FINAL REPORT 2015/016

Leaf sucrose: The link to diseases, physiological disorders such as YCS and sugarcane productivity

Final report prepared by:	Gerard Scalia, Kate Wathen-Dunn, Annelie Marquardt, Frederik Botha
Chief Investigator:	Gerard Scalia
Research organisation:	Sugar Research Australia
Co-funder:	Queensland Department of Agriculture and Fisheries
Date:	1 June 2020
Key Focus Area (KFA):	3. Pest, disease and weed management

Sugar Research Australia

Queensland Government

Please cite as: Scalia G, Wathen-Dunn K, Marquardt A and Botha FC (2020) Leaf sucrose; the link to diseases, physiological disorders such as YCS and sugarcane productivity: Final Report Project 2015/016. Sugar Research Australia Limited, Brisbane.

ABSTRACT

Yellow canopy syndrome (YCS) is a physiological disorder expressing as yellowing of the mid-canopy. Rapid growth following a stress period where growth rate of the top internodes has been compromised creates a supply demand imbalance. This results in high sucrose accumulation in the leaf which triggers yellowing. Accumulation of sucrose past an upper tolerance level causes partial stomatal closure, overheating, disruption to photosynthetic machinery, chloroplast destruction and leaf yellowing. Gene expression, protein and metabolite data all support a disruption to leaf metabolism as well as a strong association with abiotic stress. The data collectively shows that the metabolism of YCS-affected plants is compromised throughout the mid-canopy and occurs well before the onset of visual yellowing. Repartitioning of carbon to starch and other pools is an attempt to lessen the sucrose load within the source leaf, while also reducing oxidative stress. High levels of starch accumulation in the midrib veins of YCS leaves can be easily stained and viewed. This method can be used to reduce misdiagnosis when coaligned with correct symptom development and expression. There is no CCS penalty association with YCS, and crops can grow out of a YCS event. Management options to mitigate YCS involve best practice farming to reduce stress on the crop prior to and during the peak growing season. This will increase the sink capacity in the stalk and prevent a supply and demand imbalance. The data does not support a single cause and may therefore be either biotic, abiotic, or a combination of both.

EXECUTIVE SUMMARY

Yellow canopy syndrome was first noted in 2012 as an undiagnosed condition of the sugarcane mid-canopy. Yellowing of the mid-canopy is concerning as leaves in this region of the plant are responsible for sucrose production and have the highest rate of photosynthate export. These leaves are known as the sugar 'source' and any disruption to their production may reduce yield or commercial cane sugar (CCS). Healthy crops are dependent on an unimpeded supply of photoassimilate from the source to the growing or filling tissue which is known as the 'sink'. If a strong sugar gradient between the source and sink is not maintained, sugar transport out of the leaf will be compromised and a source sink imbalance will ensue. A physical blockage in the phloem or reduced physical or physiological sink strength will all reduce mass flow of sucrose between the source and sink. This could be caused by a pathogen or a product of the plant's defence response to a biotic agent or physical wounding, or by reduced sink growth. The outcome of this is sucrose accumulation in the source leaf.

In the pilot project 2014/090 it was shown that YCS plants have elevated levels of leaf sucrose and altered leaf metabolism, which included a reduction of both photosystems, reduced carbon fixation and altered partitioning of photosynthate. Based on this finding, the current project aimed to address this issue by taking an inside-out approach to identify the cause of leaf sucrose accumulation. The study presented in this report is an in-depth examination of changes to the plant's metabolism in response to reduced carbon demand from the sink, which leads to YCS symptom expression. Understanding the metabolic changes before and after the onset of visual yellowing is critical to unravelling the cause of high sucrose accumulation in the leaf. Identification of the cause of YCS symptom expression would be a critical step in the development of a potential YCS management program. To characterise the changes to metabolism, a combination of physiological

and molecular studies including transcriptome, proteome, and metabolome analyses were conducted in YCS symptomatic plants (leaf and culm). Gene expression data and protein levels support a general impact on leaf metabolism which is consistent with changes to source metabolism.

This present study revealed that YCS leaves always have elevated levels of sucrose and α-glucan (soluble and starch), with highest amounts accumulating in the midrib and leaf sheath. Metabolite analyses showed that during sucrose accumulation in the source leaf there is a reallocation of carbon to alternative pools to minimise disruption to the electron transport system. In particular, more fixed carbon is allocated to starch and soluble α-glucan and a notable upregulation of the shikimate and phenylpropenoid pathways in the leaf. A reduction in carbon partitioning to the sink will result in a yield penalty proportional to the reduction in carbon flow. In YCS symptomatic plants, the changes we see to genes associated with sugar transport, C_4 photosynthesis and mitochondrial metabolism are indicative of a response to reduced carbon flow between the source and sink. This response is an attempt to minimise changes to metabolism that lead to cellular damage.

Based on the data from this study, we postulate that YCS symptom development is a direct consequence of the accumulation of sucrose in the leaf created by reduced sucrose export. The consequence of sucrose accumulation in the leaf is partial stomatal closure, causing reduced evaporative cooling. This combined with a reduction of energy flow to the final electron acceptors of the photosystems and more heat dissipation, results in overheating. The uncoupling of the photosynthetic electron transport system and a reduction in oxidised coenzyme directly drive photo-oxidative damage, chloroplast destruction and yellowing. Evidently in the YCS symptomatic tissues, antioxidant activity is induced to try to counteract this problem. Antioxidant production of caffeoyl-quinic acids and quinate provides buffering of free radical production in the chloroplast. In healthy leaves, photosynthate export rates are sufficient to prevent sucrose build-up, and adequate levels of oxidised coenzyme are maintained ensuring full functioning of the electron transport chain.

The results presented here indicate that it is unlikely that a physical blockage is impeding sucrose translocation, and that leaf sucrose accumulation is primarily driven by changes to the sink tissue. In the current study we have only studied the culm as a sink for the photosynthate produced and exported from the leaf. However, it would be safe to argue that a disruption in any major sink or non-photosynthetic tissue in the sugarcane plant would result in a similar impact on leaf metabolism.

The internodes in YCS symptomatic plants are indicative of sink tissue that are in a ‘feast’ status i.e. not carbon starved. This would explain why no CCS penalty is associated with YCS expression. High yielding crops exhibit strong sink strength and have reduced risk of YCS development.

An insight into carbon repartitioning to starch in the midrib vascular tissue was instrumental in the development of the midrib stain test. This test has assisted researchers and service providers to identify YCS and reduce the incidence of misdiagnosis. These research outcomes address many of the concerns that have plagued the industry since 2012. They also offer an insight into the management of YCS and a means to evaluate impact on the crop.

One of the most significant outcomes from this research has been the huge advance made in our understanding of the fundamental physiology of commercial sugarcane varieties. The knowledge regarding the importance of maintaining leaf sucrose below a critical threshold will find application

in many aspects of future international sugarcane improvement, production, and stress management.

The data does not support a single cause of YCS expression and is consistent with a source sink imbalance in which reduced physical or physiological sink tissue capacity inhibits demand. YCS is not a disease, it is a physiological disorder comparable to source-sink regulated senescence.

TABLE OF CONTENTS

TABLE OF TABLES

TABLE OF FIGURES

1. BACKGROUND

1.1. Yellow canopy syndrome (YCS)

Wide-scale mid-canopy yellowing of sugarcane occurred in the peak of the growth season (December to March) in Northern Queensland in 2012. The timing and pattern of symptom expression were atypical for known sugarcane diseases and nutrient stress. Although partially similar to Yellow Leaf Syndrome (YLS) (Lehrer and Komor, 2008) there were enough differences to lead to a decision to call this phenomenon Yellow canopy syndrome (YCS). Since the first widespread occurrence in Gordonvale, Nth Queensland in 2012, YCS has been identified as far south as Maryborough in the south-east of Queensland. YCS was not characterised before 2012, so was either not present or not prevalent before this date.

There are many causes of leaf yellowing in sugarcane which are mostly due to water stress (deficit or waterlogging), pathogens, agrochemicals, nutrient and mineral deficiencies. Initial investigation ruled out water stress as a cause of YCS, as associated leaf colouring and pattern of development, morphology and total leaf canopy affliction did not correlate with YCS symptoms. Analysis of soil and leaf nitrogen, iron, and other mineral nutrients, as well as heavy metals found no deficiencies or toxicities associated with YCS. At the request of industry, early screening of YCS leaf tissue also found no evidence of the metabolite aminomethylphosphonic acid (AMPA) which is a biodegraded form of glyphosate (Gomes et al., 2016). YCS symptomatic plants also tested negative for all known sugarcane pathogens. These and other studies are detailed in the final report of project 2014/049.

Considering all obvious causes of yellowing were being ruled out, it was clear that a different approach was required to find the cause of YCS expression. It is well known that leaf yellowing is a common symptom of the *Poaceae* family when there is high carbohydrates accumulation in the source leaves (Fontaniella et al., 2003). Chlorophyll loss initiated this way is also associated with accumulation of pigments such as zeaxanthin and anthocyanins, giving the leaf a golden-yellow colour (Allison and Weinmann, 1970; Tollenaar and Daynard, 1982; Rajcan and Tollenaar, 1999). Therefore, understanding the metabolic disruptions occurring within the asymptomatic and symptomatic YCS leaf associated with carbohydrate accumulation would be essential to identifying the potential cause of this disorder.

1.1.1. Leaf sucrose, photosynthesis and metabolism

Initial investigations showed that YCS symptomatic source leaves contained high levels of sucrose and glucan. To investigate the cause of high levels of these metabolites, a clear understanding of where sucrose accumulates in the leaf (lamina, midrib, dewlap, and sheath) and location of the highest concentrations is paramount. Surprisingly, a search of the literature revealed only three other studies have been conducted in relation to the distribution of sucrose along the sugarcane leaf and within the varying tissues (Hatch and Glasziou, 1964; Mattiello et al., 2015; Bassi et al., 2018). We postulated that this information would help to reveal if leaf sucrose accumulation was due to compromised phloem loading or phloem transport in the YCS plant.

A good measure of leaf health in C_4 plants can be determined by the sucrose level in the photosynthetic cells. Under high levels of carbohydrate accumulation in the source leaf there is a downregulation of the photosynthetic genes which induces yellowing of the lamina (Tollenaar and

Daynard, 1982; Krapp and Stitt, 1995; Jensen, 1996; Russin et al., 1996; Rajcan and Tollenaar, 1999; Graham and Martin, 2000; Braun et al., 2006). Therefore, understanding the extent to which this happens in YCS leaves would be critical in determining whether there is any potential for downstream changes that would be responsible for initiating chlorosis.

Studies investigating the upstream effect of sugar accumulation on photosynthesis downregulation show that this mechanism is regulated through sugar sensing molecules. These metabolites initiate feedback inhibition of photosynthesis together with carbon redirection and partitioning to other pools (Gupta and Kaur, 2005; Braun et al., 2006; McCormick et al., 2008; Lunn et al., 2014; Nuccio et al., 2015; Figueroa and Lunn, 2016). Once again, the extent to which this may be occurring in YCS plants is important to know as this would have significant impact on the regulatory mechanisms surrounding carbon accumulation and partitioning in the leaf. Also, of interest would be the rate of carbon fixation and decarboxylation, as increased sucrose synthesis may also lead to excess accumulation in the leaf.

The disruption to these key biological functions within the plant needs to be clearly understood to characterise changes prior to and during YCS development and after the onset of visible yellowing. To study these issues, a comprehensive sugarcane leaf metabolome, transcriptome and proteome database would be required.

1.1.2. Source sink imbalance

Leaf sucrose accumulation may also occur if there is a disruption to mass flow from the source leaf to the main sink tissue of the culm or roots. Such a disruption could occur in YCS plants if there is a physical blockage of the phloem or a limitation to sink strength. To differentiate between the two would require investigation of plant defence responses, identification of an abundant microbial entity and characterisation of sink tissue strength. (Rae and Pierre, 2018) found no differences in total root and fine root length, diameter and percentage of fine roots relative to the total root length, between YCS plants and healthy controls. However, it is not plausible to rule out altered root development as a possible cause of reduced carbon demand in YCS plants from one study. It is also important to note that internodes directly beneath YCS symptomatic source leaves receive carbon well before the roots. Thus, any altered sink capacity in the internodes would initiate a faster response in the source tissue than would changes to root development. Therefore, investigations into causes of source sink imbalance would be best focussed on changes to internode development.

Phloem transport of sucrose occurs along a pressure gradient between the leaf and culm. This gradient is established and maintained by adequate loading of the phloem in the source, and efficient unloading at the sink. This is maintained by critical enzymes involved in sucrose turnover and carbon partitioning (Black et al., 1995; Koch, 1996; Morey et al., 2018). The metabolic rate and storage within the sink tissue together with the physical size of the sink organ determines sink strength (Bihmidine et al., 2013).

The metabolic processes that are responsible for maintaining healthy source sink relationships are poorly studied in general and almost none exist in sugarcane. A large part of the problem is associated with the fragmented nature of most previous studies. In this study we postulated that some of these shortfalls could be avoided by constructing comprehensive sugarcane metabolome, transcriptome and proteome databases from the relevant source and sink tissues. These databases

together with detailed complementary information regarding the physical size of the sink culm repository and growth rate would be essential to ascertain the sink strength status of YCS plants.

1.1.3. Crop stress and management

Initial reports from industry suggests there is a strong correlation between stress and YCS symptom development. When plants are under environmental stress, the growth rate is the most sensitive parameter and the first to decrease. The consequence of this is a reduction in demand for reduced carbon and hence uncoupling of the photosynthetic electron transport systems occur. This leads to increased production of reactive oxygen species (ROS). If left unchecked, photooxidation will cause the degradation of chloroplasts and chlorosis will ensue. In response to oxidative stress, plants initiate non-photochemical quenching to reduce the production of ROS, enabling a means of photoprotection (Gill and Tuteja, 2010). Therefore, knowledge of the stress status in YCS symptomatic plants and the identification of any stressors that may be contributing to reduced culm growth could help in the development of a YCS management program.

1.1.4. Diagnostic

At any one time there is a significant portion of the mature leaves on a sugarcane plant that is yellowing. This makes misdiagnosis of YCS common and creates problems for researchers, industry support services and growers alike. It also creates confusion in industry which may impact on productivity if an incorrect diagnosis is assigned to crops which otherwise could potentially have been treated to remedy an unrelated problem. Hence the problem of misdiagnosis is two-fold. Firstly, researchers may sample incorrect tissue which would compromise conclusions and research outcomes. Secondly, incorrect advice may be given to growers (or self-determined), which may impact on outputs. Therefore, development of a unique YCS biomarker or in-field diagnostic test would be of benefit to industry.

2. PROJECT OBJECTIVES

The objectives of this project were to

- Describe YCS leaf symptom expression and development
- Describe changes to leaf metabolism prior to and after the onset of visible yellowing
- Assess changes to stomatal conductance, chlorophyll fluorescence, photosynthesis, carbon turnover and partitioning, metabolome, transcriptome, and proteome
- Establish a baseline description of a healthy sugarcane leaf in terms of sucrose and starch content
- Establish whether phloem loading, or phloem transport is compromised
- Determine if leaf sucrose accumulation is primarily driven by changes to source or sink
- Identify factors that may contribute to a source sink imbalance
- Identify the processes that control sugar levels in the source leaf
- Investigate feedback inhibition of photosynthesis and leaf metabolism
- Describe the upstream and downstream effects of changes to photosynthesis and leaf metabolism

- Describe changes to sink metabolism
- Assess sink strength status
- Investigate the development of a YCS diagnostic test
- Investigate any correlation between YCS and stress
- Contribute to a potential YCS management program
- Establish where and when this physiological disorder starts and what is responsible for its induction

3. OUTPUTS, OUTCOMES AND IMPLICATIONS

3.1. Outputs

i) The major outputs delivered by this project are:

- Solving YCS by identifying that the condition is a physiological disorder without a single cause; any factor that reduces sink strength, respiration and accelerates photosynthesis could trigger the event. Thus, YCS is a condition that is comparable to source sink related induced senescence
- PhD (Annelie Marquardt)
- Masters (Kate Wathen-Dunn)
- Increased knowledge of fundamental sugarcane physiology
- Sugarcane leaf and culm metabolome, transcriptome, and proteome databases
- Establishment of sucrose, starch, and soluble α-glucan levels in a healthy sugarcane leaf
- Quantification of the leaf sucrose tolerable upper threshold in Qld commercial sugarcane genotypes before induction of photooxidation and chlorosis
- New discovery of major carbon partitioning to soluble α-glucan in sugarcane lamina, midrib, and sheath
- New discovery that the PEPCK decarboxylation pathway activity is present in Qld commercial sugarcane genotypes
- Characterisation of sugarcane feedback regulation of photosynthesis and leaf metabolism
- Identification of sucrose movement-related proteins including SWEETs, SUTs, H^+-ATPases and H^+pyrophosphatases (H^+-PPases) in Qld commercial genotypes
- Identification of the processes that control sugar levels in the source leaf of sugarcane
- Characterisation of changes to source sink balance leading to leaf sucrose accumulation in sugarcane
- Knowledge of the changes to photosynthesis, carbohydrate metabolism and carbon partitioning in sugarcane during YCS development
- Development of rapid leaf and internode sampling and microtitre assay protocol for sucrose and α-glucan quantification
- Methodology for 13C labelling of sugarcane leaf in the field
- Methodology for building a sugarcane transcriptome reference database
- Sugarcane YCS identification kit (midrib stain)

ii) Adoption

- Sugarcane researchers in Australia and internationally
- SRA researchers, SRA adoption officers and sugar service providers have adopted the YCS identification kit and trialling it in sugarcane regions throughout Qld

3.2. Outcomes and Implications

YCS is a condition that has caused concern for the industry since 2012. From the onset researchers were perplexed as to what could suddenly cause yellowing of the mid canopy in one field and not the next, in the current crop cycle but not in the following year, in one section of a field and not another, in some culms of the same stool but not others, and express at varying levels of severity and then grow out of the condition.

Progress in unravelling the YCS phenomenon was hampered by a limited understanding of the metabolism of sugarcane, especially the interaction and control of leaf (source) and culm (sink) metabolism. In contrast to other main crops there were limited 'omics' databases on the Australian Q and SRA varieties and hence, no opportunity to immediately deploy the powerful new high throughput technologies to characterise and understand the YCS phenomenon.

There were two major achievements in this project. Firstly, it allowed the development and characterisation of comprehensive sugarcane leaf and culm metabolome, transcriptome, and proteome databases of Q200$^{\phi}$, Q240$^{\phi}$, Q208$^{\phi}$ and KQ228$^{\phi}$. Secondly, it has improved the fundamental knowledge of sugarcane physiology enormously. Evidently, this knowledge and databases will be an invaluable future resource to understand sink source relationships in sugarcane. The work highlighted the importance of combining proper accurate field characterisation of a phenotype with modern high throughput technologies.

The results from this research on sugarcane and YCS have been disseminated at national and international events by using local forms of communication, formal conferences, and peer reviewed publications. This has helped the Australian and international sugarcane industries and scientific community to better understand YCS. It highlighted that mid-canopy yellowing is a phenomenon driven by sink source imbalance and the crop's response to rebalance the source sink ratio.

Identification of YCS as a physiological disorder without a single cause has significant implications for the industry. We now know that any factor that reduces sink strength, respiration or accelerates photosynthesis could trigger the event. Therefore, this condition can be described as a form of source-sink regulated induced senescence. Management of YCS must focus on best practice farming to maintain maximum growth rate and minimise crop stress to avoid initiation of a source sink imbalance. It is paramount that the industry considers how it will maintain this balance in a rapidly changing environment due to global warming and climate change at a local level. These events have contributed to a significant impact on production in the past decade. Plant crop stress is an evolving issue for growers and YCS may be the first of many such disorders that could develop without the proper implementation of mitigation practices. Low world sugar prices and increasing costs of production are major drivers of reduced capacity across the industry to prevent the ongoing occurrence of YCS. Therefore, RD&A and government policy must focus on relieving these economic pressures for growers so they may access all necessary resources to prevent the development and impact of YCS within industry. Interestingly, successful implementation of these measures to

mitigate YCS should see an increase in yield. This is not because of the impact YCS has on yield after symptom expression in the canopy, but because of preventative measures required before expression.

From a professional perspective, formal qualifications were obtained through studies of YCS, Kate Wathen-Dunn her Masters in Bioinformatics (2017) and Annelie Marquardt her PhD (2019).

4. INDUSTRY COMMUNICATION AND ENGAGEMENT

4.1. Industry engagement during course of project

Communication of objectives and results throughout the project

4.1.1. Presentations to industry and scientific research community

- Qld Minister for Agriculture onsite tour 2015, 2017
- YCS Scientific Reference Panel reviews and workshops
- Grower updates throughout Qld 2015 - 2020
- Webinar May 6th, 2020 (Appendix 3)
- Productivity and sugar services groups throughout Qld
- Grower delegates and industry representatives
- Canegrowers organisation
- International Plant & Animal Genome XXV Conference: PAG XXV San Diego, California, USA, January 2017
- ISSCT conference in Chiang Mai, Thailand, Dec. 2016
- ISSCT conference in Tucumán, Argentina, September 2019
- Global Conference on Plant Science and Molecular Biology: GPMB II, Rome, Italy, 2018 (Appendix 3)
- ASSCT conference in Mackay, April 2017 (Appendix 3)
- TropAg 2015, 2017, 2019 (presentations and posters Appendix 3 & 4)
- COMBINE Student Symposium 2016/The Australian Bioinformatics and Computational Biology Society (AB3ACBS) Conference 2016, 2019, F1000Research Poster/Speaker Prize Winner (2016).
- UQ Bioinformatics Winter School, July 3rd, 2018 School F1000 Speaker Prize
- QAFFI lab talks

4.1.2. Industry conference papers

1) Frederik C Botha, Annelie Marquardt, Gerard Scalia and Kate Wathen-Dunn: “Yellow Canopy Syndrome (YCS) is associated with disruption of sucrose metabolism in the leaf.” In: Proceedings of the International Society of Sugar Cane Technologists, Volume 29, 2016 (in press).
(presented by Frikkie Botha at ISSCT conference 2016). (See Appendix 1)

2) Annelie Marquardt, Kate Wathen-Dunn, Robert J Henry and Frederik C Botha: "There's yellow and then there's yellow – which one is YCS?" In: Proceedings of the Australian Society of Sugar Cane Technologists, Volume 39, p89-98, 3-5 May 2017.
(presented by Annelie Marquardt at ASSCT conference in 2017). (See Appendix 1)

4.1.2 Academic documents and other

1) Marquardt A (2019) 'The molecular analysis of yellow canopy syndrome-induced yellowing in the sugarcane leaf', PhD thesis, The University of Queeensland, DOI 10.14264/ uql.2019.238. (See Appendix 2)

2) Wathen-Dunn K (2017). 'Yellow Canopy Syndrome in sugarcane: Finding clues to the cause in the leaf transcriptome', Master's thesis, The University of Queensland (See Appendix 2)

3) Botha FC (2019). A research model for carbon-partitioning in sugarcane. Research Outreach Issue 106 https://issuu.com/researchoutreach/docs/ro_106_web_singlepages

4) Communication through SRA newsletters, flyers, emails, videos, and website

4.2. Industry communication messages

Key communication points:

- YCS is a physiological disorder expressing as yellowing of the mid canopy
- YCS is not a disease
- Research does not support a single cause
- YCS is always preceded by some form of stress
- The cause of YCS is any form of stress that significantly slows growth and reduces the sink size or strength
- Growth rate drives YCS development, not vice versa
- Environmental or biological stress or both can be the trigger for YCS
- Use all available resources together with best practice farming to reduce plant stress and ensure growth does not slow
- YCS usually expresses after good rain or irrigation in crops that have been previously stressed
- An imbalance between supply from the leaf (source) and demand from the stalk (sink) causes sucrose accumulation in the leaf
- YCS leaves always have high levels of sucrose and starch
- High leaf sucrose and high light intensity is required to initiate yellowing
- High leaf sucrose above an upper tolerable level initiates yellowing and accelerates senescence (aging)
- There is no commercial cane sugar (CCS) penalty associated with YCS
- YCS severity does not predict yield penalty

5. METHODOLOGY

5.1. Field visits

Field sampling conducted in this project was a continuation of sampling reported in the Final report of project 2014/090. As samples and data attained during research conducted in project 2014/090 have been used for further analysis in this project, details of all Field Visits (FV) (Table 1) and sample collection methodology are recorded in this report for completeness.

Table 1: Details of sampling field visits in this study

Field Visit	Date of sampling	Location	Genotype	FVD = Leaf # 1
2	Feb 24-27, 2014	Herbert	Q200$^{\phi}$	All leaves
		Burdekin	KQ228$^{\phi}$	
3	May 12-15, 2014	Herbert	Q200$^{\phi}$	Leaf 2 & 4
4	July 1-2, 2014	Herbert	Q200$^{\phi}$	Leaf 2 & 4
6	Jan 19-22, 2015	Herbert	Q200$^{\phi}$	Leaf 4 & 6
		Burdekin	KQ228$^{\phi}$	
		Mackay	Q208$^{\phi}$	
9	May 19-21, 2015	Herbert	Q200$^{\phi}$	Leaf 2 & 4
		Burdekin	KQ228$^{\phi}$	Leaf 2 & 4
10	Feb 3-5, 2016	Burdekin	Q240$^{\phi}$	Leaf 3, 4 & 6
11	Mar 16-18, 2016	Burdekin	KQ228$^{\phi}$	Leaf 4 & 5
12	Mar 22-24, 2016	Mackay	QC04-1411	Leaf & Internode 5 & 6
			Q240$^{\phi}$	Leaf 5 & 6
13	Mar 30-Apr 1, 2016	Maryborough	Q240$^{\phi}$	Leaf & Internode 3 & 4
14	Mar 7-10, 2017	Burdekin	KQ228$^{\phi}$	Leaf 4 & Internode 2, 4 & 6
15	Apr 11-13, 2017	Burdekin	Q240$^{\phi}$	Leaf 2-6
16	Feb 20-21, 2018	Herbert	SRA3$^{\phi}$, Q250$^{\phi}$, Q200$^{\phi}$, Q232$^{\phi}$, Q240$^{\phi}$, Q242$^{\phi}$, KQ228$^{\phi}$, Q208$^{\phi}$	Leaf 4
17	Apr 2-4 2019	Herbert-Cairns	Numerous	Leaf 4
18	July 1, 2019	Maryborough	Q240$^{\phi}$	Whole culm, all leaves
19	Nov 21, 2019	Woodford	Numerous	Leaf 4

5.2. Material sampling

As we learned more about the metabolic processes in the upper canopy of YCS symptomatic plants (2014/090) we refined our sampling strategy and methodology. Sampling evolved to the point where samples were mostly only taken (where practical) during the peak growing period of December – April. After this time there are other symptoms which include significant reduction in canopy size, natural senescence and several minor diseases which may overlay on the typical YCS symptom development. Controls were classified as culms with mid canopy leaves that had no YCS symptoms.

Sampling of control tissue may therefore be from either culms from the same or different stools to culms with YCS symptomatic leaves. The investigatory directive at the time of sampling determined the amount of sample biomass and type of tissue that was collected. Whatever the magnitude of the sampling the following was adhered to whenever possible.

5.2.1 Leaf, internode and xylem sap

In all the work reported here, leaves on each culm were numbered wherein the leaf with the first visible dewlap was deemed Leaf 1 (Figure 1A & B) (Bonnett, 2014). Unless otherwise specified, leaf samples were taken from the middle section of the leaf either by leaf punch (Figure 1C & D), or 70 mm section. Leaf punches were placed in a 2 mL screw cap tube and snap frozen with dry ice or liquid nitrogen; when these were unavailable then tubes were dropped into a Thermos filled with boiling water for 15 mins and then transferred to a -20°C freezer. Figure 2 shows sampling of each type of leaf tissue except for the 70 mm piece cut from the middle of the leaf which includes the midrib and lamina on both sides. All tissue sampled was taken from material that had the exterior surface first wiped with 70% ethanol. All instruments used for sampling were cleaned with 70% ethanol between samples.

For internode samples, a section from the bottom of the internode approximately 30 mm long was cut and a 8mm Ø cylindrical core was bored off-centre (avoiding the pith) and vertically down using a 12 mm cordless drill and Sutton Diamond Drill Bit Core Blue Ceram 8mm Ø (Model Number370400080) (Figure 1E). Cylindrical samples were placed in a labelled 2mL screw cap tube and snap frozen in liquid nitrogen and stored at -80 °C. The drill bit borer was sprayed with 70% ethanol and wiped between samples.

Xylem sap and internodes were sampled directly beneath leaf sheaths while maintaining correct orientation. Cut ends of the internodes were then blotted with tissue paper for approximately 5 seconds to absorb remnants of ruptured cells. A pressure regulated sap extractor kit was used to push sap (min 70 kPa - max 140 kPa) from the internode under constant and controlled pressure (in the direction from bottom to top) into a plastic funnel above a labelled 2 mL screw cap tube (Figure 1F). Sap was snap frozen in liquid nitrogen and stored at -80 °C. All equipment was sprayed with 70% ethanol and wiped between samples.

All samples were transferred to dry ice and either lyophilised or stored at -80 °C awaiting further processing.

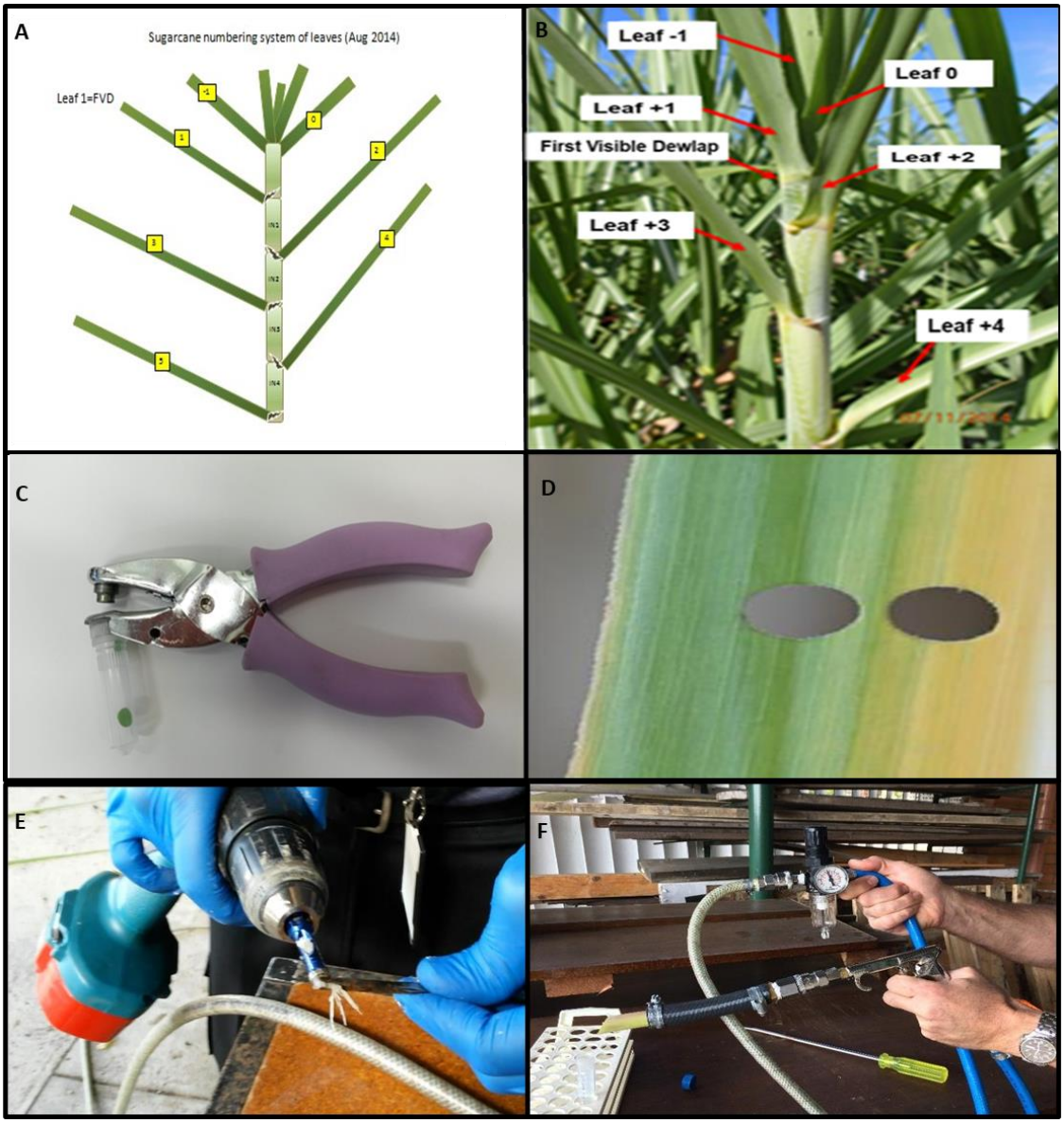

Figure 1 Schematic diagram of sugarcane leaf numbering system used during sampling (A) photograph indicating Leaf 1 in the leaf with the first visible dewlap from the top (B), modified Fiskars hole punch 6.35mm Ø and 2mL screw cap tube (C), example of leaf disk sample taken from early stage (ES) and late stage (LS) YCS lamina (also used for midrib) (D), diamond Drill Bit Core Blue Ceram (8mm Ø) used to sample internode core section, forceps used to remove sample before placing in collection tube (E), and xylem sap extracting apparatus where internode piece is inserted into rubber tubing and regulated compressed air (1 bar) released to push sap out of the xylem into collection tube (F).

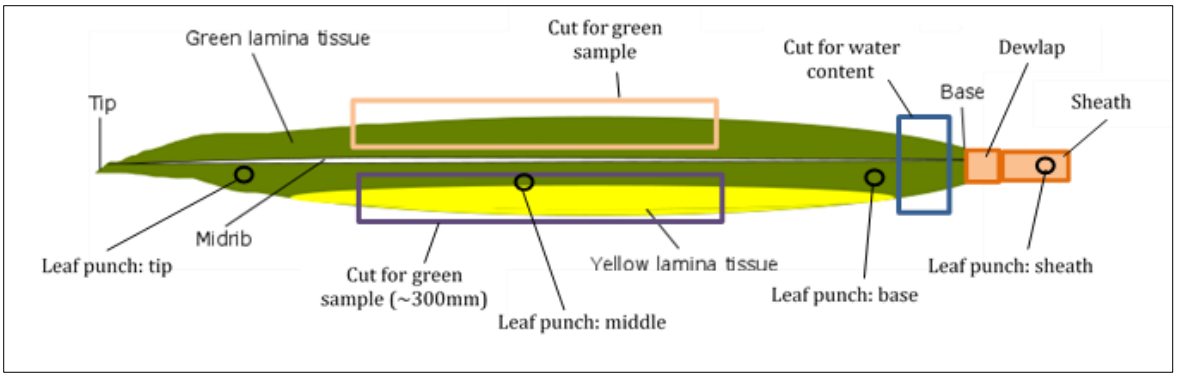

Figure 2 Types of leaf tissue sampling

5.2.2 ^{13}C Labelling and sampling

A $^{13}CO_2$ delivery bag chamber (Figure 3A) was attached to a region of the YCS symptomatic leaf where one side of the mid-rib was yellow and the other side was mostly green (Figure 3A & B) and preferably not in the lower 1/3 of the leaf. A similar leaf position was selected on the leaf directly above and the same for ^{13}C labelling of the two asymptomatic control leaves. Plastic bag chambers were sealed onto the surface of the leaf with rubber butyl sealant and evacuated with a 60mL syringe (Figure 3B). CO_2 free air from a KOH (2.5M) CO_2 sink was pushed into the chamber to inflate the bag around the leaf. A pipette and 3mL syringe were used to deliver 500 µL $NaH^{13}CO_3$ (0.1299M) solution and 500 µL of HCl (1M) to the absorbent pad inside the chamber where $^{13}CO_2$ was released to the leaf (Figure 3C-E). Approximately 16,000 ppm of $^{13}CO_2$ was available for leaf photosynthesis.

Figure 3 ^{13}C labelling Q240$^{\Phi}$ in field; ^{13}C delivery chamber (volume: ≈ 100mL) plastic acetate sheet heat sealed to form a chamber 124 x 80 mm with two 12 mm strips of Consolidated Alloys Butyl rubber sealant at each end (Bunnings part # 10266). The chamber has an internal pocket 70 x 25 mm containing a strip of TOM organic ultra-thin absorbent liner 70 x 20mm. Inserted on top of the liner is a 1.0mm Ø x 100mm clear transmission tube attached to a BD blunt end plastic cannula (303345) and Terumo Terufusion 3-way Stopcock Luer Lock (TE-TSWSR201) (A); evacuating chamber and filling with CO_2 free air (B); addition of $NaH^{13}CO_3$ + HCl and injection into chamber (C-E)

100 mm leaf sections, leaf sheaths and internode cores were harvested from labelled stalks at three time points i) 3 hr ii) 8 hr and iii) 31 hr post labelling. Leaf samples were also collected from unlabelled leaf material to determine the amount of background C^{12} in the atmosphere. All leaf and sheath material were placed in porous plastic zip lock bags and snap frozen in liquid nitrogen. Internode cores 8mm Ø were bored off-centre and vertically down using a cordless drill and

diamond drill core bit and placed in 2 mL screw cap tubes and snap frozen in liquid nitrogen. Three leaf punches were also collected above and below the labelled leaf section and from the leaf sheath.

5.3. Sample processing

5.3.1. Lyophilisation of samples

All material that was not stored at -80°C was lyophilised in a CHRIST® Alpha 1-4 LSC Plus Freeze dryer. After lyophilisation of mid leaf samples, the midrib was removed and leaves cut into approximately 3 mm^2 pieces with scissors or passed through a small shredding mill and then transferred to reinforced 2 ml tubes containing two stainless steel grade 316, 5 mm Ø balls. The sample was ground to a fine powder using a Retch MM300 bead mill (frequency 30 hz, 4 cycles of 2.5 minutes with 2 minutes pause between each cycle to allow any heat to dissipate) or 3 mg (0.0030g) of lyophilised lamina, midrib, sheath/dewlap tissue was transferred to a 2 mL screw cap Eppendorf tubes. Stainless steel ball bearings (3 x 2.8mm and 2 x 3 mm) were added plus two mini-spatula scoops of sand and samples were ground at 1500 strokes/min in a Geno/Grinder® for 10 min total (in 2 min bouts).

Powder from replicates was then equally combined and thoroughly mixed to make one stock sample. Dry powder portions of 100 mg were sent to the laboratories outlined below for metabolome and hormone analysis.

Metabolomics Australia
School of Botany
The University of Melbourne
Parkville
Victoria 3010

National Research Council of Canada
Plant Biotechnology Institute
110 Gymnasium Place
Saskatoon
Saskatchewan S7N 0W9
Canada

Approximately 250mg of ground lyophilised material was sent to APAF for protein analysis

Australian Proteome Analysis Facility (APAF)
Level 4 Building 4 Wallys Walk (formerley F7B, Research Park Drive)
Macquarie University
Sydney NSW 2109

5.3.2. Extraction method chlorophyll and carbohydrates from lyophilised material or a single fresh leaf disk

Finely ground lyophilised lamina (3.0 mg), midrib, sheath/dewlap tissue or one whole fresh leaf punch was used for the extraction. Chlorophyll was extracted in 500 µL of 100% V/V acetone (precooled to -20°C), and vortexed thoroughly, left overnight at -20°C, vortexed and then centrifuged for 5min at 6000Xg at 4°C. Acetone solution containing chlorophyll was removed and kept. A further 500 µL (V/V) acetone (precooled to -20°C) was added to the pellet and chlorophyll re-extracted as above. Both supernatants were combined for chlorophyll determination.

The pellet was then left to air-dry before 200 µL deionised water was added and incubated at 70°C for 30 minutes followed by centrifugation at 16000Xg for 10 minutes. Supernatant was removed and retained, and the pellet re-extracted with water as before. The combined supernatant was filtered through a 0.45 µm PVDF filter and used to determine sucrose, glucose, fructose, and soluble alpha-glucan. Two small spatula scoops of sterile sand and 2 x 3mm and 2 x 2.38 mm stainless steel balls were added to the residual pellet and the sample ground in a Geno/Grinder® for 12 min @1750 strokes/min. Potassium hydroxide (20 µL of 4.2M) and 400 µL deionised water was added to the residual pellet and autoclaved for 2 hrs at 121° C (~210kPa), ground for a further 5 mins, then cooled, neutralised with acetic acid (70 µL of 1M) and centrifuged at 16,000xg for 10 minutes. Supernatant was removed and used for starch determination.

5.3.3. RNA extraction from fresh mid-leaf powder

The mid-rib was removed, and the lamina tissue was ground to a fine powder under liquid nitrogen in a mortar and pestle. RNA was extracted from the laminar material using Qiagen RNeasy Plant Mini Kit (QIAGEN N.V., The Netherlands) according to the manufacturer's instructions with the addition of 2.5% (w/v) PVP-40, with the RNA eluted twice in the elution buffer. In brief, 600 µL of RLT buffer was added to tissue powder and centrifuged at 15,000 rpm for 5 minutes before passing through the QIAshredder column and eluting with 60µL RNase-free water passed through membrane twice. RNA quantity was checked with the NanoDrop for yields > 100 ng/µL and A_{260}/A_{230} > 1.0. RNA quality was checked with 1.5% TBE agarose gel containing 1 % SybrSafe to visualize 18s and 28s ribosomal RNA bands.

Internode RNA extraction: RNA from each internode sample was extracted and sequenced individually. Internode tissue was ground to a fine powder with the Geno/Grinder® (Spex SamplePrep, NJ USA) for 2 minutes at 1500 strokes/minute with liquid nitrogen, using 2x2mm plus 2x3mm stainless steel beads per tube, and the cryoplate in metal blocks. RNA was extracted from 100mg of powder per sample, using Spectrum Plant Total RNA kit (Sigma-Aldrich/Merck, Germany) according to the manufacturer's instructions with the addition of 2.5% (w/v) PVP-40 (polyvinylpyrrolidone, mw 40,000; Sigma-Aldrich/Merck), with the RNA eluted twice in the elution buffer. RNA quality was checked by agarose gel electrophoresis and spectrophotometer (ND-1000 Spectrophotometer, NanoDrop Technologies, Wilmington, DE, USA).

Approximately 20µg of RNA per sample was prepared for despatch by suspending the RNA in precipitation buffer (1/10 vol 3M sodium acetate pH 5.5 plus 3.0 x volume 100% ethanol) to:

LC Sciences

Sample Receiving

2575 West Bellfort St
Suite 270
Houston Texas 77054 USA
University of Western Sydney
Hawkesbury Institute for the Environment
University of Western Sydney
Locked Bag 1797
Penrith NSW 2751

NGS department of overseas sales
Macrogen Inc.
World Meridian Venture Center
10F, #1003, 254 Beotkkot-ro, Geumcheon-gu
Seoul, Rep, of Korea
08511 (153-781)

5.3.4. Protein extraction from lyophilised leaf material

SRA Indooroopilly

Freeze dried and crushed plant material to the weight of 125mg was denatured using 5% SDS, 25mM Tris PH8.0 and 0.07% β-mercaptoethanol (1.2 mL) at 90°C for 10 minutes. Samples were centrifuged at 16,000G for 10 minutes and supernatant transferred to a 15 mL Falcon tube. Approximately 6 times the supernatant volume of cold (kept at -20°C) 10% TCA, 0.07% β-mercaptoethanol in acetone (approximately 5.4 mL) was added to the supernatant and left at 20°C overnight to precipitate. Samples were centrifuged at 5,000G for 5 minutes and the supernatant discarded. The pellet was washed three times with cold acetone (kept at -20°C) and then dried at room temperature. The pellet was then dissolved in 100 µl of 25mM Tris PH8.0, 0.07% β-mercaptoethanol. The protein concentration was measured and precipitated in 6 volumes of cold acetone. The air-dried protein (125 µg per sample) was dispatched on dry ice to Proteomics International for proteome analysis.

Proteomics International Pty Ltd
Harry Perkins Institute of Medical Research
QQ Block, QEII Medical Centre
6 Verdun Street, Nedlands WA 6009
Australia

Australian Proteome Analysis Facility (APAF)

Similar to description by Wu et al. (2016). Samples were washed with 10% TCA containing 0.07% DTT in acetone and homogenised in 50 mM HEPES in 2% SDS buffer.

Supernatant was taken and buffer exchanged with 100 mM TEAB using 5KDa molecular weight cut-off filter (VIVASPIN 6, 5 kDa spin filter, Product #VS0612, Sartorius Stedim).

The protein concentration was determined by Direct Detect. 100 µg of sample was taken for digestion and analysis. 1D and 2D IDA nanoLC (Ultra nanoLC system, Eksigent) ESI MS/MS data were acquired for each control, ES and LS lamina samples. 2D IDA nanoLC ESI MS/MS data were acquired for lamina samples collectively (including senescent and water-stressed leaf tissues not used in this study).

After sample fractionation and peptide elution, the reverse phase nanoLC eluent was subject to positive ion nanoflow electrospray analysis in an information dependant acquisition mode (IDA). In the IDA mode a TOFMS survey scan was acquired (m/z 350 - 1500, 0.25 second), with the ten most intense multiply charged ions (1+ - 5+; counts >150) in the survey scan sequentially subjected to MS/MS analysis. MS/MS spectra were accumulated for 50 milliseconds in the mass range m/z 100 – 1500 with rolling collision energy.

Again, after sample fractionation and peptide elution, the reverse phase nanoLC eluent was subject to positive ion nanoflow electrospray analysis in a data independent acquisition mode (SWATH). In SWATH mode, first a TOFMS survey scan was acquired (m/z 350-1500, 0.05 sec) then the 60 predefined m/z ranges were sequentially subjected to MS/MS analysis. MS/MS spectra were accumulated for 60 milliseconds in the mass range m/z 350-1500 with rolling collision energy optimised for lowed m/z in m/z window +10%. To minimize instrument condition caused bias, SWATH data were acquired in random order for the samples with one blank run between every sample injection.

5.3.5. Extraction of metabolites for GC-MS (Untargeted) and LC-MS (Amino Acids and Untargeted Profiling)

Approximately 30 mg of homogenized leaf was added to a cryomill tube. Methanol (100%) (500 µL), and a quantitative internal standard containing 4% [(13C6-Sorbitol (0.5 mg/mL), 13C5-15N-Valine (0.5 mg/mL); 2-aminoanthracene (0.25 mg/mL) and pentafluorobenzoic acid (0.25 mg/mL)] was added. The sample was vortexed for 30 sec and was subsequently homogenized using a cryomill (Bertin Technologies) using program #2(6100-3 x 45 - 045) at -10°C. The sample mixture was then incubated at 30°C, and agitated at 850 rpm for 15 mins and then centrifuged at 13,000 rpm for 5 mins at 4°C. The supernatant containing methanol was then transferred into a new Eppendorf tube. Milli-Q Water (containing formic acid, 2%) (500 µL) was added to the remaining pellet in the cryo- mill tube. The sample was vortexed for 30 sec and then centrifuged at 13,000 rpm for 5 mins at 4°C. The supernatant was then combined with the previous methanolic supernatant. A (50 µL) aliquot and a (5 µL) were transferred into glass inserts and dried in vacuo for subsequent TMS polar metabolite derivatisation. Extracted leaf tissue samples were placed in a snaplock bag with silica gel prior to derivatisation for GC-MS analysis. A 10 µL aliquot of the extract was transferred into an Eppendorf tube for subsequent amino acid metabolite derivatisation (LC-QQQ-MS) and a 50 µL aliquot was used for LC-QTOF-MS Profiling. Aliquots for LC-MS (Amino acid quantitation and untargeted profiling) were stored at -20°C prior to analysis.

^{13}C metabolites

Aliquots (10 mg) of lyophilised leaf material were extracted and then derivatized using TMS N,O-bis (Trimethylsilyl)trifluoroacetamide with Trimethylchlorosilane (BSTFA with 1% TMCS, Thermo Scientific).

5.3.6. Derivatisation of Polar metabolites

The dried samples were re-dissolved in 10 µL of 30 mg mL^{-1} methoxyamine hydrochloride in pyridine and derivatised at 37°C for 120 min with mixing at 500 rpm. The samples were then treated for 30 min with 20 µL *N*,*O*-*bis*-(trimethylsilyl)trifluoroacetamide (BSTFA) and 2.0 µL retention time standard mixture [0.029% (*v*/*v*) *n* dodecane, *n*-pentadecane, *n*-nonadecane, *n*-docosane, *n*-octacosane, *n*-dotriacontane, *n*-hexatriacontane dissolved in pyridine] with mixing at 500 rpm at 37°C. Each derivatised sample was allowed to rest for 60 min prior to injection.

5.3.7. Amino acids

Two different stock solutions were used, 1) Amino acids, containing a standard mix of 25 amino acids in water 0.1% formic acid and 2) Sulphur containing compounds: a 2.5 mM stock solution containing glutathione and s-adenosyl-homocysteine in water with 10 mM TCEP and 1 mM ascorbic acid. The solutions were mixed and diluted using volumetric glassware with water containing 10 mM TCEP and 1 mM ascorbic acid, 0.1% formic acid to produce the following series of combined standards: 0.1, 0.5, 1, 5, 10, 20, 50, 100 and 150 µM

5.3.8. Preparation of xylem sap samples for analyses

Fifty microliters of xylem sap were transferred into an Eppendorf tube (2 mL). Cold methanol (100%) (100 µL), and a quantitative internal standard containing 4% [(13C6-Sorbitol (0.5 mg/mL), 13C5-15N-Valine (0.5 mg/mL); 2-aminoanthracene (0.25 mg/mL) and pentafluorobenzoic acid (0.25 mg/mL) was added on ice. The sample was vortexed for 30 sec and then centrifuged at 13,000 rpm for 5 mins at 4°C. Aliquots of 100 µL and 5 µL were transferred into glass inserts and dried in vacuo for subsequent TMS polar metabolite derivatisation. Extracted xylem sap samples were placed in a snap lock bag with silica gel prior to derivatisation for GC-MS analysis.

Twenty microliters of xylem sap were transferred into an Eppendorf tube (2 mL). Methanol (100%) (50 µL), and a quantitative internal standard containing 4% [(^{13}C6-Sorbitol (0.5 mg/mL), ^{13}C5-^{15}N-Valine (0.5 mg/mL); 2-aminoanthracene (0.25 mg/mL) and pentafluorobenzoic acid (0.25 mg/mL) was added. The sample was vortexed for 30 sec and then centrifuged at 13,000 rpm for 5 mins at 4°C. A 10 µL aliquot of the extract was transferred into an Eppendorf tube for subsequent amino acid metabolite derivatisation (LC-*QQQ*-MS) and a 50 µL aliquot was used for LC-*QTOF*-MS profiling. Aliquots for LC-MS (Amino acid quantitation and untargeted profiling) were stored at -20°C prior to analysis.

5.3.9. Callose extraction

Finely ground lyophilised lamina (5.0 mg) was used for the extraction. To remove chlorophyll, 1.2 mL of 70% ethanol was added, gently shaken for 5min @50˚C and centrifuged for 5min @ 400xg at room temperature. The supernatant was removed, and the pellet washed twice in 600µL 70% ethanol, vortexed and centrifuged for 5min @ 400g each time and supernatant discarded. The pellet was solubilized by adding 200µL 1MNaOH and shaken for 15min @80˚C. centrifuged for 5min @ 400 g at room temperature and the supernatant removed for analysis.

5.3.10. Apoplastic fluid

Two 80 mm pieces of leaf sheath were cut from the sample leaf and weighed on an analytical balance to 4 decimal places. Each sample sheath was cut longitudinally before being further cut into

10 mm lengths. All pieces were placed in a 50 mL syringe equipped with a three way stop cock and covered with Milli-Q water. The syringe plunger was inserted into the syringe, inverted and air displaced through the valve. With the valve closed the plunger was withdrawn to create a vacuum to release the air from the apoplastic space, pulse 3x40s periods. The air was then ejected through the valve in an inverted position and repeated three times as above. The valve was then opened, the water expelled, and sheath pieces recovered, and the surface carefully blotted with tissue paper avoiding the cut ends. Samples were reweighed and placed in a 15 mL Eppendorf tube and centrifuged at 1350 RPM in a portable centrifuge for 15 minutes to recover the apoplastic fluid. Samples were immediately snap frozen in liquid nitrogen and stored on dry ice until transfer to -80°C freezer for storage.

5.4. Sample analyses

5.4.1. Quantification of carbohydrates

Sucrose content was determined using the standard enzymatic method (Bergmeyer and Bernt, 1974) with a spectrophotometer (BMG-Labtech, FLUOstar Omega) and 96-well UV-clear plate (Thermo Fisher, UV Microtiter).

Glucose composition was determined using Amplex® Red/glucose oxidase enzyme assay (Life Technologies) in a 96-well plate (Thermo Fisher, Microtiter) with a spectrophotometer (BMGLabtech, FLUOstar Omega).

Fructose content was determined using a BioVision Fructose Flurometric assay kit in a 96-well plate (Thermo Fisher, Microtiter) with a spectrophotometer (BMG-Labtech, FLUOstar Omega). A 1/10 dilution of the OxiRed probe and a running temperature of 37°C was optimal for this assay.

Starch and soluble α-glucan were digested in a sodium acetate buffer (100mM, pH 5.5) containing 10 U amyloglucosidase per reaction for 2h at 37°C. After cooling down to room temperature, glucose was measured in the resulting solution as described above (Bergmeyer and Bernt, 1974).

5.4.2. GC-MS analysis

Standard metabolites

Samples (1 µL) were injected in split less (lower and higher aliquots) into a GC-MS system comprised of a Gerstel 252 autosampler, a 7890A Agilent gas chromatograph and a 5975C Agilent quadrupole MS (Agilent, Santa Clara, USA). The MS was adjusted according to the manufacturer's recommendations using *tris*-(perfluorobutyl)-amine (CF43). The GC was performed on a 30 m VF-5MS column with 0.2 µm film thickness and a 10 m Integra guard column (J & W, Agilent). The injection temperature was set at 250°C, the MS transfer line at 280°C, the ion source adjusted to 250°C and the quadrupole at 150°C. Helium was used as the carrier gas at a flow rate of 1.0 mL min^{-1}. For the polar TMS metabolite analysis, the following temperature program was used; start at injection 70°C, a hold for 1 min, followed by a 7°C min^{-1} oven temperature, ramp to 325°C and a final 6 min heating at 325°C. For the polar metabolite analysis, the following temperature program was used; start at injection 70°C, a hold for 1 min, followed by a 7°C min^{-1} oven temperature, ramp to 325°C and a final 6 min heating at 325°C. Both chromatograms and mass spectra were evaluated using either the Agilent MassHunter Workstation Software, Quantitative Analysis, Version B.05.00/Build 5.0.291.0 for GC-MS. Mass spectra of eluting compounds were identified using the

public domain mass spectra library of Max-Planck-Institute for Plant Physiology, Golm, Germany (http://csbdb.mpimp- golm.mpg.de/csbdb/dbma/msri.html) and the *in-house* Metabolomics Australia mass spectral library. All matching mass spectra were additionally verified by determination of the retention time by analysis of authentic standard substances. Resulting relative response ratios (area of analyte divided by area of internal standard, ^{13}C6-sorbitol) per sample FW (mg) for each analysed metabolite as previously described (Roessner et al. 2001). The data was also normalized in order to compare fold differences between groups. If a specific metabolite had multiple TMS derivatives, the metabolite with the greater detector response and improved peak shape within the dynamic range of the instrument was selected.

^{13}C Metabolites

Mass spectra of eluting TMS-derivatized glucose, fructose and sucrose were identified using authentic standards and the in-house Metabolomics Australia mass spectral library. The quantification methodology based on fragment detection (Saunders et al., 2015). Peak areas for the monoisotopic (unlabelled) and associated isotopomer ions were determined using Agilent MassHunter Quantitative Analysis version B.07.00. ^{13}C Enrichment was calculated based on these peak areas using an in-house R-script (Kowalski et al., 2015), with background correction (Nanchen et al., 2007).

5.4.3. LC-QQQ-MS

LC-QQQ-MS - An Agilent 1200 LC-system coupled to an Agilent 6410 Electrospray Ionisation-Triple Quadrupole MS was used for quantification experiments. Injection volumes of 1 µL of samples or standards were used. Ions were monitored in the positive mode using a Dynamic Multiple Reaction Monitoring (DMRM) method optimized for each analyte. The source, collision energies and fragmentor voltages were optimized for each analyte by infusing a derivatised standard with LC eluent. The following source conditions were used: gas flow 10 L.min-1, nebulizer pressure 45 psi and capillary voltage 3800 V.

An Agilent Zorbax Eclipse XDB-C18 Rapid Resolution HT 2.1 x 50 mm, 1.8 µm column was used with a flow rate of 300 µL min^{-1}, maintained at 30°C, resulting in operating pressures below 400 bar with a 19 minute run time as previously described *(Boughton et al., 2011)*. A gradient LC method (Table 2) was used with mobile phases comprised of (A) 0.1% formic acid in deionized water and (B) 0.1% formic acid in acetonitrile. These conditions provided suitable chromatographic separation of modified amino acids. Co-elution was observed for some of the species, but this could be accounted for by using the mass-selective capabilities of the mass spectrometer using MRM (multiple reaction monitoring).

Table 2: Gradient LC Method for 6410-QQQ

Time (min)	% B
0.00	1
2.00	1
9.00	15
14.0	30
14.1	1
19.0	1

5.4.4. Hormone analyses

An aliquot (100 µL) containing all the internal standards, each at a concentration of 0.2 ng μL^{-1}, was added to homogenized sample (approx. 50 mg). 3 mL of isopropanol:water:glacial acetic acid (80:19:1, v/v/v) were further added, and then samples were shaken in the dark for 14-16 h at 4°C. Samples were then centrifuged and the supernatant was isolated and dried on a Büchi Syncore Polyvap (Büchi, Switzerland). Further, they were reconstituted in 100 µL acidified methanol, adjusted to 1 mL with acidified water, and then partitioned against 2 mL hexane. After 30 min, the aqueous layer was isolated and dried as above. Dry samples were reconstituted in 800 µL acidified methanol and adjusted to 1 mL with acidified water. The reconstituted samples were passed through equilibrated Sep-Pak C18 cartridges (Waters, Mississauga, ON, Canada), and then the final eluate was split in 2 equal portions. One portion (#1) was dried completely (and stored) while the second portion (#2) was dried down to the aqueous phase on a LABCONCO centrivap concentrator (Labconco Corporation, Kansas City, MO, USA) and partitioned against ethyl acetate (2 mL) and further purified using an Oasis WAX cartridge (Waters, Mississauga, ON, Canada). This GA enriched fraction (#2) was eluted with 2 mL acetonitrile: water (80:20, v/v) and then dried on a centrivap as described above. An internal standard blank was prepared with 100 µL of the deuterated internal standards mixture. A quality control standard (QC) was prepared by adding 100 µL of a mixture containing all the analytes of interest, each at a concentration of 0.2 ng μL^{-1}, to 100 µL of the internal standard mix. Finally, fractions #1 and #2, blanks, and QCs were reconstituted in a solution of 40% methanol (v/v), containing 0.5% acetic acid and 0.1 ng μL^{-1} of each of the recovery standards.

5.4.5. Xylem sap analyses

A 225 µL combined total of xylem sap from replicates was snap frozen in liquid nitrogen and despatched on dry ice to Metabolomics Australia for GC-MS analysis.

5.4.6. HPLC-ESI-MS/MS

Analysis was performed on a UPLC/ESI-MS/MS utilizing a Waters ACQUITY UPLC system, equipped with a binary solvent delivery manager and a sample manager coupled to a Waters Micromass Quattro Premier XE quadrupole tandem mass spectrometer via a Z-spray interface. MassLynx™ and QuanLynx™ (Micromass, Manchester, UK) were used for data acquisition and data analysis.

The procedure for quantification of ABA and ABA catabolites, cytokinin, auxin, and gibberellins in plant tissue was performed as described (Lulsdorf et al. 2013). Samples were injected onto an ACQUITY UPLC® HSS C18 SB column (2.1x100 mm, 1.8 µm) with an in-line filter and separated by a gradient elution of water containing 0.02% formic acid against an increasing percentage of a mixture of acetonitrile and methanol (50:50, v/v).

Briefly, the analysis utilized the Multiple Reaction Monitoring (MRM) function of the MassLynx v4.1 (Waters Inc) control software. The resulting chromatographic traces were quantified offline by the QuanLynx v4.1 software (Waters Inc) wherein each trace was integrated and the resulting ratio of signals (non-deuterated/internal standard) compared with a previously constructed calibration curve to yield the amount of analyte present (ng per sample). Calibration curves were generated from the MRM signals obtained from standard solutions based on the ratio of the chromatographic peak area for each analyte to that of the corresponding internal standard, as described (Ross et al.

2004). The QC samples, internal standard blanks, and solvent blanks were also prepared and analysed along each batch of tissue samples.

5.4.7. RNA-sequencing

Leaf RNA Sequencing

RNA from the May 2014 sample set was pooled from 32 leaf samples into 4 sequencing samples, as was the July 2014 sample set, and the January 2015 sample set was all sequenced individually. Thus, the 70 leaf RNA samples sequenced for the transcriptomics work represented 126 separate leaf samples taken from 65 individual plants.

Total RNA underwent ribosomal RNA depletion prior to sequencing on the Illumina platforms using the standard Illumina protocol; HiSeq 2000/2500 (LC Sciences, USA), HiSeq 4000 (Macrogen, South Korea) and HiSeq 2500 (UWS, Australia). The leaf samples sent to LC Sciences and Macrogen were rRNA-depleted using the TruSeq Stranded Total RNA Ribo-zero Plant library kit, multiplexed four per lane, and gave between 49-116 million 2x100bp paired-end reads per sample, with an average Q30 of 90%.

The leaf, midrib and dewlap samples sent to UWS were sequenced using an Illumina HiSeq2500 platform with TruSeq strand-specific chemistry to create 125bp sequence read length paired end reads. Sequencing yielded 60-100 million reads per sample. Reads were trimmed using Trimmomatic v0.36 (Bolger et al., 2014). Quality was checked before and after trimming with FastQC v0.11.5 (Babraham Institute, bioinformatics.babraham.ac.uk/projects/fastqc/). Paired-end reads were imported into CLC Genomics Workbench version 11.01 (QIAGEN, Aarhus, Denmark) and mapped to the sugarcane PacBio sugarcane transcriptome library described in Hoang et al. (2017), with length fraction of 0.9 and similarity fraction of 0.9. These UWS samples were not used in the construction of the sugarcane YCS transcriptome, but instead were used extensively in the investigation of the molecular basis of the leaf yellowing.

Internode RNA Sequencing

Samples were collected from internodes 2, 4 and 6 of each plant replicate and sequenced individually, thus the 36 samples represented 12 individual plants. Approximately 10 µg RNA per sample was sent to Macrogen (Seoul, Republic of Korea) for total RNA 101bp paired-end sequencing on an Illumina HiSeq4000 platform (Illumina Inc. CA). All internode samples were rRNA-depleted using the TruSeq Stranded Total RNA Ribo-zero Plant library kit, multiplexed five per lane, and gave between 52-136 million paired-end reads per sample with an average Q30 of 95%.

Except for the UWS-sequenced samples, the raw RNAseq reads were trimmed for quality using the Trimmomatic (v 0.36) software tool (Bolger et al., 2014) and the quality was visualised before and after trimming using the FastQC (v0.11.4) software tool (S. Andrews, 2010. Available online from www.bioinformatics.babraham.ac.uk/projects/fastqc/). Trimmed reads were used in the downstream mapping and assembly processes.

5.4.8. Amino acid quantification

Derivatisation was done by using 10 µL aliquots of each standard or sample. These were added to 70 µL of borate buffer (200 mM, pH 8.8 at 25°C) containing 10 mM TCEP, 1 mM ascorbic acid and 50 µM 2-aminobutyric acid. The resulting solution was vortexed, then 20 µL of AQC reagent (200 mM

dissolved in 100% ACN) was added and immediately vortexed. The samples were heated with shaking at 55°C for 10 minutes then centrifuged and transferred to HPLC vials containing inserts.

5.4.9. Photosynthesis

Measurements on all available green leaves starting from one above the youngest fully expanded leaf were taken throughout the day to encompass a range of vapour pressure deficit (VPD), radiation, light, and other environmental stress conditions. Following standard settings recommended for C_4 plants, leaf gas exchange measurements were made twice a day on control and YCS-symptomatic plants using two LiCOR 6400 instruments (Long et al., 1996). The stomatal conductance, leaf level photosynthesis, internal CO_2 (Ci) and intrinsic transpiration efficiency were also measured during the day.

During gas exchange measurements, the sample CO_2 concentration and airflow rate was maintained at 400 $\mu molm^{-2}s^{-1}$ and 500 mol m^{-2} s^{-1}, respectively. The photosynthetically active radiation (PAR) was maintained at 1500 mmol m^{-2} s^{-1} with the internal red, blue, and green light sources. The intensity of blue light in the light source was 10%, while red was 80%. The standard CO_2 matching option was used after each set of measurements for greater accuracy.

5.4.10. Chlorophyll A fluorescence

Chlorophyll a O–J–I–P fluorescence transients (Strasser and Govindjee 1992) were recorded from leaves 1 to 6. Measurements were performed on the broadest midsection of the leaves, of a minimum of 10 plants for each group (with or without visual expression of YCS). Measurements were conducted with a PEA fluorescence meter (Hansatech Instruments Ltd., King's Lynn, Norfolk, PE 30 4NE, UK). The transients were induced by a red light (peak at 650 nm) of 3,200 µmol m^{-2} s^{-1} provided by the PEA instrument through an array of six light-emitting diodes (van Heerden 2014). The JIP-test (Strasser and R.J. 1995) was subsequently employed to analyse each recorded transient. The following data from the original measurements were used: maximal fluorescence intensity (FM); fluorescence intensity at 50 µs (considered as F0); fluorescence intensity at 300 µs (F300 µs) required for calculation of the initial slope (M0) of the relative variable fluorescence (V) kinetics; the fluorescence intensity at 2 ms (the J step) denoted as FJ. VJ was calculated as (FJ - F0)/(FM - F0). The JIP-test (Strasser and R.J. 1995) was used to translate the original recorded data to biophysical parameters that quantify the stepwise energy flow through Photosystem II. A multi-parametric expression performance index (P_{ABS}), was also calculated (Strasser et al. 2000). The P_{ABS} considers the three main steps that regulate photosynthetic activity by a Photosystem II reaction center (RC) complex, namely absorption of light energy (ABS), trapping of excitation energy (TR) and conversion of excitation energy to electron transport (ET). The formulae used to calculate each of these biophysical parameters from the original fluorescence measurements are as previously detailed (van Heerden et al. 2007b)

5.4.11. Callose quantification

A modified extraction protocol was used to quantify callose (1, 3-β-glucan) through micro-titre based fluorescence spectroscopy (Kohle et al., 1984; Shedletzky et al., 1997; Ko and Lin, 2004) with spectrophotometer (BMG-Labtech, FLUOstar Omega) and 96-well plate (Thermo Scientific, Black Microtiter). The choice of flurochrome was Aniline Blue, together with Curdlan (CE) standard and fluorescence parameters Excitation: 355nm, Emission: 460nm. (Aniline blue reaction mix 120µL (40 volume aniline blue 0.1% w/v , 59 volume 1M Glycine/NaOH (pH 9.5), 21 volume 1M HCl) was added

to 10µL sample extract, vortexed and incubated on a shaker @50˚C for 20 mins and then returned to room temperature for 30 mins prior to reading in spectrophotometer.

5.4.12. Statistical analyses

Statistical analysis of the metabolite data was performed using MetaboAnalyst 3.0 http://Metabolanalyst.ca, (Xia et al., 2015). Fold change was calculated as the means ratios of each treatment compared with the asymptomatic tissues and T-tests with unequal variances were performed to compare data obtained between experimental groups. The false-positive rate associated with multiple comparisons was calculated using the false discovery rate (FDR) or Bonferroni-corrected *P* values were also calculated. All tests with significance of $P < 0.05$ were considered in the analyses (Xia et al., 2015).

Statistical analysis of the transcriptome data was performed using CLC Genomics Workbench

Differential expression (DE) analysis was performed in the CLC Genomics Workbench v12.0 (QIAGEN, Aarhus, Denmark) software environment (CLC-GWB), using the 'Differential Expression for RNA-seq' pipeline. The DE was run as a two group, unpaired, YCS vs Control experiment, while controlling for tissue type, variety, and leaf/internode number. The results were subjected to statistical analysis, then filtered to give only those transcripts with an FDR-corrected p-value ≤0.01.

Statistical analysis of inhouse carbohydrates was through Statistix10

Statistical software package Statistix 10 was used to analyse carbohydrate data. An Analysis of Variance (ANOVA-completely randomised design) was used to compare starch, sucrose, glucose, and fructose means from mid-leaf extracts to identify if there are differences between sample groups. To identify which groups are significantly different a Tukey's HSD AllPairwise Comparisons Test was then applied to create confidence intervals for all pairwise differences (these are displayed as homogeneous groups A, B, AB, C etc). Different groups indicate that their means are significantly different from each another. A statistical check for normality was also performed using the Shapiro-Wilk test and where necessary the data was transformed (normalised) prior to performing the Tukey's HSD test.

5.4.13. Transcriptome Assembly

In this project, we initially made use of existing genomic and transcriptomic resources. In particular, the sugarcane transcriptome produced by Hoang *et al.* (2016) from multiple tissue types of healthy Queensland commercial Q-varieties was very helpful in elucidating the molecular basis of changes to leaf yellowing and sucrose metabolism in YCS-affected plants.

However, a dataset constructed from healthy samples cannot hold all the answers to YCS as it would not contain any transcripts that may have been expressed uniquely and specifically during YCS. For this reason, we undertook to assemble and annotate a 'YCS transcriptome' from our sequencing reads and use this to interrogate our samples for any YCS-specific metabolic signatures.

This YCS transcriptome would also be an ideal dataset to discover a unique YCS biomarker. This strategy was successful. Of the six YCS biomarker candidates described later in section 6.6.2, three of these candidates were not found in any other sugarcane transcriptomic dataset, including our preferred candidate YCS-2.

We assembled three YCS transcriptomes; leaf, internode and a combined leaf-and-internode one. The combined version became our Reference transcriptome for our analyses.

Transcriptome Assembly from leaf and internode sequences

The 106 leaf and internode RNA samples sequenced represented 152 separate samples taken from 77 individual plants.

The reads from the leaf and internode tissue were assembled separately into leaf and internode transcriptomes, and the two tissue-specific transcriptomes were combined to produce the final reference transcriptome used in the analysis (Figure 4). The raw reads are available from NCBI's Sequence Read Archive, and together with the leaf transcriptome, internode transcriptome and final combined leaf-and-internode transcriptome, are stored under BioProject PRJNA480179.

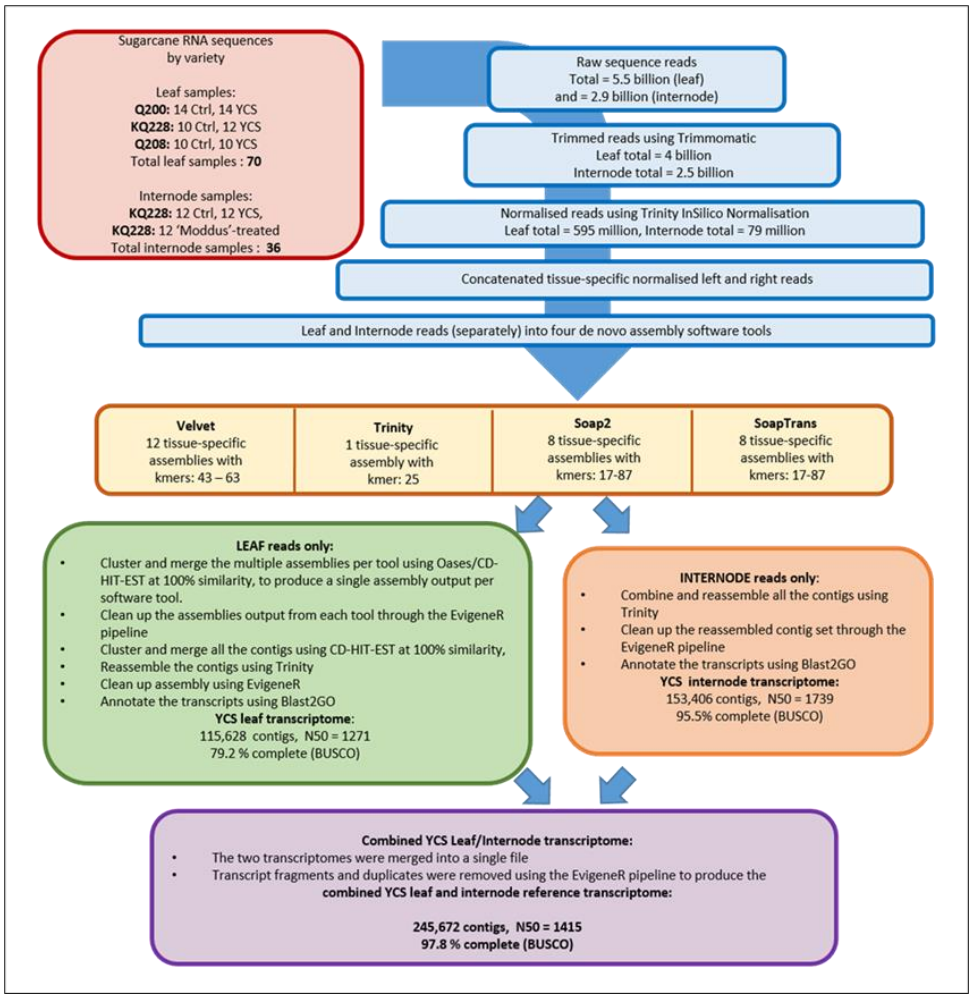

Figure 4 Bioinformatics process overview for the transcriptome assembly

Computational power

Computing resources used in this study include a Linux desktop with 256Gb of RAM running the Ubuntu 18.04 operating system, and the Stampede cluster in the Texas Advanced Computing Center (TACC), hosted by the University of Texas at Austin (https://www.tacc.utexas.edu/home). We also used the Tinaroo and FlashLite clusters, hosted by the Research Computing Centre (RCC) at the University of Queensland (https://rcc.uq.edu.au/hpc).

Leaf transcriptome

Raw RNAseq reads were trimmed for quality using the Trimmomatic (v 0.36) software tool[1] [2] (Bolger et al, 2014) and the quality was visualised before and after trimming using the FastQC (v0.11.4) software tool (S. Andrews, 2010. Available online from www.bioinformatics.babraham.ac.uk/projects/fastqc/). The Trinity (v 2.4.0) Insilico Normalisation tool was run as a stand-alone script on the trimmed reads to reduce duplication and coverage to make the assembly process easier (Haas et al, 2013). The normalised reads from all samples were concatenated into two fasta files of left and right reads, for assembly using the Velvet v1.2.10 (Zerbino and Birney, 2008), Trinity v2.4.0 (Grabherr *et al.* 2011), Soap2 v2.04 (Li *et al.* 2009) and SoapTrans v1.03 (Xie *et al.* 2014) assembly software tools. All the scripts used to create and process the assemblies are available online at https://github.com/k8hertweck/ycs and https://github.com/katewd/SugarcaneYCS .

The Velvet assembly tool was run with kmers 43, 45, 47, 49, 51, 53, 55, 57, 59, 61 and 63, and these were then combined into a single fasta file output using the Oases v0.2.8 tool (Schulz et al. 2012). The Trinity assembly tool was run using a single kmer of 25. The Soap2 and SoapTrans tools were both run with kmers of 17, 27, 37, 47, 57, 67, 77 and 87. For both Soap2 and SoapTrans, the multiple assemblies were concatenated into a single fasta file per tool, for further processing using the EvidentialGene RNA assemblies (EvigeneR) pipeline (D. Gilbert, 2013. Available online from http://arthropods.eugenes.org/genes2/about/EvidentialGene_trassembly_pipe.html). The output from each assembly tool was sent separately through the EvigeneR pipeline to remove any of the contigs that were unlikely to be coding for biologically functional proteins.

After the EvigeneR step, the 'okay.fa' contigs from the 'okayset' from each of the four assemblies were merged into a single contig set using CD-HIT-EST v4.6.6 (Li and Godzik, 2006) at 100% similarity to remove duplicate contigs. The contigs were then re-assembled using the Trinity assembly tool to reduce the segmentation score as determined by the TransRate v1.0.3 tool (Smith-Unna *et al.* 2015). The reassembled transcripts were again cleaned up through the EvigeneR pipeline to remove any nonsense or misassembled contigs.

Annotations for the transcripts were obtained using the CloudBlast service of Blast2GO, which was run with the Blast2GOPro plugin (BioBam, Spain) in the CLC-GWB software environment. Blastx-fast was run using the non-redundant protein sequences updated on the 30/01/2017, with the e-value cut off of 1.0E-3, the number of blast hits=20, word size=6, and a low-complexity filter on. Following the blast step, the Mapping, Annotation, InterProScan and Merge InterProScan steps were done subsequently in that order.

The table of blast hits was exported from the CLC-GWB environment, and the transcripts and their annotations converted into a single-column csv file for further use in a python script to add the annotations to the transcript fasta headers. The python script used was 'add_header_annotations.py' and is available from the project GitHub site (https://github.com/katewd/SugarcaneYCS).

As Figure 4 shows, the final leaf transcriptome contained 115,628 contigs with an assembly N50 of 1271.

Internode transcriptome

Similar to the leaf transcriptome, the internode reads were trimmed for quality using Trimmomatic (Bolger et al, 2014), the quality was visualised using FastQC (S. Andrews, 2010), and the reads normalised using the Trinity Insilico Normalisation script. The normalised reads from all internode samples were concatenated into two fasta files of left and right reads, for assembly using the Velvet (Zerbino and Birney, 2008), Trinity (Grabherr *et al.* 2011), Soap2 (Li *et al.* 2009) and SoapTrans (Xie *et al.* 2014) assembly software tools, using the same parameters as the leaf transcriptome assembly. However, the post-assembly processing of the internode transcriptome was different from the leaf transcriptome. Due to the smaller and more manageable dataset, the internode multiple assembly outputs were concatenated into a single fasta file and reassembled using Trinity, without the prior cluster, merge and cleanup filtering steps performed for the leaf set. The reassembled internode contigs were processed through the EviGeneR pipeline. Annotations were done in the same way as the leaf transcriptome, with the transcript Blast2GO hit annotations added to the fasta sequence headers using the python script.

The result was the final internode transcriptome with 153,406 transcripts and an assembly N50 of 1739 (Figure 4).

Combined Leaf-and-Internode Reference Transcriptome

The leaf and internode transcriptomes were concatenated into a single file, with the transcript headers retaining their tissue-specific identification and blast annotation, and were processed through the EvigeneR pipeline to remove transcript fragments and coding duplicates.

Transcriptome completeness was assessed using the embryophyta plant dataset (version odb9) of the Benchmarking Universal Single-Copy Orthologs (BUSCO) tool (Simão et al., 2015).

The combined leaf-and-internode reference transcriptome contained 245,672 transcripts, with an N50 of 1415, and contained 97.8% of expected single-copy orthologs (Figure 4).

Table 3 shows the key metrics for the de novo transcriptomes created and used in this study.

Table 3 Assembly metrics for the reference transcriptome

Assembly name	YCS Leaf transcriptome	YCS Internode transcriptome	combined YCS leaf-and-internode transcriptome
Number of transcripts	115,628	153,406	245,672
Largest transcript assembled	16,038	26,281	26,281
N50	1271	1739	1415
BUSCO completeness score	79.2%	95.5%	97.8%
MapMan bin occupancy	82.3%	91.7%	93.8%

Differential Expression

The de novo combined leaf-and-internode YCS Reference Transcriptome assembly was imported into CLC Genomics Workbench v12.0 (QIAGEN, Aarhus, Denmark) software environment. The paired,

trimmed reads for each of the samples were mapped to the reference assembly using the following mapping parameters:

mismatch cost=2, insertion cost=3, deletion cost=3, length fraction=0.9, similarity=0.8, maximum number of hits for a read=10, with the distance between paired reads automatically detected, expression values as total counts, RPKM calculated, EM estimation used, and unmapped reads discarded.

Differential expression (DE) analysis was performed in the CLC Genomics Workbench (CLC-GWB), using the 'Differential Expression for RNA-seq' pipeline. The DE was run as a two group, unpaired, YCS vs Control experiment, while controlling for tissue type, variety and leaf/internode number. Of the 106 samples used to build the reference, a subset of the samples (12) was from a set of plants that had undergone a chemical treatment. These were also not included in this analysis. The remaining 94 samples had their sucrose content measured in-house (unpublished data), and the sample sucrose content (nmol/g dry weight) was dimension-reduced to a binary of either 'above' or 'below' the median sucrose content. As high leaf sucrose content is a marker for YCS (Marquardt et al., 2016), only YCS samples with above-median sucrose values, and Control samples with below-median sucrose values, were included in the analysis. The YCS versus Control analysis was conducted using 62 samples in total, of which 24 were from internode tissue and 38 were from leaf tissue, 29 were Controls and 33 were YCS.

5.5. Field trials

5.5.1. Growth regulator

An experiment was conducted on the grounds of Sugar Research Burdekin Station, Farm #6007 Block #3-1 in Burdekin, QLD (19°34'08.0"S 147°19'30.7"E). Following soil nutrient testing, the soil was fertilised according to Six Easy Steps nutrient recommendations (N kg/ha, P kg/ha, K kg/ha and S kg/ha) and sugarcane variety KQ228$^{\phi}$ was stick planted on 23-Aug-2016. The experimental area was within a furrow irrigated sugarcane block with a seven-day flood irrigation schedule. The trial was a completely randomised design including eight treatments with four replicate plots x 10m (1.5m spacing) per treatment. Treatments were; Aviglycine (Retain) (Ethylene inhibitor), Paclobutrazol (GA inhibitor-Moddus®), 6-Benzylaminopurine (Cytokinin), Gibberellic Acid, Ethyphon (Promote 900)(Ethylene), Trinexapac-Ethyl (Moddus)(GA inhibitor), Shade (50% shade cloth) and Untreated control. Rates of application varied monthly (Table 4).

Table 4 Insecticide treatments

Date	Treatment/Rate
9/11/2016	▪ Paclobutrazol (50uM, 0.235036g/12L/plot= 4L/row watering can) ▪ Gibberelic Acid (300uM, 0.727g/7L/plot) ▪ 6-Benzylaminopurine (cytokinin) (250uM, 0.3941g/7L/plot) ▪ Aviglycine (Retain) (1/2 label rate, 415g/ha, 2.49g/7L/plot) ▪ Ethylene (Promote 900) (1/3 label rate, 333mL/ha, 2mL/7L/plot) ▪ Trinexapac-Ethyl (Moddus) (1/2 label rate, 400mL/ha, 2.4mL/7L/plot) ▪ Shade ▪ Untreated control
8/12/2016	▪ Paclobutrazol (75uM, 0.0.52884g/24L/plot= 6L/row watering can) ▪ Gibberelic Acid (150uM, 0.0.31173g/6L/plot) ▪ 6-Benzylaminopurine (cytokinin) (250uM, 0.337g/6L/plot) ▪ Aviglycine (Retain) (2/3 label, 622.5g/ha, 3.735g/6L/plot) ▪ Ethylene (Promote 900) (1/2 label rate, 450mL/ha, 2.736mL/6L/plot)

Date	Treatment/Rate
	▪ Trinexapac-Ethyl (Moddus) (1/4 label rate, 200mL/ha, 1.216mL/6L/plot) ▪ Shade ▪ Untreated control
10/01/2017	▪ Paclobutrazol (150uM, 1.05768g/24L/plot= 6L/row watering can) ▪ Gibberelic Acid (150uM, 0.31173g/9L/plot) ▪ 6-Benzylaminopurine (cytokinin) (1000uM, 2.027g/9L/plot) ▪ Aviglycine (Retain) (label, 830g/ha, 4.98g/9L/plot) ▪ Ethylene (Promote 900) (label, 900mL/ha, 5.4mL/9L/plot) ▪ Trinexapac-Ethyl (Moddus) (1/4 label rate, 200mL/ha, 1.216mL/9L/plot) ▪ Shade ▪ Untreated control
08/02/2017	▪ Paclobutrazol (150uM, 1.05768g/24L/plot= 6L/row watering can) ▪ Gibberelic Acid (150uM, 0.31173g/6L/plot) ▪ 6-Benzylaminopurine (cytokinin) (1500uM, 2.027g/6L/plot) ▪ Aviglycine (Retain) (2/3 label, 622.5g/ha, 3.735g/6L/plot) ▪ Ethylene (Promote 900) (label, 900mL/ha, 5.4mL/6L/plot) ▪ Trinexapac-Ethyl (Moddus) (1/4 label rate, 200mL/ha, 1.216mL/6L/plot) ▪ Shade ▪ Untreated control
6/03/2017	▪ Paclobutrazol (300uM, 2.1154g/24L/plot= 6L/row watering can) ▪ Gibberelic Acid (300uM, 0.6234g/6L/plot) ▪ 6-Benzylaminopurine (cytokinin) (1500uM, 2.027g/6L/plot) ▪ Aviglycine (Retain) (label, 830g/ha, 4.98g/6L/plot) ▪ Ethylene (Promote 900) (label, 900mL/ha, 5.4mL/6L/plot) ▪ Trinexapac-Ethyl (Moddus) (label rate, 800mL/ha, 4.8mL/6L/plot) ▪ Shade ▪ Untreated control

5.5.2. Insecticide Trial

The insecticide trial was established September 2017 in the same field as the growth regulator trial on the grounds of Sugar Research Burdekin Station, Farm #6007 Block #3-1 in Burdekin, QLD (19°34'08.0"S 47°19'30.7"E), KQ228(ᵬ 1st ratoon. Following soil nutrient testing, the soil was fertilised according to Six Easy Steps nutrient recommendations (N kg/ha, P kg/ha, K kg/ha and S kg/ha). All other conditions were maintained except for new treatments. Treatments were November bifenthrin - foliar applied weekly; December bifenthrin - foliar applied weekly; January bifenthrin - foliar applied weekly; February bifenthrin - foliar applied weekly; March bifenthrin - foliar applied weekly; Continuous bifenthrin - foliar applied weekly November to March; $MgSO_4$ foliar applied weekly; Untreated control. Bifenthrin was applied at 320 ml/ha and $MgSO_4$ at 104 kg/ha (based on 9.6 % Mg to deliver 10 kg/ha Mg).

6. RESULTS AND DISCUSSION

The results displayed in this study continue the pilot study conducted in project 2014/090. Presented here are the results of our research into the cause of high sucrose accumulation in YCS leaves, and the metabolic disruption to the source and sink tissue prior to and after the onset of visible yellowing. Detailed analyses of the perturbances to photosynthesis, carbon fixation, turnover and partitioning, phloem transport, and sink strength are discussed. Identification of symptom expression, diagnostics, and management options to mitigate YCS are also addressed.

6.1. YCS symptom expression

YCS symptom expression is more likely to occur during the summer months from December to March. This is notably the time of highest photosynthetic carbon fixation (photoassimilation) and the highest growth rate period for the crop. Any disruption to carbon export when sucrose synthesis is highest increases the chance that sucrose accumulation in the source leaf will exceed upper tolerance levels. Therefore, YCS symptom expression is more likely to occur during this time of year than in the cooler shorter daylength months. However, YCS may occur at any time of the year if sucrose synthesis exceeds the rate of export from the source leaf or demand from the sink tissue (internodes).

The first leaf to show symptoms will the one with the highest rate of photoassimilate export and this is typically Leaf 4 (Leaf #1 = FVD). Yellowing typically starts close to and on one side of the midrib, approximately midway along the leaf blade (Figure 5A).This section of the leaf is where the leaf usually bends under its own weight, receives most of the light and has the highest photosynthetic activity (Mattiello et al., 2015; Marquardt et al., 2016). However, yellowing can occur at any position along the leaf depending on its orientation to the sun in the canopy. Expression of yellowing and chlorosis is dependent on high light intensity in maize tie-dyed mutants (Braun and Slewinski, 2009). Hence, it is common to see higher levels of YCS expression in the outer rows or on the ends of a field and away from building and vegetation shading (Figure 5B). The midribs of afflicted leaves remain white on the upper surface (Figure 5C) and green on the abaxial side of the leaf.

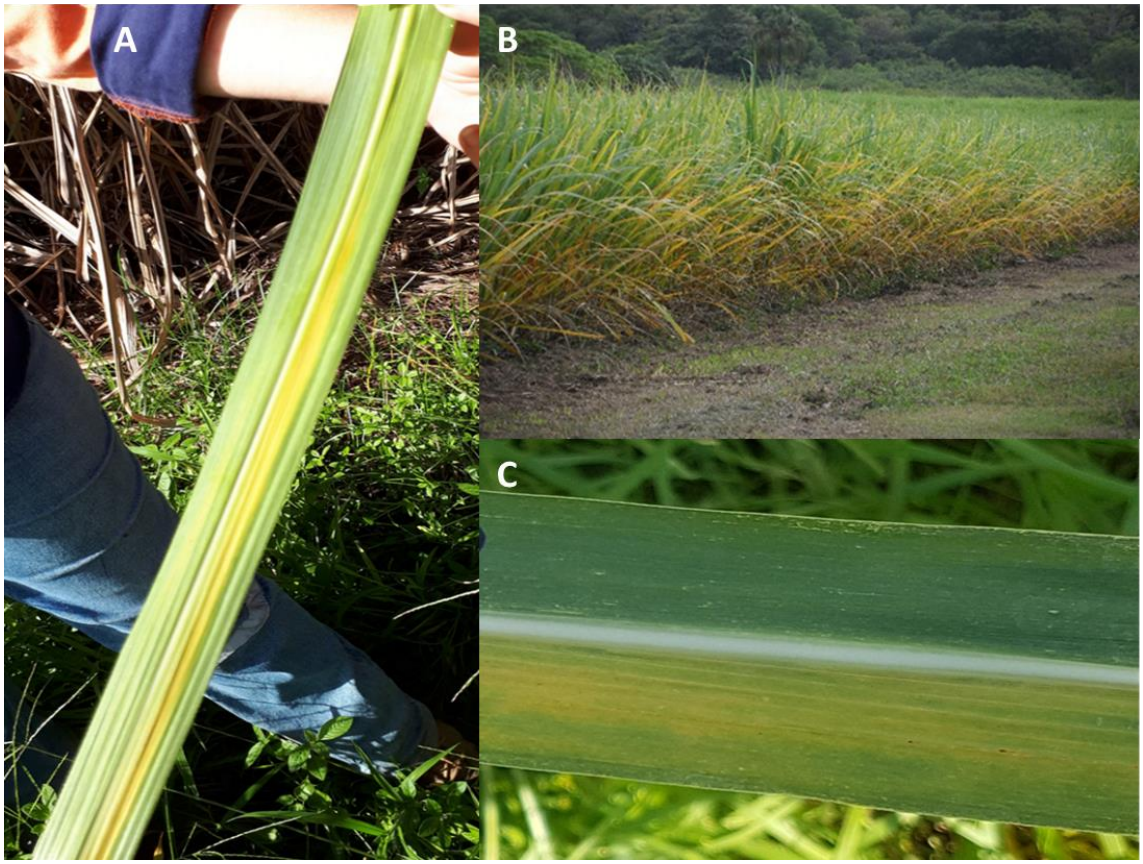

Figure 5 YCS symptom expression usually starts where light interception is highest in the middle of the leaf and on one side of the midrib A) YCS symptoms worse on field margin where exposure to sunlight is highest B) white midrib C)

Leaf yellowing occurs when leaf sucrose accumulation exceeds a tolerable upper threshold, after which a cascade of events leads to metabolic disruption and the early onset of leaf senescence. Yellowing is more golden in colour, can be solid or blotchy, spreading toward the tip, base, and outer margin of the lamina, culminating in irreversible leaf senescence. Subsequent expression will continue in the younger leaves above as they mature and become the predominant exporter of sucrose. Yellowing will cease to develop in new leaves when sucrose accumulation fails to exceed the tolerable threshold.

YCS is usually more prevalent after a period of slow growth followed by a period of increased photoassimilation and rapid growth. Symptoms can develop in all commercially grown genotypes and across all stages of the crop cycle. The typical YCS season is during the peak photosynthetic period of December to March.

6.2. Leaf yellowing – disruption to source

Leaf chlorosis or yellowing is due to reduced chlorophyll content. To understand the development of yellowing it is important to determine the pattern of chlorosis and the dependence of this on the presence of light. To do this we investigated changes in the transcriptome and metabolome to better understand chlorophyll turnover which drives YCS development. Chlorophyll turnover is determined by the magnitude of:

1) Chlorophyll synthesis (biotic stress)

2) Chlorophyll breakdown (abiotic stress)

3) Photooxidation (uncoupling of electron transport from coenzyme reduction and carbon fixation causing changes to carbon partitioning)

Source leaf health in C_4 plants can be determined by the sucrose level in the photosynthetic mesophyll and bundle sheath cells and the effect on photosynthesis. Previous studies have shown that high carbohydrate accumulation in the leaf induces yellowing of the lamina (Tollenaar and Daynard, 1982; Krapp and Stitt, 1995; Jensen, 1996; Russin et al., 1996; Rajcan and Tollenaar, 1999; Graham and Martin, 2000; Braun et al., 2006). It is important to understand whether yellowing occurs around the primary or secondary veins as this will reveal if YCS expression is associated with disruption to phloem transport or phloem loading. Another consequence of chlorophyll loss from the leaf in many species of the Poaceae family is the accumulation of pigments such as zeaxanthin and anthocyanins, giving the leaf a golden-yellow colour (Allison and Weinmann, 1970; Tollenaar and Daynard, 1982; Rajcan and Tollenaar, 1999). As golden-yellow colour is a discernible characteristic of YCS, it is therefore important to understand the mechanisms causing chlorophyll loss and the expression of other pigments.

6.2.1. Leaf sucrose

In a healthy leaf, sucrose and starch levels rise throughout the day as the photosynthetic rate increases. As the sink calls for carbon, sucrose is loaded into the phloem and excess is sent to starch storage to ensure sucrose concentrations never rise above a tolerable upper threshold. By mid-afternoon, the photosynthetic rate peaks and sucrose levels start to decline while starch synthesis continues in preparation for the dark period. Approximately 80% of the total fixed carbon is typically exported during the day period. During the night, the remaining 20% is exported to meet the energy needs of the plant and both sucrose and starch pools are depleted. Maintenance of this circadian rhythm is the role of regulatory enzymes and metabolic precursors of sucrose and starch synthesis and breakdown. Therefore, the diurnal change is dependent on the rate of carbon exchange, sucrose content and feedback mechanisms (Stitt and Quick, 1989; Weise et al., 2011). In contrast, the level of disruption to the diurnal rhythm in YCS plants is evident with high levels of both sucrose and starch recorded in leaf tissue at first light (Marquardt et al., 2016). As starch synthesis is ultimately controlled by sucrose synthesis (Stitt and Quick, 1989), it is the accumulation of sucrose that will be the initial focus of this study in understanding YCS development and expression.

To gain insight into the distribution of sucrose along the leaf and to determine any correlation with leaf yellowing, we quantified this key metabolite in different leaf sections of control and YCS symptomatic (Leaf 4) and asymptomatic (Leaf 3) leaves. Figure 6 shows the sucrose content in sectioned quarters between the leaf tip and sheath base. YCS asymptomatic (Leaf 3) and symptomatic (Leaf 4) from the same culm have significantly higher sucrose levels compared to their control counterparts. The pattern of sucrose accumulation along the lamina is similar between controls and YCS, albeit much higher in YCS, and only deviates at the base of the YCS leaf. Interestingly the rapid rise in sucrose content at the base of the YCS leaf does not correlate with where the onset of yellowing is first visualised. The highest photosynthetic rates in sugarcane occurs in the middle section of the leaf (Mattiello et al., 2015).This is not unexpected as most varieties have leaves that naturally bend over at the mid-section and therefore this segment receives the highest amount of solar radiation. Interestingly, this is also where yellowing usually commences in

YCS leaves and indicates that leaf position and amount of solar intercept play an important role together with sucrose accumulation in the development of YCS expression.

To ascertain the tolerable upper threshold of sucrose accumulation that a leaf can endure before yellowing is induced required analysis of thousands of samples across genotypes grown in each of the four agro-climatic regions in Queensland. Figure 6 is indicative of the levels of sucrose assayed across these samples. Surprisingly, the tolerance level is relatively conserved (approximately 200 µmol/g Dry Mass (DM)) across the commercial varieties This tolerable threshold offers a guide to determine the physiological fitness of the leaf and predict its level of susceptibility to developing YCS. YCS symptomatic leaf 4 shows a direct correlation between the mid-section of the leaf that receives the most light and sucrose content in excess of 200 µmol/g DM, while YCS asymptomatic leaf 3 and controls do not (Figure 6). Therefore, the onset of yellowing in leaf lamina of plants with YCS is dependent on two factors i) high photosynthetic rate (high solar radiation intensity and leaf inception) and ii) sucrose accumulation above a tolerable upper threshold of approximately 200 µmol/g DM. The mechanisms and key roles that sucrose and light play in disrupting the photosystems and plant's metabolism will be discussed in detail later in this report.

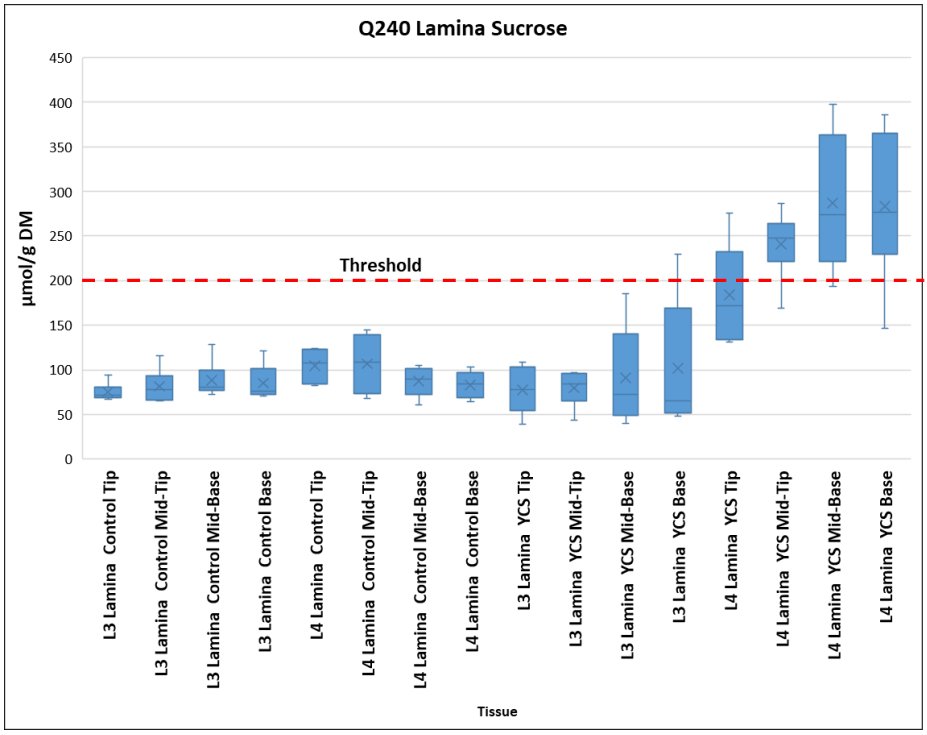

Figure 6 Q240$^{\Phi}$ Lamina quarters sucrose content in Leaf 3 and 4 from Control and YCS stalks; YCS Leaf 3 is asymptomatic and YCS Leaf 4 is symptomatic. Samples taken in the morning soon after first light

6.2.1.1. Consequences of elevated sucrose in the source leaf

Sucrose levels are consistently high in YCS symptomatic leaves. Our research also shows elevated levels of sucrose in asymptomatic mid-canopy leaves of the same culm. This is true for commercial genotypes grown across four agro-climatic zones from the northern wet tropics to the subtropical temperate south east of Queensland. Elevated levels of sucrose in the leaf triggers a suite of changes to water content, stomatal conductance, photosynthesis, gene expression, carbohydrate metabolism and carbon partitioning in the source tissue. If levels rise above a tolerable upper

threshold of approximately 200 µmol/g DM under high light intensity irreversible leaf yellowing is induced.

6.2.2. Water content

YCS symptomatic leaves from four genotypes sampled across four field visits and three agro-climatic regions have significantly less water content ($p<0.05$) than controls (Figure 7A-D). It is worth noting that the YCS asymptomatic leaf (younger of the two leaves Fig. 7B-E) shows no significant difference in water content to the control leaf (Figure 7B-D). The same trend also follows for the leaf sheath (Figure 7E). These finding suggest that translocation of water is compromised in YCS plants.

High leaf sucrose content induces a reduction in stomatal aperture and heat stress in sugarcane culminating in reduced water content in leaves, despite adequate water availability in soils (Wahid and Close, 2007; Kelly et al., 2013).

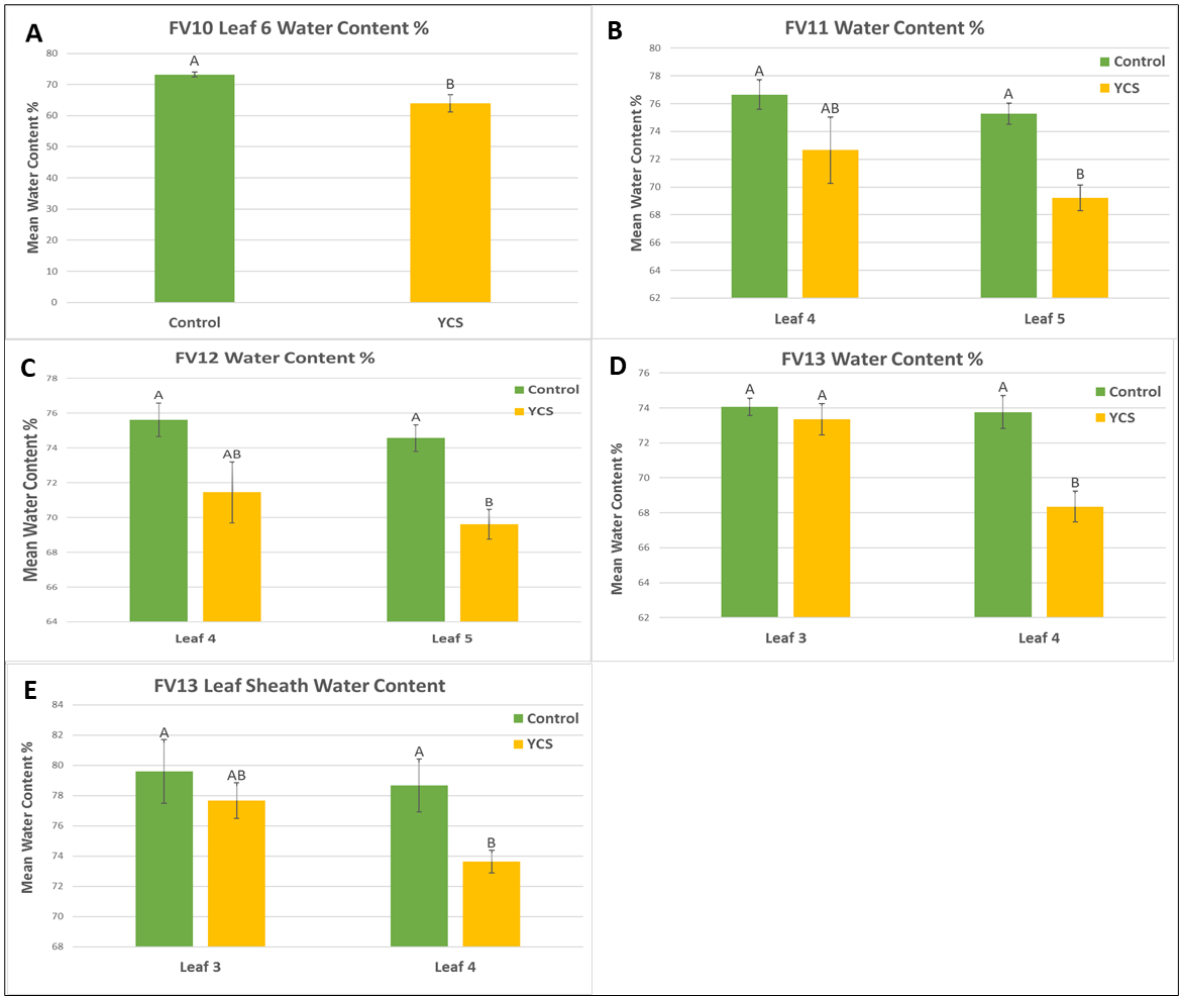

Figure 7 Leaf water content across four field visits (FV), 3 genotypes and three climatic regions. FV10 Q240$^{\Phi}$ Burdekin – lamina A), FV11 KQ228$^{\Phi}$ Burdekin - lamina B), FV12 QC40411 Mackay – lamina C), FV13 Q240$^{\Phi}$ Maryborough – lamina D and Leaf sheath E) Tukey HSD All-Pairwise Comparisons ($p<0.05$)

6.2.3. Stomatal conductance and photosynthesis

To gain an understanding of the extent of photosynthetic disruption in YCS leaves we needed to measure the levels of stomatal conductance, gas exchange, internal CO_2, carbon fixation, light harvesting, electron transport coupling and chlorophyll (chl) a fluorescence (photosynthetic energy conversion) in healthy and YCS tissue.

In crops affected by YCS, photosynthesis and stomatal conductance is suppressed in the mid-canopy leaves of both YCS asymptomatic and symptomatic leaves with older source leaves being most effected. Studies by Marquardt (2016) found the carbon fixation and stomatal conductance penalty rate due to YCS to be approximately 36% and 42% respectively in the source leaves of the mid-canopy (Figure 8, Figure 9). The extent of stomatal closure can be directly attributed to high leaf sucrose content. Our investigation of apoplastic fluid composition confirmed sucrose levels to be 3-fold higher than controls (Figure 51). High apoplastic sucrose ultimately leads to some diffusion into the transpiration stream. Here, abscisic acid (ABA) mediated sucrose induces increased hexokinase expression in guard cells, accelerating stomatal closure (Kelly et al., 2013).

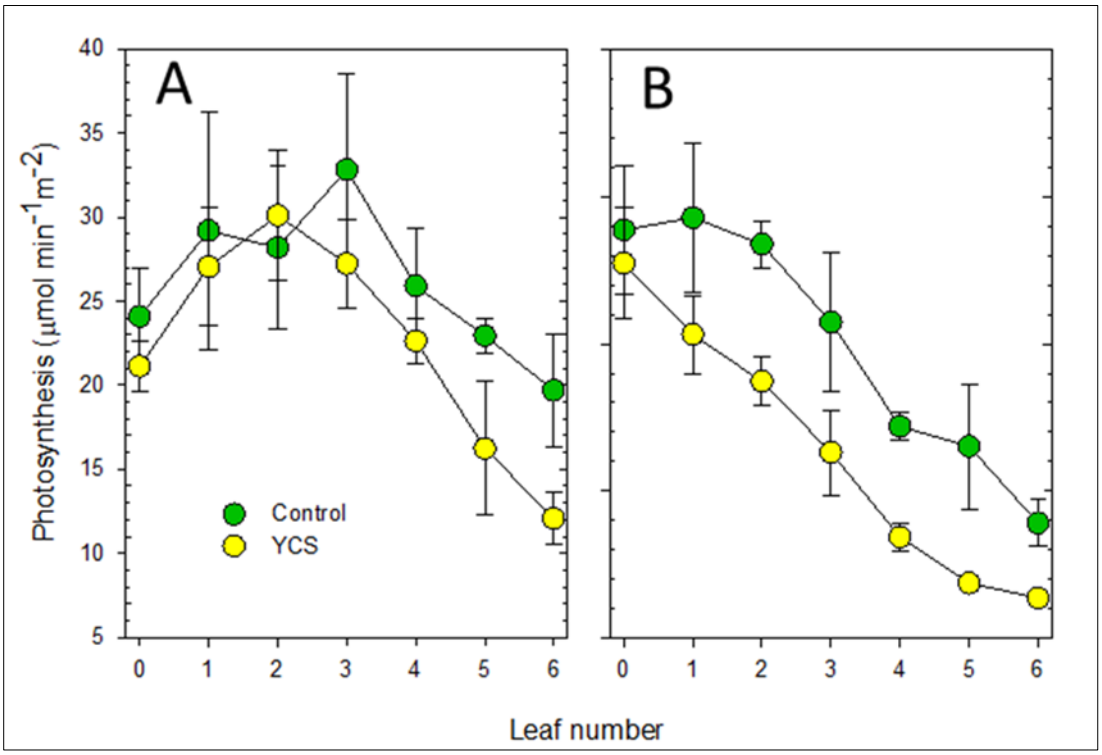

Figure 8 Photosynthesis rates in leaves of the canopy of KQ228$^{\Phi}$ in the Burdekin (A) and Q200$^{\Phi}$ in the Herbert (B) yellow canopy syndrome (YCS) symptomatic and asymptomatic (control) sugarcane plants. Values ± standard deviation (Marquardt, 2019)

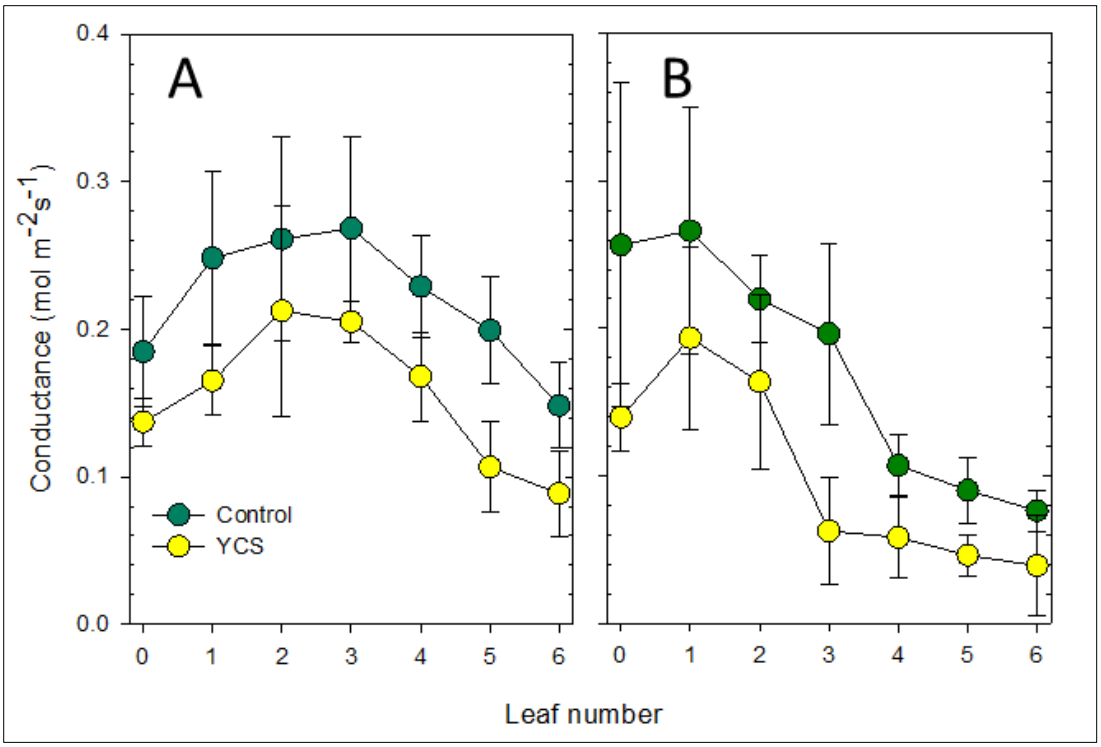

Figure 9 Stomatal conductance in leaves of the canopy of KQ228$^{\Phi}$ in the Burdekin (A) and Q200$^{\Phi}$ in the Herbert (B) yellow canopy syndrome (YCS) symptomatic and asymptomatic (control) sugarcane plants., YCS. Values ± standard deviation (Marquardt, 2019)

Such a profound reduction in stomatal conductance causes significant decline in gas exchange. Figure 10 shows the internal CO_2 concentration in YCS symptomatic leaves to be approximately 20% lower than controls. Studies show that healthy tissue should have relatively constant internal CO_2 and a lineal relationship between photosynthesis and stomatal conductance. Sustained reduction in gas exchange will also lead to a decrease in biomass production (Long et al., 1996; Chaves et al., 2008; Ghannoum, 2009). YCS mid-canopy leaves clearly show complete disorder across these parameters. Furthermore, stomatal closure will lead to a reduced transpiration rate and ultimately increased internal leaf temperature. Chl a fluorescence studies show a distinct K-step in the O-K-J-I-P transient which is indicative of elevated leaf temperature (Figure 13). In fact, when oxygenic plants are under heat stress and the water splitting system (oxygen evolving complex) is inhibited, the K-

step is always present (Srivastava et al., 1997; Jiang et al., 2006)

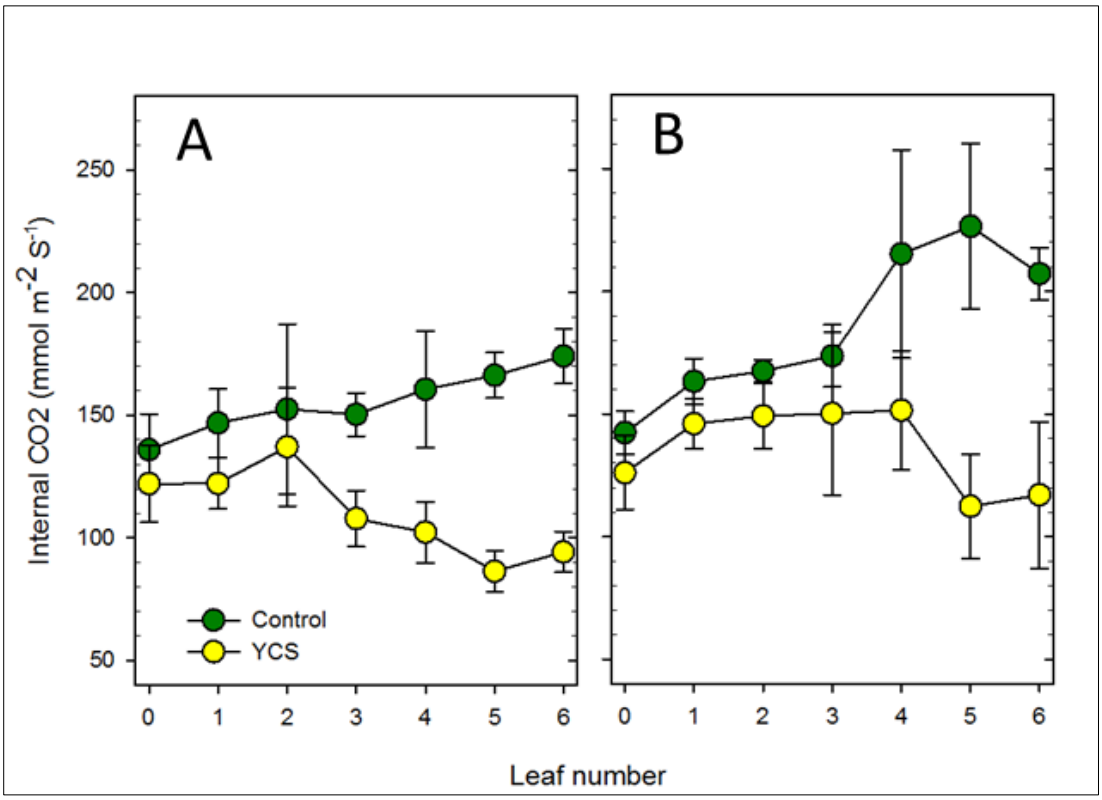

Figure 10 Internal CO_2 concentration in leaves of the canopy of KQ228$^{\Phi}$ in the Burdekin (A) and Q200$^{\Phi}$ in the Herbert (B) yellow canopy syndrome (YCS) symptomatic and asymptomatic (control) sugarcane plants., YCS. Values ± standard deviation (Marquardt, 2019).

The study of chl a fluorescence kinetics provides insight into the capacity of photosystems I and II and physiological fitness of the photosynthetic tissue (Strasser et al., 2000). Figure 11 shows changes in chl a O-J-I-P fluorescence transients at specific locations along the lamina of a YCS symptomatic leaf. Interestingly the green side of the leaf is already showing signs of electron uncoupling, trailing slightly behind in fluorescence intensity. There is also a notable disruption to the electron transport system progressing from the green to less green or yellow tissue within each side of the leaf.

Figure 12 shows a comparison in photosystem efficiencies between control leaf 5 & 6 and YCS (asymptomatic) leaf 5 and symptomatic leaf 6. Analysis of the biphasic response in delta fluorescent curves, indicates a first major peak around 500 µs to 1000 µs (Figure 12A). This is reflective of a disruption of photosystem II. However, the second peak around 10,000 µs is indicative of a disruption of electron flow between photosystem II and photosystem I. Detailed analyses of the different components of the OJIP curve at the base, middle and tip of the leaf (Figure 12B) indicates an overall suppression or decrease in the efficiency of electron flow through the electron transport systems. Uncoupling of the ETC becomes progressively worse from the leaf base (youngest tissue) to the tip (oldest tissue). PI abs is an indicator of how well photosystems II and I are functioning and also gives a quantitative measure of the plants physiological fitness under stress conditions (Strasser et al., 2000).

Figure 12C shows the electron transport system is seriously disrupted in YCS (symptomatic) leaf 6 and already compromised in YCS (asymptomatic) leaf 5 well before the onset of visible yellowing. Evaluation of the efficiency of electron movement of trapped excitation into the transport chain is

one of the main parameters of PI abs. (Kruger et al., 1997; Tsimilli-Michael and Strasser, 2013). YCS leaves clearly show an uncoupling of the electron transport chain and a huge decline in photosynthetic efficiency.

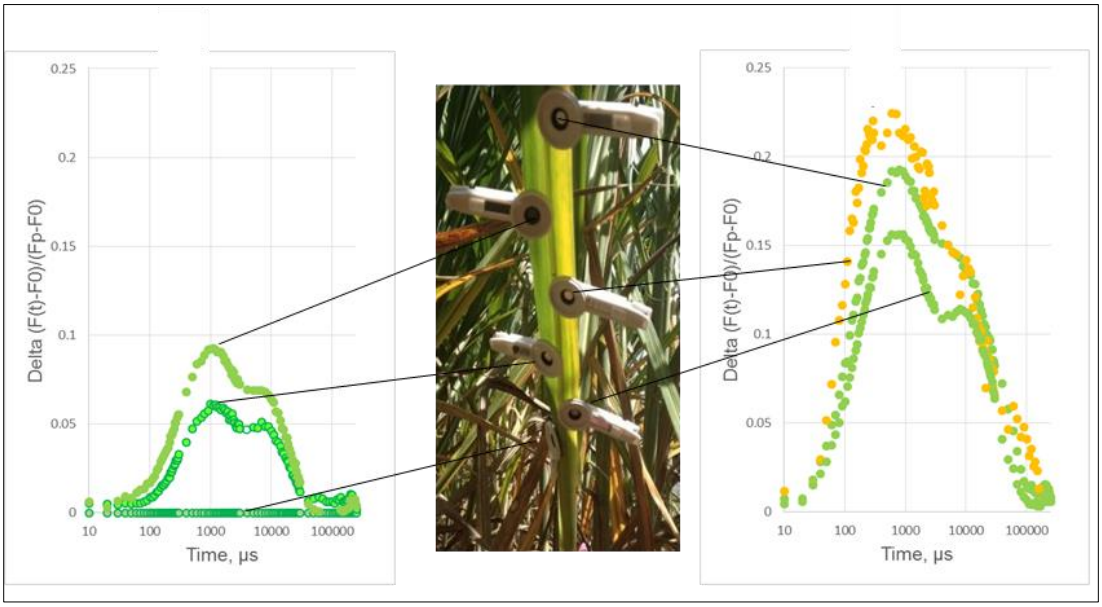

Figure 11 Difference in variable fluorescence kinetics on different positions of the same leaf. OJIP fluorescence transients were normalised (O.P) and subtracted for the first clip on the greenside of the leaf.

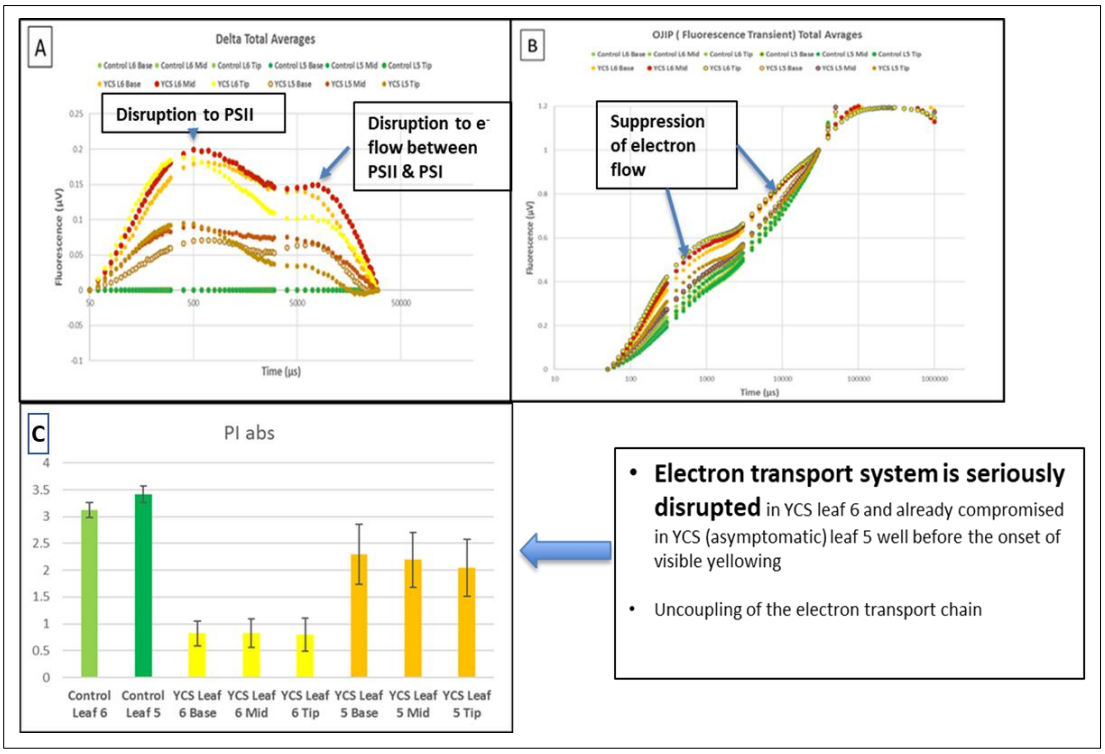

Figure 12 Difference in variable fluorescence along the lamina constructed by subtraction of normalised (O–P) fluorescence values for the asymptomatic leaves from that recorded for the same age symptomatic leaves. The O–J–I–P fluorescence transients A) recorded in leaves 5 and 6 of asymptomatic (control) and symptomatic (YCS) Q240$^{\Phi}$ plants B) performance index (PIABS) control, YCS leaf 5 (asymptomatic) and YCS leaf 6 (symptomatic) C)

Figure 13 shows a significant increase in O–J–I–P fluorescence transient intensity starting at approximately 2 ms represented by the J-step. The calculated increase in ΔJ is associated with an accumulation of the reduced primary quinone acceptor of PSII (Q_A) and plastoquinone (PQ) pools. This disruption on the electron acceptor side of PSII is most likely due to a blockage of electron flow further downstream (I-step) on the acceptor side of PSI (Schreiber and Neubauer, 1987; Strasser et al., 2000; Schansker et al., 2005; van Heerden et al., 2007). Therefore, this disruption to the electron transport system in YCS leaves would lead to a reduction in CO_2 fixation.

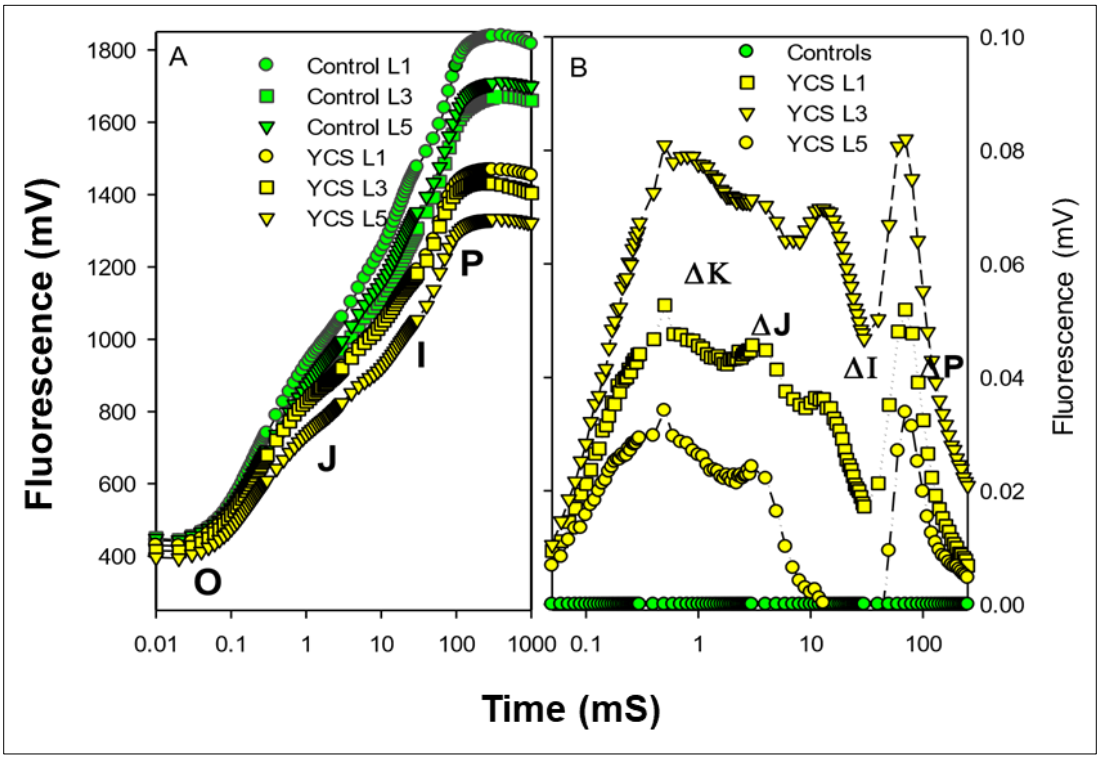

Figure 13 Chlorophyll a fluorescence transients (A) recorded in leaves 1, 3 and 5 of asymptomatic (control) and symptomatic (YCS) KQ228ϕ plants. The different stages in the fluorescence transient (OJIP) are indicated. Difference in variable fluorescence curves (B) constructed by subtraction of normalised (O-P) fluorescence values for the asymptomatic leaves from that recorded for the same age symptomatic leaves.

F_v'/F_m' is a good measure of the quantum efficiency of open PSII reaction centres. Studies by Marquardt (2016) comparing two commercial genotypes (KQ228ϕ & Q200ϕ) showed this ratio decreased significantly between leaf 3 and 5 in YCS symptomatic plants compared to controls. Also noted was the decrease in maximal fluorescence intensity (F_m) without a corresponding reduction at at 50 µs (F_0). This anomaly is indicative of inactivation of the photosynthetic reaction centres and not antenna quenching (Tsimilli-Michael and Strasser, 2008).

The inhibition of the oxygen evolving complex (OEC) due to heat stress and the subsequent disruption to the electron acceptor side of PSII could lead to damage of D1 proteins and the accumulation of reactive oxygen species (ROS) (Tsimilli-Michael and Strasser, 2008; Pokorska et al., 2009; Tsimilli-Michael and Strasser, 2013).Therefore disruption to the electron transport system in YCS leaves will result in significant production of free radicals and oxidants, unless buffered by cellular metabolism.

6.2.4. Gene expression and protein

6.2.4.1. Light reactions

It is well established that an increase in leaf sucrose level represses photosynthetic gene expression and chlorophyll abundance leading to chlorosis (Sheen, 1990; Goldschmidt and Huber, 1992; Sheen, 1994; Krapp and Stitt, 1995; Jeannette et al., 2000; Braun et al., 2006; Baker and Braun, 2008; Braun and Slewinski, 2009; Slewinski and Braun, 2010). This disruption leads to an imbalance between the production of ATP and NADPH and metabolic consumption. The resultant decrease in available oxidised coenzyme NADP+ initiates an excess capacity of the light reactions, increased ROS production and ultimately photo-oxidation of the photosynthetic apparatus, culminating in leaf yellowing. (Ahmad, 2014; Schöttler and Tóth, 2014).

Major changes are evident in the levels of transcripts and the proteins associated with photosystem I and II of the photosynthetic electron transport chain in YCS leaves (Figure 14). There is significant downregulation of genes encoding light interception proteins (chlorophyll a/b binding), through to ATP and NADPH production (ATP synthase subunit and ferredoxin-NADP+ reductase (FNR), respectively). Major impacts are observed in the reaction centres of Photosystem I and II, with the majority of changes occurring in PSII, as well as water-splitting (oxygen-evolving complex (OEC), and D1 and D2 proteins (Figure 15). In early stage (ES) YCS there was already significant decreases in PSII core protein D1 (Figure 16A), Psbo and PsbQ of the OEC (Figure 16B & C). However, disruption to PSI is most evident in more advanced YCS yellow leaf tissue. This infers there is early disruption to both nuclear and chloroplast gene expression during YCS expression (Marquardt, 2019). In summary, electron flow is reduced, and the system required for light conversion to photochemical energy is disrupted. Furthermore, this is supported by chl a fluorescence data

Figure 12, Figure 13).

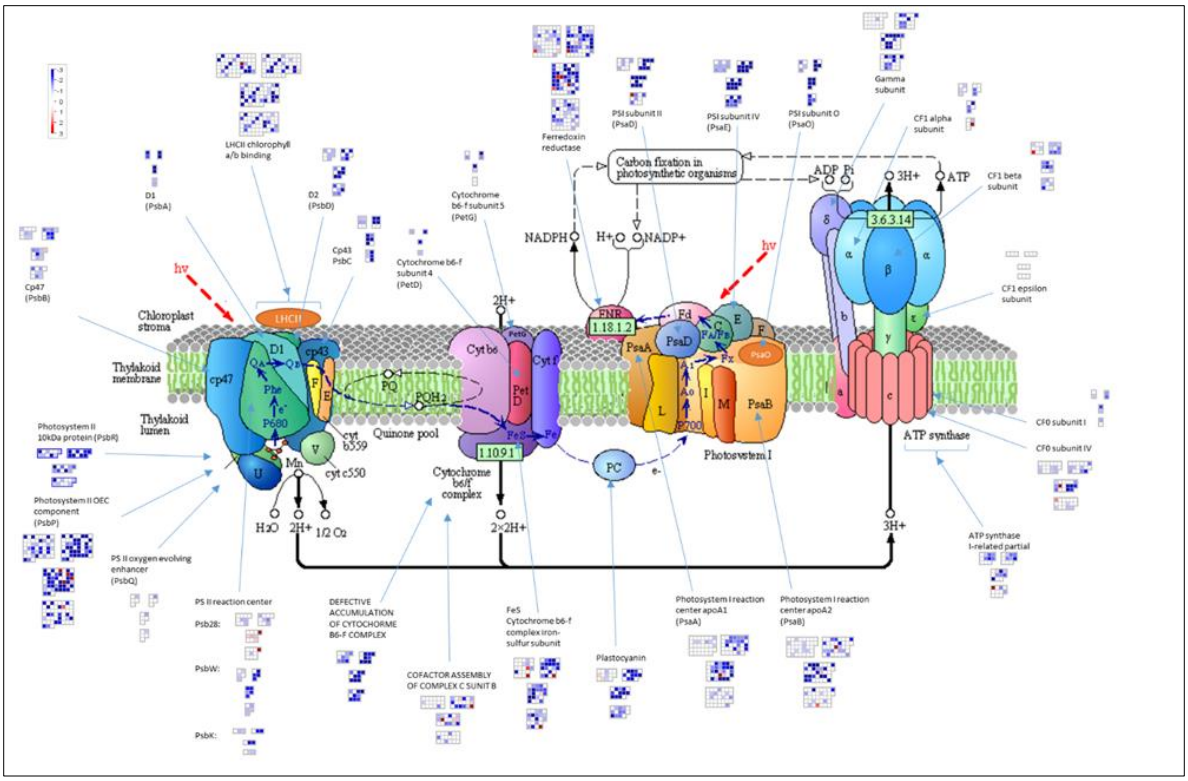

Figure 14 Representation of photosynthetic electron transport chain proteins embedded in thylakoid membrane of chloroplast, populated with differential gene expression (DE) data corresponding to proteins of YCS leaves compared to control leaves. Embedded gene expression data is displayed as individual transcripts (squares) with a uniform annotation (block of squares). Each annotation contains four blocks of transcripts: top left shows DE results for green YCS leaf lamina, top right shows yellow YCS leaf lamina, middle shows YCS midrib results and bottom shows YCS dewlap results. Corresponding squares in each block are directly comparable (represent the same transcript). Red represents significant upregulation in YCS tissue compared to control, and blue represents downregulation. White represents no significant change in gene expression to control tissue. All DE results are significant to false-discovered rate-corrected P-value of < 0.01.

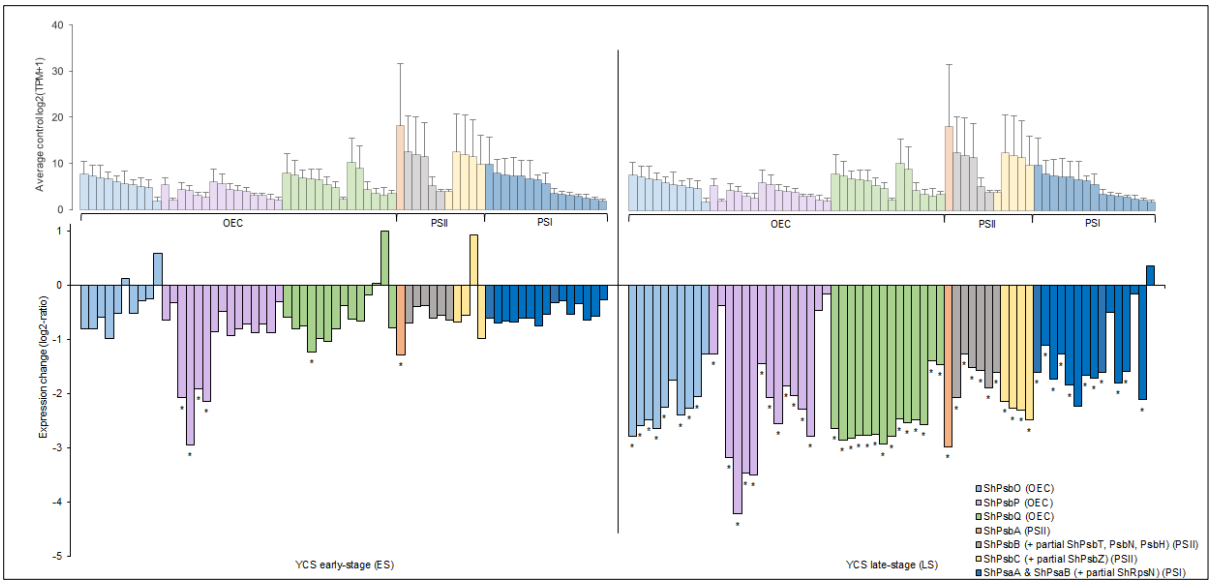

Figure 15 Oxygen-evolving complex (OEC), photosystem II (PSII) and photosystem I (PSI) subunit gene expression change from control in pre-symptomatic (early-stage; ES) lamina, and post-symptomatic (late-stage; LS) lamina of yellow canopy syndrome (YCS)-affected sugarcane leaves. Shown as log2(TPM+1) of average control sample expression (paled, top graph) and log2-fold change from control (fold change; bottom graph), for each protein coding sequence of OEC components of PsbO (light blue; *ShPsbO*; 10 genes), PsbP (purple; *ShPsbP*; 15 genes) and PsbQ (green; *ShPsbQ*; 14 genes), PSII components of PsbA (*ShPsbA*; D1; orange; one gene), PsbB (*ShPsbB*, where each also contained partials of *ShPsbT*, *ShPsbN* and *ShPsbH*; grey; six genes), PsbC (*ShPsbC*, where each also contained partials of *ShPsbZ*; yellow; four genes), and PSI components of PsaA and PsaB (*ShPsaA*, and *ShPsaB* genes were found on the same contig; dark blue; 15 genes). Asterisk symbol (*) denotes significant change in YCS-affected tissue from control based on false discovery rate (FDR)-corrected p-value <0.001 (Marquardt, 2019).

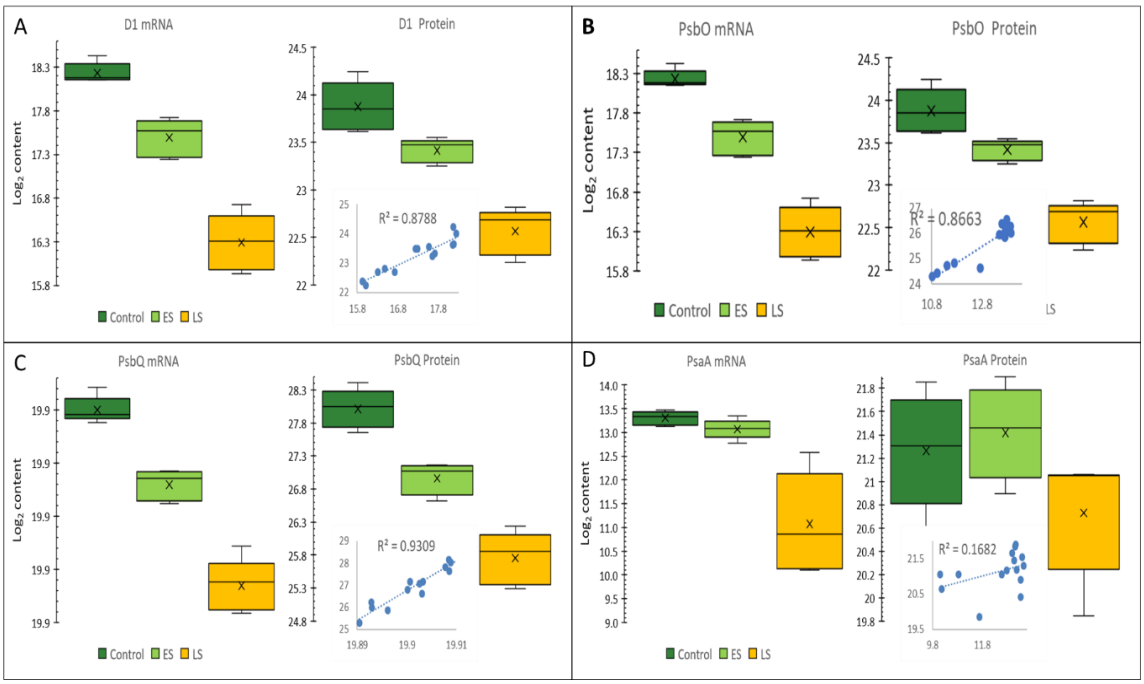

Figure 16 Photosystem II (PSII), Oxygen-evolving complex (OEC), and photosystem I (PSI) subunit gene expression and protein change from control in pre-symptomatic (early-stage; ES) lamina, and post-symptomatic (late-stage; LS) lamina of yellow canopy syndrome (YCS)-affected sugarcane leaves; PSII components of PsbA (*ShPsbA*; D1; one gene) (A), OEC components of PsbO (*ShPsbO*; 10 genes), PsbP (*ShPsbP*; 15 genes) (B & C) PSI components of PsaA (*ShPsaA*; 15 genes) (D).

6.2.4.2. Primary Carbon fixation

In C_4 plants carbon fixation occurs in the cytosol of the mesophyll cells where CO_2 is trapped by phosphoenolpyruvate carboxylase (PEPC) to form C_4 acids. Gene expression analysis of not only PEPC activity but all of the primary carbon fixation reactions of carbonic anhydrase, phosphoenolpyruvate carboxylase, NADP malate dehydrogenase and pyruvate phosphate dikinase shows downregulation in both early and late stage YCS (Figure 17) (Marquardt, 2019).

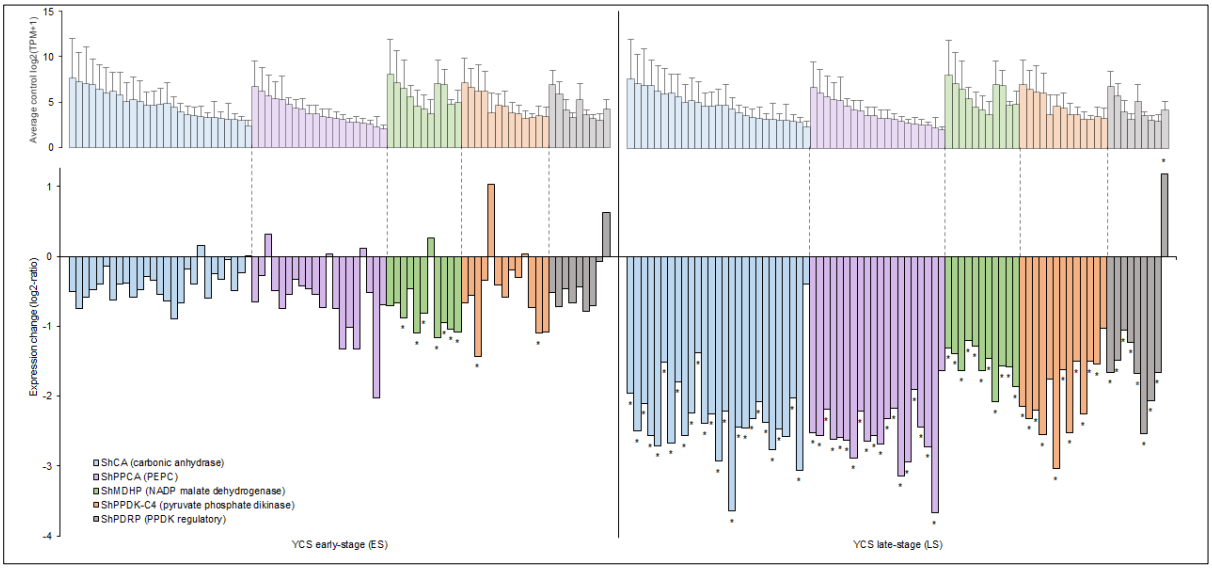

Figure 17 Initial carbon fixation in mesophyll cell gene expression change from control in pre-symptomatic (early-stage; ES) lamina, and post-symptomatic (late-stage; LS) lamina of yellow canopy syndrome (YCS)-affected sugarcane leaves. Shown as log2(TPM+1) of average control sample expression (paled, top graph) and log2-fold change from control (fold change; bottom graph), for each protein coding sequence of carbonic anhydrase (blue; *ShCA*; 27 genes), phospho*enol*pyruvate carboxylase (purple; *ShPPCA*; 20 genes), NADP-dependent malate dehydrogenase (green; *ShMDHP*; 11 genes), C4-specific pyruvate phosphate dikinase (orange; *ShPPDK-C4*; 13 genes) and pyruvate phosphate dikinase regulatory protein (grey; *ShPDRP*; nine genes). Asterisk symbol (*) denotes significant change in YCS-affected tissue from control based on false discovery rate (FDR)-corrected p-value <0.001 (Marquardt, 2019).

6.2.4.3. Decarboxylation

Carbon fixation in C_4 plants is a complex process starting with PEPC as the primary enzyme of CO_2 fixation and the formation of a C_4 acid oxaloacetate (OAA). OAA is converted to malate or aspartate and shuttled to the bundle sheath cell where decarboxylation takes place and CO_2 is released for refixation in the Calvin cycle. This decarboxylation may occur via one or more of three possible pathways, i) NADP-malic enzyme (NADPME) - malate pathway, ii) NAD – aspartate pathway and iii) PEP carboxy kinase (PEPCK)– aspartate pathway (Figure 18).It is thought that the main decarboxylation pathway in the bundle sheath cells of sugarcane is through NADP-malic enzyme (NADPME). In this pathway, OAA is first reduced to malate in the mesophyll chloroplasts by NADP-malate dehydrogenase (NADPMD) before being shuttled. Whereas in the other two pathways OAA is converted to aspartate in the cytosol of the mesophyll cell by aspartate aminotransferase before being shuttled to the bundle sheath cell where it is once again converted back to OAA for decarboxylation. In these two pathways decarboxylation takes place through either NAD-malic enzyme or PEPCK as per their pathway name sake (Figure 18) (Furbank, 2011). Figure 19 shows all three decarboxylation pathways are present in three main commercial sugarcane varieties. This is an

exciting discovery as evidence of PEPCK pathway activity had not been detected in sugarcane before. This suggests that while NADPME is the dominant decarboxylation pathway in sugarcane there may be flexibility to preference the other two pathway options depending on developmental or environmental queues. Comparison of gene expression data of water stress, senescence and YCS tissue shows that there is a preference for the PEPCK decarboxylation pathway in stressed plants (Figure 20) (Botha 2017 Appendix 4). Further investigation into early and late stage YCS shows that in contrast to NADPME, PEPCK was upregulated at a gene expression and protein level in both tissue stages of expression (Figure 21) (Marquardt, 2019).

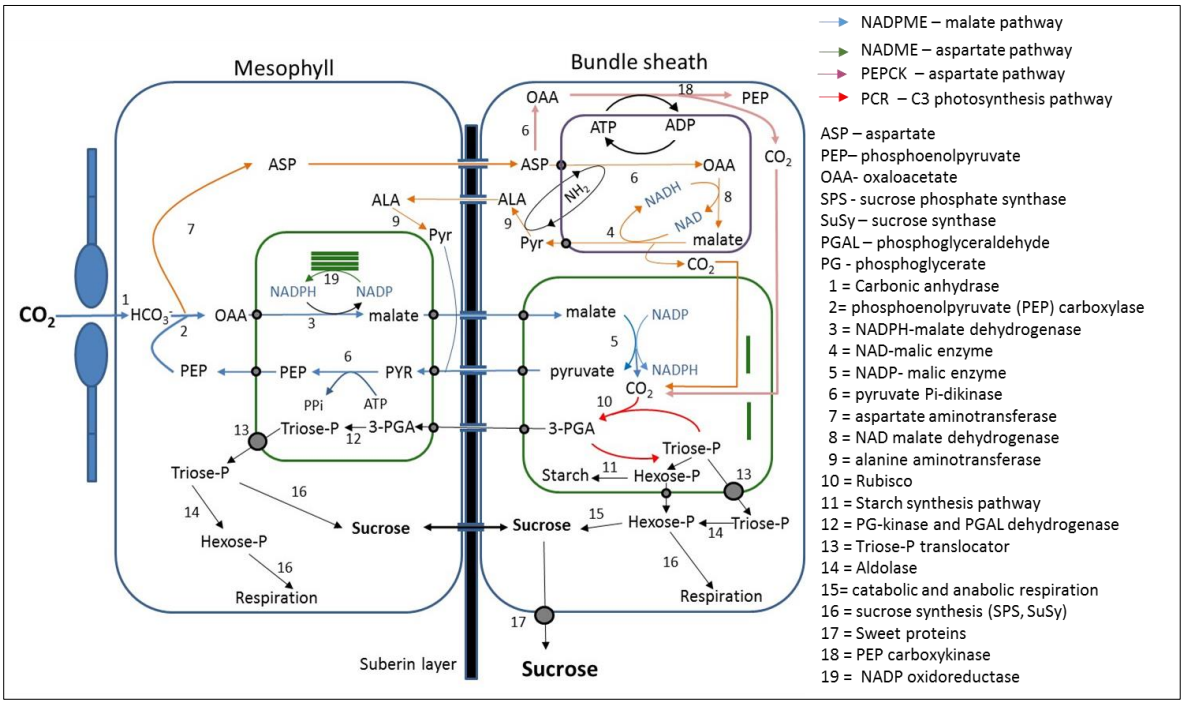

Figure 18 C_4 photosynthetic mechanisms. There are two pathways for production and translocation of C_4-acids to the bundle sheath. Three decarboxylation mechanisms exist, but there are doubts whether PEPCK (reaction 18) is present in the bundle sheath cells. (Botha 2017 Appendix 4)

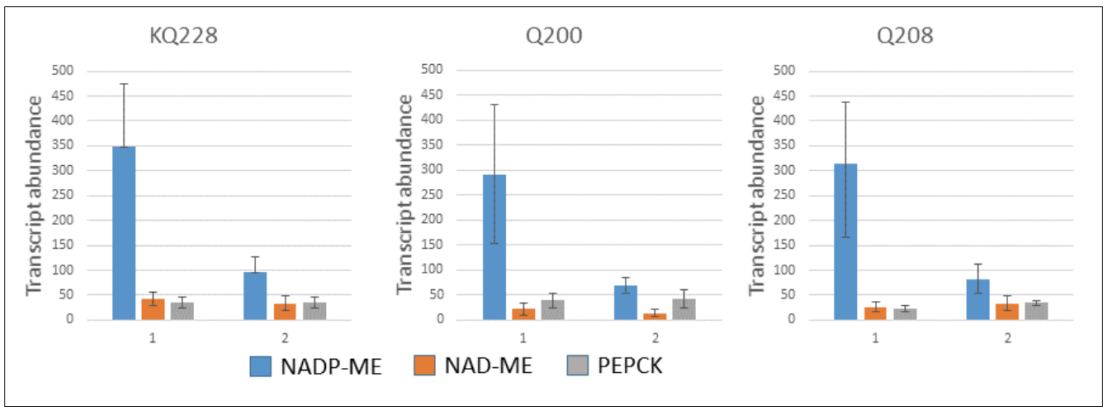

Figure 19 Expression of the three decarboxylation mechanisms in three sugarcane varieties in three very different production environments (Botha 2017 Appendix 4)

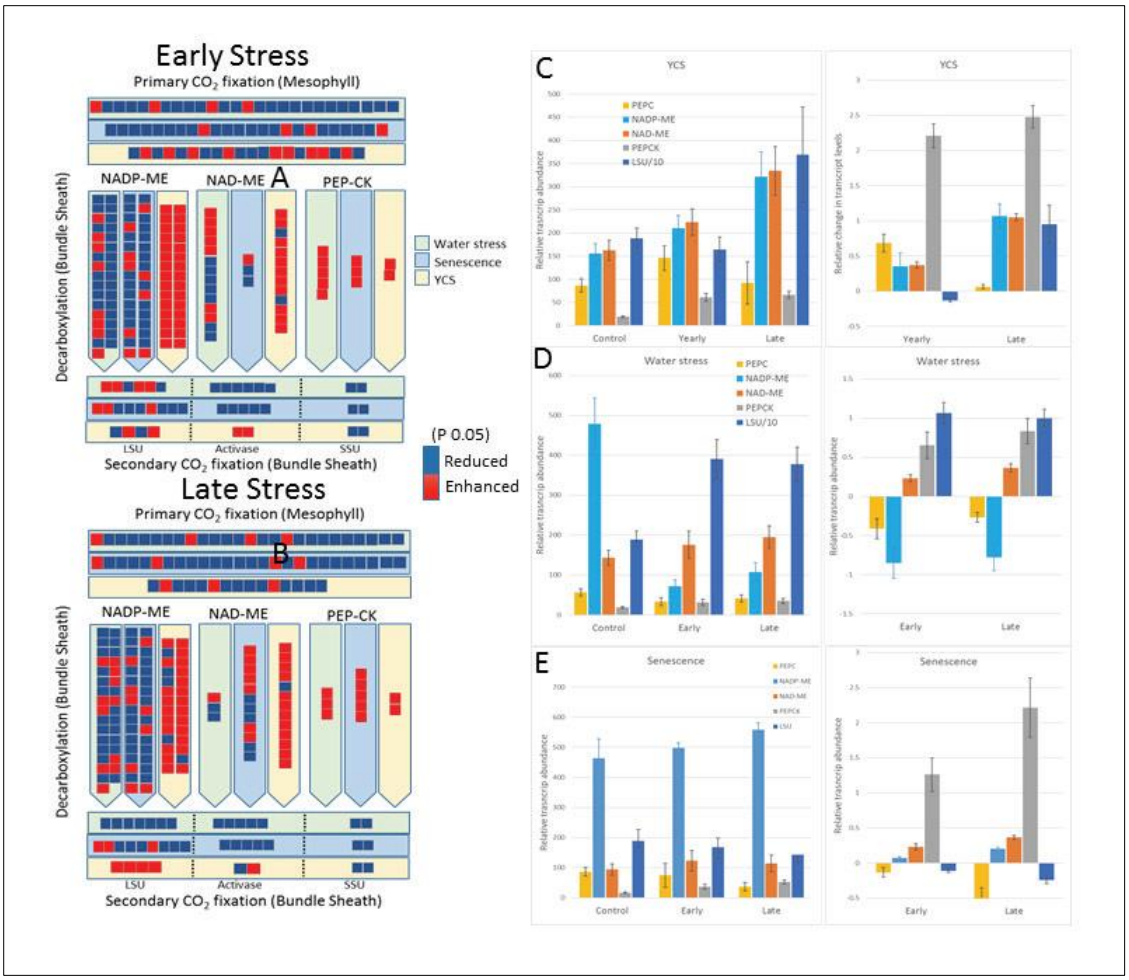

Figure 20 Expression of mesophyll and bundle sheath carboxylation, and bundle sheath decarboxylation, genes during early (A) and late stage stress (B). Expression of NADP-ME, NAD-ME, PEPC, PEPCK and Rubisco LSU during YCS symptom development (C), water stress (D) and senescence (E). (Botha 2017 Appendix 4)

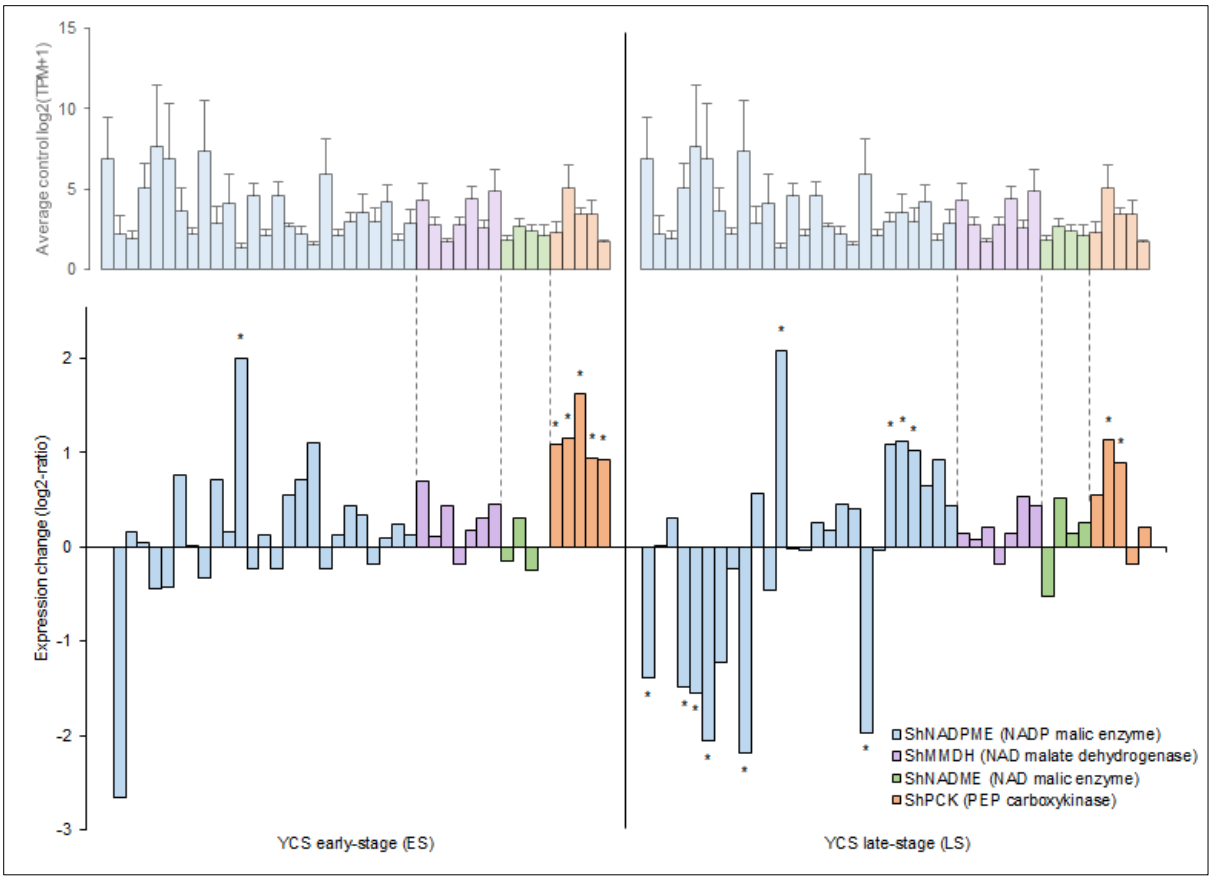

Figure 21 Decarboxylation pathways in bundle sheath cell gene expression change from control in pre-symptomatic (early-stage; ES) lamina, and post-symptomatic (late-stage; LS) lamina of yellow canopy syndrome (YCS)-affected sugarcane leaves. Shown as log2(TPM+1) of average control sample expression (paled, top graph) and log2-fold change from control (fold change; bottom graph), for each protein coding sequence of NADP-dependent malic enzyme (blue; *ShNADPME*; 26 genes), NAD-dependent malate dehydrogenase (purple; *ShMMDH*; seven genes), NAD-dependent malic enzyme (green; *ShNADME*; four genes) and phospho*enol*pyruvate carboxykinase (orange; *ShPEPCK*; five genes). Asterisk symbol (*) denotes significant change in YCS-affected tissue from control based on false discovery rate (FDR)-corrected p-value <0.001. (Marquardt, 2019)

6.2.4.4. Refixation

The two components of Ribulose bisphosphate carboxylase/oxygenase (Rubisco) [the large subunit (RbcL), encoded in the chloroplast DNA as a single-copy gene, the small subunit (RbcS) which is nuclear-encoded with multiple copies] and the binding of Rubisco activase (RbcA)], were analysed at a transcript abundance and protein level. Interestingly, the results do not follow the accepted model that during leaf sucrose accumulation Rubisco is an early downregulation response of feedback inhibition. Rather, they show it is a late-stage response in both gene expression and protein abundance, indicating there is more disruption in bundle sheath fixation in late stage YCS tissue (Figure 22) (Marquardt, 2019).

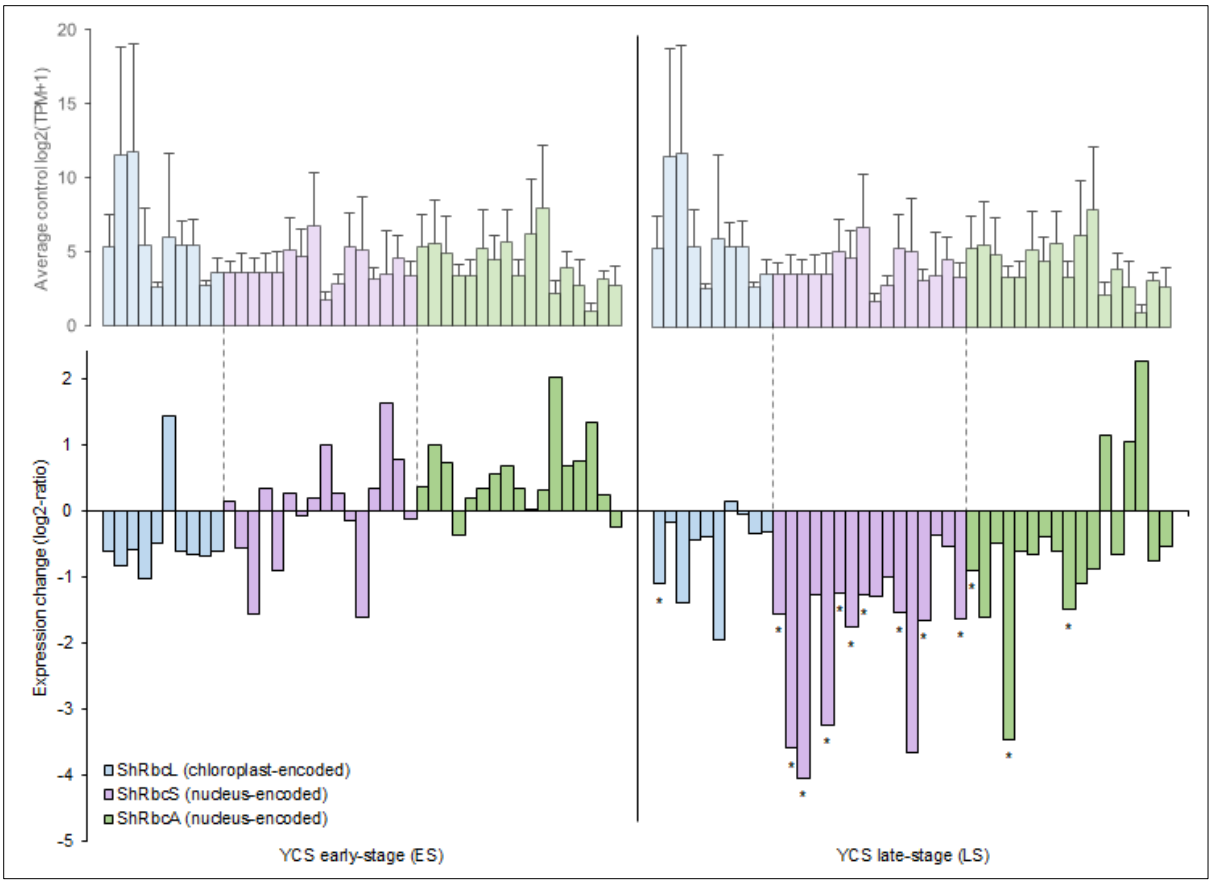

Figure 22 Ribulose bisphosphate carboxylase/oxygenase (Rubisco) components in bundle sheath cell gene expression change from control in pre-symptomatic (early-stage; ES) lamina, and post-symptomatic (late-stage; LS) lamina of yellow canopy syndrome (YCS)-affected sugarcane leaves. Shown as log2(TPM+1) of average control sample expression (paled, top graph) and log2-fold change from control (fold change; bottom graph), for each protein coding sequence of Rubisco large subunit (blue; *ShRbcL*; ten genes), Rubisco small subunit (purple; *ShRbcS*; 16 genes) and Rubisco activase (green; *ShRbcA*; 17 genes). Asterisk symbol (*) denotes significant change in YCS-affected tissue from control based on false discovery rate (FDR)-corrected p-value <0.001 (Marquardt, 2019).

6.2.4.5. Calvin cycle

CP12 is an important protein which is linked to Calvin cycle activity through its bonds to glyceraldehyde-3-phophate dehydrogenase (GAPDH), and phosphoribulokinase (PRK). Figure 23 shows reduced Calvin cycle activity in both early and late stage YCS expressing tissue (Marquardt, 2019).

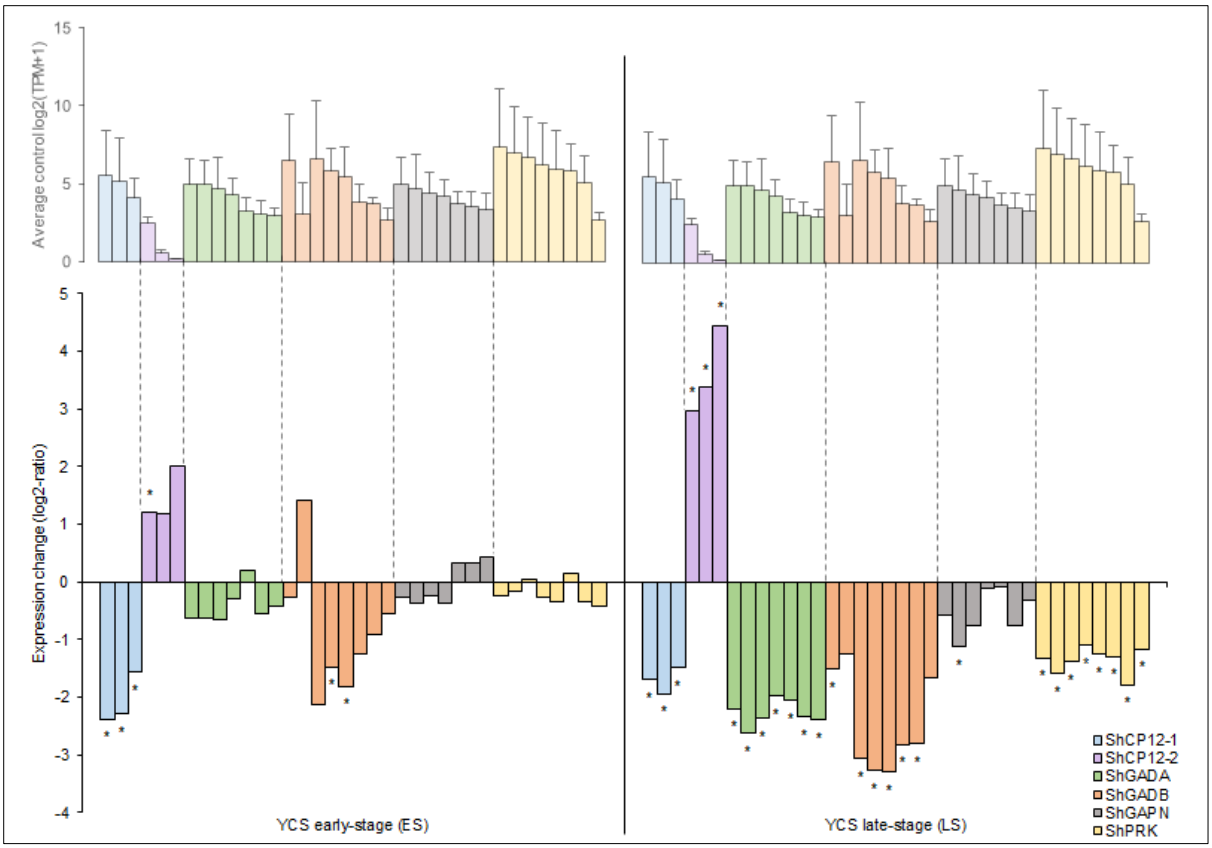

Figure 23 Calvin cycle-related gene expression change from control in pre-symptomatic (early-stage; ES) lamina, and post-symptomatic (late-stage; LS) lamina of yellow canopy syndrome (YCS)-affected sugarcane leaves. Shown as log2(TPM+1) of average control sample expression (paled, top graph) and log2-fold change from control (fold change; bottom graph), for each protein coding sequence of CP12-1 (blue; *ShCP12-1*; three genes), CP12-2 (purple; *ShCP12-2*; three genes), glyceraldehyde-3-phosphate dehydrogenase (GAPDH) A, (green; *ShGADA*; seven genes, GAPDH B (orange; *ShGAPB*; eight genes), NADP-dependent GAPDH (grey; *ShGAPN*; seven genes), phosphoribulokinase (yellow; *ShPRK*; eight genes). Asterisk symbol (*) denotes significant change in YCS-affected tissue from control based on false discovery rate (FDR)-corrected p-value <0.001 (Marquardt, 2019).

6.2.4.6. Pigment biosynthesis & breakdown

Pigment metabolism is affected during YCS onset (Figure 24). Downregulation of chlorophyll biosynthesis and upregulation of chlorophyll breakdown was found on the gene expression level. This is consistent with a loss of chlorophyll observed during YCS symptoms. Carotenoids (carotenes and xanthophylls) show a similar reduction in genes relating to biosynthesis; however, carotenoid breakdown-associated genes are also downregulated. These results support the reduction in chlorophyll and retention of carotenoid pigments observed during development of the YCS leaf phenotype.

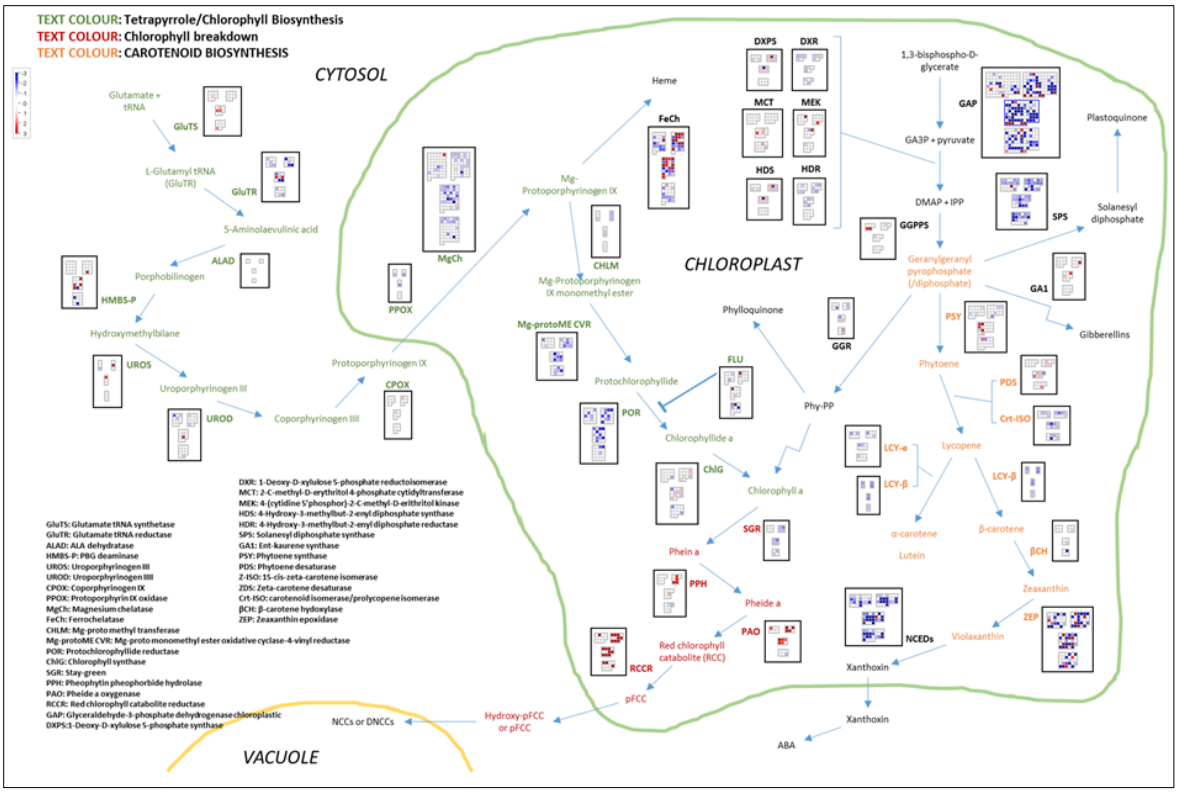

Figure 24 Overview of chlorophyll biosynthesis & breakdown, and carotenoid biosynthesis & breakdown pathway, populated with differential gene expression (DE) data corresponding to proteins of YCS leaves compared to control leaves. Embedded gene expression data is displayed as individual transcripts (squares) with a uniform annotation (block of squares). Each annotation contains four blocks of transcripts: top left shows DE results for green YCS leaf lamina, top right shows yellow YCS leaf lamina, middle shows YCS midrib results and bottom shows YCS dewlap results. Corresponding squares in each block are directly comparable (represent the same transcript). Red represents significant upregulation in YCS tissue compared to control, and blue represents downregulation. White represents no significant change in gene expression to control tissue. All DE results are significant to false-discovered rate-corrected P-value of < 0.01.

6.2.5. Carbohydrate metabolism

Sucrose is the major product of photoassimilation, and the main form of carbon exported from the source leaf in sugarcane and most other plants. It is well accepted that cellular metabolism in plants is regulated by sucrose and its hydrolytic products. The stoichiometry between sucrose and starch is a good indicator of leaf metabolic status and physiological fitness. Therefore, analysis of carbohydrate cellular content in all YCS leaf tissue (lamina, midrib, sheath) is imperative to understanding the mechanism behind the induction of leaf yellowing.

Carbohydrate-induced feedback regulation of photosynthesis is evident in YCS leaves. These changes are present in the early and late stage YCS leaf lamina, as well as the dewlap and midrib. Noteworthy is the decrease in carbon fixation in the mesophyll and bundle sheath cells through downregulation of PEPC and RuBisCo respectively (Figure 25).

Trehalose-6-phosphate (T6P) is synthesised from UDP-glucose and glucose-6-phosphate through T6P synthase. The non-reducing glucose disaccharide trehalose is then synthesised from T6P through trehalose phosphate phosphatase (TPP). T6P is a sugar status-signalling molecule and is a major regulator of plant metabolism, increasing when carbon availability is high and regulating growth and development with respect to environmental conditions. Gene regulation of growth and

development by T6P is through the protein kinase SnRK1. Together SnRK1 and T6P coordinate metabolic regulation of growth in response to stress (Nuccio et al., 2015). T6P has been linked to signalling the downregulation of photosynthesis during the presence of excess sucrose. Levels of T6P change in parallel with sucrose synthesis and also influence the amount of starch accumulation and degradation during the day and night, respectively. Therefore, this signalling molecule is very important in maintaining balance between sucrose and starch levels to meet the plant's sucrose demands during the normal circadian rhythm (Gupta and Kaur, 2005; Lunn et al., 2014; Nuccio et al., 2015; Figueroa and Lunn, 2016). Both starch synthase (starch synthesis) and breakdown (AGPase) genes are upregulated in YCS plants This indicates starch turnover is occurring in the leaf lamina, midrib, and dewlap. Furthermore, T6P is a precursor to trehalose synthesis through TPP and TPS levels are upregulated in all three YCS leaf tissues (Figure 25). Trehalose metabolism strongly correlates with sugar and anthocyanin levels in plants (Lunn et al., 2014). Figure 26 shows increased levels of trehalose in symptomatic YCS leaves across three varieties and regions. Anthocyanin synthesis is initiated by light and high sucrose content in leaves which is synonymous with YCS symptom development and expression.

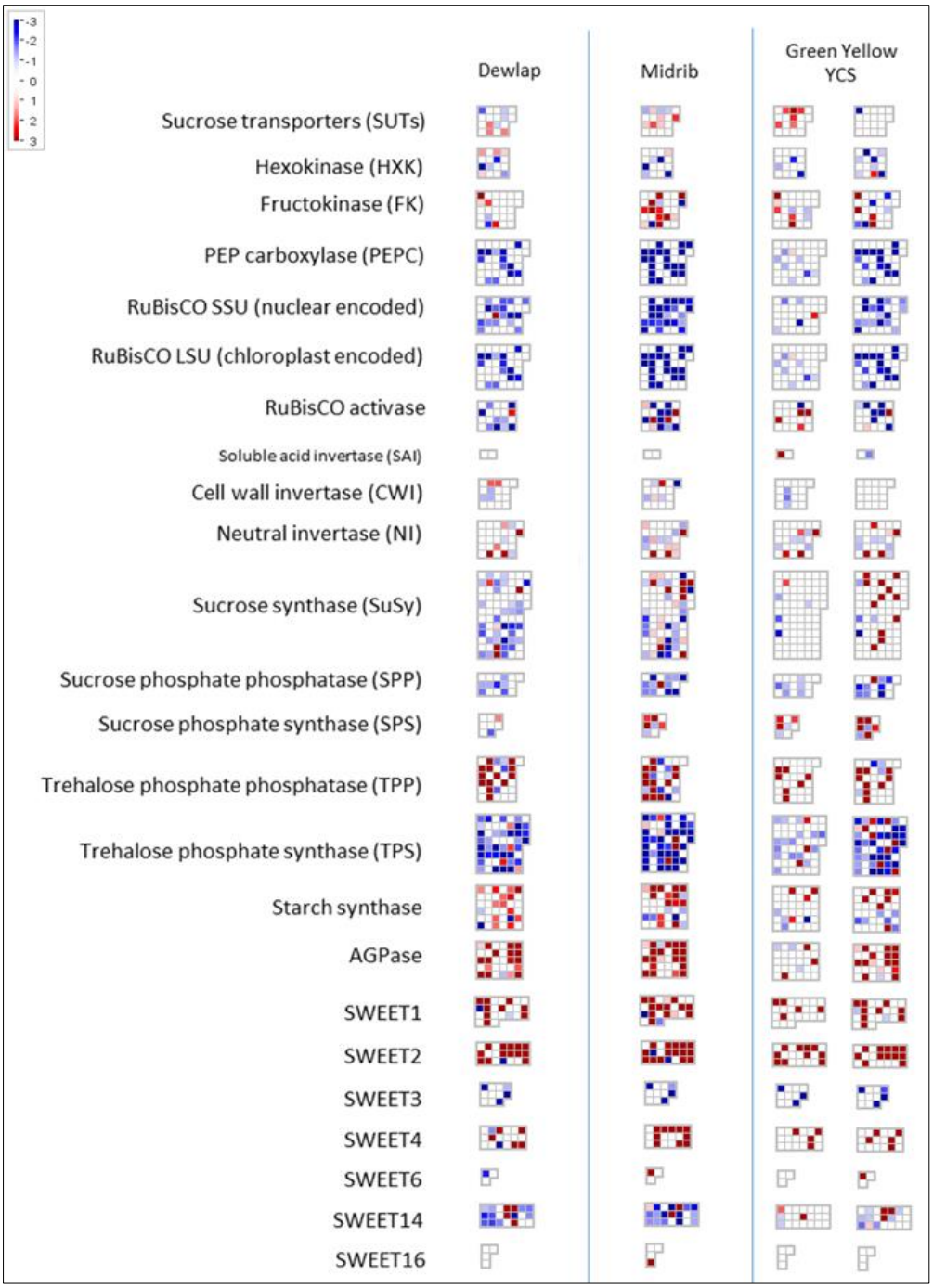

Figure 25 Differential gene expression (DE) data of genes associated with carbohydrate metabolism, feedback regulation of photosynthesis and sucrose transport in YCS leaves compared to control leaves. DE data is displayed as individual transcripts (squares) with a uniform annotation (block of squares). Each gene row shows four blocks of transcripts: DE results for YCS dewlap, midrib, and green and yellow leaf lamina. Corresponding squares in each block are directly comparable (represent the same transcript). Red represents significant upregulation in YCS tissue compared to control, and blue represents downregulation. White represents no significant change in gene expression to control tissue. All DE results are significant to false-discovered rate-corrected P-value of < 0.01.

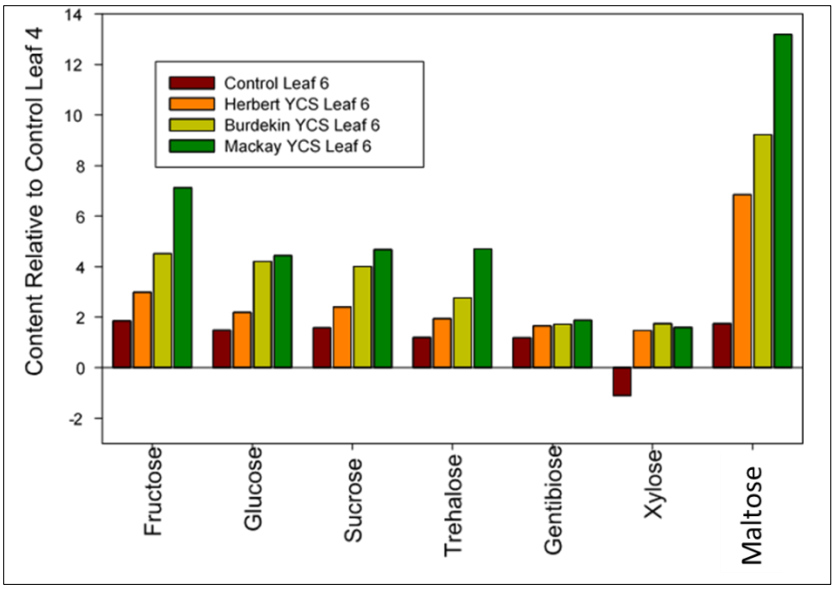

Figure 26 Changes in the levels of sugars in YCS symptomatic sugarcane plants (Herbert - Q200$^{\Phi}$, Mackay - Q208$^{\Phi}$, Burdekin - KQ228$^{\Phi}$). Data is normalised against the control leaf four. All these values have a t-test value below P< 0.05 (Bonferroni-corrected P value). (Botha et al., 2015)

Analysis of leaf carbohydrate content across three commercial genotypes (Q200$^{\Phi}$, Q208$^{\Phi}$, KQ228$^{\Phi}$) and three geographical regions showed seven distinct sugars and sugar phosphates to be significantly higher in YCS leaves than asymptomatic controls (Figure 26). Increased levels of xylose may be attributed to cell wall degradation in YCS-induced senescing tissue. Gentiobiose is a rare disaccharide that has been shown to change concentrations in parallel with invertase in the herbaceous perennial *Gentiana* and has been implicated as a signalling molecule. Research suggests that gentiobiose is hydrolysed from gentianose and modulated by invertase (Takahashi et al., 2014). It is tempting to speculate that high levels of gentiobiose in YCS leaves could be linked to neutral invertase activity and sucrose hydrolysis to prevent high levels of sucrose accumulation in the cytosol (Figure 25). Indeed, significantly higher levels of the reducing sugars glucose and fructose are evident in YCS leaf tissue (Figure 26). Studies have linked high maltose concentrations to increased plant stress and high transitory starch breakdown (Lu and Sharkey, 2006). Gene expression analysis shows transcript abundance of β-amylase to be significantly higher in both water stressed and YCS symptomatic plants than controls (Figure 27).

Figure 27 represents the changes in gene expression of the main enzymes surrounding sucrose and starch synthesis and degradation. Sucrose synthesis to the right of the chloroplast membrane shows that gene expression is mostly upregulated, but on examination of the transcript abundance for Sucrose phosphate synthase (SPS) and UDP glucose pyrophosphorylase there is no significant difference between controls and YCS. Since we know there is sucrose accumulation in YCS leaves this would suggest that sucrose synthesis is mostly under metabolic control. The accumulation of sucrose in the cytosol most likely downregulates the triose phosphate transporter through feedback regulation which in turn results in a retention of carbon in the chloroplast. The result of this is clearly seen with an increase in gene expression for starch synthesis and breakdown through an upregulation of ADP GlcPPase and alpha & beta amylase, respectively. Therefore, starch synthesis and breakdown are regulated by gene expression during YCS symptom development.

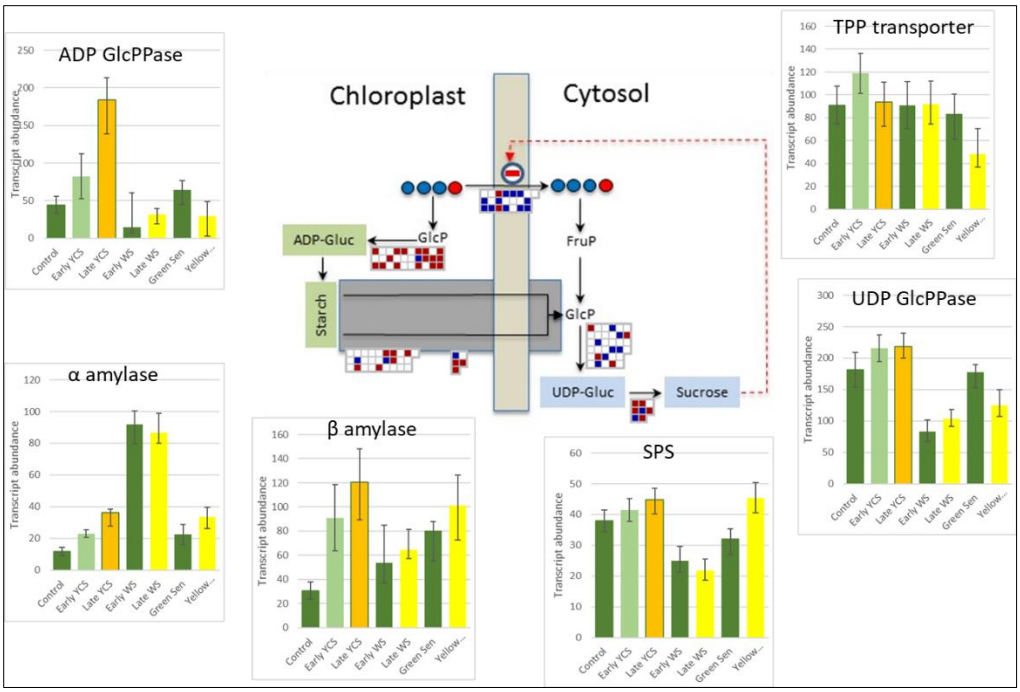

Figure 27 Regulation of sucrose and starch levels in asymptomatic control and early and late stages of YCS, water stress and senescent leaf tissue.

It has been demonstrated that sucrose and its hydrolytic products (glucose and fructose) are heavily involved in signalling and control of cellular metabolism through the SNF1- related protein family (Gupta and Kaur, 2005). As high sucrose and YCS development are strongly correlated it is therefore important to determine any relationship with the two reducing sugars. All three sugars are significantly higher in YCS asymptomatic Leaf 3 and symptomatic Leaf 4 than controls (Figure 28A-C). Quantities of both reducing sugars are of equal proportions within controls and YCS samples. However, hydrolysis ratios in YCS symptomatic Leaf 4 are approximately three-fold higher than in asymptomatic Leaf 3. This suggests that to curtail high sucrose accumulation, breakdown of sucrose has been upregulated. This is supported by an upregulation in cytosolic neutral invertase (Figure 25).

Another insight to the status of leaf carbohydrate metabolism is through starch levels. Excess sucrose is usually converted to starch and stored in the bundle sheath chloroplasts. This is a useful mechanism that the plant deploys in preparation for energy needs during the night period or in times of stress. Hence, quantities stored are highly dependent on daylength and environmental conditions (Weise et al., 2011). Therefore, the true status of starch accumulation can only be ascertained if sampling is conducted at first light. YCS leaf samples analysed under such conditions show levels to be much higher than their control leaf counterpart (Figure 28D). The disruption to cellular carbohydrate metabolism is also evident in asymptomatic Leaf 3 even before the onset of visual yellowing. This correlates with the disruption to the photosystems of these leaves caused by high sucrose accumulation (see section 6.2.3 of this report

Figure 12).

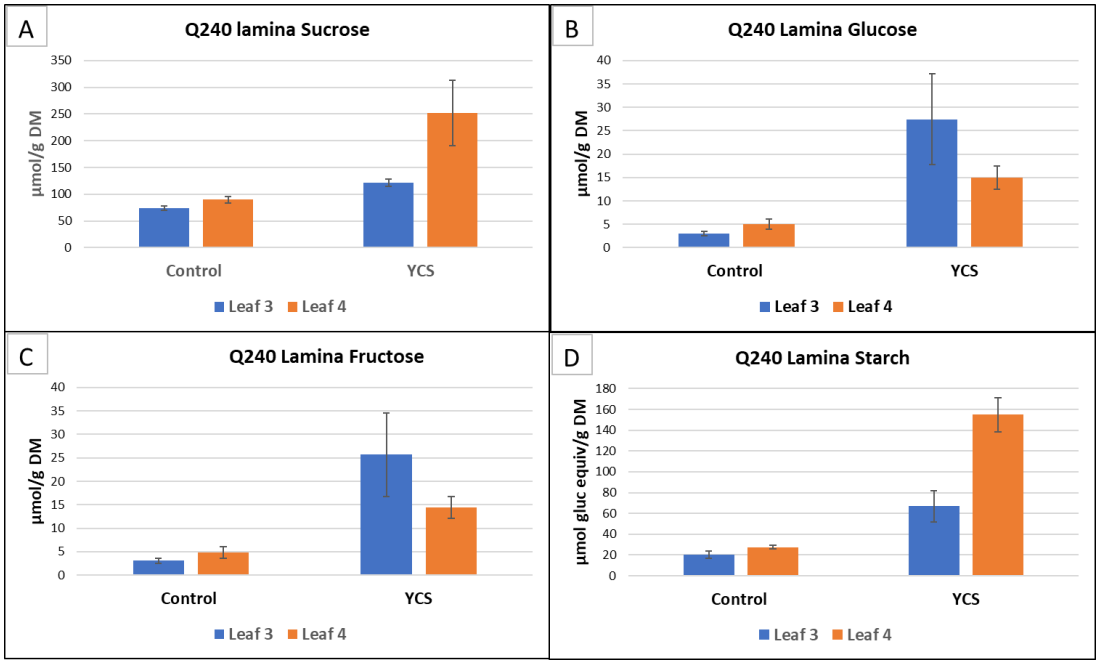

Figure 28 Changes in the levels of sucrose, glucose, fructose, and starch in control, YCS asymptomatic Leaf 3 and symptomatic Leaf 4 in genotype Q240$^{\Phi}$.

6.2.6. Carbon partitioning

The disruption to the diurnal rhythm evident by high sucrose and starch levels recorded in the lamina of YCS plants at first light has serious repercussions for the health of the leaf if accumulation is not maintained below a tolerable upper threshold. To ascertain whether elevated sucrose and starch content was confined to the lamina, analysis of other types of leaf tissue was conducted. Interestingly we not only discovered high levels of both sucrose and starch (insoluble α-glucan) in midrib, dewlap and sheath but also extremely high levels of soluble α-glucan (Figure 29). This is an exciting discovery that has not been reported in sugarcane leaf anywhere in the world literature.

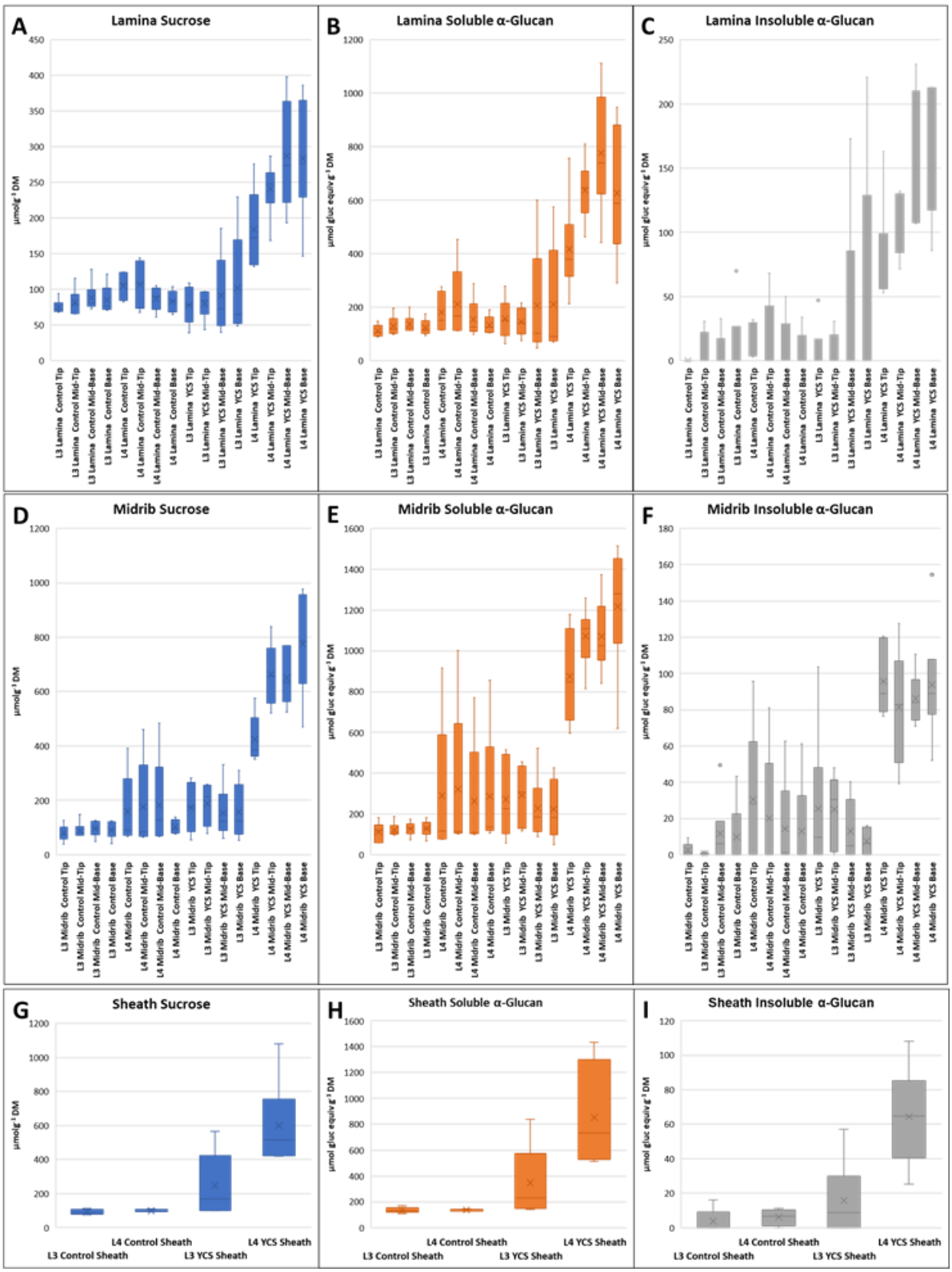

Figure 29 Q240Φ Lamina sections tip to base (A-C), Midrib sections tip to base (D-F) and Sheath (G-I); sucrose, soluble and insoluble α-glucan content in Control, YCS asymptomatic Leaf 3 and symptomatic Leaf 4. Samples taken in the morning soon after first light.

Glucans can be classified as polysaccharides composed of glucose units. Starch, an insoluble form of α-glucan is a mixture of water insoluble amylose (10-30%) and water-soluble amylopectin (70-90%). Amylose is linear with α-1,4-glycosidic linkages which form a coil structure that can accommodate an

iodine molecule. This forms an amylose-iodine complex that gives a blue-violet colour. Amylopectin has both α-1,4 and α-1,6 linkages. The α-1,6 bonds are responsible for branching of this molecule and disrupts the helical shape. Due to this a less intense reddish-brown colour is produced when iodine is added (Smith, 2007; Geigenberger, 2011). This is clearly visible in cross-section staining of the midrib from YCS symptomatic tissue between the vascular and parenchymatous tissue (Figure 30).

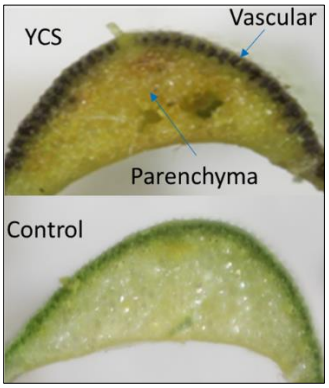

Figure 30 Control and YCS symptomatic leaf midrib stained with 1% iodine solution.

Clearly, excess carbon in the YCS leaf is redirected to the soluble α-glucan and starch pools to prevent further build-up of sucrose. Figure 29 shows the bulk of carbon is stored in the soluble pool as C_4 plants are not anatomically or physiologically capable of storing and synthesising large quantities of starch like C_3 plants. In C_4 plants this is limited by the quantity of bundle sheath cells in which the chloroplasts synthesise transitory starch during the day. Carbon partitioning in different leaf tissue components (lamina, midrib and sheath) show that sucrose and soluble α-glucans are highest in the sheath and base of the midrib and lamina (Figure 29). These two metabolites mirror each other in all three tissue types (Figure 31A-C). However, insoluble α-glucan (starch) levels are closely aligned to tissue anatomy with highest levels measured where bundle sheath chloroplasts are more abundant. Starch content is highest in the lower half of the lamina, followed by uniform distribution throughout the midrib and lowest levels recorded in the sheath (Figure 29C, F & I). Interestingly, asymptomatic (control) Leaf 4 shows a similar pattern of sucrose and soluble α-glucan accumulation to asymptomatic Leaf 3 on the YCS culm, in both the lamina and midrib (Figure 29A, B, D, & E). This indicates that the crop is in a constant state of leaf carbohydrate flux. Therefore, the plant's physiological fitness will determine its tolerance threshold to metabolic perturbance and whether it advances to YCS expression.

In C_4 plants the starch-sucrose ratio never exceeds 1.0 and averages at approximately 0.5 (Kingston-Smith et al., 1998). Unlike maize, sugarcane lacks the physiological ability to store starch in the mesophyll cells and ratios vary between 0.1- 0.15 (Figure 31D-F). Comparable ratios are maintained between sucrose, soluble α-glucan, and insoluble α-glucan in all three tissues for both asymptomatic Leaf 3 and YCS symptomatic Leaf 4. This shows that as metabolic disruption develops to the point of leaf yellowing a carbon balance between these three metabolites is maintained. Hence, the onset of yellowing is the true start of YCS. Maintenance of this metabolic balance is upheld (even when a source sink imbalance exists) until cell death and senescence occurs (Figure 32). Completely senescent or dead leaves from the Burdekin 2018/19 insecticide trial (treated with bifenthrin – project 2014/049) show that YCS symptomatic untreated controls (UTC) still contain significantly higher levels of all three metabolites in the lamina, midrib, and sheath than the asymptomatic

leaves. The lamina and midribs retain the highest levels of metabolites after leaf death except for sucrose which has almost been completely degraded, repartitioned or translocated from the lamina (Figure 32).

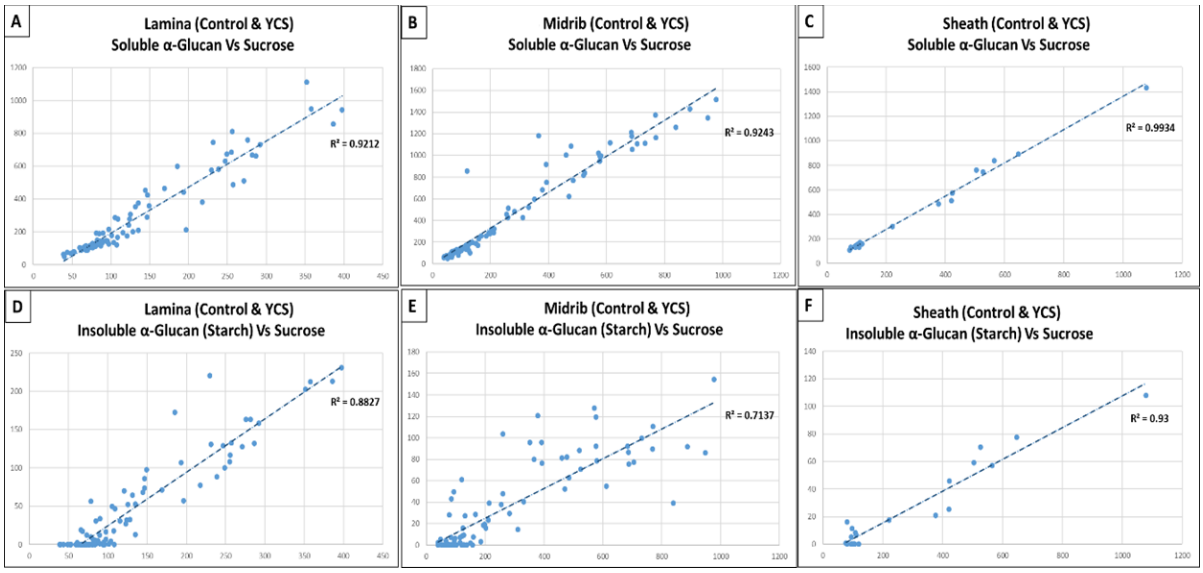

Figure 31 Q240$^{\Phi}$ Leaf 3 and 4, Sucrose: Soluble (A-C) and Insoluble α-Glucan (D-F) ratios in lamina, midrib and sheath

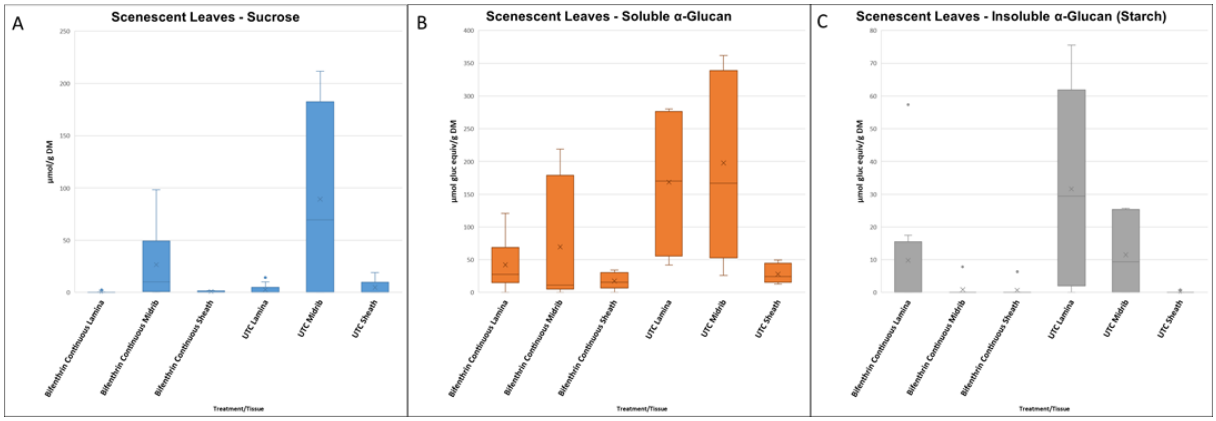

Figure 32 KQ228$^{\Phi}$ Insecticide treated and Untreated Controls (UTC) senescent leaf Sucrose, Soluble & Insoluble α-Glucan content.

To curb sucrose synthesis transitioning from a healthful to a harmful state, a combination of signalling and changes to metabolism is induced in the leaf to maintain homeostasis (source sink balance). Feedback inhibition of photosynthesis is initiated together with carbon redirection and partitioning to other pools (Braun et al., 2006; McCormick et al., 2008). Noteworthy changes to carbon partitioning are to the shikimate and the phenylpropenoid pathways which are associated with amino acid synthesis and protection against oxidative stress, respectively. Figure 33 shows metabolism divided into seven clusters (Figure 33a–g) representing the major changes to carbon partitioning. In addition to the expected changes to carbohydrate metabolism (Figure 33a) there is significant upregulation of the phenylpropanoid (Figure 33e) and shikimate (Figure 33c) pathways (Marquardt et al., 2017). It is well known that the phenylpropanoid pathway is associated with protection against oxidative stress (Osmond et al., 2000) . Important to note is that metabolites in this pathway serve as precursors in the yellow and orange carotenoid pigment biosynthesis (Figure

24) (Gray et al., 2012). The upregulation of amino acid synthesis in the shikimate pathway indicates YCS has a significant impact on protein hydrolysis.

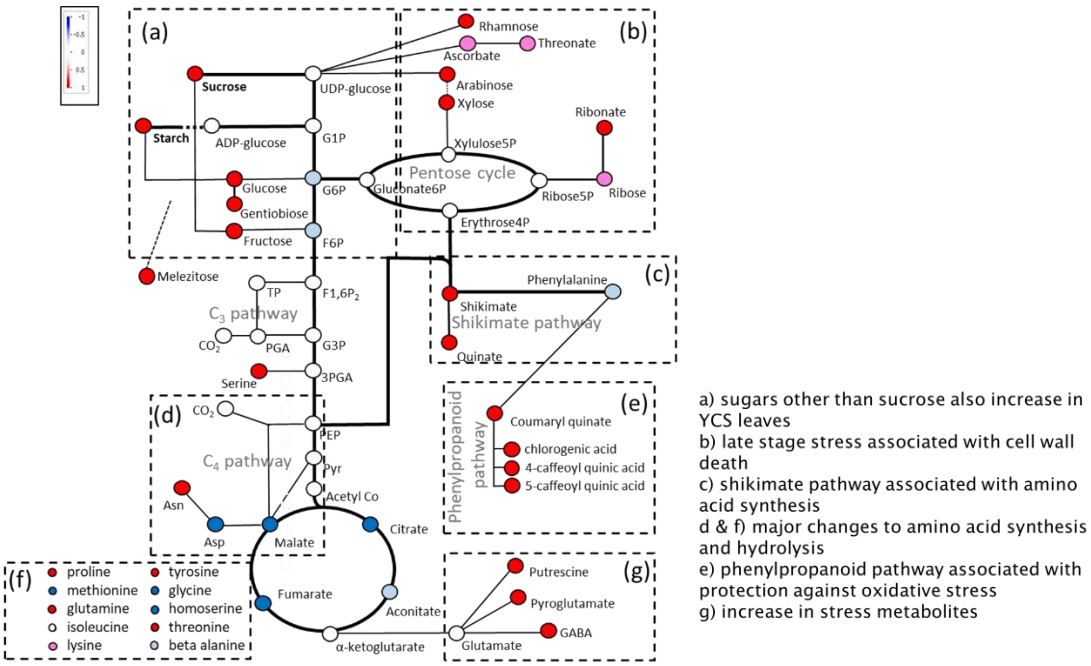

Figure 33 Overview of carbon partitioning pathways overlaid with metabolite data. Coloured circles display change in metabolite level compared to control. Results normalized where red indicates upregulation, blue indicates downregulation, on a scale between 1 and -1 (Marquardt et al., 2017)

While carbon repartitioning to other pools is useful in mitigating further accumulation of sucrose, the bulk of the carbon is redirected to the soluble and insoluble α-glucan pools in the lamina (source) and midrib (mostly sink-like) tissue. By the time leaf sucrose accumulation exceeds the tolerable upper threshold (approx. 200 µmol/g DM), the lack of coenzyme and level of electron transport disruption is sufficient to cause adequate free radical production to initiate photooxidation and leaf yellowing (Figure 34). Therefore, it is not sucrose per se that directly causes the yellowing, but rather the disruptions in energy flow which results in increased photooxidation. Hence the areas of the leaf where maximum light capture occur are particularly vulnerable to photooxidation and yellowing. However, sucrose is the critical metabolite triggering events which lead to irreversible leaf yellowing. If sucrose reaches intermediate levels of accumulation or when the supply demand imbalance passes a healthful state of stasis, carbon will likely be redirected to other main carbohydrate pools in the following order:

1. Soluble α-glucan – levels higher than 200 µmolg^{-1} DM measured in asymptomatic leaves
2. Insoluble α-glucan (starch) – once stored as granules, this insoluble metabolite will represent metabolically inactive reduced carbon
3. Sucrose – tolerable threshold breached after which photooxidation and leaf yellowing occur

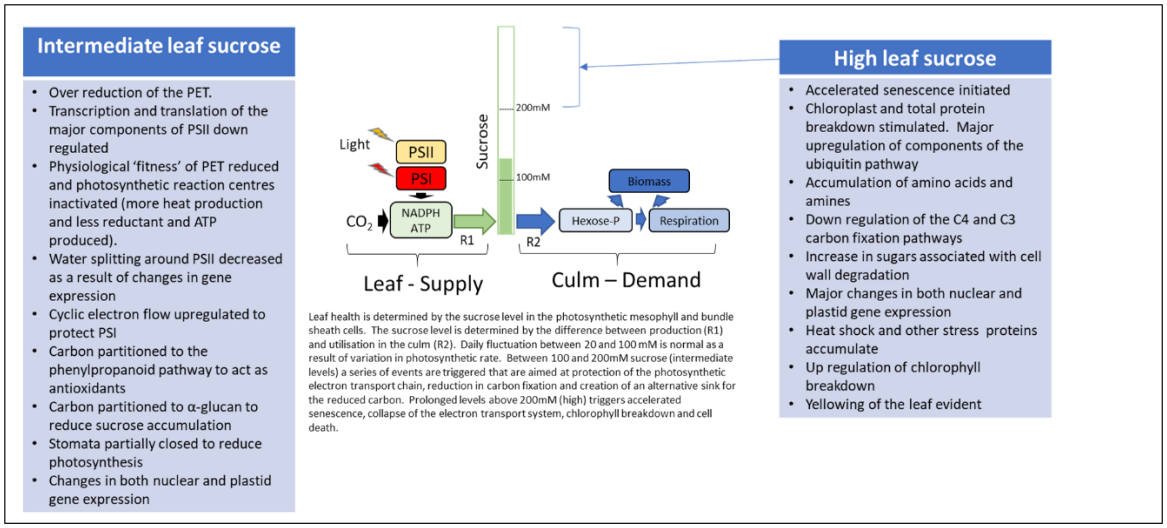

Figure 34 Carbon partitioning and source sink model centres around sucrose levels of accumulation

It is evident from the data presented in section 6.2 of this report that sucrose accumulation in the lamina above a tolerable upper threshold (approx. 200 µmol/g DM) is detrimental to leaf health. In order to prevent further sucrose accumulation, excess carbon is repartitioned to other metabolic pools. The bulk of the carbon is redirected to soluble α-glucan and starch. As alternative carbon pools fill toward capacity, sucrose levels will continue to rise and reduced photosynthetic leaf metabolism will be induced through feedback inhibition signalling (Marquardt et al., 2016; Marquardt, 2019). Downregulation of the photosynthetic rate reduces stomatal conductance, CO_2 intake, transpiration, and major components of photosystem II (PSII). Reduced water splitting and CO_2 supply to the Calvin-Benson cycle (light-independent reactions) creates an imbalance between production and metabolic consumption of photosynthetic ATP and NADPH. This causes a disruption to cellular redox homeostasis leading to a decrease in available oxidised coenzyme NADP+. Such a limitation causes i) a reduction in available electrons for carbon fixation to carbohydrates, and ii) reduced electron flow through photosystem I (PSI). This over-reduction of the photosynthetic electron transport (PET) chain increases available energy for the production of reactive oxygen species (ROS) (Schöttler and Tóth, 2014). It is worth noting that this is very common in plants under environmental stress, particularly where there is high light intensity (Braun et al., 2006). The increased production of free radicals together with an increase in internal leaf temperature due to reduced transpiration causes photo-oxidation of the photosynthetic apparatus (Ahmad, 2014). This initiates events leading to the destruction of cell membranes, chlorophyll, loss of cellular function and leaf yellowing.

6.3. Is leaf sucrose accumulation primarily driven by changes to source or sink?

Determining that sucrose, soluble α-glucan, and starch are present in all leaf tissue, and identifying where content is lowest and highest, gives us a significant insight into the internal distribution and partitioning of excess carbon in the YCS leaf. It also shows whether there is more or less accumulation of a particular metabolite at a specific location, leaf section or leaf tissue. This is invaluable information to help understand the possible cause of sucrose accumulation. Is it a physical blockage in the phloem within either the lamina, midrib or sheath or does it sit outside the leaf in the culm tissue? Do the varying levels of sucrose accumulation correlate with the pattern of chlorosis in the leaf and the kinetics of symptom development? This knowledge will be of great

benefit in ascertaining whether there is any likely disruption to phloem loading and translocation from the site of photoassimilation, or whether the cause of leaf sucrose accumulation is some other physiological disruption.

Sucrose accumulation in the source leaf may be caused by:

A) Increased synthesis exceeding export rates of sucrose to the sink
B) Disruption to phloem loading
C) Compromised phloem transport
    i) physical blockage
    ii) reduced sink strength
        - diminished sink size (internode volume)
        - metabolic disruption to carbon demand (feast or famine)

In this section of the report we will address these issues to determine whether leaf sucrose accumulation is primarily driven by changes to source or sink tissue.

6.3.1. Phloem loading, transport, and carbon turnover

6.3.1.1. Sucrose synthesis and active phloem loading

The first known cause of stress in the leaf associated with YCS onset is sucrose accumulation (Marquardt et al., 2016). This accumulation causes substantial downstream effects on leaf metabolism (Marquardt et al., 2017). The 'upstream' metabolic processes of sucrose accumulation in YCS leaves was investigated using omics data.

For sucrose to accumulate in the leaf, there must be an imbalance between how much sucrose is synthesised and how much is exported. Either sucrose synthesis must be increased while export rate is maintained/decreased, or export rate decreases while synthesis rate is maintained/increased. To investigate whether an increase in sucrose synthesis is responsible for leaf sucrose accumulation, a differential gene expression analysis for key enzymes of sucrose synthesis pathways in bundle sheath cells was conducted. This is expressed as a series of heat maps comparing control tissue with early (green tissue) and late stage (yellow tissue) YCS lamina (Figure 35). The regulation of enzymes after triose phosphate production in the chloroplast is of particular interest as this provides a clear insight to any metabolic regulatory preference towards the synthesis of either sucrose or starch. The level of expression within early stage green YCS tissue shows no increase in sucrose synthesis driving the continued sucrose accumulation past the tolerable upper threshold measured in YCS symptomatic leaves. Similarly, there is no increase in starch synthesis. Therefore, an increase in sucrose synthesis enzymes and related transcripts was not consistent in the data in YCS-affected leaves.

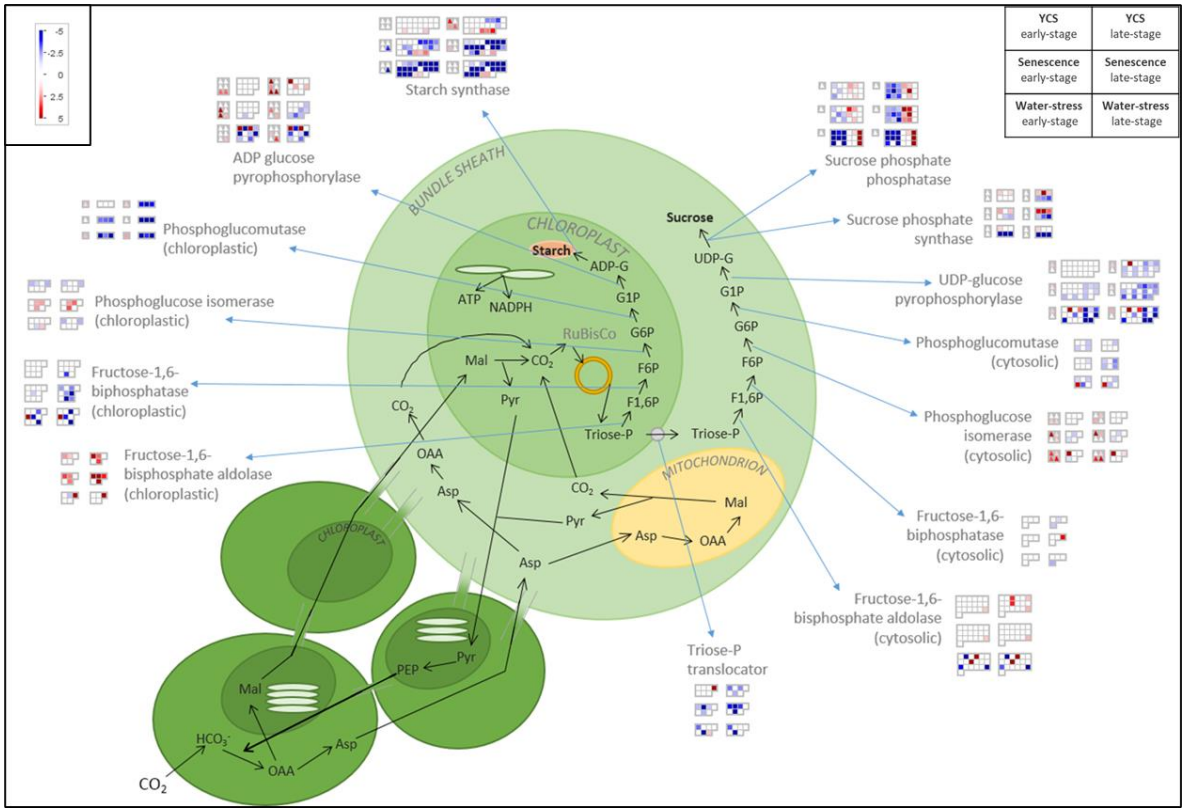

Figure 35 Differential gene expression (DE) data of genes associated with sucrose and starch synthesis in YCS, senescent and water stress leaves compared to control leaves. DE data is displayed as individual transcripts (squares) with a uniform annotation (block of squares). DE results for early and late stage YCS, senescent and water stress lamina. Corresponding squares in each block are directly comparable (represent the same transcript). Red represents significant upregulation in YCS tissue compared to control, and blue represents downregulation. White represents no significant change in gene expression to control tissue. All DE results are significant to false-discovered rate-corrected P-value of < 0.01. (Marquardt 2017 Appendix 3).

Protein abundance and gene expression were analysed to establish whether down regulation of key enzymes and transporters might be responsible for decreased sucrose export from the leaf (Marquardt et al., 2019). The way in which sucrose moves from where it is made in leaf cells involves crossing membranes facilitated by transport proteins. These are encoded by known genes, which include sucrose transporters (SUTs and SWEETs), H^+-ATPases and H^+-Pyrophosphatases (H^+-PPases). For sucrose to move from the source photosynthetic cells to the phloem requires either symplastic or apoplastic loading. Symplastic loading occurs by diffusion from high to low sucrose concentration, whereas apoplastic loading requires active transport of sucrose from the apoplast into the phloem. In active loading, SWEET proteins facilitate the diffusion of sucrose from the symplast (where it is synthesised), into the apoplastic space (where it is loaded into the companion cells of phloem sieve elements) (Chen et al., 2010). In this process ATP is used to generate a H^+ gradient across the cell membrane. Together with symporters (SUTs), sugars are transported from the apoplast into the phloem (Figure 36) (Zhang et al., 2016). Reduced abundance (and activity) of SWEET proteins could slow sucrose movement out of the leaf. The genes encoding for sucrose-transporting SWEET proteins (Figure 37g, h & i) did not show downregulation before or after YCS-symptoms were visible. Two SWEET proteins showed an upregulation during YCS symptoms (Marquardt et al., 2019) (Figure 37h & i) .

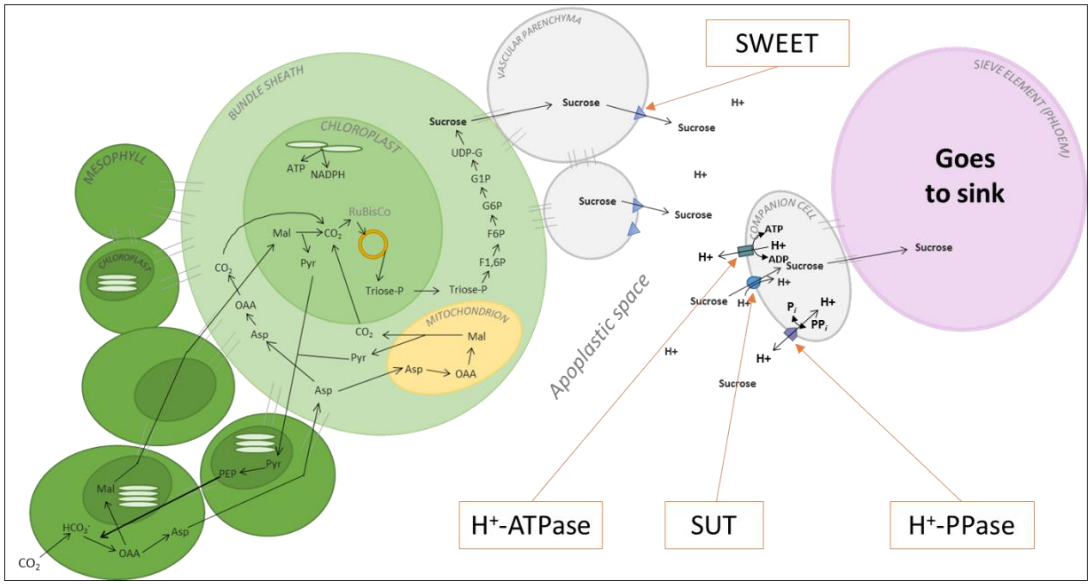

Figure 36 Sugarcane active phloem loading: sucrose transporters (SUTs and SWEETs), H⁺-ATPases and H⁺-Pyrophosphatases (H⁺-PPases) (Marquardt 2017 Appendix 3).

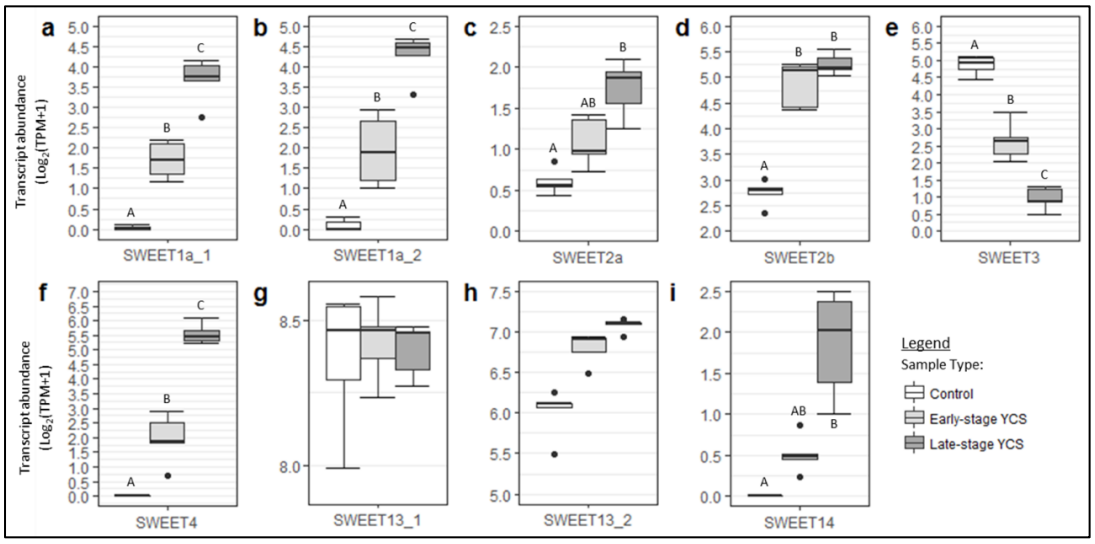

Figure 37 Transcript abundance of expressed SWEET transcripts in control, early-stage (ES)- and late-stage (LS)-yellow canopy syndrome (YCS)-affected Q240$^{\Phi}$ sugarcane leaves.
Data displayed as Log_2(TPM+1) value of reads mapping to reference transcript. (a) SWEET1a_1, (b) SWEET1a_2, (c) SWEET2a, (d) SWEET_2b, (e) SWEET3, (f) SWEET4, (g) SWEET13_1, (h) SWEET13_2, (i) SWEET14. Letters above (or below) sample type within graphs represent significant difference-groupings between sample types (differential expression analysis result false-discovery rate (FDR)-corrected P-value<0.05; fold-change>1.5). If letters not displayed within graph - no significant difference between sample types was present.

A downregulation in SUT, H+-ATPase or H+-PPase proteins could lead to decreased sucrose leaf export. SUTs actively transport sucrose from the apoplastic space into the companion cells of the phloem (Figure 36). This process requires a proton gradient, which is generated by H⁺-ATPase. ATP must be available for this to occur, which comes from the breakdown of a small fraction of sucrose in the companion cells. The energy for this breakdown is provided by H⁺-PPases.

Of the three groups of sucrose-H⁺ symporter (SUT) genes ShSUT1 had the most transcript abundance across the three leaf tissues and none showed differential expression in YCS (Figure 38). SUT1 is

implicated in phloem loading/reloading in maize, sugarcane and other plant species (Slewinski et al., 2009; Glassop et al., 2017). The SUT1 transcript was upregulated in YCS-affected leaves, both before and after visual yellowing.

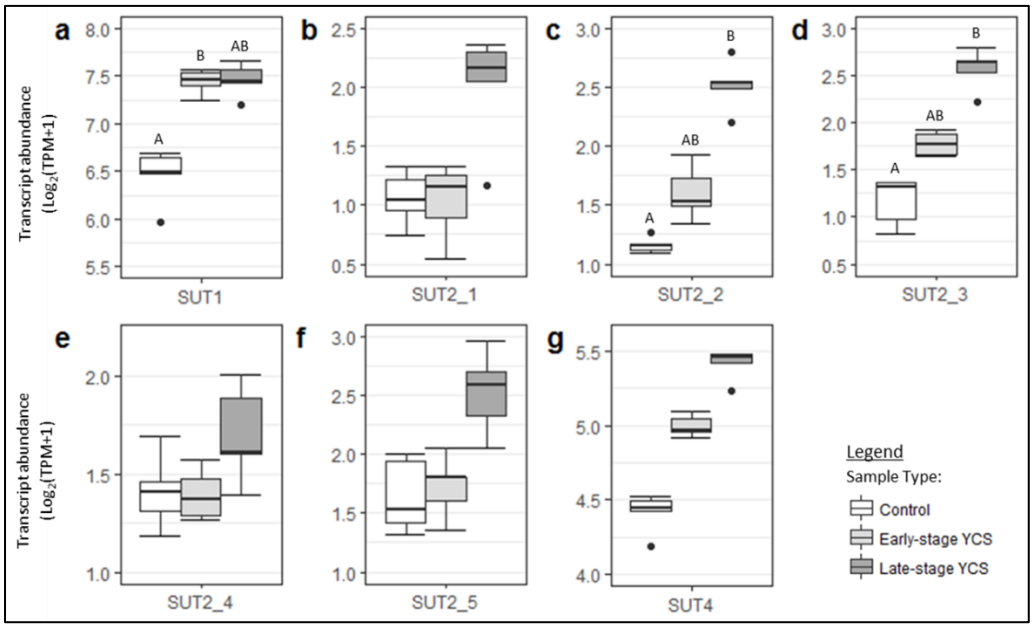

Figure 38 Transcript abundance of expressed SUT transcripts in control, early-stage (ES)- and late-stage (LS)-yellow canopy syndrome (YCS)-affected Q240$^{\Phi}$ sugarcane leaves. Data displayed as Log_2(TPM+1) value of reads mapping to reference transcript. (a) SUT1, (b) SUT2_1, (c) SUT2_2, (d) SUT2_3, (e) SUT2_4, (f) SUT2_5, (g) SUT4. Letters above sample type within graphs represent significant difference-groupings between sample types (differential expression analysis result false-discovery rate (FDR)-corrected P-value<0.05; fold-change>1.5). If letters not displayed within graph - no significant difference between sample types was present.

Investigation into the functionality of the H^+-pyrophosphatases (H^+-PPases) showed significant variation with both up and down regulation in YCS tissue (Figure 39). However, H^+-ATPase gene expression showed greatest differentiation in late stage YCS tissue (Figure 40) (Marquardt, 2019; Marquardt et al., 2019). In the data, both H^+-ATPases and H^+-PPases had multiple transcripts with the annotation, where currently available information in the literature did not allow the discerning of which transcript(s) or protein(s) are involved in the phloem loading process (both are involved in other cell membrane processes). However, wherever a transcript showed downregulation in YCS-affected leaves – and hence could pinpoint a cause of reduced sucrose phloem loading – the corresponding protein showed either no abundance change, or an increase in abundance.

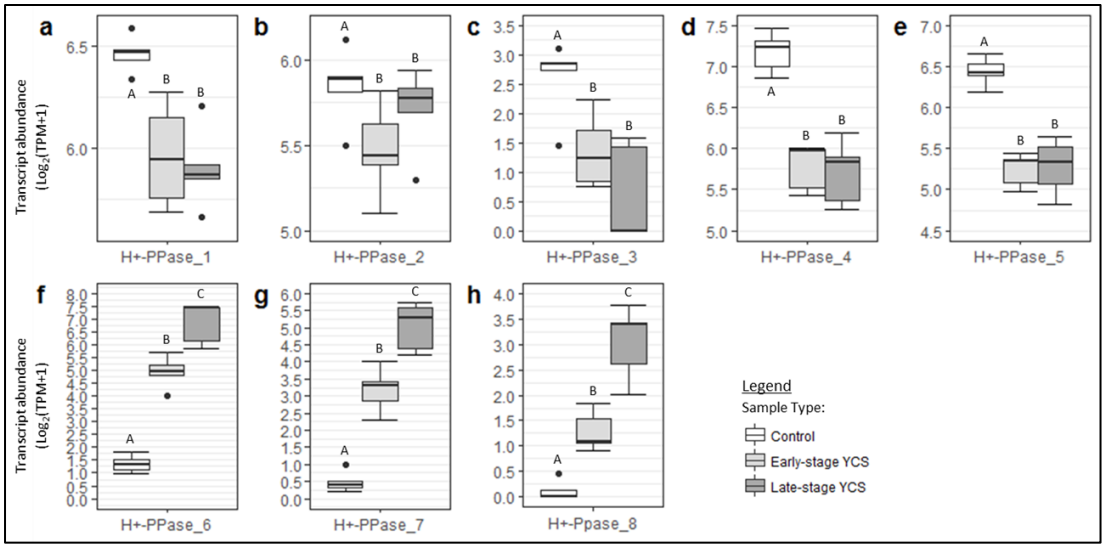

Figure 39 Transcript abundance of expressed H⁺-Pyrophosphatase (H⁺-PPase) transcripts in control, early-stage (ES)- and late-stage (LS)-yellow canopy syndrome (YCS)-affected Q240Φ sugarcane leaves. Data displayed as Log_2(TPM+1) value of reads mapping to reference transcript. (a) H⁺-PPase_1, (b) H⁺-PPase_2, (c) H⁺-PPase_3, (d) H⁺-PPase_4, (e) H⁺-PPase_5, (f) H⁺-PPase_6, (g) H⁺-PPase_7, (h) H⁺-PPase_8. Letters above (or below) sample type within graphs represent significant difference-groupings between sample types (differential expression analysis result false-discovery rate (FDR)-corrected P-value<0.05; fold-change>1.5). If letters not displayed within graph - no significant difference between sample types was present.

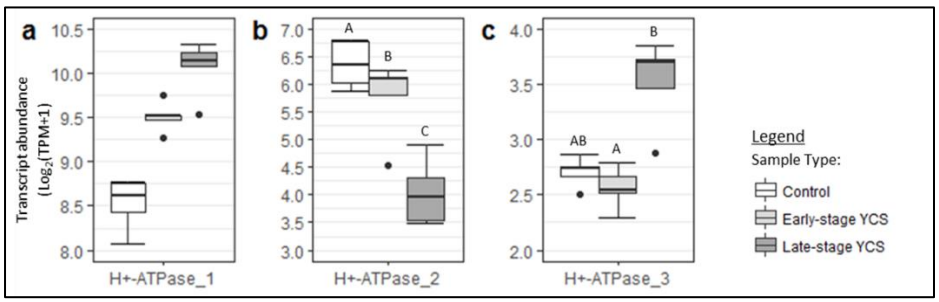

Figure 40 Transcript abundance of expressed H⁺-ATPase transcripts in control, early-stage (ES)- and late-stage (LS)-yellow canopy syndrome (YCS)-affected Q240Φ sugarcane leaves. Data displayed as Log_2(TPM+1) value of reads mapping to reference transcript. (a) H⁺-ATPase_1, (b) H⁺-ATPase_2, (c) H⁺-ATPase_3. Letters above sample type within graphs represent significant difference-groupings between sample types (differential expression analysis result false-discovery rate (FDR)-corrected P-value<0.05; fold-change>1.5). If letters not displayed within graph - no significant difference between sample types was present.

The combined data suggests that cellular regulation of sucrose movement, by the genes and proteins analysed, is not hindering sucrose export from the YCS leaf. Indeed, there is significant upregulation of transcripts involved in phloem loading and sucrose transport. This probably indicates that the loading and movement of sucrose is regulated by the prevailing sucrose levels in the leaf.

6.3.1.2. Sucrose translocation and carbon turnover (^{13}C labelling)

The synthesis and degradation of starch is essential for buffering and maintaining sucrose levels in the leaf. This is required to ensure that gene expression and metabolism is buffered against short term oscillation in sugar levels. It probably also ensures there is a constant stable supply of sucrose for export during the diurnal phase and oscillations in photosynthesis in events like cloud cover (Weise et al., 2011). In sugarcane, the priority of carbon assimilation is for sucrose with partitioning to starch regulated by sucrose synthesis (Stitt and Quick, 1989). Plants supplied with $^{13}CO_2$ can be

sampled at different time points to investigate carbon partitioning of photosynthates and carbon turnover (Sasaki et al., 2007; Uehara et al., 2009). Our research in this area was critical for us to understand the observed accumulation of sucrose and starch and carbon turnover within YCS asymptomatic and symptomatic leaves. A $^{13}CO_2$ pulse chase experiment in field grown sugarcane was conducted from early morning to the following afternoon (30-hour period). Through this we were able to measure the extent of disruption to carbon partitioning between starch and sucrose and the rate of carbon turnover. ^{13}C enrichment analysis across three sampling time points (AM & PM1 day 1, PM2 day 2) gave us insight into how phloem loading, and transport is linked to YCS and the effect it has on reduced carbon between the source leaves and the sink. In this section of the report we show how ^{13}C labelling enabled a better understanding of sucrose and starch accumulation, phloem loading, translocation, and carbon turnover within YCS source leaves.

The turnover of sucrose and starch in YCS leaves determines photosynthate partitioning in the leaf and other parts of the plant. The ^{13}C study revealed how much labelled fixed carbon was partitioned to sucrose and starch and how much remained in the leaf section after a period of 31 hours. We used this data to calculate turnover. The amount of heavy carbon in these two cellular components provides an insight to the diurnal changes that occur over the pulse chase period and disruption to diurnal metabolism in YCS plants. Table 5 shows the diurnal rate of change based on ^{13}C enrichment. YCS symptomatic Leaf 4 sucrose turnover is 1.5-fold lower and 2.5-fold higher than controls during the day and night period, respectively. Starch turnover is 5-fold lower in YCS than controls during the day period and 17-fold lower at night.

Table 5 ^{13}C sucrose and starch turnover rates during the light and dark periods YCS and control Leaf 4

	^{13}C sucrose % change of total pool during Light	^{13}C sucrose % change of total pool during Dark	^{13}C starch % change of total pool during Light	^{13}C starch % change of total pool during Dark
Control Leaf 4	-5.75%/hr	-0.625%/hr	+19.25%/hr	-12.7%/hr
YCS Leaf 4	-3.75%/hr	-1.54%/hr	+3.75%/hr	-0.75%/hr

^{13}C labelling shows that both metabolic pools fluctuate by varying amounts over the chase period. The percentage change between the sucrose pools is similar for control and YCS whereas the change in starch is much higher in controls (Table 5). More fixed carbon is allocated to starch in YCS leaf tissue (Figure 41) as this is most likely linked to the high sucrose levels effecting a preferential allocation of triose-phosphate (Triose-P) to starch (Figure 42). Sucrose and starch synthesis pathways are both dependent on the triose-phosphate precursor exported from the chloroplasts (Du et al., 2000; Weise et al., 2011) . During the 3-hour ^{13}C pulse there is a preference to partition more carbon as starch within YCS leaves than in the controls (Figure 41)

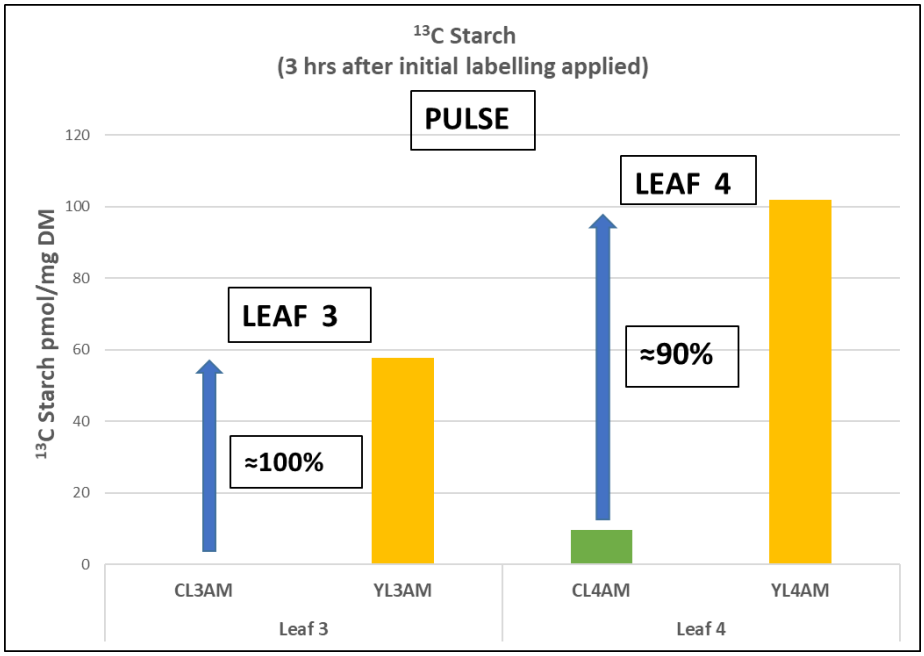

Figure 41 ^{13}C starch synthesis during pulse period

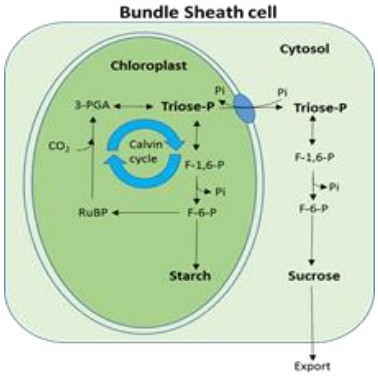

Figure 42 Carbon partitioning between sucrose and starch in the bundle sheath cell

There is approximately 2.5 times more ^{13}C sucrose in YCS leaf 3 & 4 than in control counterparts (Figure 43). Asymptomatic YCS leaf 3 (L3) has already started to accumulate sucrose and starch well before the onset of yellowing (Figure 43 & Figure 45) In maize, studies also saw accumulation of carbohydrates well before any visible yellowing. This suggests that yellowing is not the cause of carbohydrate hyperaccumulation but rather a secondary consequence (Braun et al., 2006). Yellowing in leaf 4 (L4) was clearly visible at the time of sampling and contains the highest sucrose content. YCS L3 & L4 lamina show increased accumulation of sucrose immediately after ^{13}C pulse as they contain approximately 60% more ^{13}C sucrose than the controls (Figure 44A). By end of chase YCS L3 & L4 show they have accumulated 40% & 60% more ^{13}C sucrose respectively than controls (Figure 44B). However, both the control and YCS leaf export (or convert to other metabolic products) approximately 70 - 85% of their respective ^{13}C sucrose pools by the end of the chase period (Figure 43). This is noteworthy considering the magnitude of the YCS ^{13}C sucrose pool which has been drawn down. The reduction in the ^{13}C sucrose pool in YCS leaves by the end of the chase, could be due to transport of sucrose out of the lamina, or the conversion to other metabolic products (Figure 44B).

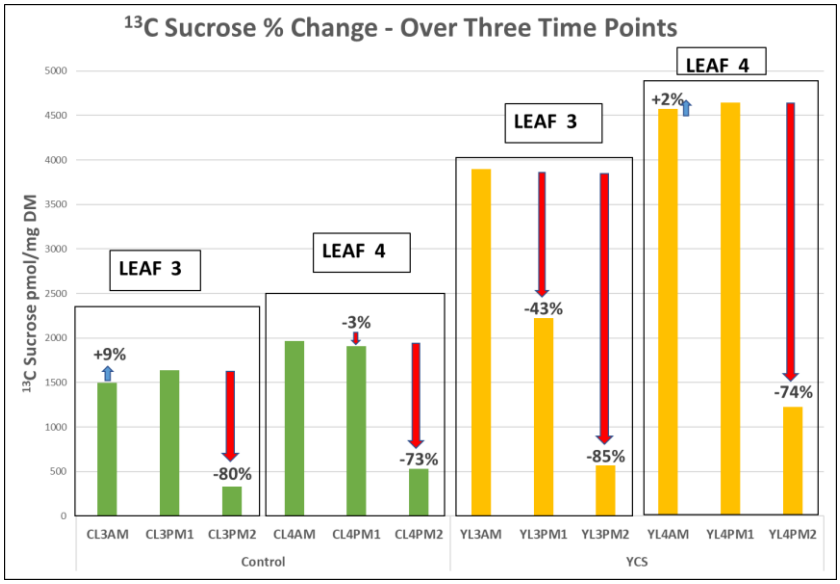

Figure 43 ^{13}C sucrose synthesis and proportional change across the pulse chase period; AM1 (3 hours), PM1 (8 hours) and PM2 (31 hours) post labelling, control and YCS Leaf 3 and 4.

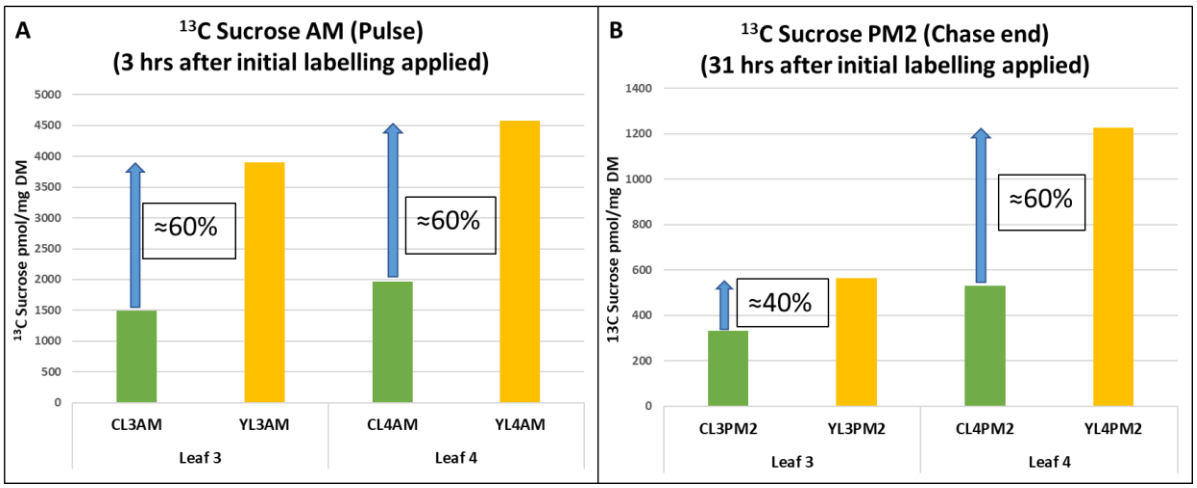

Figure 44 ^{13}C sucrose content L3 & 4 at the end of the pulse A) and chase end B) periods

Studies by Du (2000), observed synthesis and degradation of starch in sync with the diurnal rhythm. This mechanism is essential for a balanced control of sucrose synthesis and export, while at the same time ensuring a continuous supply of carbon throughout the 24-hour period (Weise et al., 2011). Figure 45 shows that Control L3 has not synthesised any starch by the end of the ^{13}C pulse. However, by the afternoon it has partitioned carbon as starch in preparation for the night period and by chase end all starch has been turned over. This oscillation is typical of the diurnal rhythm exhibited in a healthy plant. Control L4 which is more mature and displays a higher photosynthetic rate also displays a similar day night pattern. In contrast, asymptomatic YCS L3 had already begun to synthesise starch by the end of the ^{13}C pulse (similar quantity to control L4) and by the end of the chase it has turned over 81% of its starch. Symptomatic L4 on the other hand, had synthesised 10-fold more starch than its control counterpart by pulse end and only turned over 40% of its starch by chase end (Figure 45). It is worth noting at this point that the YCS leaf had a significantly higher total

sucrose pool (Figure 46) at the point of ^{13}C labelling (pulse) and this may have significantly influenced the partitioning of carbon towards starch.

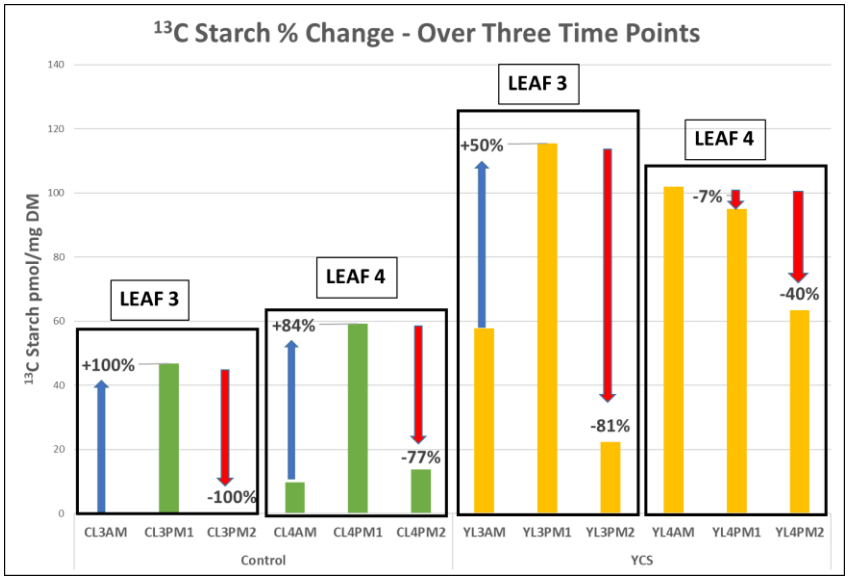

Figure 45 ^{13}C starch synthesis and proportional change across the pulse-chase period; AM1 (3 hours), PM1 (8 hours) and PM2 (31 hours) post labelling, control and YCS Leaf 3 and 4.

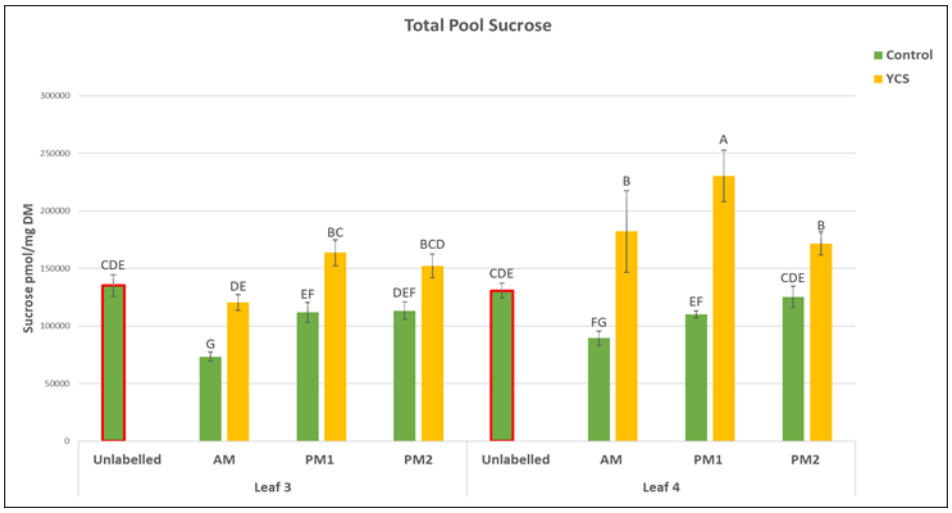

Figure 46 Sucrose total pool across the pulse-chase period. Tukey HSD All-Pairwise Comparisons (p<0.05)

In sugarcane, transitory starch is synthesised in the bundle sheath chloroplasts during the day to provide a carbon store for use during the night in the absence of photosynthesis. Starch synthesis also enables a higher rate of photosynthesis to be maintained during periods of high light and CO_2 when carbon assimilation exceeds the rate of sucrose synthesis and export. On the other hand, sucrose synthesis is favoured over starch when the photosynthesis rate is low (Baker and Braun, 2008; McCormick et al., 2008; Weise et al., 2011). Therefore, starch synthesis is an important function that enables a peak photosynthetic rate to be maintained by assimilating carbon overflow when photosynthesis is high, and also provides a means for carbon storage when photosynthesis is low (Baker and Braun, 2008; Weise et al., 2011), However, Figure 45 also shows there is a preference for starch synthesis in YCS leaves which have pre-existing elevated levels of sucrose (Figure 46). This

suggests that starch synthesis may have a third role, functioning as a safety net mechanism for carbon partitioning over sucrose when the internal environment of the leaf is not conducive for further sucrose synthesis. This is an extremely interesting finding, as unlike other crops the priority of carbon assimilation in sugarcane is for sucrose with partitioning to starch regulated by sucrose synthesis, not vice versa (Stitt and Quick, 1989).

The collective data of how YCS affects sucrose and starch metabolism strongly suggest that sucrose accumulation in the leaf (source) is likely the result of an overflow problem where carbon fixation and loading of sucrose in the source phloem exceeds the sink capacity. Such a system would result in sucrose accumulation throughout the phloem and eventually in the primary cells of synthesis (mesophyll and bundle sheath). Sucrose build up in the phloem and sites of production would also result in accumulation of sucrose in the apoplastic space (leakage from the phloem and facilitated diffusion out of the mesophyll and bundle sheath cells). Once sucrose levels exceed a threshold in the mesophyll and bundle sheath cells, photosynthesis and chlorophyll synthesis is inhibited resulting in yellowing. This mechanism seems to be universally present in the Poaceae (Braun et al., 2006; Baker and Braun, 2008).

Analysis of the 'total carbon pool' in this ^{13}C field study shows there is a significant difference in sucrose and starch content in the leaf sheath between control and YCS in both the morning and afternoon (Figure 47). This demonstrates that photosynthesis is still active in the YCS symptomatic leaves and translocation is occurring. However, within both control and YCS sheath there is no significant difference in sucrose or starch content between morning and afternoon (Figure 47). This result is not unexpected as the leaf sheath lacks some of the more specialised cells present in the lamina and no stomata to allow for gas exchange and carbon fixation. The sheath's main role is one of structural support and as a conduit to facilitate translocation of photosynthates between the lamina and the culm (Rae et al., 2014).

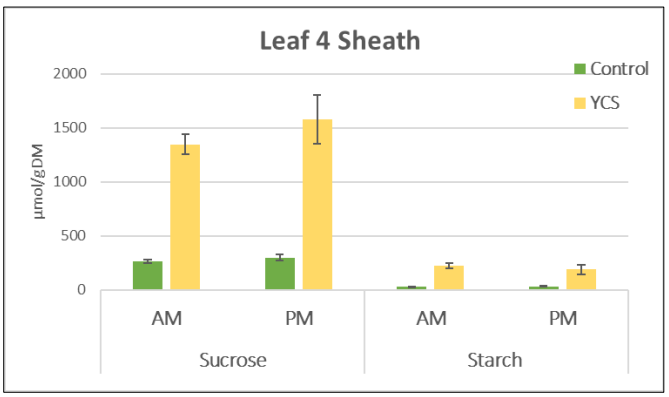

Figure 47 Q240$^{\Phi}$ Leaf 4 sheath sucrose and starch content, AM & PM

As expected for a healthy, green control leaf partitioning carbon in sync with the diurnal rhythm, the lamina has significantly higher sucrose and starch levels in the afternoon than the morning. However, YCS lamina exhibits a complete disruption in this mechanism as there is no significant difference to both sucrose and starch content throughout the day (Figure 48). This pattern of sucrose and starch accumulation is evident of a carbon partitioning imbalance resultant of impeded translocation of sucrose out of the leaf.

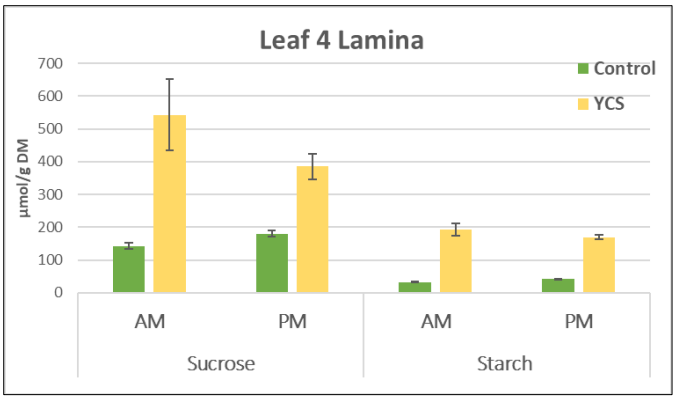

Figure 48 Q240Φ Leaf 4 lamina sucrose and starch content, AM & PM

It is important to note that the cellular composition of both the lamina and sheath is proportionally different. When studying the structure of the sheath it is apparent that this tissue contains large pads of sclerenchymatous fibre and a larger proportion of vascular bundles per unit area than that of the lamina (Rae et al., 2014). It would therefore be inappropriate to draw conclusions by comparing sucrose and starch content on a one to one basis between sheath and lamina as a quantity per unit mass fresh or dry mass. Hence, investigation of the sheath to lamina ratio for both sucrose and starch is a more apposite method to gain an understanding of where these carbohydrates accumulate in the leaf. Figure 49 shows that YCS symptomatic leaf 4 has significantly higher sucrose content in the sheath than the lamina in the afternoon than that of the control (4:1 & 1.6:1 respectively). This is also evident in the morning, but to a lesser extent (YCS 2.5:1, control 1.8:1). Noteworthy is the 1.6-fold increase in the sucrose sheath to lamina ratio of the YCS leaf between the morning and afternoon. As there was no significant difference in YCS lamina sucrose content between AM & PM this implies that the leaf lamina is continuing to synthesise and export sugars throughout the day. However, sucrose is beginning to accumulate in the sheath during this period (Figure 48). The reason for this accumulation may be due to a full or partial blockage of the phloem or a decrease in sink strength. No such pattern is visible in the controls. This evidence also supports the results obtained in the ^{13}C labelling field experiment where 70-85% of the ^{13}C sucrose pool had been drawn down from the lamina across the pulse chase period of 31 hours (Figure 43).

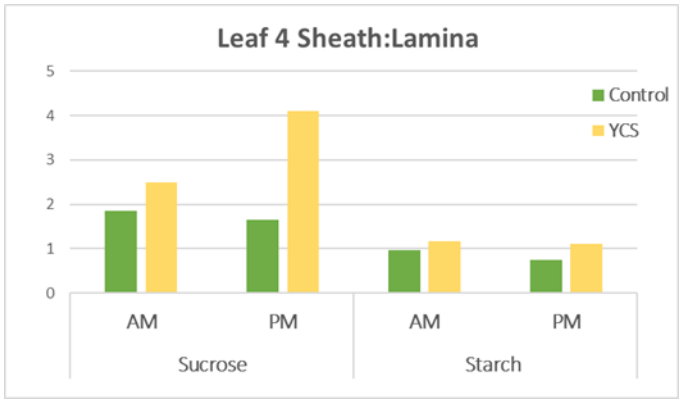

Figure 49 Q240Φ Leaf 4 sucrose and starch sheath:lamina ratio, AM & PM

The sheath to lamina starch ratio is unremarkable for the morning period but interestingly there is a 1.5-fold difference in the ratio between YCS and control in the afternoon (Figure 49). This is consistent with the world literature that states starch synthesis enables a higher rate of photosynthesis to be maintained during periods of high light and CO_2 when carbon assimilation

exceeds the rate of sucrose synthesis and export (YCS: physical blockage of phloem or impeded sink strength). Assimilation of carbon overflow into starch synthesis also provides a means for carbon storage (Baker, 2008). The YCS sheath to lamina starch ratio also supports the ^{13}C results which clearly showed a preference for starch synthesis in YCS leaves when a pre-existing elevated level of sucrose exists. Therefore, in the high sucrose environment of the YCS sheath (Figure 47) starch synthesis is favoured as a mechanism for carbon partitioning over sucrose when the internal environment is not conducive for further sucrose synthesis. As synthesis of sucrose or starch is dependent on the triose-phosphate precursor, the metabolic needs of the plant can direct which pathway is followed (Figure 42) (Du et al., 2000; Weise et al., 2011).

There is significantly more sucrose and starch in YCS lamina than controls but no significant difference in sucrose and starch content between the tip and the base within control and YCS leaves. The YCS sheath also has significantly higher levels of sucrose and starch than controls. The link between leaf sucrose and starch supports the hypothesis that the retention of photoassimilates is involved in YCS yellowing. Examination of the sucrose and total α-glucan pools from the leaf sheath to the tip, for both the morning and afternoon period, also gave an insight to disruptions to mechanisms surrounding carbon partitioning in different age (YCS leaf 3 asymptomatic & YCS leaf 4 symptomatic) sections of the YCS leaf. Interestingly, the pattern of change in the sucrose to total α-glucan ratio is the same between YCS and control leaf 4 in both the morning and afternoon (Figure 50A & B). The same pattern is also evident for leaf 3, strengthening the argument that the changes are happening well before the onset of visual symptoms.

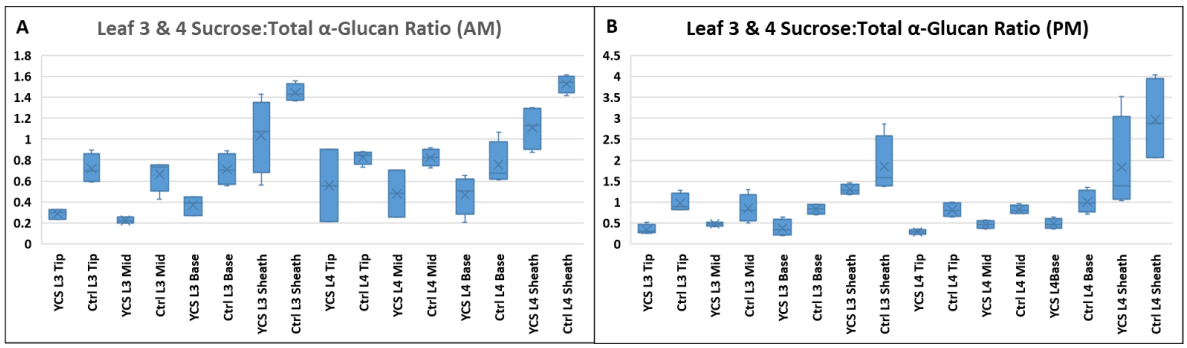

Figure 50 Control and YCS asymptomatic Leaf 3 and symptomatic Leaf 4 sucrose to total α-glucan ratio morning A) afternoon B)

There is disruption to carbon partitioning in YCS leaves with a preference to starch and soluble α-glucan synthesis over sucrose when hyperaccumulation of sucrose occurs. The fact that sugar/α-glucan is higher in the YCS sheath, despite YCS symptomatic leaves being photosynthetically less active, is consistent with the model that the carbon export from the sheath is compromised. There is no significant difference in sucrose and α-glucan content along the leaf blade between the tip and the base, the ratio between sucrose and α-glucan (including the sheath) shows a similar pattern change between YCS and control both in the morning and afternoon. Maintenance of this metabolic balance supports earlier observations that there appeared to be equilibrium between the cytosol and apoplast of the phloem, bundle sheath and mesophyll cells for both phenotypes even when there is a source sink imbalance. Therefore, the collective ^{13}C and total carbon pool data indicates that the sucrose accumulation in the YCS source leaf is the result of an overflow problem where carbon fixation and loading of sucrose in the source phloem exceeds the sink capacity.

In a leaf unable to export more carbon than is assimilated, sucrose will eventually push through the tolerable upper threshold unless synthesis is curtailed. Therefore, an efficient regulatory mechanism to reduce sucrose synthesis while protecting the photosystems from oxidation would be required. Unless the plant possesses the means to reduce incoming solar energy at the same time this mechanism will be limited, as excess energy leads to the production of ROS during photosynthetic downregulation. Furthermore, as sugarcane has the physiological ability to produce a new leaf approximately every seven days (approximately 150 °Cd) it is most likely more energy efficient to sacrifice compromised leaves and redirect energy to the younger source and sink leaves. Obviously, there is a cost benefit ceiling that would be determined by plant vigour. This model adds support to observations pertaining to the lack of YCS severity in high yielding crops which have both vigour and high sink strength (see section 6.7.1 of this report).

6.3.2. Leaf sucrose accumulation at a cellular level

Sucrose synthesised in the cytoplasm of the mesophyll and bundle sheath cells diffuses through the plasmodesmata into the vascular parenchyma cell via the symplast. As discussed in section 6.3.1.1 of this report, sugarcane is an active phloem loader and uses a combination of sweet proteins to move sucrose from the symplast to the apoplast of companion cells, and sucrose symporters (SUTs) then actively load the sieve elements against the concentration gradient. Analysis of apoplastic fluid sugars allows further insight into the status of phloem loading and where sugar is accumulating at a cellular level.

6.3.2.1. Apoplastic sugar levels

It is notoriously difficult to extract apoplastic fluid from sugarcane leaf but subsequent attempts to do so from leaf sheath and midrib have proved successful (Husted and Schjoerring, 1995). An optimized methodology consisting of pressure infiltration and low speed centrifugation was implemented under field conditions to extract apoplastic fluid from KQ228$^{\phi}$ control and YCS leaf sheath. The extract was analysed for sugars using standard enzymatic assays (Bergmeyer and Bernt, 1974).

Sucrose hydrolysis by cell wall acid invertase in the apoplast should liberate equal proportions of glucose and fructose. However, Figure 51B shows the ratio of sucrose to glucose and fructose is not equal for either control or YCS plants. However, the ratio in the controls is much closer to 1:1 than in YCS. Glucose concentrations are also significantly lower than fructose in both controls and YCS (Figure 51A). The disproportionate amounts of YCS sucrose to glucose and fructose may indicate that an opportunistic organism is hydrolysing sucrose and consuming large quantities of both glucose and fructose in this space. Sucrose levels in the YCS apoplast are significantly higher than controls (approx. 3 fold), which is consistent with levels measured in total tissue assays of the lamina and midrib (see section 6.2.6 of this report Figure 29A & D). This would suggest that there is equilibrium between the cytosol and apoplast of the phloem, bundle sheath and mesophyll cells for both phenotypes as previously noted in the lamina and midrib. High levels of sucrose accumulation in the apoplast of YCS tissue implies that sweet proteins are functional in their transport of sucrose across the parenchyma cell membrane. As our studies have shown there is significant upregulation of transcripts involved in phloem loading and sucrose transport, it is therefore unlikely that an apoplastic pathogen is the cause of high sucrose levels in the apoplastic space. Upregulation

suggests the cells are constantly trying to move excess sugars out of the source cells, implying that both the cytosol and apoplast are saturated with sucrose.

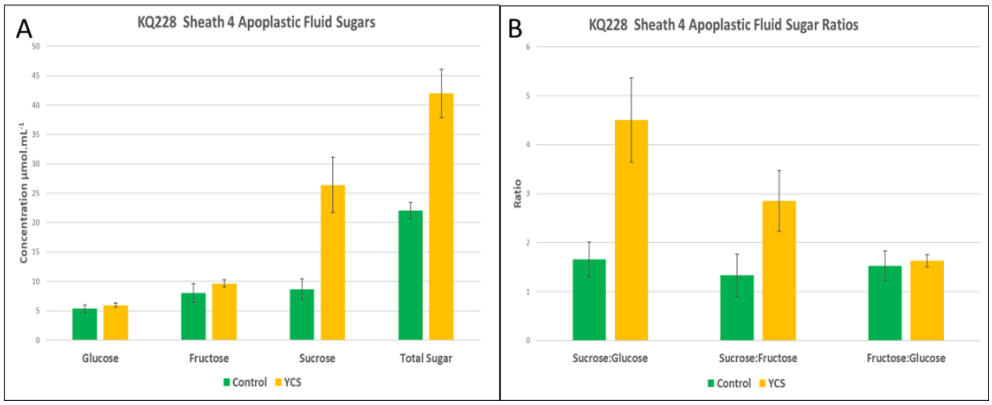

Figure 51 Apoplastic sugar concentrations; sucrose and reducing sugars A) apoplastic sugar ratios B)

The apoplastic data supports ^{13}C studies that sucrose accumulation in the YCS source leaf is likely an overflow problem from the phloem into the surrounding tissue. This could result from a physical blockage in the phloem.

6.3.3. Physical blockage of the phloem and plasmodesmata

The integrated YCS program initiated a directive to analyse our current leaf transcriptome and proteome data for phytoplasma signatures in the search for a phloem blocker. This directive was derived through consultation with Dr Owain Edwards (CSIRO).

6.3.3.1. Bioinformatic analyses of both the reference YCS transcriptomes (leaf and internode) and the raw reads for sequences from phytoplasmas and other micro-organisms

Bioinformatic analyses of reference transcriptomes was done using Kraken software (Wood and Salzberg, 2014) to identify any sequences that did not originate from sugarcane and may instead have come from micro-organisms like phytoplasmas.

A search of the YCS Leaf transcriptome assembly failed to find any matches to phytoplasma sequences (see Appendix 5), even when the search was expanded to include the broader 'mollicute' class. However, the analysis did reveal a high number of matches to the bacterium Ralstonia pickettii. This organism is known to be a contaminant of common laboratory and hospital solutions and has most likely been accidently sequenced and transcript assembled. Taking this information into consideration and the lower abundance of this microorganism in YCS samples, we conclude that Ralstonia pickettii is unrelated to YCS (see Appendix 5).

Similarly, a search was conducted for the broader 'mollicute' sequences, sourced from the NCBI RefSeq database, in the internode transcriptome assembly. The best match was to an 'ATP synthase subunit' from 'Mycoplasma sp. HU2014' with a 70 % (546/776) identity match on a contig that was 6771 bases long. However, taking that entire contig sequence and blasting it to the wider 'nr' database, the contig's annotation comes up as 'Saccharum officinarum mitochondrial chromosome 2 DNA, complete genome, cultivar: Khon Kaen 3' with a 99 % (3860/3870) identity match. This showed that the contig was not from mycoplasma, but instead was just mitochondrial transcript from sugarcane. No phytoplasma sequences were found in the YCS Internode assembly.

Across the transcriptome assemblies, the analysis of non-sugarcane sequences showed no microbial signature of any significance in association with YCS.

6.3.3.2. Phytoplasma proteins

Australian Proteome Analysis Facility (APAF) performed an initial analysis of leaf protein data to identify potential phytoplasma protein sequences (1D). Signatures for 16 different phytoplasma species were detected with reasonable confidence in the leaf tissue.

Further analyses were performed in an attempt to quantify the phytoplasma signatures between samples using protein matches to gene expression data (a “rough” idea). Results indicated a potentially greater abundance of phytoplasma in YCS leaf samples, however this was also the case in senescent leaf tissue (Figure 52).

Similar 1D (i.e. lacking quantitation) analysis of internode proteome data was performed. Approximately 20 different phytoplasma species (early-stage analysis) were detected and likely to be in control (healthy), Moddus-treated and YCS-expressing internode samples. At this stage, quantification between internode sample types has not been determined (requiring transcriptome cross-referencing).

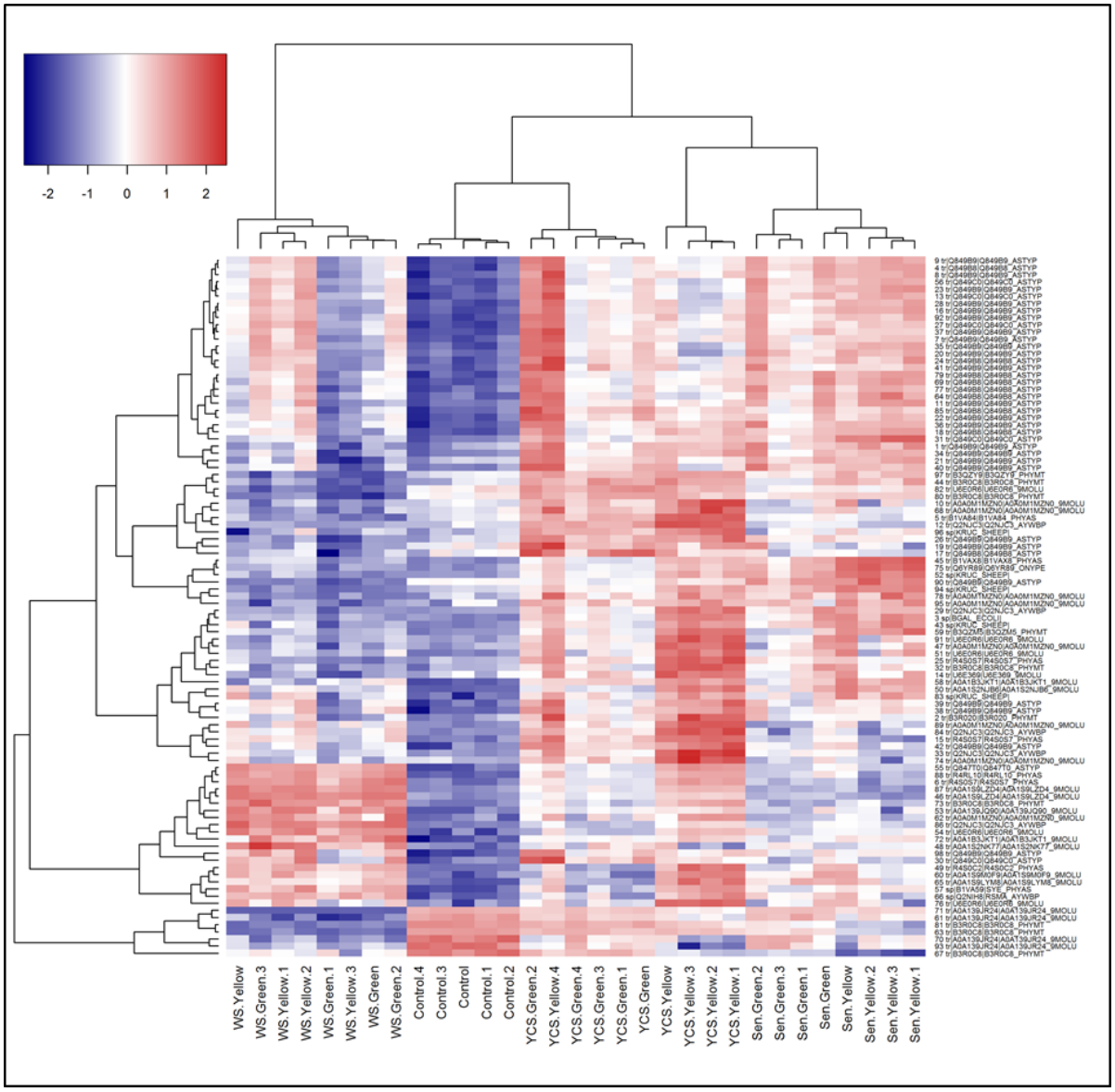

Figure 52 Heatmap of Q240$^{\Phi}$ sugarcane leaf samples and phytoplasma peptide matches, quantification comparison through transcriptome contig expression levels. Blue indicates lower abundance; red indicates higher abundance. Sample replicates listed along base of heatmap (control = healthy, YCS = yellow canopy syndrome, Sen = senescence, WS = water-stress. Green = early-stage of stress, yellow = late-stage of stress)

6.3.3.3. Non-sugarcane organisms as potential causal agent of YCS

Bioinformatic analyses of the raw RNAseq reads was also done using Kraken software (Wood and Salzberg, 2014) to identify any sequences that did not originate from sugarcane and may instead have come from micro-organisms like phytoplasmas.

Analyses of leaf, midrib, dewlap, and culm tissue collected across five field visits and three regions (Herbert, Burdekin, and Mackay) failed to identify the involvement of a micro-organism or phytoplasma in YCS development or expression. While some species of type Candidatus, mycoplasma and spiroplasma were detected, they were equally present, or more abundant, in the Control samples rather than the YCS samples. While Curtobacterium does figure prominently as the most identifiable microorganism, with YCS fold change differences to control in the number of reads counted (Lamina: 1.46, Midrib: 3.3, Dewlap: 2.11, Internode: 0.61), the signature became

insignificant when a differential expression analysis was conducted. The same was true of the bacterium Bacillus cereus m 1293 and Banana Streak CA virus.

Across the multiple RNAseq datasets produced in this project, the analysis of non-sugarcane sequences showed no microbial signature of any significance in association with YCS.

6.3.3.4. Callose

Changes to gene expression associated with a physical blockage in vascular tissue

Callose is a β-1,3-glucan polysaccharide (1,3-β-linked glucose residues) that is transiently produced by plants during development, and in response to both abiotic and biotic stress (Chen and Kim, 2009). It occurs intrinsically within the sieve plates of the phloem, cell plates of dividing cells, plasmodesmata canals, reproductive organs, and root hairs. Accumulation is usually transitory and bulk flow of phloem sap can be regulated by callose deposition or degradation. Therefore, control of callose deposition is a key mechanism of phloem sap transport. It can be synthesized rapidly with deposition localised in response to wounding, abiotic stress, mechanical stress and pathogen infection (Kohle et al., 1984).

As a defence mechanism, callose deposition can be deployed by plants to limit access to nutrients by restricting solute movement between plant cells (Varsani et al., 2019). This method is effective against both pathogens (like viruses), and pests (like sap-sucking insects). Defensive callose deposition occurs within the phloem and plasmodesmata, and contributes to sieve element and plasmodesmata occlusion (Will and van Bel, 2006; Julius et al., 2018). In this way, plants can restrict movement and feeding opportunities, and effect a measure of control over populations of phloem-feeding insects (Will and van Bel, 2006).

Callose quantification

Quantification of lamina, midrib, and sheath callose through fluorescence spectroscopy indicates uniform content between control and YCS plants within each of the three leaf tissues. Callose content within lamina and midrib is comparable between leaf 3 and 4, whereas leaf 4 sheath levels are approximately 2-fold that of leaf 3 in both control and YCS tissue (Figure 53A & D). A similar pattern also holds for the gradient between the leaf tip and sheath within in all three tissue types (Figure 53B & C). Interestingly the mid-tip region in both controls and YCS has less callose than any other region in the lamina and midrib (Figure 53B & C). Further investigation of any correlation between sucrose and callose is unremarkable (Figure 54A-D). This data suggests that callose deposition in the lamina, midrib or sheath is unlikely to be responsible for reduced sucrose translocation and leaf accumulation. However, it cannot accurately describe accumulation at a specific site within the plasmodesmata or other vascular tissue. As each of these tissue types has a different proportion of vascular tissue there may be differences at the micro level. Nonetheless, it does suggest that on a µg/mg leaf dry mass basis there is no evidence of variation between the vasculature of controls and YCS leaves.

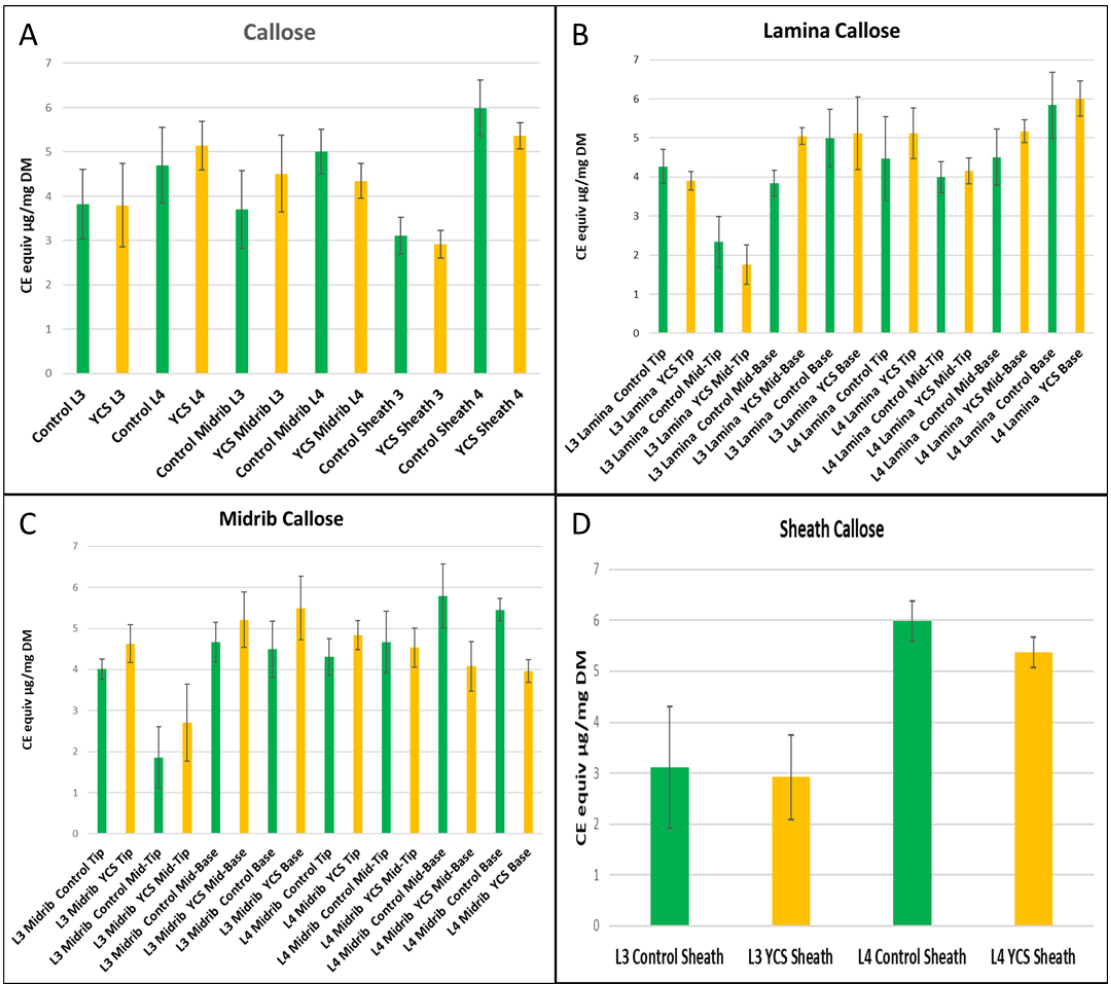

Figure 53 Q240$^{\Phi}$ Callose content-Curdlan (CE) equivalent, Control and YCS asymptomatic Leaf 3 and symptomatic Leaf 4, lamina, midrib and sheath A) Lamina gradient B) Midrib gradient C) Sheath D)

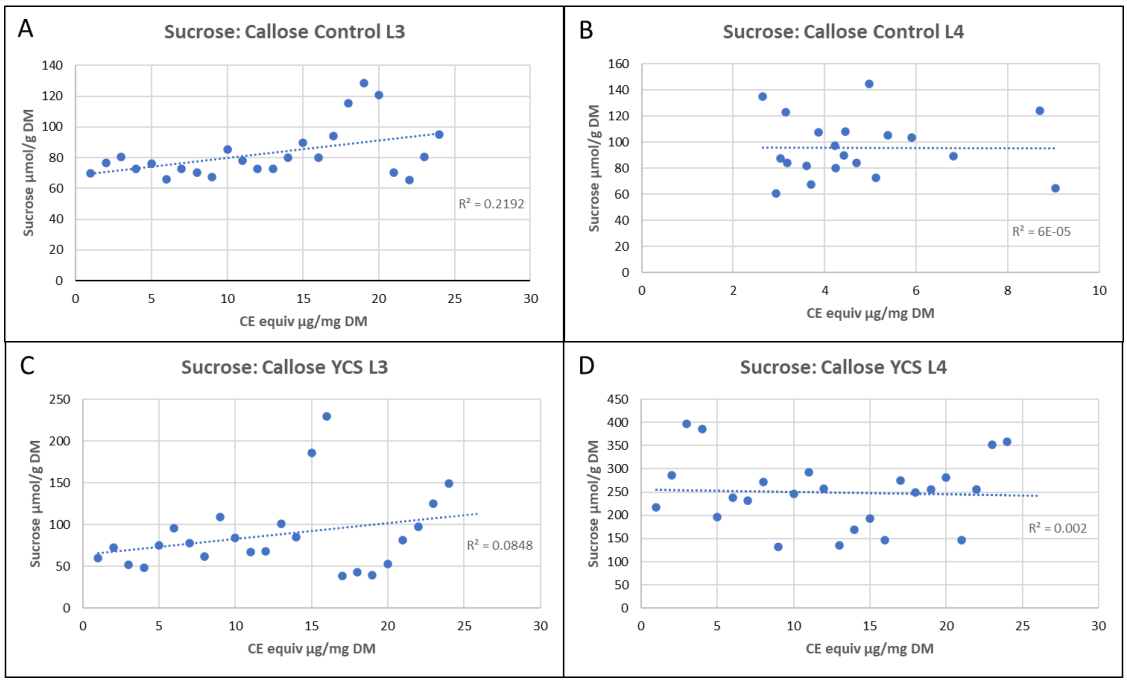

Figure 54 Lamina Sucrose callose correlation, Control and YCS asymptomatic Leaf 3 (A, C) and Control and YCS symptomatic Leaf 4 (B, D)

Callose is produced by callose synthase (CalS) enzymes (alternatively called glucan synthases, although the isoform numbering is not transferable between the two), and degraded by β-1,3-glucanases (Chen and Kim, 2009). There are twelve known isoforms of callose synthase, divided into 4 main sub-families (Chen and Kim, 2009). Loss-of-function analyses have identified the specific role played by many of the isoforms (Chen and Kim, 2009).

From this work, we know that CalS-3 and CalS-8 are involved specifically in plasmodesmatal deposition, and CalS-7 in phloem deposition (Barratt et al., 2011; Cui and Lee, 2016). Higher expression and abundance of CalS-3, CalS-8 and CalS-7 would occlude the plasmodesmata and phloem sieve elements, either partially or fully, and thus limit sucrose export from leaf.

Given that we know sucrose export is hindered in YCS, we looked for transcriptomic evidence of these callose synthase isoforms expression in YCS. We found increased expression in YCS of all three isoforms, plus another callose synthase without an isoform designation (Figure 55).

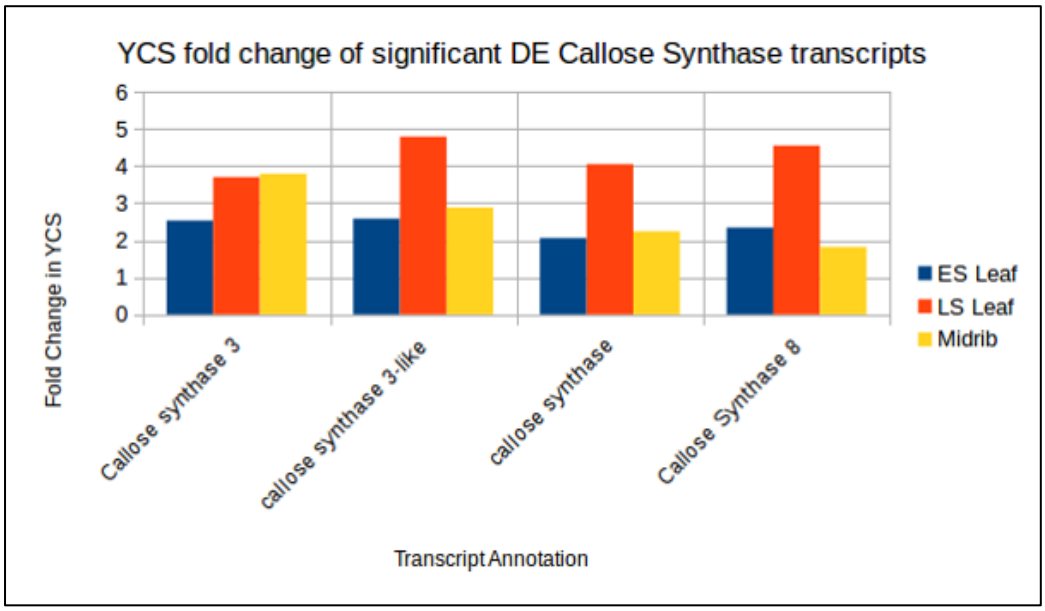

Figure 55 Increased expression of plasmodesmata- and phloem-specific callose deposition CalS isoforms in YCS (ES = early stage YCS lamina, LS = late stage YCS lamina)

While CalS-3 and CalS-8 (and the unidentified CalS isoform) were in higher abundance in YCS, the biggest fold change is in the CalS-7 expression. Callose synthase 7 isoform was expressed only in the phloem sieve elements (Barratt et al., 2011). The transcript, YCS-internode-contig_105736 'Callose synthase 7', (2544 bases long), was the only callose-related transcript that was significantly differentially expressed in YCS (Bonferroni < 0.0001) in each of leaf, midrib and dewlap tissue, and internode tissue (Bonferroni = 0.03). Fold change in YCS of this transcript by tissue type is shown in Figure 56.

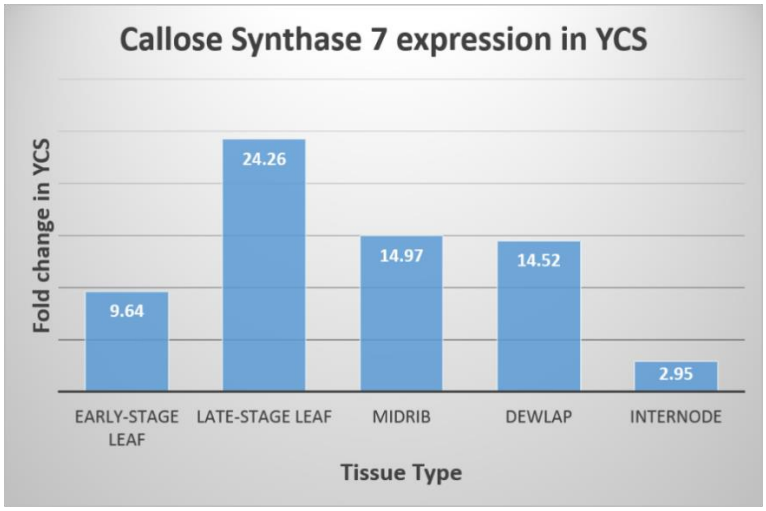

Figure 56 Fold change in YCS expression of callose synthase 7, by tissue type

These results suggest that there is not a tight correlation between callose synthase gene expression and callose levels (Figure 53).

Plasmodesmata-associated proteins involved in plasmodesmata permeability

There are many plasmodesmata-located and -associated proteins that regulate plasmodesmata permeability. For example, beta-glucanase and plasmodesmata-associated protein complexes play a role in callose turnover in plasmodesmata, as do proteins involved in plasmodemata callose binding (Ueki and Citovsky, 2014). In addition, calreticulin, glycosyltransferase, reversibly glycosylated polypeptides, receptor-like proteins, remorin, PDLP, HopW1, and Gpi-anchor plasmodesmal neck proteins are all associated with plasmodesmata permeability (Ueki and Citovsky, 2014).

We looked for transcriptomic evidence of these proteins being upregulated in YCS. While the YCS Reference transcriptome contained many of these transcripts, only one (YCS-internode-contig_137580 'Remorin family', size 5421 bases) was significantly differentially expressed in YCS (Bonferroni 0.03) but was weakly expressed overall and only two fold in higher abundance in YCS. In summary, plasmodesmata-associated permeability proteins are unlikely to play a role in restricting sucrose export in YCS.

At the time of this report, extensive research conducted across the YCS Integrated Research Program has failed to find conclusive evidence in support of a physical blockage in the leaf phloem or plasmodesmata. This is aligned with the findings of this report. A more likely explanation would be carbon fixation and loading of sucrose in the source phloem exceeding the sink demand.

6.3.4. Changes to the metabolome, transcriptome, and proteome

Although visual yellowing is usually only evident in the lower leaves of the canopy (older than leaf 5) photosynthesis and stomatal conductance are reduced both in yellowing leaves and the leaves not yet showing any visible yellowing. On a canopy basis, photosynthesis is reduced by 14% and 36% in YCS symptomatic KQ228$^{\phi}$ and Q200$^{\phi}$ plants, respectively (Marquardt et al., 2016). Sucrose levels increased significantly and reflects some of the earliest changes that are induced in the YCS symptomatic plants. In addition, there are disruptions on both electron acceptor and donor side of photosystem II (Marquardt et al., 2016). Some of these changes are characteristic of a degree of disruption of the protein structure associated with the electron transport chain. Based on the

results, we proposed that the first change in metabolism in the YCS symptomatic plants is an increase in sucrose and that all the other changes are secondary effects modulated by this increased sugar levels.

To form a better understanding of the above, we studied the metabolic, gene expression and protein changes that accompany the expression of YCS in sugarcane (Botha et al., 2016). This information would be important to assist in developing management strategies as well as in the identification of potential causal factors.

6.3.4.1. Metabolites

More than 200 metabolites were detected in the leaf samples and 84 of these could be identified. The results revealed intrinsic differences ($p < 0.05$) between the metabolomes of the YCS symptomatic and asymptomatic plants. It was evident that significant metabolic changes occurred well before the development of leaf yellowing. The major metabolic changes were associated with sugar metabolism, the pentose phosphate cycle, and phenylpropanoid and α-ketoglutarate metabolism. The diurnal changes of sucrose concentrations (low in the morning and high at the end of the day) are absent in the YCS symptomatic plants even before symptom expression. Comparing the leaf transcriptomes of the symptomatic and asymptomatic plants shows that a complex network of changes in gene expression underpins the observed changes in the metabolome.

PCA analysis separates Control and YCS metabolite samples into distinct clusters (Figure 57). However, the overlay of YCS AM and PM is indicative of disruption to the diurnal rhythm in YCS plants. While there is overlap in control samples, clear separation between the morning and afternoon metabolites is indicative of healthy transitioning in preparation for the night period. The main metabolites driving the separation between controls and YCS are the soluble sugars reported in section 6.2.5 (Figure 58).

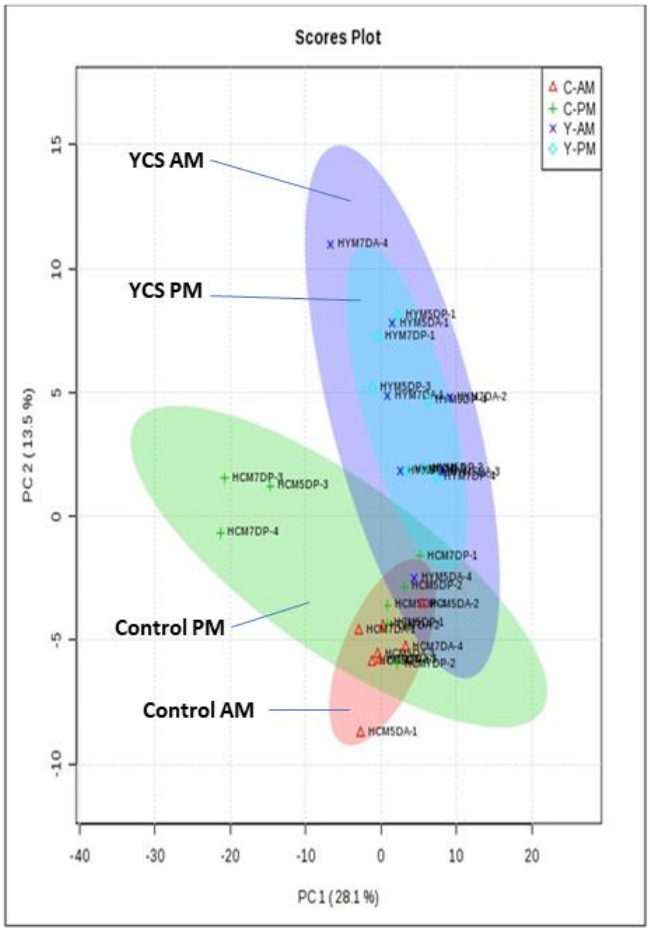

Figure 57 PCA analysis Control and YCS AM & PM (Botha et al., 2015)

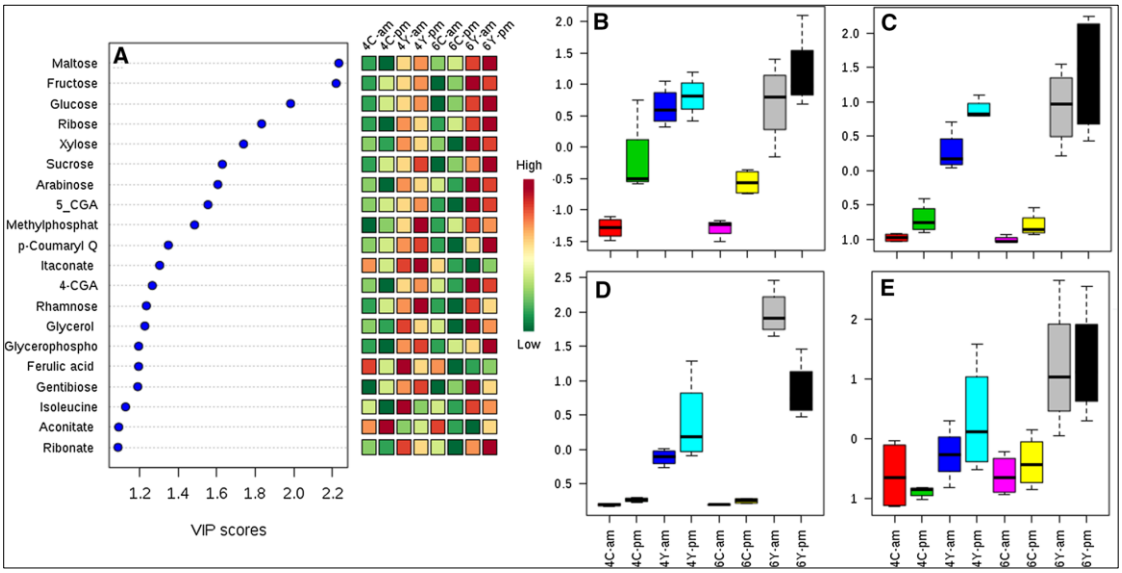

Figure 58 VIP scores with the corresponding heat map of statistically significant metabolites from YCS symptomatic (4Y, 6Y) and asymptomatic (4C, 6C) leaf tissue in the morning and late afternoon (a). Green and red indicate decreased or increased metabolite levels. Relative abundance of sucrose (b), glucose (c), fructose (d) and maltose (e) (Marquardt et al., 2017)

Figure 59 shows changes to the metabolites derived from the pentose phosphate cycle and associate phenylpropanoid pathway. No significant variation is noted in these metabolites between the morning and afternoon of YCS asymptomatic Leaf 4 and symptomatic Leaf 6. This is evident of an early response to oxidative stress in YCS leaves before the onset of yellowing (Marquardt et al., 2017).

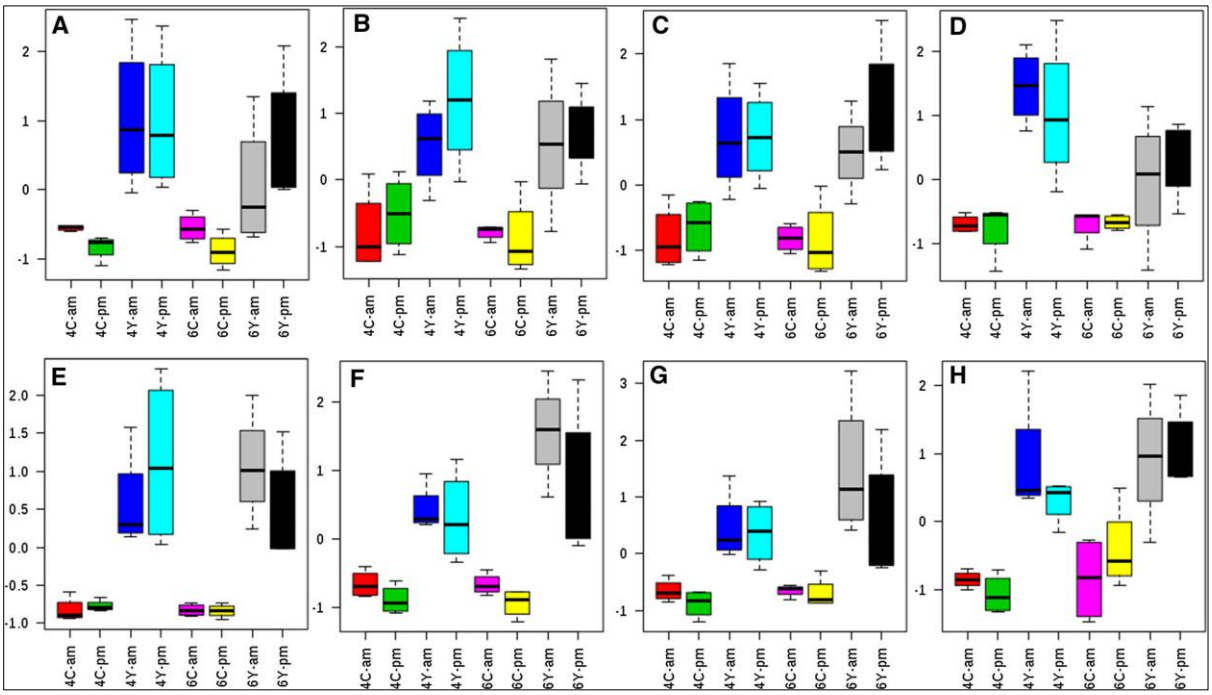

Figure 59 Relative changes in metabolites from YCS symptomatic (4Y, 6Y) and asymptomatic (4C, 6C) leaf tissue associated with the phenylpropanoid pathway (A–D), and the pentose phosphate cycle (E, F). Shikimate (A), caffeoyl quinate (B), coumaroyl quinate (C), quinate (D), rhamnose (E), xylose (F), arabinose (G) and ribose (H) (Marquardt et al., 2017)

6.3.4.2. Gene expression

For this analysis, the RNAseq reads were mapped to the PacBio (v1.02) sugarcane transcriptome (Hoang et al., 2018). Analysis of upregulated genes for identification of metabolic pathways (GO analysis; Blast2G0) unique to YCS yellowing showed carbohydrate metabolism and the phenylpropanoid pathway were foremost impacted (Figure 60). Notable is the gluconeogenesis category, containing the largest number of genes with altered expressed. Gluconeogenesis channels triose phosphate into sucrose and starch (Sung et al., 1988). Importantly, sugar metabolism pathways, including fructose, mannose and carbohydrate phosphorylation were also affected, as was starch synthesis and breakdown (malate metabolism). These results are consistent with sugar and starch accumulation found to be associated with YCS leaf symptoms, indicating these pathways are affected in a unique way during YCS symptom development.

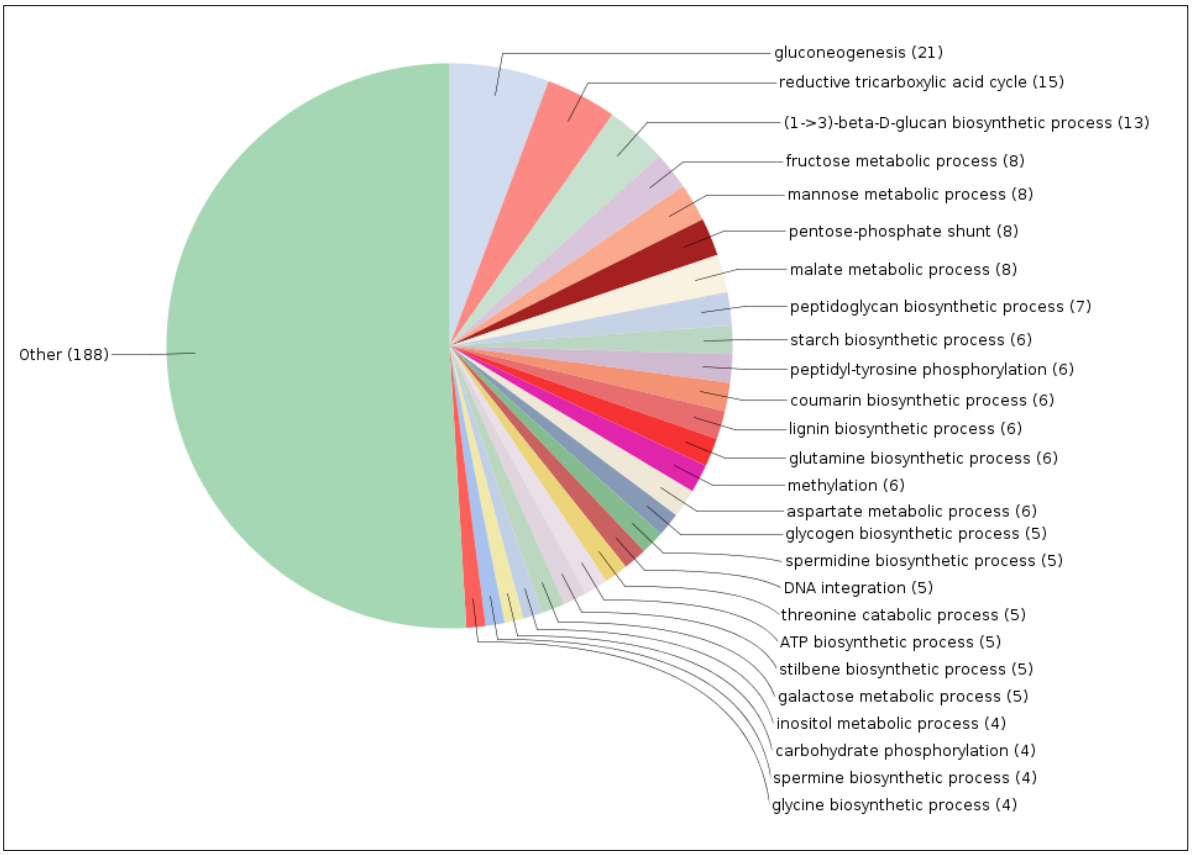

Figure 60 Pie chart of Biological Process, subgraph Metabolic Process GO ontology categorization of 808 upregulated genes unique to YCS leaf yellowing (FDR-corrected P-value < 0.001). Numbers in brackets represent number of genes within category. Category "Other" blankets categories containing < 0.5% of total number of genes.

RNA sequencing data from samples obtained across four genotypes and three geographical regions were mapped against the sugarcane transcriptome reference database (Hoang et al., 2017; Hoang et al., 2017; Hoang et al., 2018) using CLC Genomics Workbench v9.5.3 software. A two-group unpaired differential expression analysis using Baggerley's proportions was done, separating the samples into Control versus YCS, including a statistical analysis of the results with Bonferroni-corrected p-values, to find the statistically significant differentially expressed transcripts. Figure 61 shows the volcano plot of fold change against p-values. From this analysis, a total of 109 transcripts were found to be differentially expressed with a Bonferroni-corrected p-value of less than 0.05. Of the 109, only 9 had a fold-change in expression greater +/- 1.4. Looking at those 9 and starting with the transcripts with lower abundance in YCS samples, there are 4 which are expressed in the Control samples but not in the YCS samples at all, which gives them a fold-change of minus infinity. These 4 include

- c110365f1p05811 U-box domain-containing 4
- c66641f1p0949 clathrin light chain
- c39217f2p01829 von Willebrand factor type A domain-containing protein
- c61736f1p0907 probable NAD(P)H dehydrogenase (quinone) FQR1-like 1.

The U-box domain-containing transcript is involved in the E3 ligase step of protein ubiquitination. This process leads to the degradation of unwanted proteins within the cells and is a necessary part of normal metabolism (Amm et al., 2014). Not having this transcript expressed in the YCS samples

was surprising, as stress conditions are known to require more of the protein ubiquitin process so we would expect to see a higher abundance of this transcript in the YCS samples instead.

The clathrin light-chain transcript is involved in intracellular protein transport, particularly across membranes, and regulation of the same (Wang et al., 2006; Wang et al., 2013). That this transcript was not expressed in YCS implies a breakdown in the movement of proteins in the different cellular compartments.

The FQR1-like transcript is involved in the transfer of electrons from NADH and NADPH to several quinones in the electron transport chain (Laskowski et al., 2002). It also acts as an oxidoreductase in stress response, so it was surprising to see this transcript not expressed in the YCS plants. It indicates that the electron transport chain is not functioning properly in the YCS plants, and this supports our previous findings on analysis of chlorophyll fluorescence (see Section 6.2.3. of this report)

Most interestingly in this group, the transcript c39217f2p01829 von Willebrand factor type A domain-containing protein is from a gene called Lagging Growth and Development 1 (LGD1). LGD1 regulates developmental signals for growth. From studies in rice, (Thangasamy et al., 2012), disruption in the expression of this gene negatively impacts the plant growth, morphology, internode length and yield. While more work needs to be done to explore the role of this transcript in YCS, it may provide some insight into the sugarcane reduced growth phenomenon.

The transcript c65847f1p11543 probable glutathione S-transferase GSTU6 is also in lower abundance in YCS samples, with its expression 12-fold lower. This enzyme is involved in the glutathione biosynthesis pathway, which in turn is involved in protecting the cell from oxidative stress (Foyer and Noctor, 2005). Together, this suggests that the YCS plants have an impaired stress response capability, which makes them more susceptible to stress conditions. In addition, each of these biochemical reactions involve ATP and may point to a problem in YCS plants having insufficient energy to drive their metabolism. This is likely due to the disruption to the electron transport chain.

The remaining significant transcripts with a fold change above 1.4 were in higher abundance in the YCS samples. These included

- c97367f1p02843 serine threonine- kinase BLUS1
- c111113f1p03909 senescence-associated
- c106391f1p04490 O-linked-mannose beta-1,4-N-acetylglucosaminyltransferase 2-like
- c17952f5p41542 GDSL esterase lipase At5g55050-like.

The BLUS1 transcript is involved in phototropin signalling and stomatal opening (Takemiya et al., 2013). With the assumption that higher abundance of this transcript would lead to more stomatal opening, this contrasts with the data we have previously obtained, which determined that YCS plants had reduced stomatal conductance. However, upregulation may be an attempt to counter the abscisic acid (ABA) mediated sucrose induction of guard cell closure and reduce internal heat stress within the leaf.

The transcript c106391f1p04490 O-linked-mannose beta-1,4-N-acetylglucosaminyltransferase 2-like is involved in protein post-translational modification through glycosylation (Yoshida-Moriguchi et al.,

2013). This points again to some disruption in the protein modification processes in the YCS symptomatic plants.

The GDSL esterase lipase transcript is a lipolytic enzyme that is involved in plant immunity and induced systemic resistance to infections and abiotic stress (Kwon et al., 2009; Chepyshko et al., 2012). It is over 4-fold higher abundance in the YCS plants and is an indication of the stress the YCS plants are under.

The transcript c111113f1p03909 is senescence-associated and being present in higher abundance likely indicates that the YCS symptoms are terminal in the leaf and the leaf is entering an early-senescence stage.

These 109 transcripts were subjected to Blast2GO analysis to identify any enrichment in the biological processes represented within the group (Figure 62). From the Blast2GO analysis, more than 40% of the transcripts (44/109) in the group were involved in DNA integration, recombination, and biosynthesis. This group also includes 15 transposable elements, including three from the retrotransposon Ty1-copia subclass, eight Retrovirus-related Pol poly from transposon TNT 1-94 and four unclassified transposons. It is unclear what role these transposable elements play in YCS.

In addition, 6% of the transcripts (7/109) were methylation-related. Methylation status is a way of regulating gene expression and is indicative of plant stress (Peng and Zhang, 2009).

The remaining processes identified include sugar metabolism, protein modification and movement, carotenoid biosynthesis, oxidative stress metabolism and circadian rhythm processes.

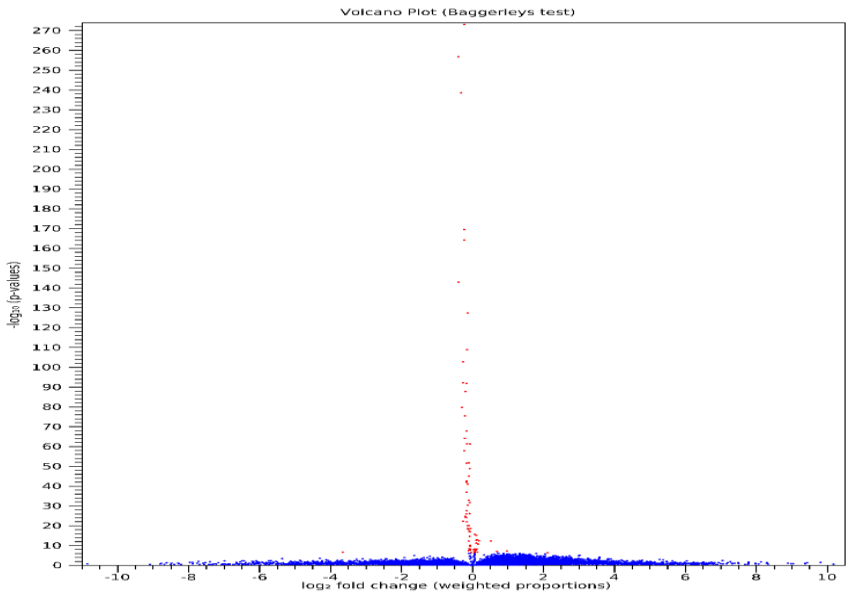

Figure 61 Volcano plot of the expression data. The red dots show the 109 statistically-significant results.

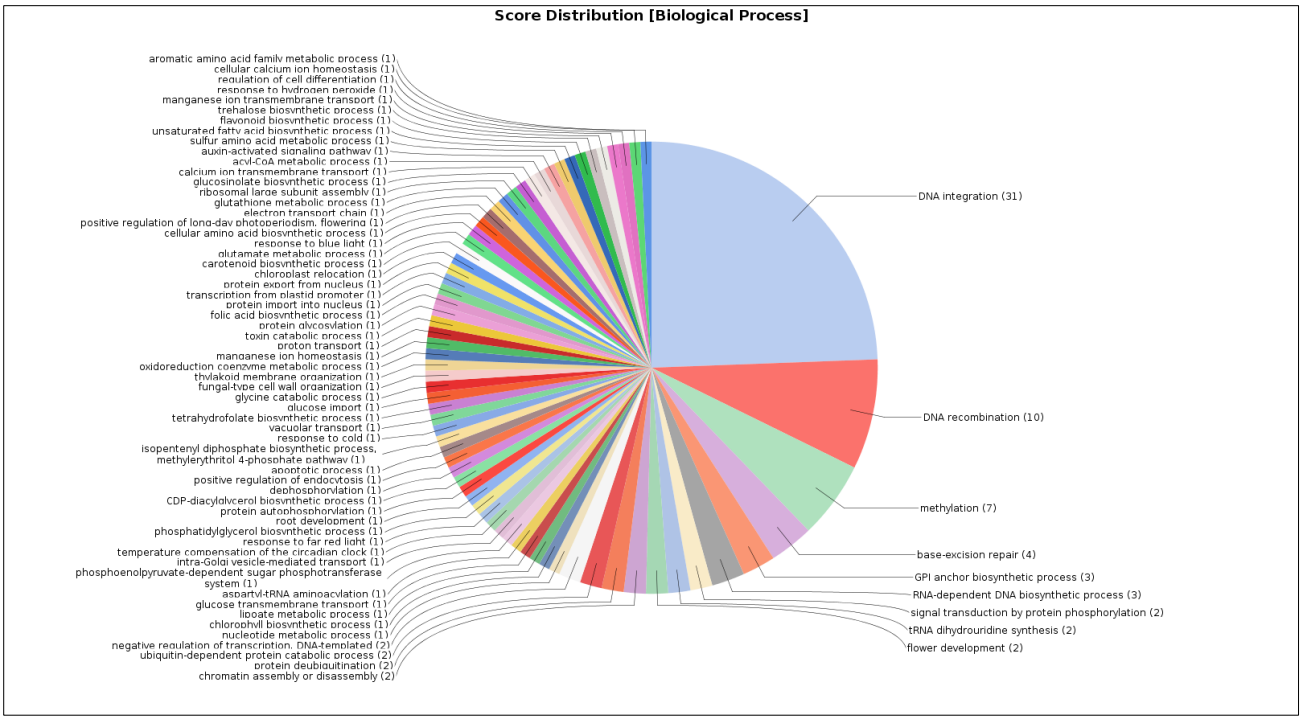

Figure 62 Summary of the biological processes represented by the 109 statistically-significant contigs differentially expressed in the YCS vs Control analysis of data from (Field Visits 3, 4 and 6 combined) against sugarcane PacBio transcriptome (Hoang et al., 2018)

Combining this analysis with a further analysis across water stress and senescent samples identified 11 transcripts significantly expressed in YCS (Table 6).

Table 6 DE expressed transcripts in YCS samples from genotypes Q200$^{\Phi}$, Q208$^{\Phi}$, Q240$^{\Phi}$ & KQ228$^{\Phi}$

c57334f1p01569 flagellar radial spoke 5 isoform X1
c111765f1p14596 phosphatase 1 regulatory subunit pprA
c52126f1p12255 mitogen-activated kinase kinase kinase YODA-like isoform X2
c119406f1p45922 Retrovirus-related Pol poly LINE-1
c114609f1p04644 disease resistance RPP13 2
c28783f1p02310 hAT dimerisation domain-containing -like
c107022f1p04513 clathrin assembly
c88737f1p02730 Sugar transporter ERD6-like 6
c119233f1p06987 exportin-4 isoform-X2
c105044f1p24618 DUF1296 domain-containing family [Zea mays]
c51679f1p11333 retrotransposon unclassified

The flagellar radial spoke 5 isoform X1 transcript is involved in the movement of proteins and molecules within the cell (Vale, 2003). The phosphatase 1 regulatory subunit pprA transcript is involved in DNA repair, particularly with double-stranded breaks (http://string.embl.de/newstring_cgi/show_network_section.pl?identifier=pprA). The mitogen-activated kinase kinase kinase YODA-like isoform X2 transcript regulates the formation and architecture of stomatal cells (http://www.uniprot.org/uniprot/Q9CAD5). The retrovirus-related Pol poly LINE-1 and retrotransposon unclassified transcripts are transposable elements, as is the hAT dimerisation domain-containing -like transcript (https://www.ebi.ac.uk/interpro/entry/IPR008906). The disease resistance RPP13 2 transcript is involved in resistance to fungal pathogens, particularly

downy mildew (https://www.wikigenes.org/e/gene/e/823806.html). The clathrin assembly transcript is involved in intracellular protein movements across membranes as described above. The sugar transporter ERD6-like 6 transcript is involved in transporting glucose across membranes (http://www.uniprot.org/uniprot/Q9FRL3). The exportin-4 isoform-X2 transcript is involved in transporting proteins out of the nucleus of the cell (Lipowsky et al., 2000). The DUF1296 domain-containing family [Zea mays] transcript is involved in abiotic stress response (Shiriga et al., 2014).

Taking all these together, YCS plants have changes to protein and glucose movement within the cells, and the formation of the stomata. They are dealing with biotic and abiotic stress, DNA damage and are impacted in some way by transposable elements.

6.3.4.3. Proteins and amino acids

The protein reference database required for protein identification from samples was improved by providing RNA-seq data to the Australian Proteome Analysis Facility (APAF) in Sydney to generate protein sequences. Over 1,800 were identified, where previous protein identification samples had yielded < 300 proteins. These results showed a large number of protein abundance differences between YCS-symptomatic and healthy leaves. Over 600 proteins had significantly higher presence in YCS leaves, particularly various heat-shock proteins and proteins involved in transcription, translation, and carbon metabolism. Of the 190 proteins significantly reduced in abundance in YCS leaves, the largest proportion were involved in photosynthesis in the chloroplast. Cellular locations of the higher and lower abundance proteins can be seen in Figure 63 Cellular location of protein proportional abundance in YCS leaf

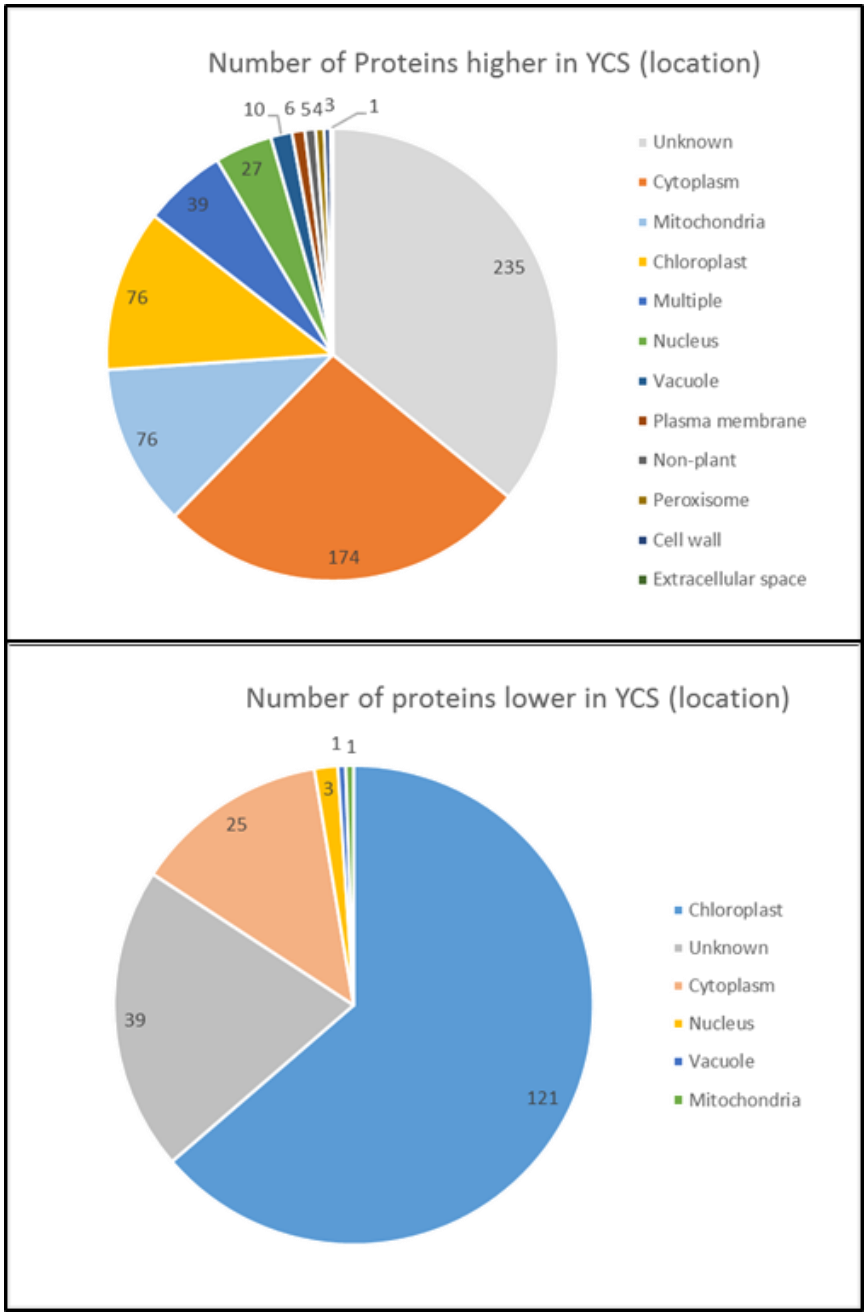

Figure 63 Cellular location of protein proportional abundance in YCS leaf

Figure 64 Number of identified proteins in yellow canopy syndrome (YCS)-affected leaf tissue in dewlap, midrib, lamina early-stage (ES) and lamina late-stage (LS). Blue end indicates number of proteins with decreased level, red end indicates number with increased level, and grey indicates number with no level change compared to controls. Differential abundance (level change) defined as false discovery rate (FDR)-corrected Pvalue <0.05. (Marquardt, 2019)shows the distribution of protein abundance between green and yellow YCS lamina, midrib, and dewlap. Of these, twenty-seven were higher in abundance in YCS lamina and midrib than in controls and five proteins were consistently decreased in abundance across all dewlap, midrib, YCS ES and LS leaf lamina (Table 7). Noteworthy is the greatest fold-change decrease recorded in the late stage yellow lamina and the midrib associated with the photosynthetic electron transport chain - PSII D1, ATP synthase and oxygen-evolving complex enhancer. The data is evident of significant

downregulation of the photosynthetic apparatus through feedback regulation (Marquardt, 2019).

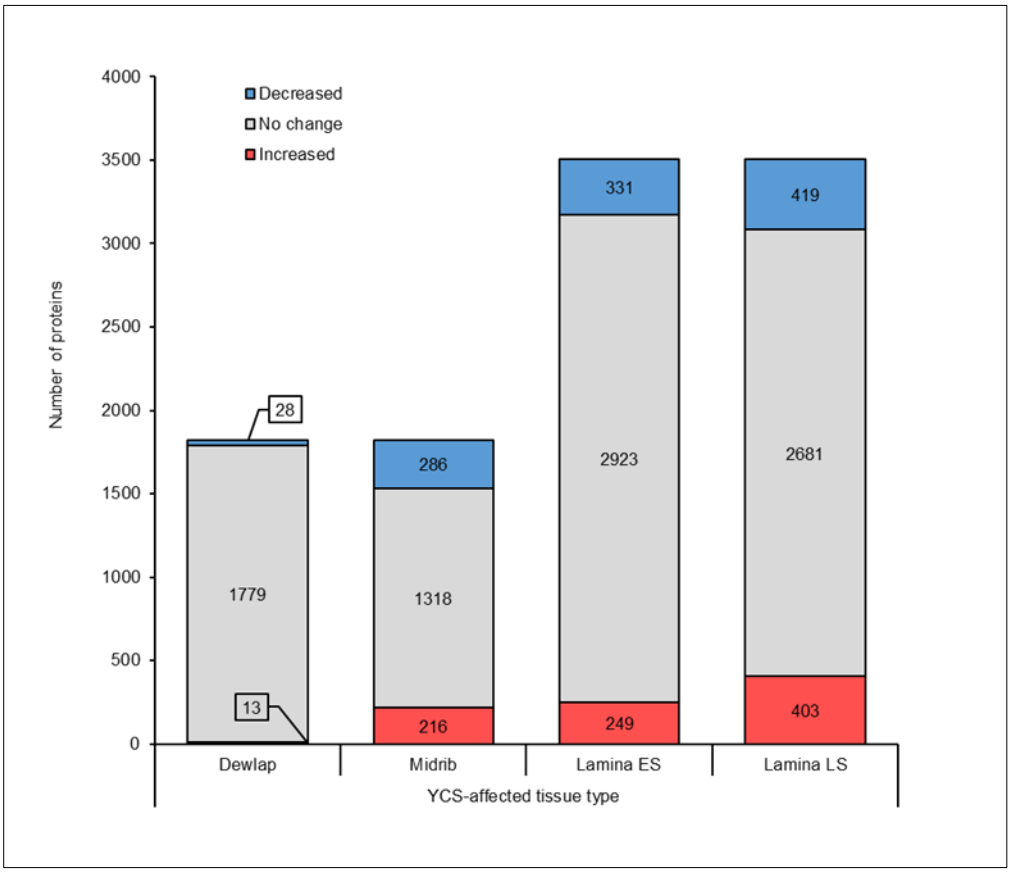

Figure 64 Number of identified proteins in yellow canopy syndrome (YCS)-affected leaf tissue in dewlap, midrib, lamina early-stage (ES) and lamina late-stage (LS). Blue end indicates number of proteins with decreased level, red end indicates number with increased level, and grey indicates number with no level change compared to controls. Differential abundance (level change) defined as false discovery rate (FDR)-corrected Pvalue <0.05. (Marquardt, 2019)

Table 7 Proteins with lower abundance in yellow canopy syndrome (YCS)affected dewlap, midrib, early-stage (ES) lamina and late-stage (LS) lamina compared to controls including fold changes. (Marquardt, 2019)

			Fold-change in YCS from control			
					Lamina	
Protein ID	Description	UniProt ID	Dewlap	Midrib	Early-stage (ES)	Late-stage (LS)
gi|195628120	ATP synthase B chain, chloroplastic	C5WPC6	-36.13**	-7.1**	-2.63**	-3.86**
gi|241915488	fructose-bisphosphate aldolase 5, cytosolic	C5Z5R1	-2.55**	-3.88**	-1.5**	-5.63**
gi|241924815	oxygen-evolving enhancer protein, chloroplastic	C5X9F7	-1.93**	-4.5**	-1.73**	-4.8**
gi|413939455	unknown (predicted on chloroplast membrane)	C5XVU8	-1.86**	-3.51**	-1.99**	-3.58**
gi|893641155	Photosystem II protein D1	A0A109NDD5	-2.85**	-5.14**	-1.66**	-3.94**

***Differential abundance at significance value of false discovery rate (FDR)-corrected P-value <0.01.*

There are nine amino acids which increase in abundance in YCS leaves normalised against control Leaf 4 (Figure 65). This increase is asparagine and tryptophan as YCS symptoms develop is supported by research showing a strong correlation of these two amino acids with increased chlorosis (Kenyon and Turner, 1990). A strong correlation also exists between abiotic stress and high GABA and proline levels in plants (Widodo et al., 2009; Witt et al., 2011; Rodziewicz et al., 2014). This adds weight to the mounting evidence implicating abiotic stress as a precursor to YCS development and expression.

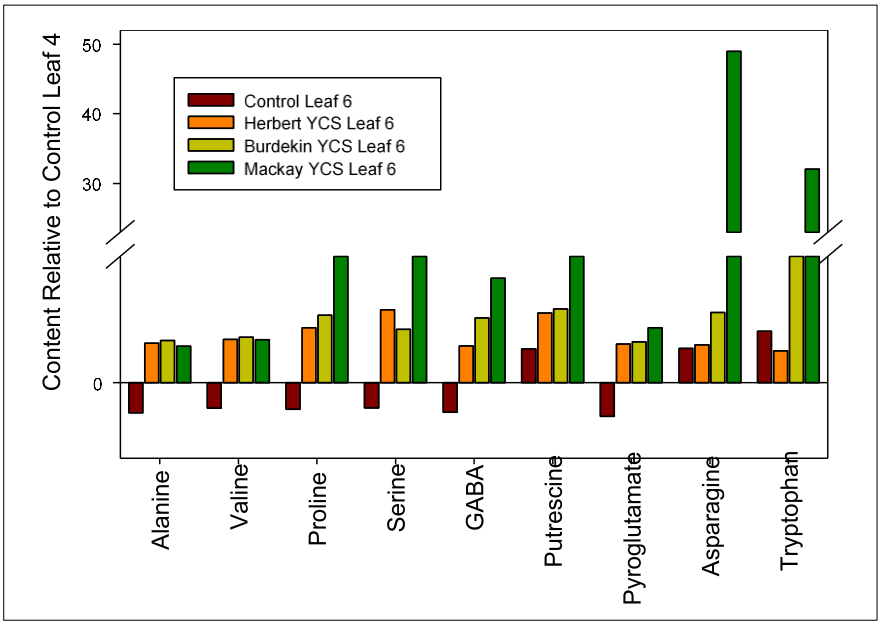

Figure 65 Changes in the levels of amino acids in YCS symptomatic sugarcane plants. Data is normalised against the control leaf two. All these values have a t-test value below P< 0.05 (Bonferroni-corrected P value).

The collective data presented in section 6.3 of the report indicates there is massive disruption to source leaf metabolism as YCS develops. This metabolic perturbance is evident of a secondary effect in direct response to sucrose accumulation in the leaf, or an induced response to reduce sucrose synthesis through downregulation of the photosystems. As there is no evidence of reduced phloem loading and transport, or a physical blockage of the vasculature, the cause of leaf sucrose accumulation must primarily be driven by changes to the sink. While research conducted by the CSIRO found no differences in root system structure between YCS plants and healthy controls (Rae and Pierre, 2018), the roots should not be ruled out as a possible cause of sink source imbalance. It is important to note that a more immediate source response is likely differentiated in changes to internodes sink strength than at the root level due to the proximity of internode sink tissue to the source. It is evident from our data that sucrose accumulation in the source leaf is driven primarily by sink limitation within the culm. It should also be noted that xylem sap sucrose and its reducing sugars extracted from internodes show no consistent difference between control and YCS (Figure 66A-C). This suggests that a xylem vessel microbial entity is not responsible for reducing water movement that may limit sink size. Furthermore metabolite analysis of xylem sap (data not shown) did not show a single compound across the regions and genotypes that changes in association with YCS expression (Botha et al., 2015).

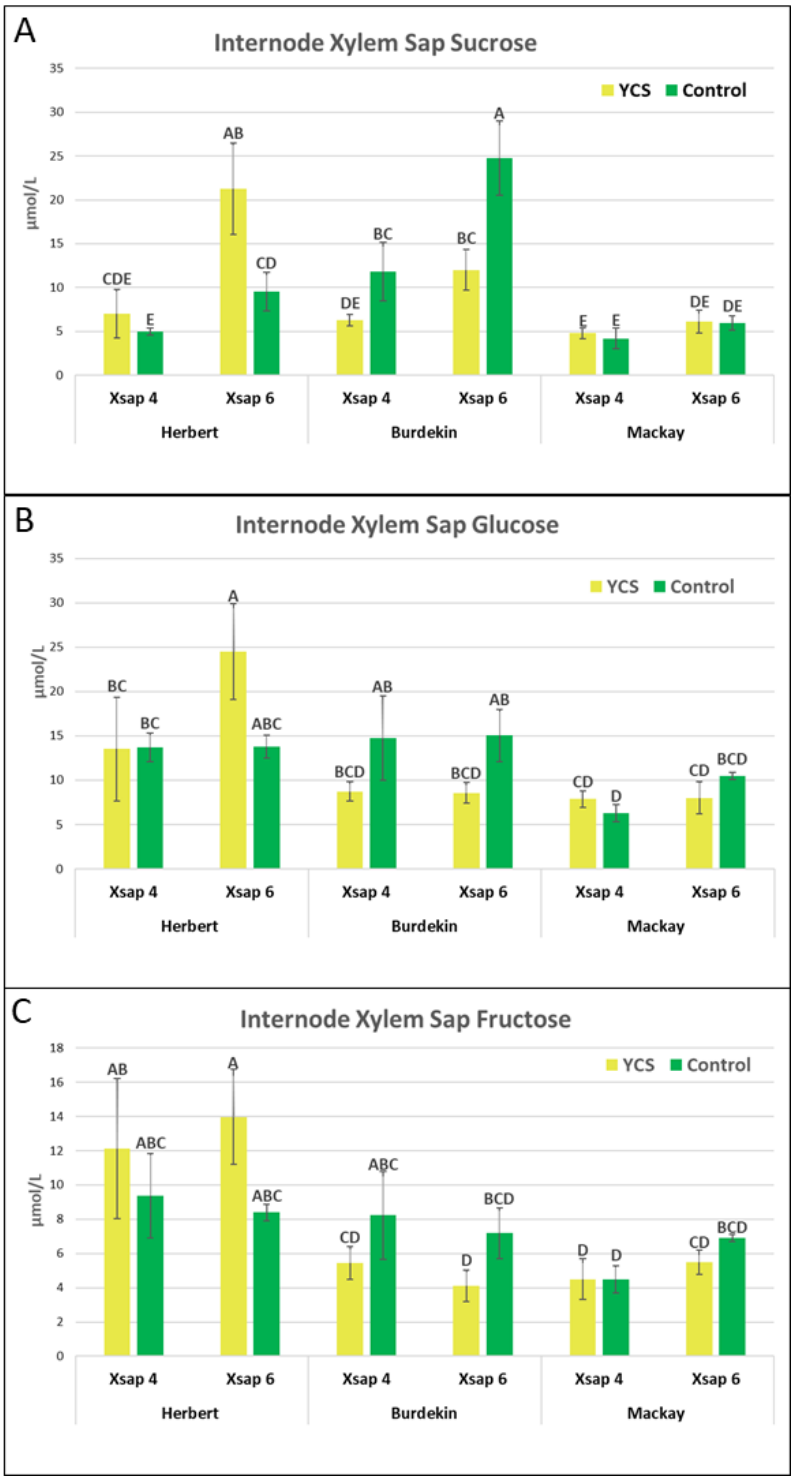

Figure 66 Internode 4 & 6 xylem sap sucrose A), glucose B) and fructose C), Q200$^{\Phi}$ Herbert, KQ228$^{\Phi}$ Burdekin, Q208$^{\Phi}$ Mackay. Tukey HSD All-Pairwise Comparisons (p<0.05)

6.4. Source sink imbalance

^{13}C studies showed that there was carbon overflow assimilation to starch (insoluble α-glucan) as a means of carbon offset in asymptomatic leaves which had already started to accumulate sucrose. Both sucrose and α-glucans synthesis are linked to the triose-phosphate produced from CO_2 fixation in the chloroplast (Myers et al., 2000). The carbon storage potential of starch will quickly reach saturation as sugarcane lacks the machinery outside of the chloroplasts of bundle sheath cells to

synthesise this polysaccharide (Lunn and Furbank, 1997). Measurements of high leaf starch and sucrose at first light indicate limited capacity to turnover starch. Studies have shown that this mechanism is synchronised to the diurnal rhythm and any disruption to this will result in a change to carbon partitioning in the leaf and whole plant (Du et al., 2000; Watt et al., 2005; Weise et al., 2011). In sugarcane the priority of carbon assimilation is for sucrose with partitioning to starch regulated by sucrose synthesis.

To gain a better understanding of the diurnal profile of the source leaf and any link to sink tissue, YCS symptomatic and control Leaf 4 midribs were sampled 13 hours apart (dusk and dawn). Midrib vascular bundle (VB) tissue was separated from parenchymatous tissue (PT) (Figure 67) and assayed for sucrose, soluble and insoluble α-glucan content (Figure 68).

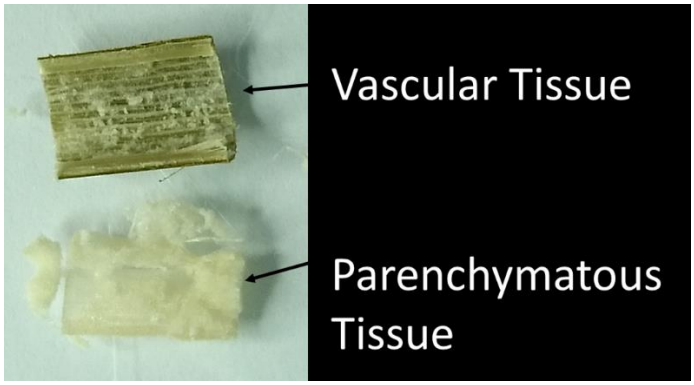

Figure 67 Separation of KQ228Φ Leaf 4 midrib vascular and parenchymatous tissue using a lino cutting chisel

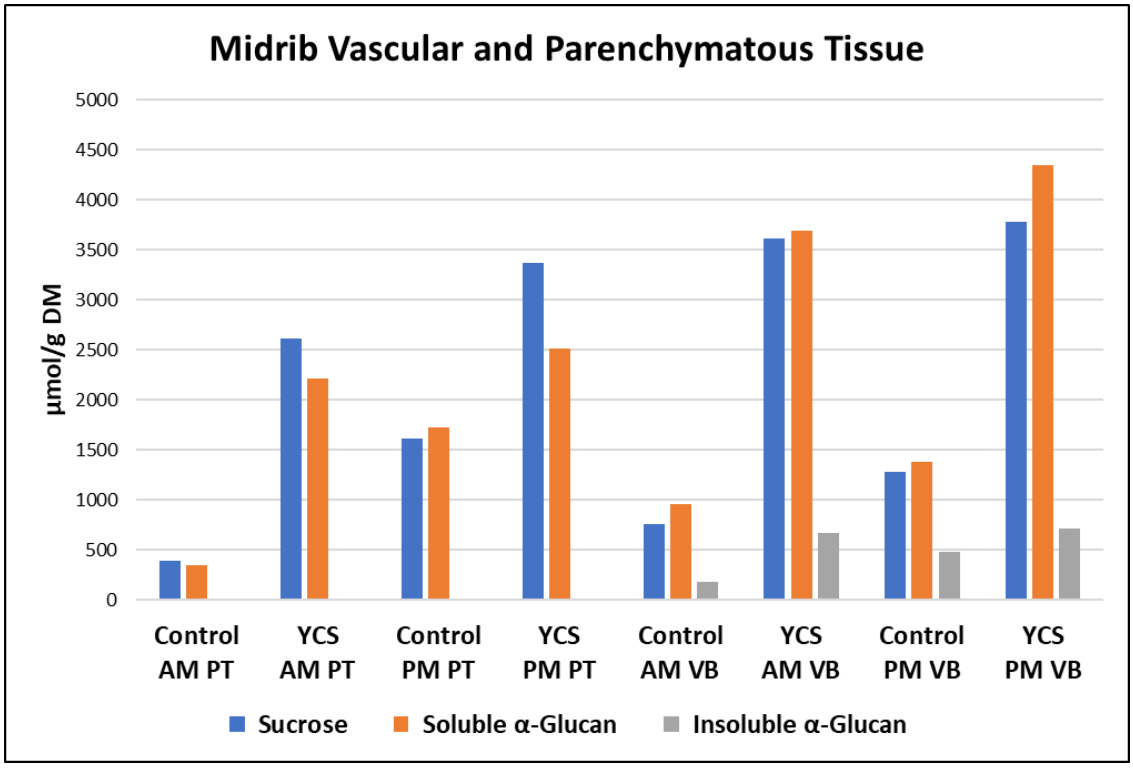

Figure 68 KQ228Φ Leaf 4 midrib Vascular bundle (VB) and Parenchymatous tissue (PT) sucrose, soluble & insoluble α-glucan content (AM & PM). (note: sucrose units µmol/g DM; α-glucan units µmol glucose equivalent/g DM)

The flow rates of each soluble metabolite (sucrose and soluble α-glucan) and turnover of the insoluble starch pool can be used as a proxy for sink strength. A strong gradient between the source leaf and the sink (internode) is indicative of high sink strength or demand and vice versa for a weak sink strength (Black et al., 1995; Koch, 2004; Morey et al., 2019). As carbon is only translocated in the phloem as sucrose, calculating flow rates of soluble and insoluble α-glucans would be misleading. These two polymers are converted to hexose units and then reused for sucrose synthesis. Therefore, the change in total pool size of sucrose, soluble and insoluble α-glucans would be an indication of carbon flux out of the source tissue and indicative of sink demand. It is important to also note that the midrib parenchymatous tissue is devoid of bundle sheath cells and therefore lacks the cellular machinery to synthesise starch. Figure 69 shows hexose unit rate of change, represented by the total hexose equivalent pool from both PT and VB control tissue, is approximately 2-fold higher than YCS tissue. This is a significant difference and gives a better understanding of the variance in sink strength impacting sucrose and α-glucan export from the leaf. Also of note are the large quantities of glucan and sucrose in vascular and non-vascular tissue of the midrib. This is indicative of this tissue serving as an alternate sink to offset excess carbon accumulation in the lamina (Marquardt et al., 2017).

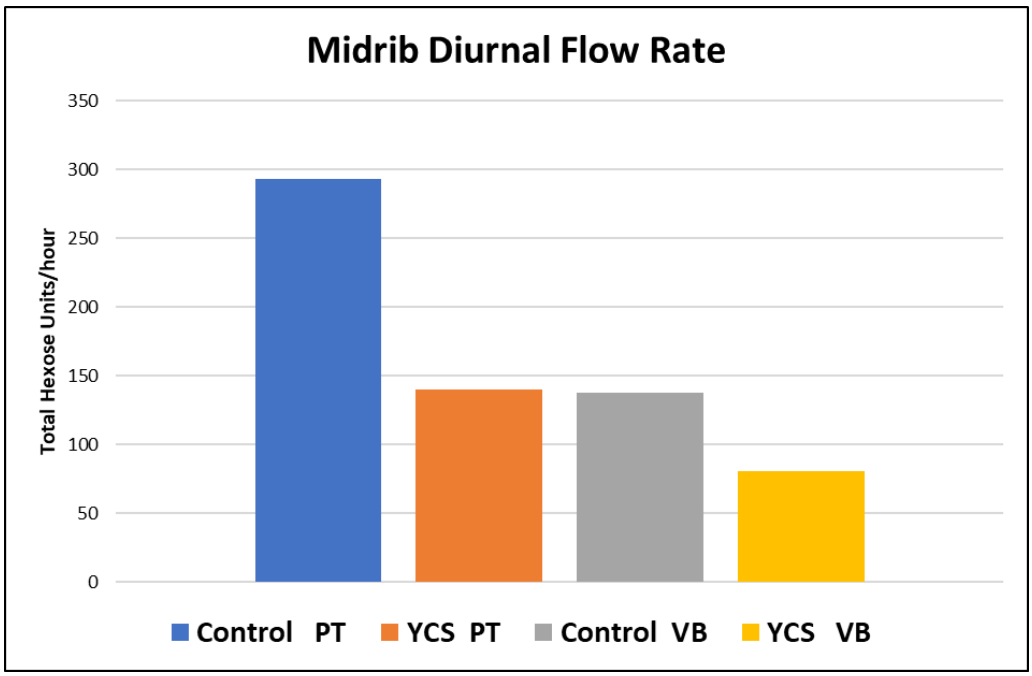

Figure 69 KQ228$^{\Phi}$ Leaf 4 midrib diurnal flow rate (Total hexose units/hour). Vascular bundle (VB) and Parenchymatous tissue (PT).

A reduction in sink strength can occur if i) the physical size or ii) the metabolic rate of the internode is reduced. If the physical size of the internode is reduced, the capacity of the sink to accommodate exported sucrose from the source leaf will obviously be diminished. The magnitude of internode volume reduction will be one factor that contributes to the sink strength status, the other will be its metabolic rate. Maintenance of a sucrose concentration gradient in the phloem between the source and sink tissue is imperative for unencumbered export from the leaf. It is also true that a sluggish metabolic rate in an internode of adequate physical capacity will have a diminished call for carbon, as respiratory requirements are unable to maintain an adequate concentration gradient between the source and sink tissue. In either scenario, sucrose accumulates in the leaf due to a source sink

imbalance. Therefore, if internode growth is slowed physically or metabolically, sink strength will be diminished causing a source sink imbalance.

6.4.1. Manipulation of supply and demand

A growth regulator trial was conducted on the SRA Brandon station to investigate whether YCS could be induced through manipulation of the supply and demand function using growth regulators to alter the size of the source or sink. Of the 5 treatments investigated i) Benzylaminopurine (BAP), ii) Gibberellic Acid (GA), iii) Gibberellic Acid inhibitor (Moddus®), iv) Shade, v) Ethylene, only GA inhibitor Moddus® had sucrose and total α-glucan levels comparable to YCS and significantly higher than controls in both the lamina and midrib (Figure 70A-D). It is therefore reasonable to assume that the application of a GA inhibitor has induced sucrose and α-glucan accumulation in the source tissue. It is also worth noting that only Moddus-treated plants displayed a similar phenotype to YCS in symptomatic Leaf 4 in the field.

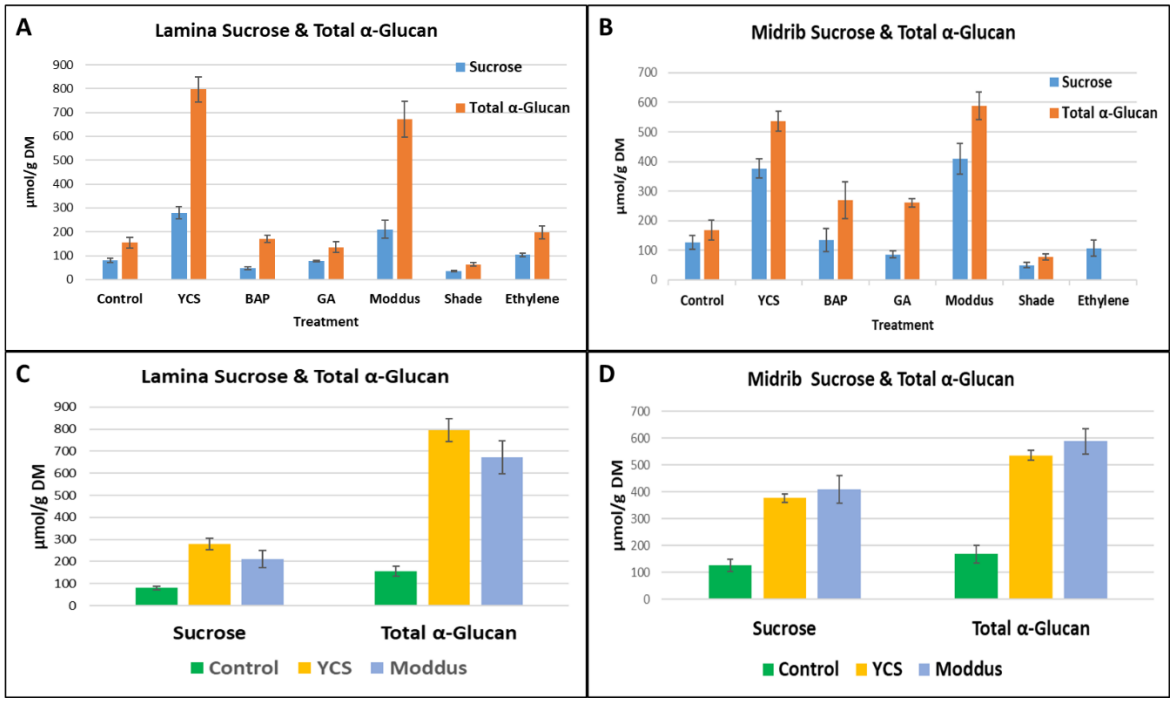

Figure 70 Growth regulator treatments KQ228$^{\phi}$ Leaf 4 sucrose and Total α-Glucan content lamina A & C), midrib B & D)

Sugarcane internodes of commercial varieties grown in Qld elongate for approximately 380-degree days (°Cd) with most growth occurring in the first 150°Cd. Internode growth is highly dependent on water and nutrient availability (Inman-Bamber, 1994; Moore and Botha, 2013). Internode length is often used to measure growth rates, but this parameter alone is inadequate for estimating sink size. Internode volume, which also considers the variations in girth, is a better measure of the plant's sink capacity. Figure 71 shows treatments Moddus, ethylene and YCS all have significantly smaller internode volumes than controls above internode 6. These two treatments and YCS group together at internode 4 and above; similarly, the remainder of treatments do so with the control. This is an extremely interesting result as it indicates a strong correlation between leaf sucrose/α-glucan content (Figure 70A-D) and sink size (Figure 71). However, ethylene, with notably the smallest sink size (Figure 72A), is the exception to this with leaf sucrose and starch content comparable to that of controls. This result is not surprising as ethylene is an early ripener, which slows the entire plant

growth. Ethylene is also the only treatment to have a significantly smaller leaf area (Figure 72B) than controls and hence its photoassimilate production is not likely to exceed the sink capacity to cause accumulation of sucrose above the upper tolerable threshold in the source tissue.

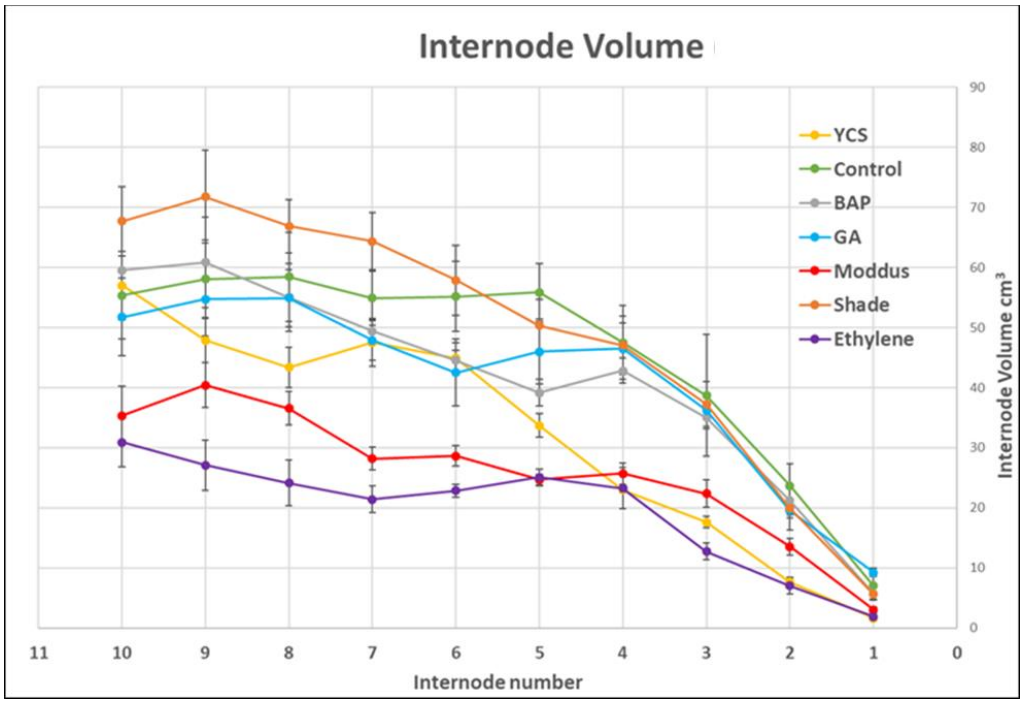

Figure 71 KQ228$^{\Phi}$ growth regulator trial, internode (1-10) volume cm^3. Internode # 1 directly beneath leaf sheath of true leaf #1 (FVD)

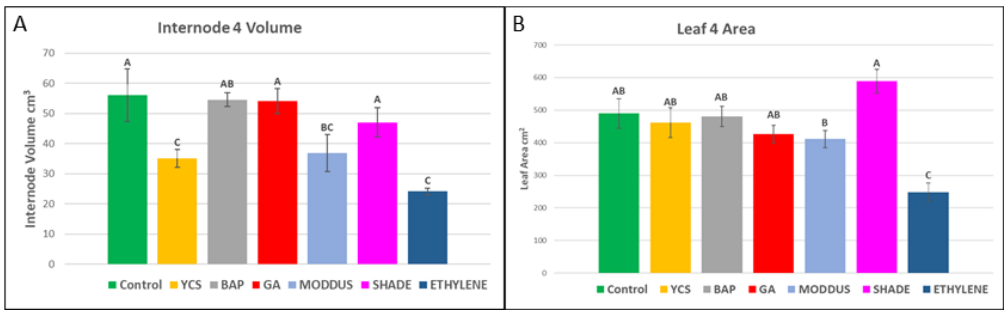

Figure 72 KQ228$^{\Phi}$ internode 4 volume by treatment A) and leaf area B). GA inhibitor (Moddus) and YCS have a larger supply to demand function than control. Tukey HSD All-Pairwise Comparisons (p<0.05)

There is a clear sucrose concentration gradient between Control, YCS and Moddus in internode 4 which sits directly beneath the YCS symptomatic leaf. Interestingly, Moddus has a significantly higher internode 6 sucrose concentration than YCS and control (Figure 73). It is worth noting that YCS internode 6 volume does not vary much to that of control, whereas Moddus internode 6 is significantly smaller (Figure 71). Accordingly, YCS leaf 6 showed no sign of yellowing in any of the reps (only leaf 4 was YCS symptomatic), which suggests source supply does not exceed the sink capacity or demand.

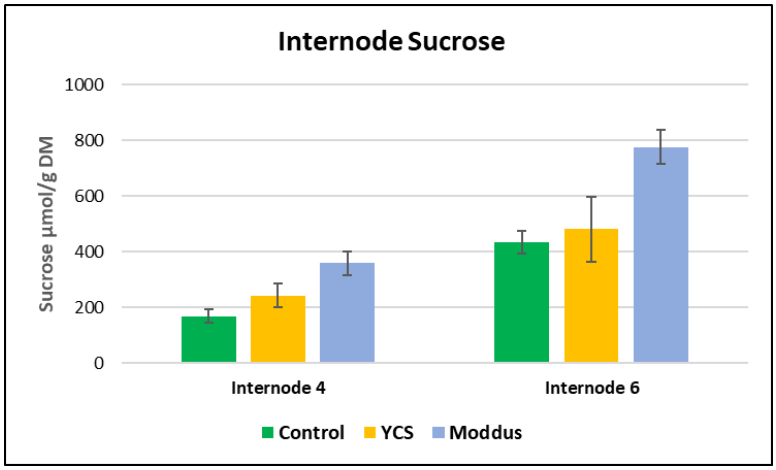

Figure 73 KQ228$^{\Phi}$ Internode 4 & 6 sucrose concentration; control, YCS and Moddus

The results from the growth regulator field trial show that limiting the internode size through application of a GA inhibitor induced a YCS-like response. This culminates in sucrose and starch accumulation levels comparable to that measured in YCS samples. The correlation between physical sink size and photoassimilate accumulation was a major step forward in understanding potential triggers that induce a YCS event. This also helped to explain why growers report a flush of yellow across a field directly after a rainfall event that followed an extended dry period during the peak photosynthetic months of December to March. If optimum conditions for photosynthesis occur following a period in which internode elongation has been compromised, sugars rapidly build up in the source leaves and trigger premature leaf senescence. Yellowing of the lamina will usually occur when levels of sucrose exceed ≈200µmol/g DM. Once this tipping point is surpassed, the damage to cells and tissue is irreversible.

YCS plants exhibit a major disruption to the supply and demand balance where supply is much greater than sink demand or capacity.

6.4.2. Source sink imbalance & sink strength

As discussed in section 6.3.1.1 of this report, sugarcane loads the phloem through an apoplastic step, requiring energy and specialised sucrose transporters to move sucrose against a concentration gradient. Gene expression of sugar transporters and other required proton pumps in YCS leaves do not indicate an issue with phloem loading. The ^{13}C carbon turnover and hexose unit flow rates in the midrib in YCS source leaves indicate there is reduced sap flow between the source and the sink tissue. This implies reduced sink strength or a physical occlusion (see section 6.3.3. of this report) of the phloem. In this section of the report we will address the issue of sink strength and the likelihood of it being a cause of compromised sucrose transport between source and sink tissue.

Sucrose arrival in sink tissues (e.g. internodes) is determined by its movement along a pressure gradient, created by the sucrose concentration and available water between the leaf and sink. This gradient is maintained by adequate photoassimilation in the source, and a low sucrose concentration in the parenchyma cytosol. Sucrose synthase and invertase are two critical enzymes necessary for sucrose turnover and carbon repartitioning to take place and their activity is strongly correlated with the import of sucrose by the sink tissue (Black et al., 1995; Morey et al., 2018). The consumption and storage of sucrose along the transport path (metabolic rate and storage within the

sink tissue) together with the physical size of the sink organ determines sink strength (Bihmidine et al., 2013).

In sugarcane, photoassimilates are initially used for growth and development but when the internodes have ceased to elongate after approximately 380 ˚Cd (internode 8 & older) the culm transitions to a storage organ. A reduction in sucrose usage by sinks occurs normally as internodes mature. In mature internodes (internode 10 & older) sucrose hydrolysis slows to near zero and there is a very much reduced metabolic rate (Botha et al., 1996; Moore and Botha, 2013). Sucrose metabolism is therefore not a critical driver of sink strength in mature internodes. Where the supplied sucrose is in excess of internode metabolic requirements and capability, it remains 'unused' by the internode and results in a disrupted concentration gradient between the leaf source and internode sink. The disrupted sucrose gradient influences the sink strength signal. Maintenance of sink strength is therefore highly dependent on a balance between storage and respiration (growth, development, and maintenance). Sucrose levels at a given site is the net result of its import and use at that point of ontogeny (Botha et al., 1996; Geiger et al., 1996; Bihmidine et al., 2013).

To gain an understanding of sink strength status at a molecular level in YCS plants, analysis of leaf and internode gene expression data associated with changing levels (abundance and depletion) of sugars is crucial. In order to understand if there is availability of sucrose to internode, or whether sucrose is not reaching the internode, we investigated gene expression data of sucrose metabolism genes.

Table 8 shows the main genes enhanced during either a feast or famine carbohydrate state in both leaf and internode. The expression of photosynthetic genes and the remobilisation of reserves (starch) is repressed by elevated levels of sucrose and glucose, while genes associated with sucrose import and use are enhanced (initial sucrose cleavage, respiration, biosynthesis, and storage). Differential expression analyses of carbohydrate regulated genes will also give an insight to the important role played by these genes in maintaining a supply demand balance (photosynthesis Vs utilisation) in response to environmental change (Geiger et al., 1996; Koch, 1996; Bihmidine et al., 2013). Environmental factors can affect transport from the source to sink by influencing i) source: e.g. photosynthetic rate, phloem loading ii) sink: e.g. internode and root growth, pathogens iii) path between source and sink: e.g. callose, bacteria and viruses (Lemoine et al., 2013). It is worth noting that the "omics" analyses across all samples analysed since the commencement of this research project reveal a common thread of metabolic perturbance associated with abiotic stress.

Table 8 Feast & Famine genes

Plant sugar feast/famine genes	
source 1: Koch, K.E. (1996) CARBOHYDRATE-MODULATED GENE EXPRESSION IN PLANTS Annu. Rev. Plant Physiol. Plant Mol. Biol. 1996. 47:509–40	
"Famine" genes: enhanced by sugar depletion:	**"Feast" genes: enhanced by sugar abundance:**
Genes enhanced under carbohydrate FAMINE conditions	**Genes enhanced by FEAST conditions**
Photosynthesis:	Polysaccharide biosynthesis (starch and other):
Rubisco S–subunit [rbcS]	AGPase [Sh2] (starch)
Rubisco L–subunit [rbcL]	starch phosphorylase
chl a/b–binding protein (cab, Lhcb)	starch synth [GBSS]
atp-δ thylakoid ATPase	branching enzyme [BE]
malic enzyme, C4 [Me1]	Storage proteins:
PEP carboxylase, C4 [Pepc1]	sporamin, A & B types
triose-phosphate translocator	β-amylase (storage protein?)
pyruvate PPdikin [Ppdk1]	patatin class I
C4-pyruvate phosphodikinase	proteinase inhibitor II [Pin2]
Remobilization (starch, lipid, and protein breakdown):	lipoxygenase (storage protein)
Amy3D, Amy3E α-amylase	Pigments and defense:
α-amylase	chalcone synth (pigment/path.)
plastid starch phosphorylase	RT locus (pigment synth)
phosphoglucose mutase	dihydroflavonol-reductase
isocitrate lyase [Icl] (glyox cycle)	Mn-superoxide dismutase
malate synth (glyox cycle)	hrp (pathology)
proteases	chaperonin 60B (protein synth)
asparagine synthetase (N cycling	Respiration:
Sucrose and mannitol metabolism (synthesis and breakdown):	PGAL-dehydrog. (GapC) cyto
acid invertase	β-isopropylmalate dehydrog.
S synth	apocytochrome 6 (co6)
SPS	PP-F-6-P phosphotransferase (cytosolic enzyme)
Mtol dehydrogenase	Sucrose metabolism:
	invertase
	S synth
Abbreviations: 2dG, 2-deoxy-glucose; acet, acetate; cult, culture; endo, endosperm; F, fructose; G, glucose;	SPS
Lhcb, light-harvesting chlorophyll-binding protein (also cab); lvs, leaves; M, mannose; Mal, maltose; Mtol,	Other:
mannitol; PEP, phosphoenolpyruvate; PPdikin, phosphodikinase (cytosolic); rts, roots; scutel, scutellum; Sh1,	nitrate reductase
Shrunken1; S, sucrose; SPS, sucrose phosphate synthase; trans expr, transient expression; synth, synthase.	SAM synth
	ro/C gene of Ri plamid
	30-kD Rubisco-assoc. protein
	Abbreviations: 6dG, 6-deoxy-glucose; AA, amino acids; cult plts, cultured plants; F, fructose; G, glucose;
	GapC, PGAL-dehydrogenase (cytoplasmic); Gln, glutamine; Glu, glutamate; lvs, leaves; Mal, maltose; MeJA,
	methyl jasmonate; Met, methionine; p-coumar, p-coumaric acid; PGAL, glyceraldehyde-3-phosphate
	dehydrogenase; pgal a., polygalacturonic acid; PP-F-6-P phosphotransferase, pyrophosphate:fructose-6-
	phosphate-phototransferase; S, sucrose; SPS, sucrose phosphate synthase

Table 9 shows a summary of the expected gene expression status for leaf and internode tissue induced by feast and famine conditions compared to YCS tissue. Investigation of these two tissue types (leaf 4 & internodes 2, 4 & 6) collected from the Growth Regulator Trial (FV14) unsurprisingly showed YCS leaf tissue is in a feast status due to sucrose accumulation resultant of compromised phloem transport. In a feast situation, photosynthetic activity and sucrose synthesis is inhibited by feedback regulation (decrease in sucrose synthase) while excess carbon is directed to starch synthesis (20-fold increase in starch phosphorylase). Investigation into the two main sucrose cleavage enzymes associated with sink strength yields some interesting results. Firstly, soluble acid invertase (vacuolar invertase) is approximately 15-fold down regulated in internodes 2, 4 and 6 of YCS stalks. While vacuolar invertase gene expression is not a direct measure of enzyme activity, it can be used as a proxy of sink strength and to also reflect the possible hexose-to-sucrose ratios which are instrumental to the regulation of the sucrose gradient (Morey et al., 2018). In sugarcane, soluble acid invertase activity reduces significantly as the culm transitions to storage of sucrose in the vacuole. Secondly, the increase in expression of sucrose synthase is not surprising as its catalysis of the reversible cleavage of sucrose to UDP-glucose and fructose in the cytosol is known not to be inhibited by high substrate concentrations (Black et al., 1995). These results suggest that all three YCS internodes (2, 4 & 6) have weak sink strength (sucrose is available, but not "used"), more indicative of a mature culm.

It is therefore highly probable that reduced physiological capacity together with reduced physical capacity is the cause of reduced sap flow between the source and sink tissue which culminates in leaf sucrose accumulation. The underlying factors that cause a reduced physical and physiological capacity may be many and varied and could explain the sporadic nature of YCS occurrence and severity within and between fields and between sugarcane growing regions.

Table 9 YCS tissue specific feast and famine gene expression

Tissue	Expected Plant Transcriptional Response		
Leaf	**Feast**	**Famine**	**YCS**
Photosynthesis			
ATPase	↓	↑	↓
Pyruvate phosphodikinase	↓	↑	↓
Remobilisation (breakdown of starch, lipids & proteins)			
Alpha amylase	↓	↑	↓
Lipase	↓	↑	↓
Proteinase	↓	↑	↓
Sucrose/Starch metabolism			
Sucrose synthesis (sucrose synthase)	↓	↑	↓
Starch synthesis (branching enzyme & starch phosphorylase)	↑	↓	↑ (20-fold)
Internode			
Sucrose metabolism			
Soluble acid invertase (vacuole)	↓	↑	↓ (15-fold)
Sucrose synthase	↓	↑	↑ (2-fold)

6.4.3. Supply & Demand Balance

The readily available carbon for export from the leaf is a good measure of supply function while the internode dry biomass is indicative of sink strength. At the stage where the leaves are symptomatic, the sucrose and total α-glucan levels in the leaf represent 80% of the dry mass of the internode attached to that leaf (Figure 74B). In comparison, this would only be 10% in the control tissue (Figure 74A). Mass flow between the source leaf and the internode in a symptomatic plant would therefore be significantly impeded.

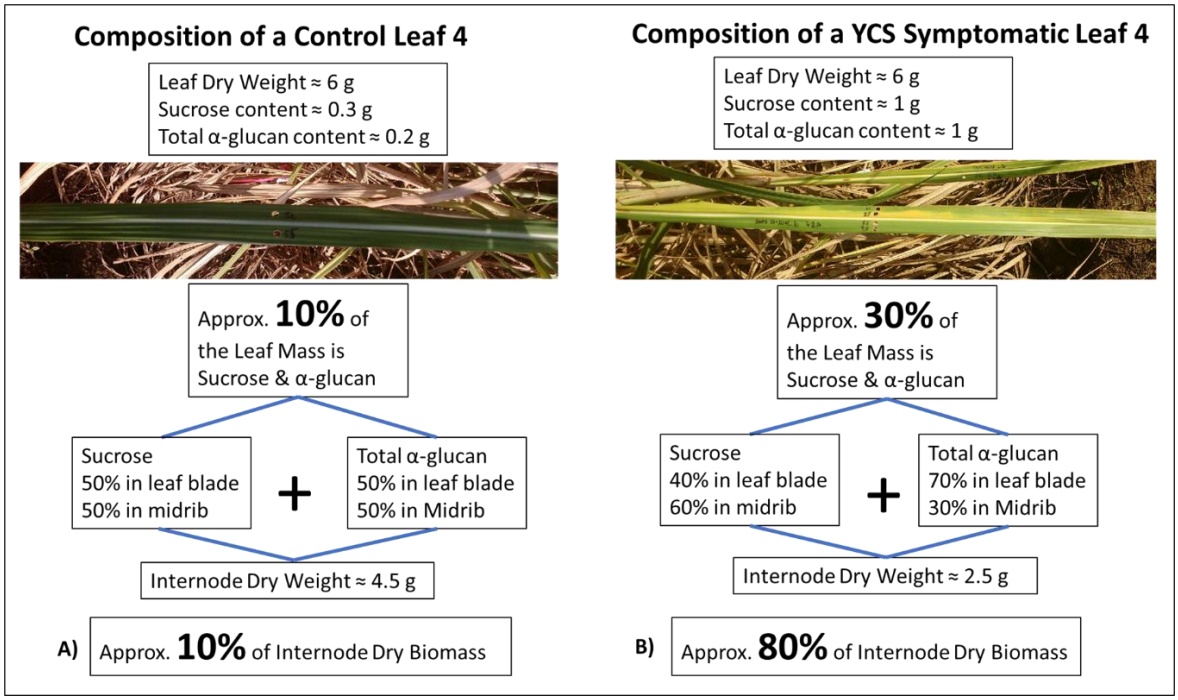

Figure 74 Supply and demand balance, Control A) and YCS B)

Total leaf (lamina and midrib combined) sucrose and α-glucan is a good measure of readily available carbon for export to the sink. Conversely, the internode biomass is a reliable estimate of sink demand. Therefore, the ratio between available carbon in the leaf and internode biomass can be used to evaluate the balance between supply and demand.

An asymptomatic control plant has a supply demand balance of approximately 0.1 between the fourth source leaf (counted from the first visible dewlap) and the internode directly beneath it (Figure 75). Therefore, it can be assumed that values close to or equivalent to this benchmark are indicative of an equilibrium between source and sink. Both YCS and Moddus treated plants clearly show that supply significantly exceeds demand with ratios respectively eight and five-fold higher than control (Figure 75). This evidence supports the hypothesis that carbon fixation and loading of sucrose in the source phloem exceeds the sink demand or capacity. Quantification of readily available carbon in a YCS symptomatic Leaf 4 shows there is approximately one gram of both sucrose and total α-glucan on hand for export (Figure 76). These results confirm there is a significant excess of carbon accumulating in the YCS leaf (sucrose:3-fold & total α-glucan:5-fold greater than control). Failure to mobilise adequate amounts of carbon from the source tissue to maintain an equilibrium with the sink leads to disruption of the supply and demand balance.

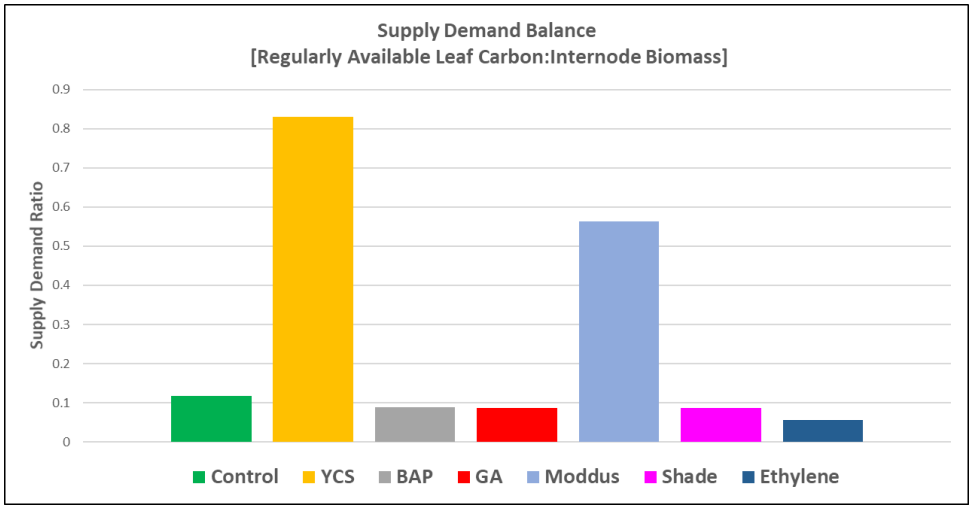

Figure 75 KQ228$^{\Phi}$ leaf & internode 4 supply demand balance

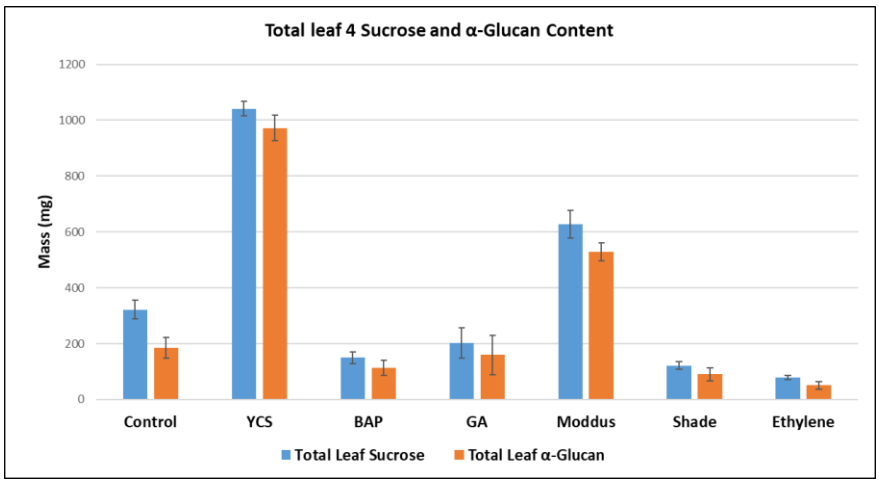

Figure 76 KQ228$^{\Phi}$ Leaf 4 (lamina and midrib inclusive) total sucrose and α-glucan content

In plant physiology it is generally accepted that the 'source' refers to photosynthetic tissue that is mainly responsible for carbon fixation and export, while the 'sink' refers to tissue which is the store of photoassimilation. Application of this definition '*loosely*' to the source leaf shows that the sucrose and two α-glucan pools in samples collected from the growth regulator field trial have distinct differences between the cellular compositions of source and sink tissues with respect to these metabolites (Figure 77). Our studies have noted that sucrose accumulation is highest in the midrib and sheath with starch levels greatest in the lamina of a YCS symptomatic leaf 4. The same correlation is evident when considering soluble α-glucan and insoluble α-glucan (starch) pools respectively (Figure 78A-C). Interestingly, both YCS and the GA inhibitor 'Moddus' have very similar quantities and patterns of distribution between the three tissue types for all three metabolites (Figure 78A-C). This suggests that the metabolic response (carbon redirection and partitioning) to reduced phloem export within the lamina of these two treatments is closely linked. Metabolomic studies support this finding with a significant ($p<0.0001$) difference of only 5 major metabolites (ribitol, proline, 9-12-15-octadecatrienoic acid, benzioic acid and β-sitosterol), between the YCS and Moddus treatment.

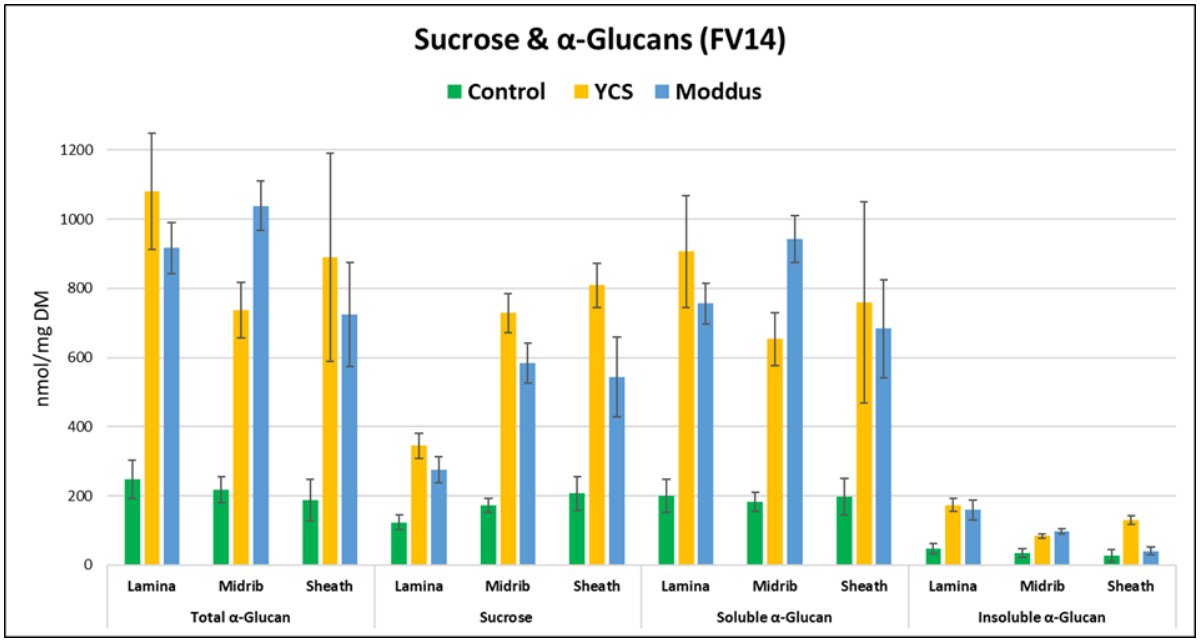

Figure 77 Source sink tissue, sucrose, and α-glucans

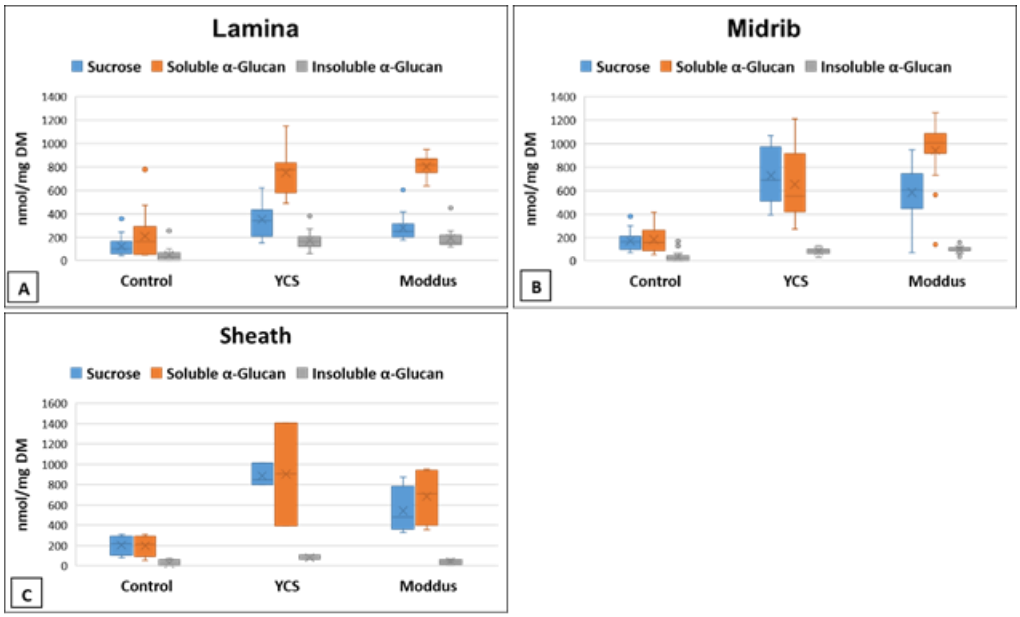

Figure 78 Leaf source (A) and sink (B & C) tissue sucrose & α-glucan content; treatments: control, YCS and Moddus (GA inhibitor)

The segregated portions within the total α-glucan pool show most of the carbon is partitioned as soluble α-glucans rather than starch in the source tissue (lamina). This is not surprising given that C_4 plants like sugarcane are not anatomically or physiologically capable of synthesising and storing large quantities of starch like their C_3 counterparts. One parameter that limits the synthesis and storage of starch in C_4 plants is the number of available bundle sheath cells in which the chloroplasts synthesise transitory starch during the day. It is well documented that starch synthesis also enables a higher rate of photosynthesis to be maintained during periods of high light and CO_2 when carbon assimilation exceeds the rate of sucrose synthesis and export. On the other hand, sucrose synthesis is favoured over starch when the photosynthetic rate is low. This regulatory control maintains a source sink balance to prevent the accumulation of sucrose in the source tissue (Baker and Braun,

2008; Weise et al., 2011). Interestingly, our ^{13}C studies showed there was a preference for starch synthesis in YCS leaves which have pre-existing elevated levels of sucrose. This also supports our gene expression studies (transcript abundance) of Sucrose phosphate synthase (SPS) and UDP glucose pyrophosphorylase that show sucrose synthesis is mainly under metabolic control. When sucrose accumulates in the cytosol of YCS plants it triggers the downregulation of the triose phosphate transporter through feedback regulation which results in carbon retention in the chloroplast (Figure 79) (Du et al., 2000; Weise et al., 2011). This is supported by an upregulation of both ADP GlcPPase (α-glucan synthesis) and α-amylase (α-glucan breakdown). An appreciation of the extent of the soluble α-glucan pool provides a better understanding of the metabolic response in the source tissue when sucrose export is compromised.

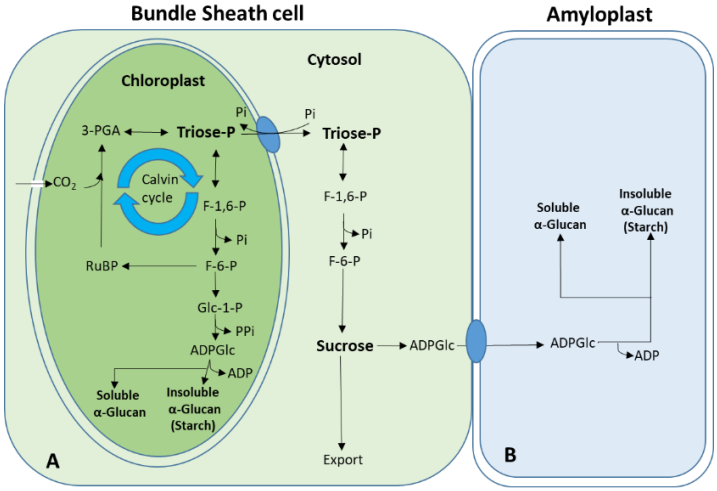

Figure 79 α-Glucan synthesis through CO_2 fixation A) sucrose breakdown B)

In contrast, the midrib and sheath which are mostly composed of sink tissue have lower levels of insoluble α-glucan (starch) and higher levels of soluble α-glucan than the lamina across all treatments (Figure 80A-C). This is most likely due to anatomical differences between the tissue types. Even though the midrib contains chloroplasts on its abaxial surface, it does not possess stomata and therefore cannot fix carbon through photosynthesis. Therefore, in the sink tissue the carbon required for synthesis of soluble and insoluble α-glucans is derived from sucrose breakdown, whereas in the photosynthetically active tissue it is derived from CO_2 fixation (Figure 79) (Myers et al., 2000). Higher levels of soluble α-glucan in sink tissue than in lamina also supports previous findings that phloem loading is not compromised. Also, the ability to partition excess carbon into alternative pools such as the phenylpropenoid and shikimate pathways seen in the lamina does not appear to be an option in the mostly sink tissue of the midrib and sheath. This may reflect reduced cellular diversity and metabolic plasticity.

Another point of note is that the insoluble proportion of the total α-glucan pool is approximately the same for all three tissue types (lamina, midrib and sheath) and treatments (control, YCS and Moddus) (Figure 80A-C).

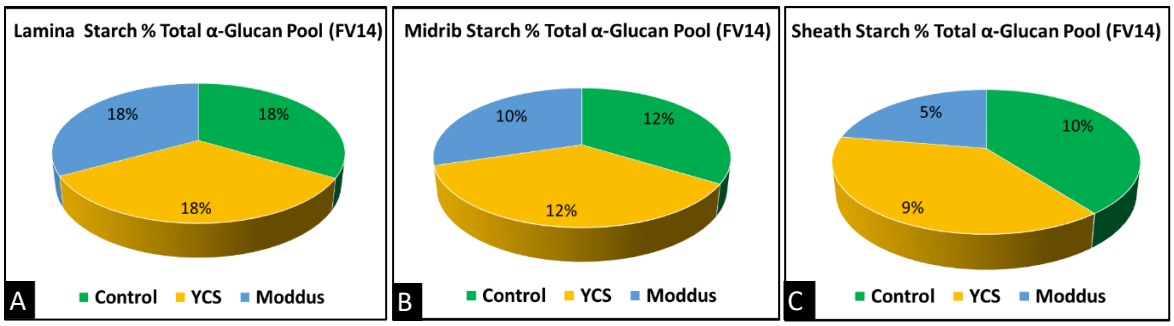

Figure 80 Starch proportion of total α-glucan pool Lamina A) Midrib B) Sheath C)

While this may seem unusual, it is consistent with uniform ratios of sucrose and starch reported between the source and sink tissues as well as the apoplastic fluid in YCS and control plants. This suggests that the cause of sucrose accumulation in YCS leaves and subsequent increases in the α-glucan pools is not due to a major physical blockage of the phloem that would ultimately disrupt these ratios. To prevent the accumulation of sucrose above the upper tolerable threshold, carbon is uniformly redirected or repartitioned to other pools in order to maintain homeostasis. The proportions within each pool is ultimately dictated by the cellular composition and available metabolic machinery of the tissue affected.

The combined data shows that the cause of sucrose accumulation in the YCS leaf, and the ensuing onset of yellowing, is the result of a physiological disorder triggered by reduced sink strength or carbon fixation rates that exceed maximum possible translocation rates through the phloem. Anything that can cause a source sink imbalance by significantly impeding mass flow of sucrose from the source leaf to the culm will induce early senescence. Therefore, YCS does not have a single cause; any factor that reduces sink strength, respiration and accelerates photosynthesis could trigger the event. Thus, YCS is a condition that is comparable to source sink regulated induced senescence.

6.5. Crop stress & YCS

Many research programs focus on understanding the stress response of plants. The objective is to improve productivity in existing fields and open up more marginal, higher stress environments to agriculture to meet the ever-growing world population and needs of the consumer. A C_4 crop like sugarcane fills a specific niche as it has one of the highest biomasses of any crop in the world and can tolerate a wide range of environmental conditions. The other attractive feature of C_4 photosynthesis is the operation of a CO_2-concentrating mechanism in the leaves, which serves to saturate photosynthesis and suppress photorespiration in normal air. Unfortunately, less is known about C_4 photosynthesis than C_3.

C_4 photosynthesis is highly sensitive to stress, with three defined phases

i) an early stomatal phase which may or may not be detected as a decline in assimilation (CO_2 fixing capacity and refixing in bundle sheath)
ii) a mixed stomatal and non-stomatal phase (damage to ETC) and,
iii) a mainly non-stomatal phase (carbon partitioning and cell death).

The main non-stomatal factors include

iv) reduced activity of photosynthetic enzymes; inhibition of nitrate assimilation, induction of early senescence,

v) sucrose and starch accumulation

vi) and changes to the leaf anatomy and ultrastructure

When plants are under environmental stress the photosynthetic light-dependent reactions are downregulated. This results in an over-reduction of the PET chain and generates reactive oxygen species (ROS). Non-photochemical quenching dissipates excess excitation energy (EEE), enabling photoprotection through the reduction in ROS production (Gill and Tuteja, 2010). Alternatively, the deleterious effects of ROS can be reduced through the activities of scavenging molecules such as antioxidant enzymes and metabolites. In both YCS asymptomatic and symptomatic tissue we see an increase in antioxidant enzymes such as the peroxidases, ascorbate peroxidases, superoxide dismutase, glutathione reductase and catalase. Metabolites of note include carotenoids, tocopherols, glutathione and ascorbate (Marquardt, 2019).

Cyclic electron flow is another mechanism that can reduce the effects of EEE in combination with antioxidant enzymes and alternative electron sinks (Strand et al., 2015). The production of ROS and redox molecules are thought to be involved in signalling between chloroplasts and the nucleus during plant stress (Mueller and Berger, 2009). This mechanism would allow for the regulation of nucleus-encoded genes for the chloroplast proteins. It is well documented that chloroplasts act as excellent sensors of environmental stress, linking plant metabolism and carbon reactions (Ahmad, 2014).

Oxidative stress can be caused by both biotic (pests and pathogens) and by abiotic (photosynthesis, metabolism, high light and temperature, water and nutrient limitations, high salt and heavy metal soils and elevated ozone) means (Apel and Hirt, 2004; Cakmak and Kirkby, 2008; Nishizawa et al., 2008; Keunen et al., 2013; Sham et al., 2014). It is worth noting here that our analyses have found no evidence of any YCS-associated biotic factors like bacterial, viral, or archaeal microorganisms in our sequencing data. It is far more likely that the oxidative stress response we see here in YCS-affected plants is due to abiotic factors.

6.5.1. Transcriptome Results and Discussion

Our transcriptome data shows an overwhelming correlation between YCS and abiotic stress. YCS shows similarity to abiotic stress responses on the protein level through chloroplast and photosynthetic ETC process down-regulation, increased oxidative stress, chaperonins, and protease upregulation. YCS also shows protein changes often associated with a leaf “feast” state, in addition to general abiotic stress associated with disruptions to sugar and starch turnover, sugar transport, carbohydrate/energy balance and organic acid metabolism. This is supported by transcriptome analyses that consistently feature upregulation of cell membrane degradation and oxidative stress (Figure 81, Figure 82). For this analysis, the RNAseq reads were mapped to the YCS reference Transcriptome produced during this study.

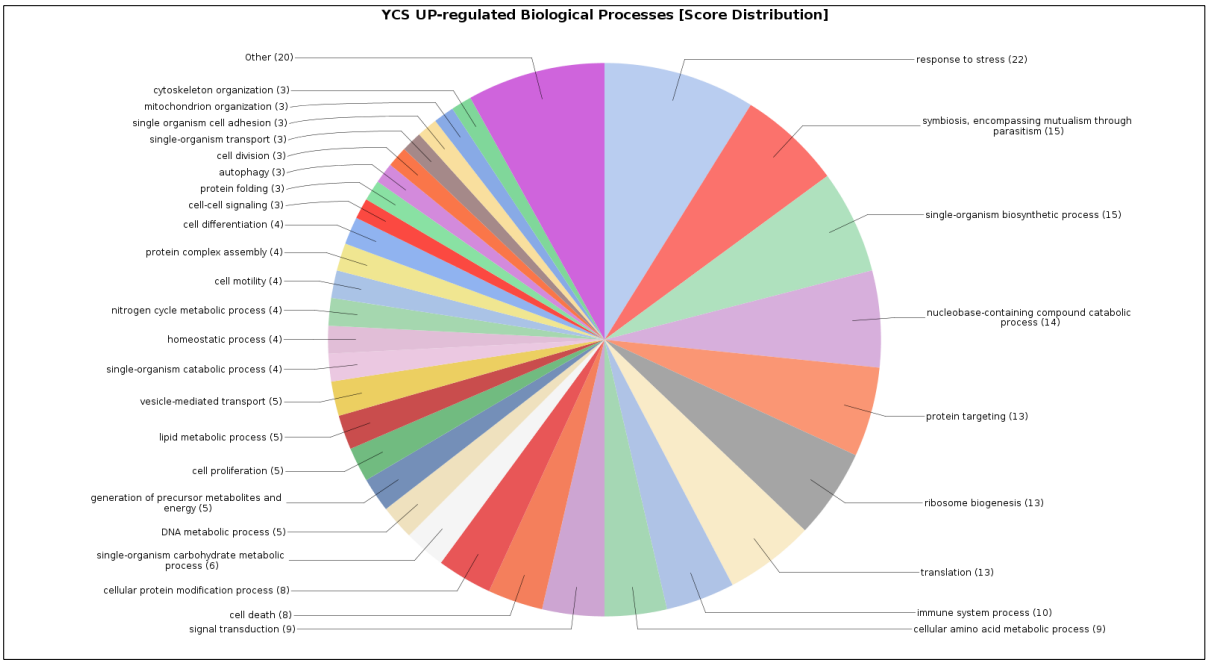

Figure 81 Transcriptomic differential expression analysis showing the biological processes enriched in the transcripts up-regulated in YCS-affected plants

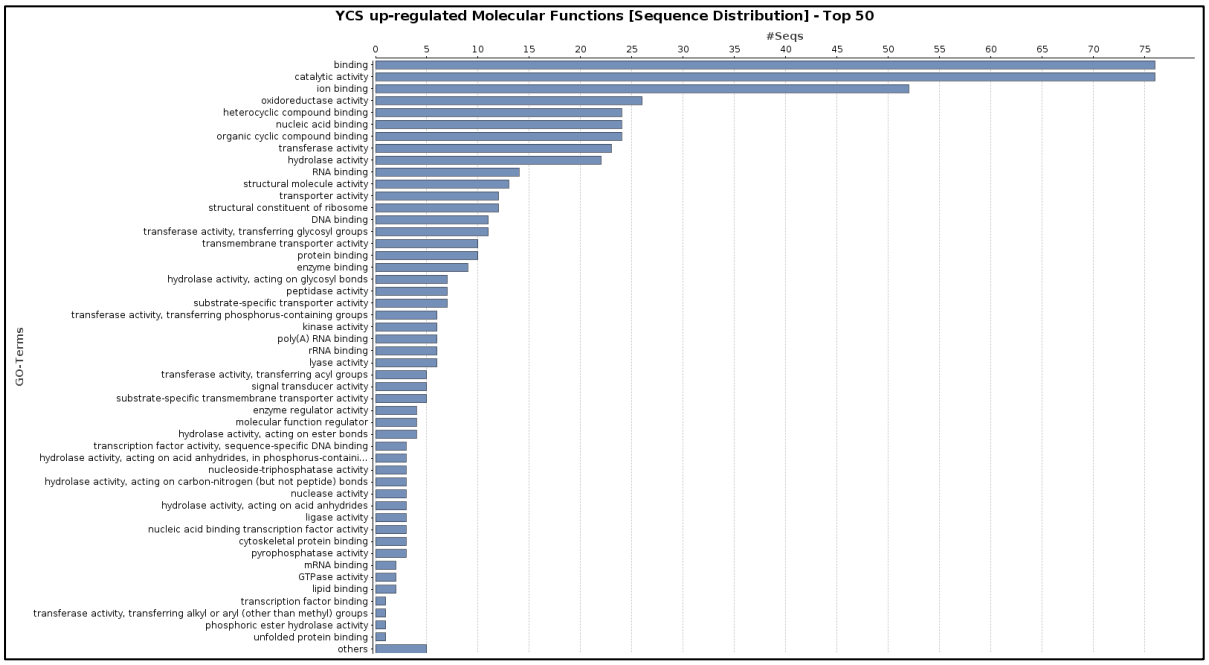

Figure 82 Molecular functions enriched in the transcripts in higher abundance in YCS

The following differential expression analysis revealed 327 transcripts whose expression changed directly in response to YCS. These transcripts, with a Bonferroni-corrected p-value of 0.0 and a $\log_2$ fold change of greater than the absolute value of 1, are highlighted in red in Figure 83. The link between water or osmotic stress and reduced stomatal conductance, growth rate (stem elongation)/sink strength, increased heat, cell membrane and mechanical damage, disruption to metabolism, photosystems, and induced senescence is clearly evident.

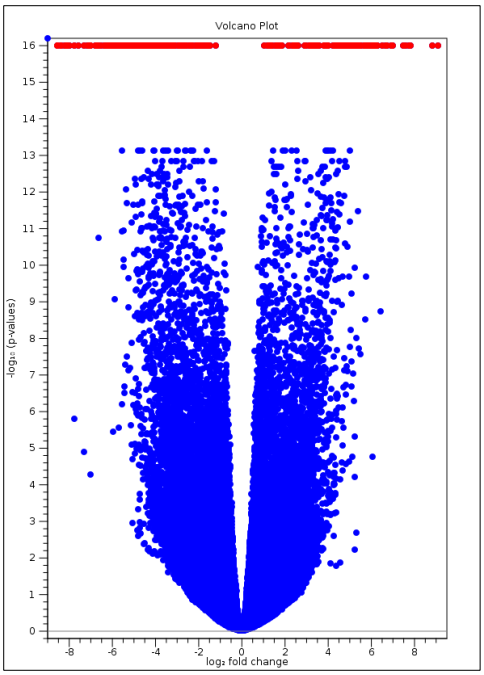

Figure 83 Volcano plot (log fold change against log p-value) of YCS differential expression results, with the highly significant transcripts (Bonferroni-corrected p-value = 0.0 and log_2 absolute fold change >1) shown in red.

A Bonferroni-corrected p-value of zero means that there is practically zero likelihood of these expression changes occurring by chance. While the analysis could have been done using a less stringent statistical threshold, we have chosen to focus on those transcript expression changes that have occurred in direct response to YCS. This focus removes much of the noise and makes the results clearer to interpret. Using this measure, 327 transcripts were found to be highly significant in YCS.

These highly significant transcript expression changes were split into those in higher abundance in YCS (123 transcripts) and those in lower abundance in YCS (204 transcripts) as compared to the healthy controls, for the next section.

6.5.2. Higher abundance transcripts in YCS

Small subsets of the full expression table are included below. The full expression table forms part of the supplementary material.

Table 10 shows the transcripts with an over 50 times greater abundance in YCS, sorted by Fold Change in descending order.

Table 10: Transcript abundance in YCS over 50-fold greater than in the healthy controls.

Transcript Name	Transcript Annotation Description	Fold change in YCS
YCS-internode-contig_66889	thioredoxin h2	557.0873
YCS-leaf-contig_51243	PREDICTED: uncharacterized protein LOC101760134	454.8396
YCS-internode-contig_117452	retrotransposon unclassified	225.4676
YCS-leaf-contig_72328	disease resistance RPM1-like	215.6185
YCS-internode-contig_61030	rRNA N-glycosidase	193.5763
YCS-leaf-contig_12893	Zinc knuckle family expressed	179.7022
YCS-internode-contig_123895	ricin-agglutinin family	130.0371
YCS-internode-contig_59004	hypothetical protein Ccrd_002160	121.9336
YCS-internode-contig_28969	disease resistance RPM1	108.4387
YCS-leaf-contig_22368	thioredoxin H2-like	100.9698
YCS-internode-contig_65157	receptor kinase At4g00960	92.40045
YCS-internode-contig_87450	retrotransposon unclassified	78.50381
YCS-internode-contig_58254	Disease resistance RPP13	76.08452
YCS-internode-contig_126434	no homology found during annotation	75.82117
YCS-internode-contig_148991	disease resistance TAO1-like isoform X1	73.36546
YCS-internode-contig_73083	probable LRR receptor-like serine threonine- kinase At3g47570 isoform X1	72.40314
YCS-leaf-contig_116952	poly	67.8532
YCS-internode-contig_84764	disease resistance RPP13 2	66.61418
YCS-internode-contig_31065	PREDICTED: uncharacterized protein LOC9269814	65.04132
YCS-internode-contig_136782	no homology found during annotation	60.82665
YCS-internode-contig_28044	disease resistance RPP13 2	59.78355
YCS-internode-contig_23999	no homology found during annotation	57.74354
YCS-internode-contig_17589	hypothetical protein SORBI_3001G311601	53.92115
YCS-internode-contig_33452	60 kDa jasmonate-induced -like	53.54455
YCS-internode-contig_55760	hypothetical protein SORBI_3005G003400	52.26274
YCS-internode-contig_32540	disease resistance RPM1-like	51.55303

These results show that oxidative stress and perturbed electron transport are key molecular features of YCS. The transcript with the highest expression fold change in YCS was (YCS-internode-contig_66889) annotated as ‘thioredoxin h2’, which was 557 times more abundant in YCS samples. Another transcript (YCS-leaf-contig_22368) with a similar ‘thioredoxin H2-like’ annotation was also 100 times more abundant in YCS samples. Thioredoxin is involved in regulating photosynthesis through electron transport, and functions in defence against oxidative stress (Arnér and Holmgren, 2000). As electron acceptors, thioredoxins play an important role in regulating carbon photo-assimilation (Schürmann and Jacquot, 2000).

Drought water stress was revealed to be directly related to YCS expression. At 454-fold higher abundance, the transcript (YCS-leaf-contig_51243) was the second-highest upregulated in YCS and is annotated as ‘PREDICTED: uncharacterized protein LOC101760134’. The expression of this protein has been shown to be highly induced in sugarcane cultivars subjected to prolonged water deficit (Belesini et al., 2017).

Heat stress is also implicated in YCS. The transcript (YCS-internode-contig_59004) annotated as 'hypothetical protein Ccrd_002160' was 121-fold more abundant in YCS. The transcript was BLAST matched to a similar Arabidopsis protein (AT4g17250/dl4660w, https://www.uniprot.org/uniprot/Q93ZA8 , accessed 02/04/20). This protein has been shown to be upregulated in Arabidopsis in response to heat stress (Lim et al., 2006). Our data show there is reduced stomatal conductance and a distinct K-step in the O-K-J-I-P transient Chl a fluorescence studies and inhibition of the OEC in YCS plants. These are all indicative of elevated leaf temperature (see section 6.2.3 of this report).

Plant stress is further implicated in YCS with the two retrotransposon transcripts (YCS-internode-contig_117452 and YCS-internode-contig_87450) that appeared in the list, at 225- and 78-fold higher abundance in YCS respectively. Retrotransposons are known to be transcriptionally activated by various biotic and abiotic plant stresses (Grandbastien, 1998; Kumar and Bennetzen, 1999). This indicates the high levels of stress that YCS plants endure and underlines the importance of plant stress in triggering expression of typical YCS symptoms in crops.

In addition to stress, disease resistance response appears to be important in YCS. Three types of disease resistance (RPM1, TAO1 and RPP13) responses from seven separate transcripts were upregulated more than 50-fold in YCS. These transcripts confer protection to the plants from bacteria and fungi and are involved in triggering a hypersensitive response (https://www.uniprot.org/uniprot/Q39214 /Q9FI14 and /Q9M667 , accessed 2/4/20). Given that previous research (Hamonts et al., 2018) failed to find a consistent biotic signal in YCS plants, these upregulated transcripts may be indicative of a secondary, opportunistic response of various microorganisms feeding on the high sucrose levels retained in the leaf tissue of YCS-symptomatic plants.

Plant defence is also implicated in YCS, by the three transcripts (YCS-internode-contig_61030, YCS-internode-contig_123895 and YCS-internode-contig_33452) that were annotated with 'rRNA N-glycosidase', 'ricin-agglutinin family' and '60 kDa jasmonate-induced -like', which were 193-, 130- and 53-fold more abundant in YCS respectively. These transcripts may play a role in protecting plants from viruses or herbivorous insects (Dunaeva et al., 1999; Peumans and Damme, 2001).

Circadian rhythm disruption has been reported previously in YCS-symptomatic plants and is supported in this study with the transcript (YCS-leaf-contig_12893) 'Zinc knuckle family expressed' having a 179 times higher abundance in YCS (Marquardt et al., 2016; Marquardt et al., 2017). Zinc knuckle proteins have been shown to regulate growth-related genes in a circadian manner in response to light, with experimental over-expression resulting in extended elongation phases for growing plant organs (Loudet et al., 2008). Therefore, this transcript upregulation may serve to counteract the source-sink imbalance linked to YCS development as postulated in this final report.

Protein modification is upregulated in YCS, with two transcripts (YCS-internode-contig_65157 and YCS-internode-contig_73083) annotated as 'receptor kinase At4g00960' and 'probable LRR receptor-like serine threonine- kinase At3g47570 isoform X1' being 92-fold and 72-fold more abundant respectively in YCS than in the healthy controls. These transcripts are involved in protein phosphorylation (https://www.uniprot.org/uniprot/O23082 and https://www.uniprot.org/uniprot/C0LGP4 accessed 02/04/20). While it's not clear which proteins

are being phosphorylated in this situation, such modifications serve to regulate enzyme activity and form part of complex signalling pathways within the cell (Olsen et al., 2006).

While the remainder of the transcripts in the table were without functional annotation, we submitted all of the upregulated transcripts to the MapMan4 webtool (https://plabipd.de/portal/mercator4 accessed 28/03/20; (Schwacke et al., 2019) to investigate the metabolic pathways upregulated in YCS. The results show that the pathways upregulated in YCS include carbohydrate metabolism, amino acid metabolism, nucleotide metabolism, polyamine metabolism, redox homeostasis, protein modification, solute transport and enzyme classification. The sequence of events that lead to the disruption of leaf metabolism, the development and expression of YCS are put forward in the following conceptual model (Figure 84).

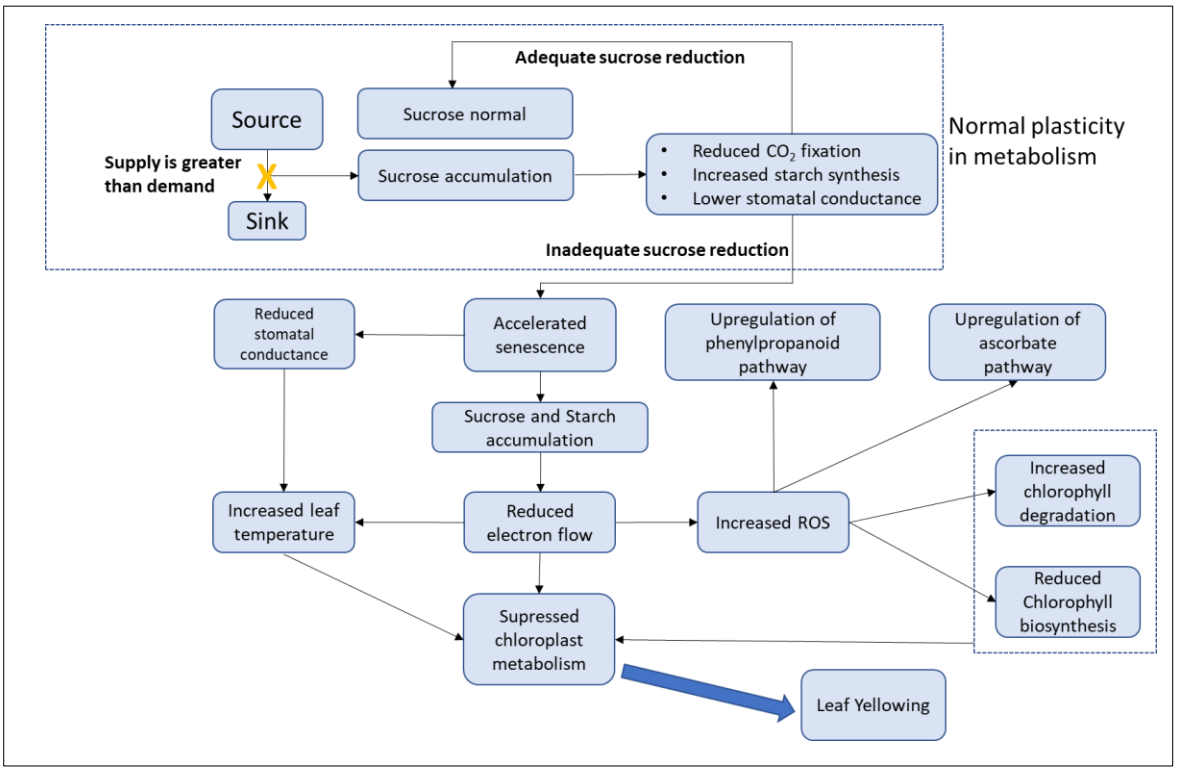

Figure 84 Simplified conceptual model of YCS development. The symptoms of YCS (leaf yellowing) are the result of sucrose feedback regulatory effects upon photosynthesis in leaf lamina, due to inadequate sucrose movement out of the leaf whereby sucrose movement through the phloem (out of the leaf) is influenced at a point beyond the leaf sheath and linked to reduced sink strength.

6.5.3. Lower abundance transcripts in YCS

The 204 downregulated transcripts were similarly submitted to the MapMan4 webtool (https://plabipd.de/portal/mercator4 accessed 28/03/20; (Schwacke et al., 2019) to investigate the metabolic pathways downregulated in YCS. The results show that the pathways downregulated in YCS include chromatin organisation, protein modification and enzyme classification. While two of these pathways were also upregulated in YCS, the transcripts involved in each group were placed into different bin sub-compartments. This is indicative of the complex signalling pathways involved in YCS.

Table 11 shows the transcripts with an over 50 times lower abundance in YCS, sorted by Fold Change in descending order.

Table 11 Transcripts abundance over 50 times lower in YCS than in the healthy controls.

Transcript Name	Transcript Annotation Description	Fold change in YCS
YCS-leaf-contig_17098	thiol protease SEN102-like	-372.745
YCS-leaf-contig_12909	disease resistance RPP13	-365.571
YCS-leaf-contig_80039	inactive disease susceptibility LOV1 isoform X1	-333.769
YCS-internode-contig_54680	NC domain-containing -related	-325.06
YCS-internode-contig_96292	disease resistance RPP13 3	-290.497
YCS-leaf-contig_12015	ERBB-3 BINDING PROTEIN 1	-279.421
YCS-internode-contig_147271	disease resistance RPP13 3	-269.705
YCS-internode-contig_40467	disease resistance RPP13 2	-268.712
YCS-internode-contig_152225	probable disease resistance At4g27220	-252.498
YCS-internode-contig_120597	no homology found during annotation	-214.248
YCS-internode-contig_38877	1-aminocyclopropane-1-carboxylate oxidase homolog 1-like	-189.846
YCS-leaf-contig_117596	Disease resistance RPP8 3	-158.031
YCS-internode-contig_107136	Tyrosine-sulfated glycopeptide receptor 1	-143.016
YCS-internode-contig_90793	disease resistance RPP13 3	-134.642
YCS-internode-contig_129275	disease resistance RPP13 1	-128.337
YCS-internode-contig_123845	disease resistance RPP13 3 isoform X1	-128.268
YCS-internode-contig_114126	disease resistance RPP13-like	-109.382
YCS-leaf-contig_1275	receptor kinase At3g47110 isoform X1	-105.622
YCS-internode-contig_50228	serine threonine kinase	-100.356
YCS-internode-contig_140218	no homology found during annotation	-97.3528
YCS-internode-contig_47899	no homology found during annotation	-92.1182
YCS-internode-contig_90491	hypothetical protein SORBIDRAFT_05g026310	-81.5799
YCS-internode-contig_88793	NC domain-containing family	-79.7855
YCS-internode-contig_85963	cysteine-rich receptor kinase 12 isoform X1	-74.5204
YCS-internode-contig_94217	PREDICTED: uncharacterized protein LOC100836056 isoform X1	-74.1727
YCS-internode-contig_40527	ALTERED XYLOGLUCAN 4	-72.9392
YCS-leaf-contig_123249	very low-density lipo receptor isoform X1	-67.8642
YCS-leaf-contig_40936	disease resistance RPP13-like	-67.1522
YCS-internode-contig_121112	disease resistance RGA1	-65.9965
YCS-internode-contig_77154	no homology found during annotation	-63.6156
YCS-internode-contig_123374	hypothetical protein SORBIDRAFT_05g022610	-61.4649
YCS-leaf-contig_10567	proline-rich receptor kinase PERK4 isoform X1	-60.7898
YCS-internode-contig_50581	disease resistance RPM1-like	-58.2054
YCS-internode-contig_67000	ubiquitin-like-specific protease 1B	-54.2002
YCS-internode-contig_9130	Nitrate transporter	-53.9854
YCS-internode-contig_135620	Retrovirus-related Pol poly LINE-1	-53.8903
YCS-leaf-contig_58531	condensin-2 complex subunit H2	-53.1811
YCS-internode-contig_64173	retrotransposon expressed	-51.5089
YCS-leaf-contig_38936	hypothetical protein SORBI_3002G343901	-50.7295
YCS-internode-contig_51648	no homology found during annotation	-50.5671

These results indicate that YCS-affected sugarcane may be in a developmental stage related to the ripening off stage that normally occurs just prior to harvest. Here, the transcript (YCS-leaf-contig_17098) annotated as 'thiol protease SEN102-like' was 372-fold less abundant in YCS than in the healthy controls. This protein has been shown to be downregulated in plants, particularly fruits, when ripening occurs (Drake et al., 1996). Alternatively, as the ripening process in sugarcane is metabolically similar to mild water stress, affecting stalk elongation (Morgan et al., 2007), so this highly down-regulated transcript may instead be indicative of plant stress caused by a water deficit.

Interestingly, like the higher abundance transcripts, many of the transcripts in lower abundance in YCS were ones related to disease resistance. Five disease resistance annotations (RPP13, At4g27220, RPP8 3, RGA1, RPM1-like) from thirteen different transcripts were significantly down-regulated in YCS, with expression changes ranging from 58- to 365-fold lower abundance in YCS. This result suggests that plant pathogens are not involved in YCS, and may instead reflect the complex, multicomponent regulatory system involved in plant immunity (Andersen et al., 2018).

Leaf tissue abscission may be important in YCS. The transcript (YCS-leaf-contig_80039) annotated as 'inactive disease susceptibility LOV1 isoform X1' is 333-fold lower abundant in YCS. The transcript annotation is a synonym for 'LONG VEGETATIVE PHASE 1', and this protein is a transcription factor that has been shown to regulate leaf abscission through a decrease in expression as the abscission process develops (Kim et al., 2016). In addition, LOV1 expression is thought to be controlled by the photoperiod pathway and regulates abiotic stress response where a decrease in expression triggers a hypersensitive response (Yoo et al., 2007). This suggests that YCS leaf yellowing is terminal for that leaf and may result in the leaf being sacrificed by the plant. This would not have a serious impact as sugarcane can grow a new leaf approximately every 150°Cd or about every 7-10 days in summer (Inman-Bamber, 1994; Inman-Bamber et al., 2005)

Abiotic stress response is again highlighted in YCS, with the two transcripts annotated as 'NC domain-containing -related' (YCS-internode-contig_54680 and YCS-internode-contig_88793) expressed 325-fold and 79-fold lower abundance respectively in YCS. Low expression of this protein under drought and salt stress regulates plant growth (Nounjan et al., 2018).

Reduced growth in YCS is also supported by the 'ERBB-3 BINDING PROTEIN 1' transcript (YCS-leaf-contig_12015) having a 279-fold lower abundance in YCS. Expression of this protein regulates plant growth and affects plant organ size, with low expression resulting in reduced growth (Horváth et al., 2006).

Reduced cell elongation may contribute to the reduced growth phenomenon in YCS. The transcript '1-aminocyclopropane-1-carboxylate oxidase homolog 1-like' (YCS-internode-contig_38877) was down-regulated 189-fold in YCS. This protein is involved in ethylene biosynthesis and reduced expression results in reduced stem elongation (Qin et al., 2007). In addition, the transcript (YCS-leaf-contig_10567) annotated as 'proline-rich receptor kinase PERK4 isoform X1' was 60-fold less abundant in YCS. This transcript codes for a protein that regulates the ABA-mediated growth inhibition in response to water deficit stress, with particular effect on cell elongation (Sharp et al., 1994; Davies et al., 2005; Bai et al., 2009). In section 6.2.5 of this report we showed upregulation of trehalose synthesis through TPP and TPS in all YCS leaf tissue. This is dependent on the T6P precursor (Figueroa and Lunn, 2016). T6P has been implicated in regulating growth and development through the protein SnRK1 which suppresses photosynthesis, carbohydrate and amino

acid pathways (Nuccio et al., 2015). Furthermore, T6P has been linked to ABA-mediated stress responses in plants (Li et al., 2014). ABA levels in YCS symptomatic leaf tissue are approximately 2 to 4-fold higher than asymptomatic controls (Figure 85).

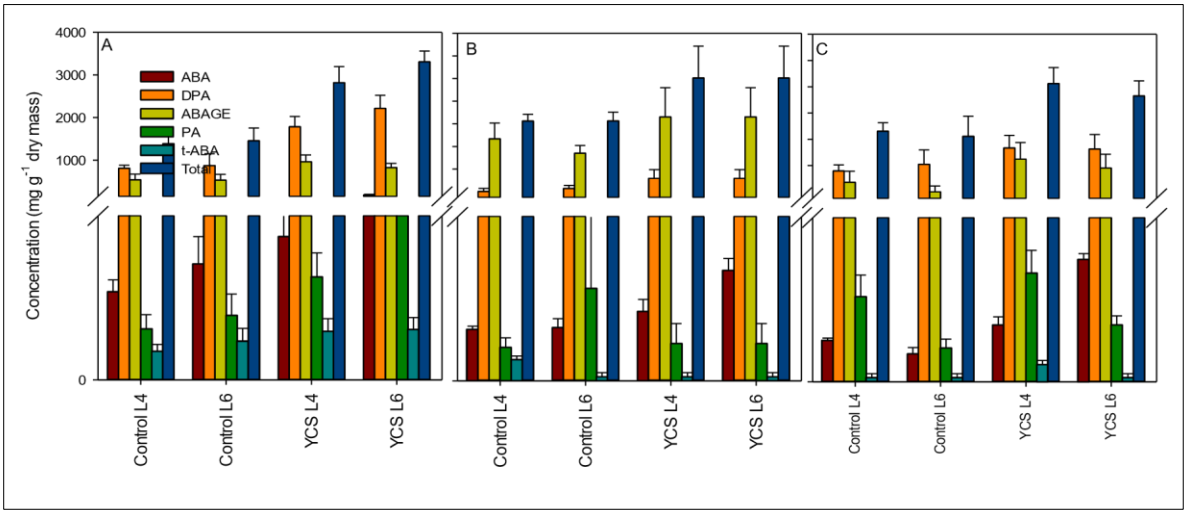

Figure 85 Changes in ABA and ABA catabolites in YCS symptomatic and asymptomatic leaves. Q200$^{\Phi}$ in the Herbert (A), KQ228$^{\Phi}$ in the Burdekin (B) and Q208$^{\Phi}$ in Mackay (C). Values ± standard deviation (Botha et al., 2015)

Reduced growth in YCS is further supported by the transcript (YCS-internode-contig_107136) annotated as 'Tyrosine-sulfated glycopeptide receptor 1' which was 143-fold lower in abundance in YCS. This protein mediates a signalling pathway that regulates plant growth, plant immunity and energy production (https://www.uniprot.org/uniprot/Q9C7S5 accessed 03/04/20; (Amano et al., 2007).

The two transcripts (YCS-leaf-contig_1275 and YCS-internode-contig_50228), annotated as 'receptor kinase At3g47110 isoform X1' and 'serine threonine kinase' respectively, were 105- and 100-fold down-regulated in YCS. Both these proteins play a role in the MAPK signalling pathway, specifically with pathogen infection (https://www.genome.jp/kegg-bin/show_pathway?ko04016+K13420), and their down-regulation in YCS is further support that plant pathogens are not involved in YCS and that the underlying cause of YCS is most likely to be abiotic in origin.

Early senescence in YCS is indicated by the 74-fold down-regulation of the transcript (YCS-internode-contig_85963) annotated as 'cysteine-rich receptor kinase 12 isoform X1'. In transgenic studies, the knockout model for this protein exhibited an early flowering and early leaf senescence phenotype (Idänheimo, 2015), so presumably a significant down-regulation would have a similar effect. This supports our research conclusion that YCS is a form of source sink related senescence

The transcript (YCS-internode-contig_40527) annotated as 'ALTERED XYLOGLUCAN 4' was 72-fold in lower abundance in YCS. This protein is involved in O-acetylation of the hemicellulose xyloglucan in the plant cell wall (Gille et al., 2011). In transgenic studies, non-functional mutant versions of this protein had very little phenotypic effect, although it was hypothesised that the cell wall structure may play a role in plant defence and xylem structure (Gille et al., 2011; Schultink et al., 2015). It is unclear what the consequence of the reduced expression of this protein in YCS would be.

Equally unclear is the effect of the downregulation of the transcript (YCS-leaf-contig_123249) annotated as 'very low-density lipo receptor isoform X1', which was 67-fold less abundant in YCS. This protein is involved in molecular signalling, with the Sorghum homolog annotated as 'G protein-coupled receptor signalling pathway' (https://www.ebi.ac.uk/QuickGO/term/GO:0007186 and https://www.kegg.jp/ssdb-bin/ssdb_best?org_gene=ptr:455722 accessed 06/04/20). It is not known which signal this protein is mediating in YCS.

Changes in signalling pathways and regulation are further supported by the 61-fold lower abundance in YCS of the transcript (YCS-internode-contig_123374), annotated as 'hypothetical protein SORBIDRAFT_05g022610'. This protein was BLAST matched to a putative retrotransposable element in rice (GenBank accession AAN04214.1). In addition, the transcript (YCS-internode-contig_64173) annotated as 'retrotransposon expressed' was also 51-fold less abundant in YCS. Transposons are well known to modulate gene expression and plant response, particularly under stress conditions (Negi et al., 2016; Dubin et al., 2018), and this result further illustrates the role of plant stress underlying YCS.

Turnover of abnormal or short-lived proteins may be impacted in YCS. The transcript (YCS-internode-contig_67000) annotated as 'ubiquitin-like-specific protease 1B' was 54-fold less abundant in YCS. This transcript codes for a sumoylation protease involved in essential protein degradation and turnover of abnormal and short-lived proteins (Yan et al., 2000; Schulz et al., 2012). Plant stress is implicated here too, as the transcript is expressed in Cajal bodies, which are distinct sub-nuclear structures. Cajal bodies are known to be functionally affected during a plant stress response and indeed may play a role in regulating abiotic stress responses in the plant (Love et al., 2017) .

The transcript (YCS-internode-contig_9130) annotated as 'Nitrate transporter' was 53-fold less abundant in YCS. Nitrate transporters have a multitude of functions within the plant, particularly in mediating plant growth and stress response (Fan et al., 2017). Of relevance to YCS, the expression of several nitrate transporters has been shown to be downregulated in plants undergoing osmotic or drought stress (Fan et al., 2017).

The transcript (YCS-leaf-contig_58531) annotated as 'condensin-2 complex subunit H2' was 53-fold less abundant in YCS. This protein is involved in DNA replication and repair during mitosis, and it's lower abundance may be indicative of less cell replication occurring in YCS, resulting from a reduced growth rate (Fujimoto et al., 2005); https://www.uniprot.org/uniprot/Q9LUR0 accessed 06/04.20.

6.5.4. Principle component analysis

To investigate the underlying structure of the data and the factors influencing YCS expression, the samples were clustered by the principal components of the YCS Reference transcript expression data and were visualised in the following figures.

In Figure 86, the two principal components 1 and 2 show that the biggest impacts on transcript expression were firstly the sample batch (when and where the sample was taken, processed and/or sequenced), with PC1 explaining 22.3% of the variation, and secondly the sample tissue type, with PC2 explaining 7% of the variation.

Figure 87 show the same plot as Figure 86, this time with the sample's cultivar (variety) labelled, to demonstrate that while the cultivars could be separated out, the sample batch was a better explanation for the data.

Figure 88 shows the principal components PC3 against PC5. It is only in this plot that the YCS and Control samples start to cluster away from each other by treatment. Here, PC3 and PC5 explain 3.8% and 2.6% of the expression data, respectively.

Together, these PCAS results show that the batch effect and tissue type were more influential than the cultivar on the transcript expression, and that the treatment type (YCS or Control) explained only a small proportion of the result.

Similarly, Figure 89 shows a heat map analysis of the 327 highly significant transcripts differentially expressed in YCS. As the heatmap demonstrates, the batch, tissue and variety type all help explain the clustering, and the transcripts cannot be clearly grouped only by treatment type.

This supports our conclusion that YCS is a physiological disorder and our samples display varying degrees of metabolic disruption dependent on the degree of sink limitation or source sink imbalance. This also supports our findings that YCS is not the result of a single cause.

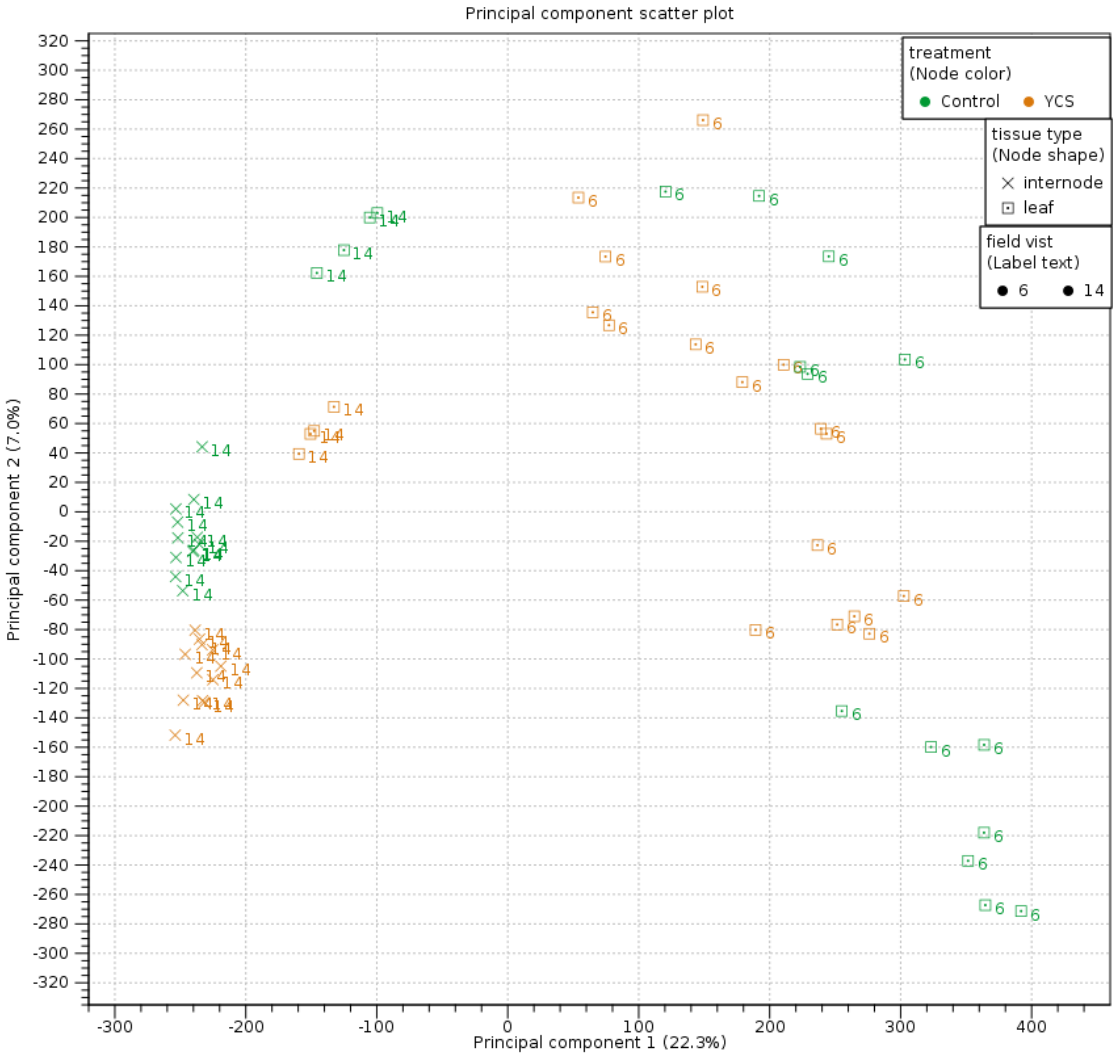

Figure 86 PCA plot of YCS and Control expression data, showing PC1 against PC2.

Figure 87 Another PCA plot of YCS and Control expression data, showing PC1 against PC2, this time with the variety type labelled.

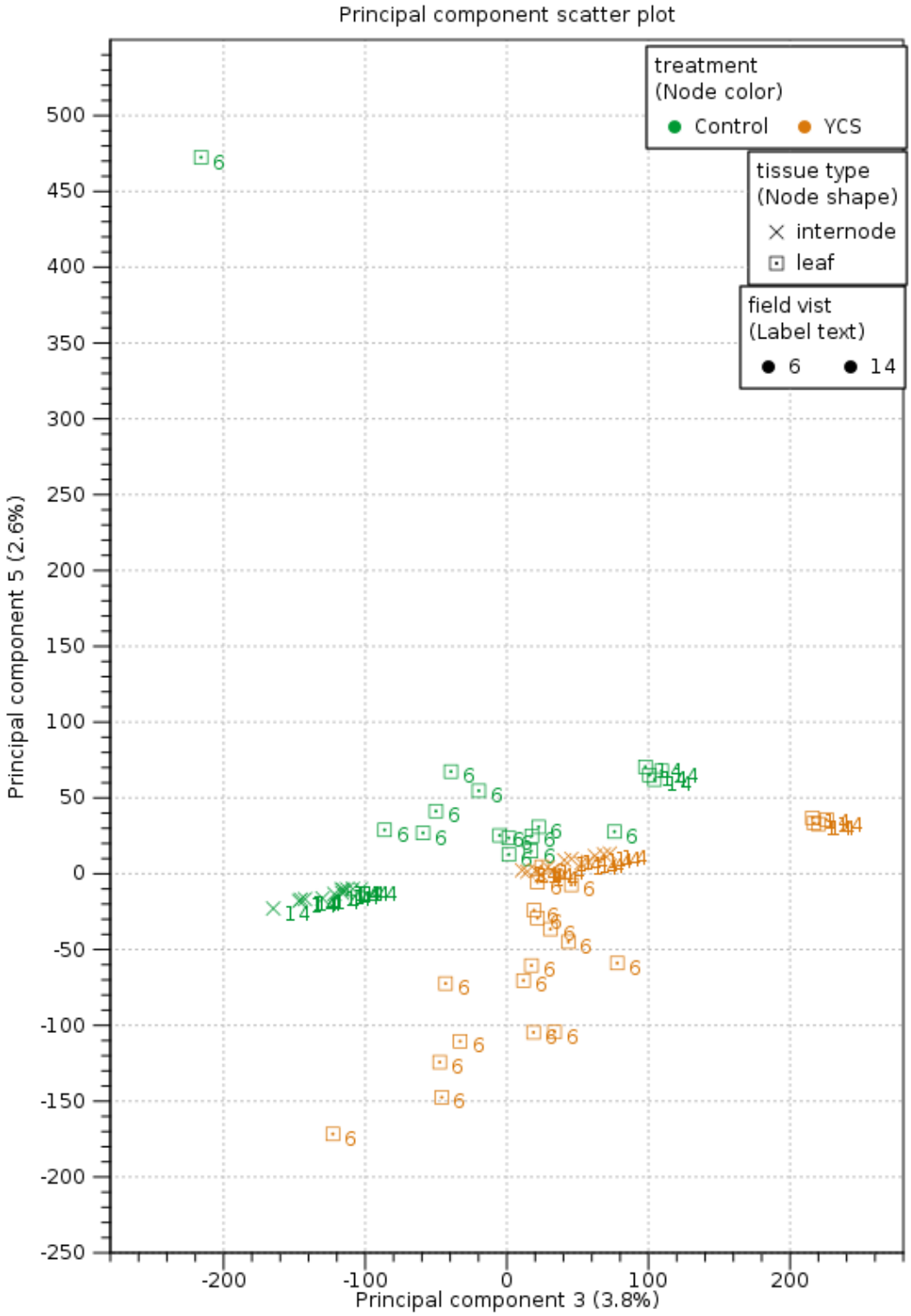

Figure 88 PCA plot of YCS and Control expression data, showing PC3 against PC5

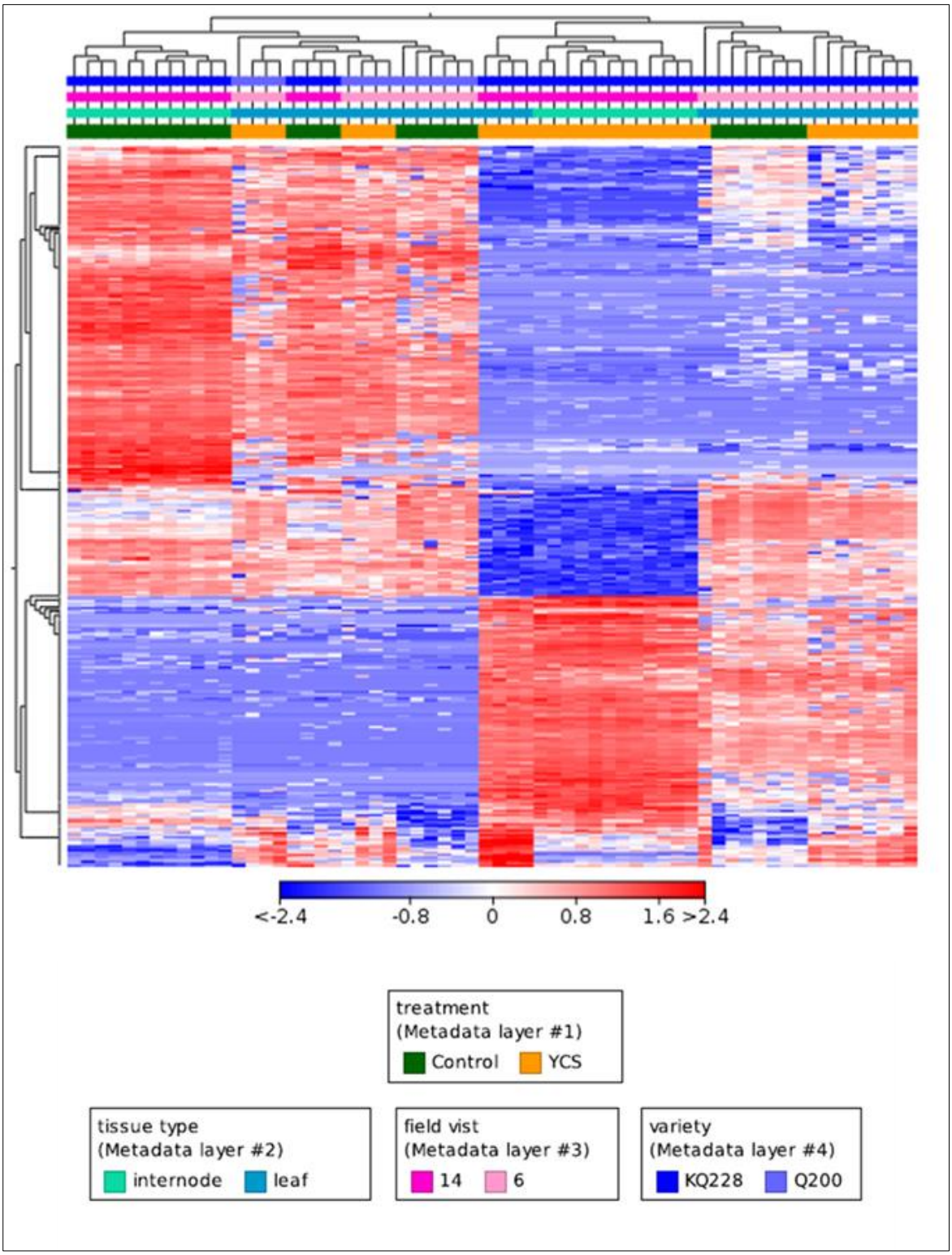

Figure 89 Expression heat map of the 327 highly significant transcripts (Bonferoni = 0.0, log_2 fold change > abs 1). Heat map was clustered using the mean Euclidean distance.

This collective data confers with results and conclusions presented within this report that the key driver of YCS is reduced growth rate. This is primarily associated with abiotic and not biotic causal agents. Reports from industry also concur that YCS expression is always preceded by some form of stress.

6.6. Diagnostics

6.6.1. Sucrose/ Starch YCS Diagnostic

It is notoriously difficult to identify YCS in sugarcane fields where a significant portion of the sugarcane leaves are yellowing as a result of many other factors. However, our studies have shown that YCS symptomatic and asymptomatic leaves from the same culm always have higher sucrose and starch levels compared to their control counterparts. While YCS asymptomatic and symptomatic leaves always have elevated levels of sucrose and starch, it is not only confined to the yellow sections of the lamina. Sugars and starch also accumulate in the green parts of the leaf lamina, midrib, dewlap, and sheath, with the highest content located in the leaf sheath and midrib (see section 6.2.5 of this report). Therefore, early detection of either sucrose or starch accumulation in asymptomatic leaves may inform growers of an impending development of YCS. If growers could identify factors that may have contributed to a slowdown in crop growth (leading to a source sink imbalance) and the subsequent sucrose and starch accumulation, then this will assist them to better manage the crop to prevent or reduce further incidence of YCS.

6.6.1.1. Midrib stain test

It is difficult to measure leaf sucrose in the field without the assistance of expensive and cumbersome equipment, which made starch the choice of metabolite to test for. Excessive starch accumulation in the source leaves will occur when sucrose transport from the leaf to the culm is impeded. As sucrose levels begin to build-up in the leaf, more carbon is redirected to starch in the lamina, midrib, and sheath. This allows the leaf to store carbon in an inert form to slow down the disruption to metabolism. Starch (insoluble α-glucan) is easily stained with iodine solution to produce a blue-black colour (see section 6.2.5 of this report) which is clearly visible with the naked eye or with the help of a simple inexpensive X10 magnifying hand lens. Using high starch content as the criterion for tissue selection for the diagnostic, it was decided to use midrib over sheath as the sample material. Also considered was the ease of accessing this tissue from the plant. The sheath, while attainable, is tightly held to the culm in the mid-canopy and makes for a more time consuming and arduous sampling task. Furthermore, the cross-sectional area of the midrib is much larger than that of the sheath, or other leaf tissue for that matter, making visual diagnosis in the field easy and fast. The use of 1% iodine solution (optimised in the lab - data not shown) also made this test very safe for the user. Figure 90 shows the composition of the midrib stain kit.

Figure 90 Midrib stain kit contains 1% iodine solution dropper bottle, 10X magnifying hand lens and lanyard, safety data sheet

To investigate the accuracy of the midrib stain diagnostic, lamina and midrib tissue was collected at first light from eight commercial varieties (SRA3$^{\Phi}$, Q240$^{\Phi}$, Q250$^{\Phi}$, Q242$^{\Phi}$, Q200$^{\Phi}$, KQ228$^{\Phi}$, Q232$^{\Phi}$and Q208$^{\Phi}$) cultivated in Ingham (HCPSL RVT Trial site - Reinaudo 0127A). Leaf 4 was selected for sampling as it displayed strong YCS symptoms across the genotypes and the asymptomatic counterpart was also attainable within the same four row plot. Figure 91 shows an example of YCS leaf symptoms in genotype SRA3$^{\Phi}$. Sucrose and starch quantification analysis was conducted on the leaf and midrib disks to validate the samples collected. Staining of midrib sections and starch content in the lamina and midrib from these same leaves is represented in Figure 92. It is evident from this experiment that there is a strong correlation between midrib staining and starch content.

Figure 91 SRA3$^{\Phi}$ YCS symptomatic and asymptomatic Leaf 4 from the same plot (Herbert RVT trial)

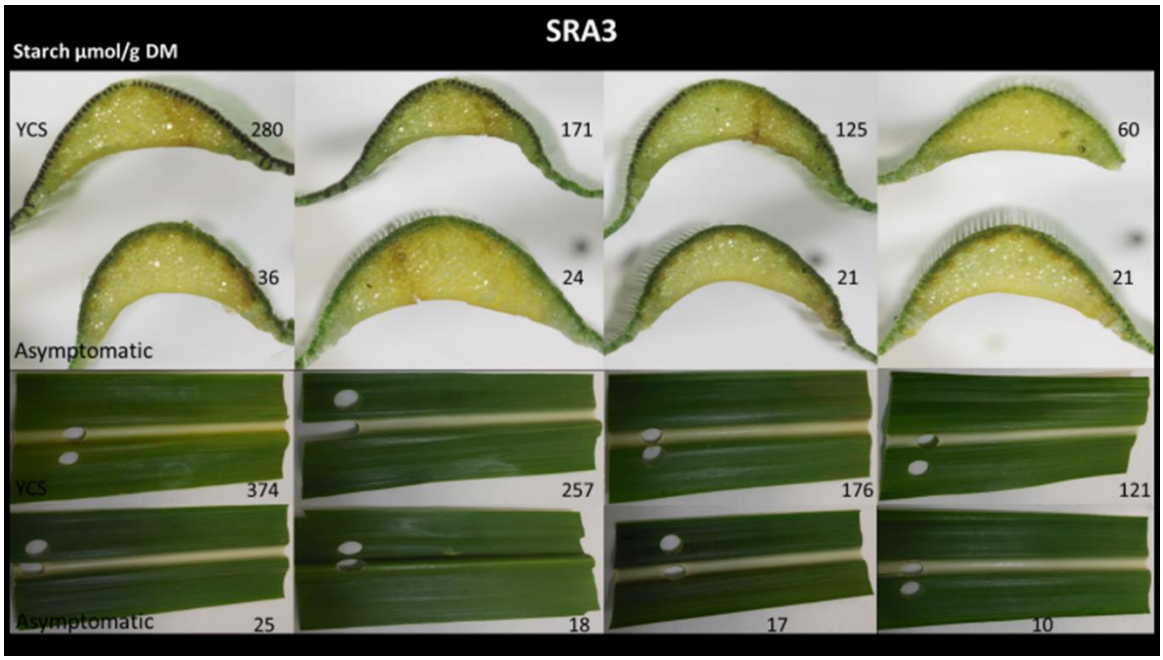

Figure 92 SRA3$^{\Phi}$ YCS symptomatic and asymptomatic Leaf 4 midrib staining and corresponding lamina and midrib starch content µmol/mg DM noted beside each section (Herbert RVT trial).

It is important to note that starch accumulation in the midrib of sugarcane is not unique to YCS. Tests conducted on leaves from YCS and water deficit stress plants (Figure 93A, B) shows staining of the starch in the bundle sheath cells surrounding the midrib vascular bundles/veins (Figure 94A-D).

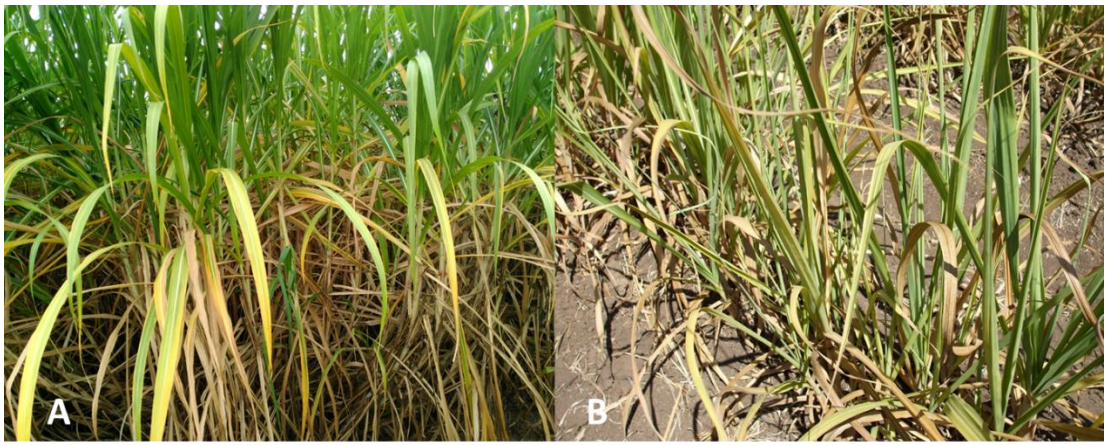

Figure 93 Sugarcane symptoms – Yellow canopy syndrome A) water deficit stress B)

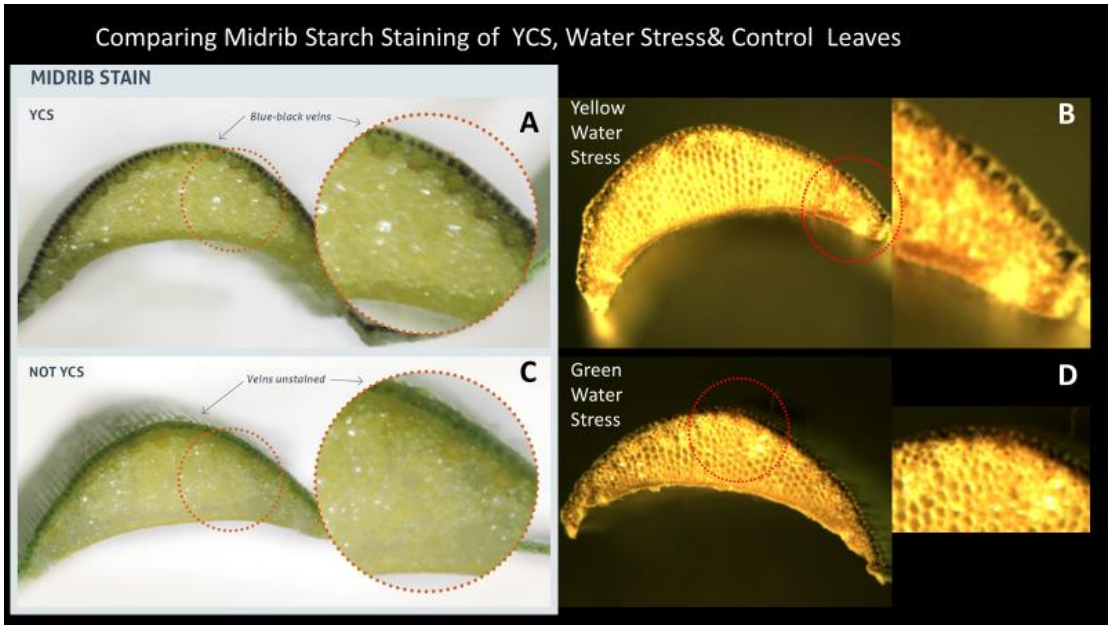

Figure 94 Leaf 4 midrib cross-section stains (1% iodine solution) YCS A) yellow water deficit B) control C) and green water deficit D)

Studies of plants testing positive to sugarcane yellow leaf virus (ScYLV) also show reduced sugar export from the leaf. Sucrose accumulation in these plants is likely cause by mechanical plugging of the sieve tubes through callose formation in response to the virus or a leak in turgor pressure from viral movement protein expression of the companion cell-sieve tube complex (Esau, 1957; Herbers et al., 1997). High sucrose accumulation leads to changes in chloroplast ultrastructure and degradation of the chlorophyll resulting in yellowing of the midrib and lamina (Yan et al., 2008) (Figure 95A, B). Like YCS, plants infected with ScYLV also have high starch content at first light which is evident of a major disruption to the diurnal rhythm. While ScYLV midrib and lamina symptom expression is different to YCS, staining of the midrib produces a similar response compared to the control (Figure 95C, D).

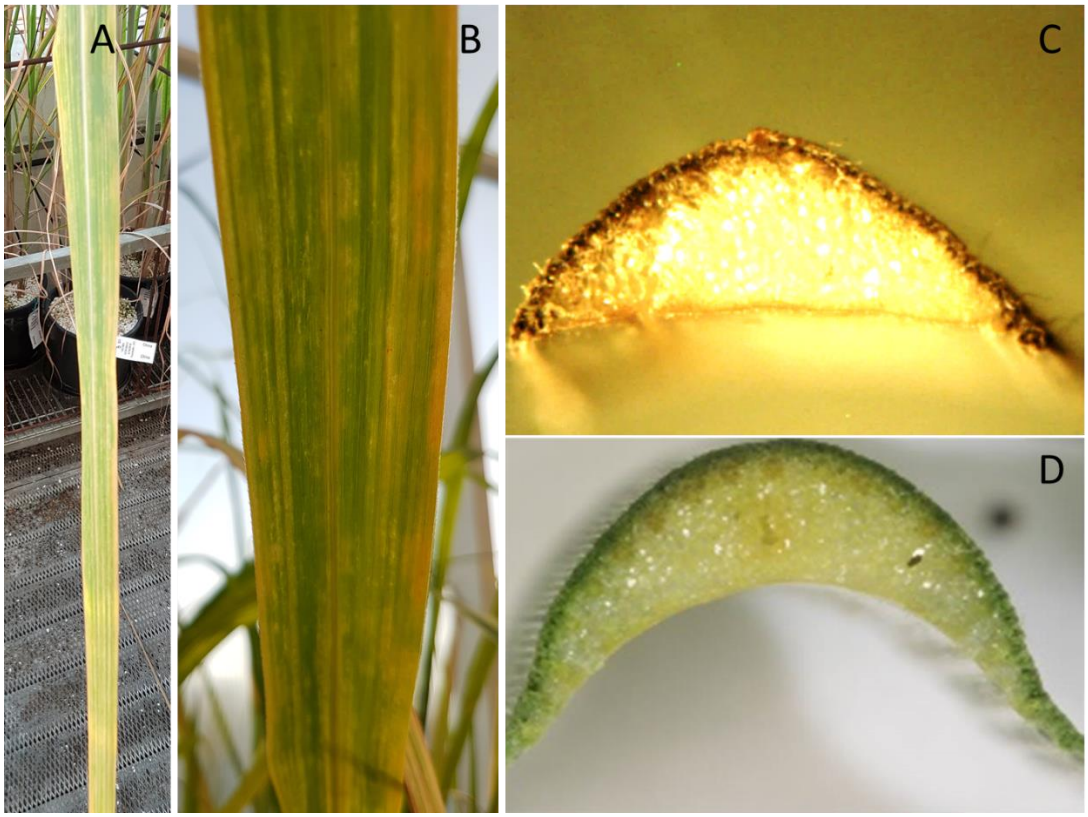

Figure 95 Sugarcane yellow leaf virus (ScYLV) symptomatic Leaf 3 A) close-up showing yellow midrib and lamina B) ScYLV midrib cross section stained with 1% iodine solution C) and control Leaf 3 midrib cross section stained with 1% iodine solution D). ScYLV (Vietnam genotype) confirmed sample and control obtained from quarantine glasshouse SRA Indooroopilly, Brisbane Qld

Attainment of a positive midrib stain in plants afflicted by both abiotic (water deficit) and biotic (ScYLV) stress indicates that the test is not unique to YCS, and at best, a good test for stress. To improve the accuracy of the test and to reduce misdiagnosis of YCS or false positives, flash cards were included in the diagnostic kit. These flash cards were designed to assist the user to identify key characteristics that are common to YCS prior to performing the midrib stain. These include identification of the YCS zone in the mid-canopy, the pattern of development and colour of expression in the leaf, a decision key 'to test or not' and instructions on how to perform the test (Figure 96A-D).

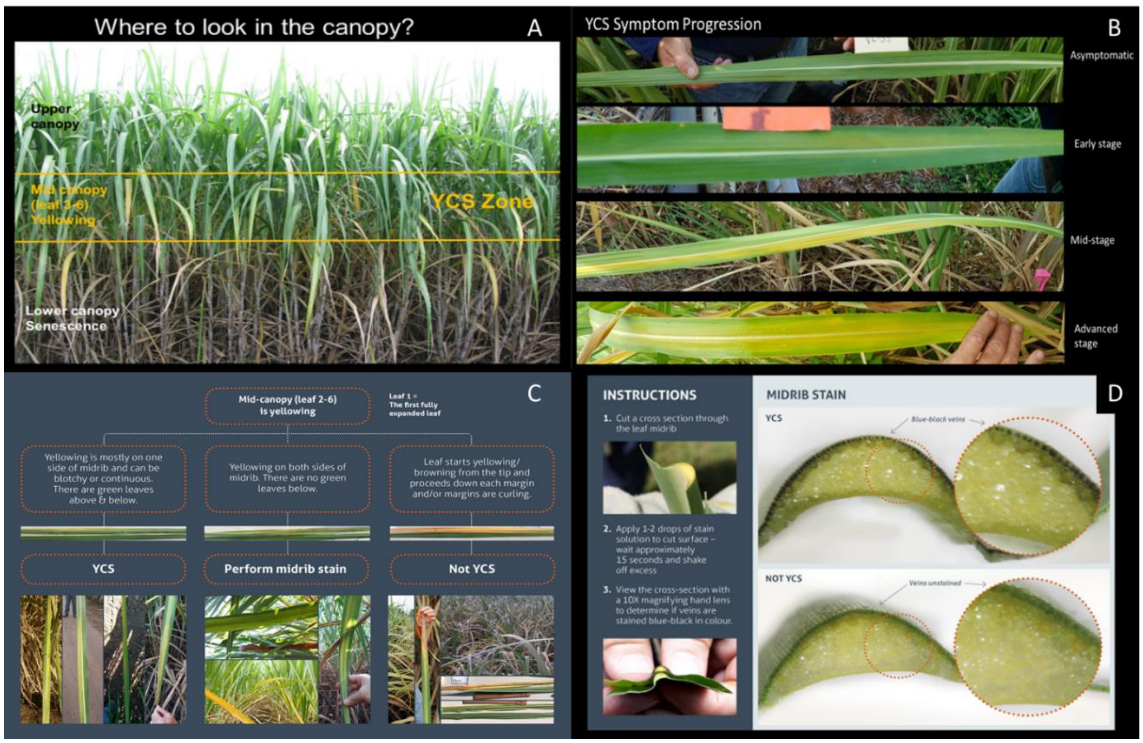

Figure 96 Midrib stain kit flash cards; YCS zone A) YCS symptom progression B) midrib stain determination key C) staining instructions and comparative vascular bundle cross section stains D)

The YCS in-field test kit was distributed to key SRA and sugar service personnel across the sugarcane growing regions in Qld. The aim of the kit was to reduce misdiagnosis of YCS and to provide industry and researchers with a tool to confidently predict the development and onset of the syndrome and gather accurate information regarding its prevalence. Operators were requested to record the variety, crop cycle, grower detail, GPS coordinates and to photograph the stool/field, leaf and midrib cross section stain for each sample test conducted. Sampling and staining were always performed as soon as possible after first light and always before 8AM. All data was uploaded to a central database for review and comment. Leaf punch samples were also collected at the same time as midrib staining in Bundaberg and despatched to the SRA Indooroopilly molecular laboratory for sucrose and α-glucan analysis (Bergmeyer and Bernt, 1974; Beutler, 1984). Quantitative values were correlated with the field results to determine the accuracy and reliability of the midrib stain in identifying YCS correctly. Results from the 2018/19 season in the Bundaberg region indicate an 87% accuracy rate (data not shown). The collation of all the data and results over the 2018-2020 period will be presented in the Final Report for project 2014/049 in December 2020.

While the midrib starch stain per se is not a novel test for YCS, it is still a useful measure of plant/leaf health at that point in time. If used in conjunction with flash cards included in the YCS identification kit, it is an invaluable support tool which helps train industry service providers and researchers to better identify YCS in the field and ultimately reduce misdiagnosis.

6.6.2. Novel biomarker

A biomarker for identifying YCS, as distinct from other conditions that cause leaf yellowing, is important to enable early detection before any signs of visual yellowing, to inform YCS management practices and to drive the research forward. Using an RNAseq and bioinformatic approach, we

looked at differential gene expression in YCS-affected plants using a YCS-specific reference transcriptome, de novo assembled from Illumina HiSeq2500/4000 paired-end reads. Using this reference transcriptome, we performed YCS differential expression (DE), gene ontology (GO) and MapMan pathway bin enrichment analyses. In addition, DE analysis comparing YCS to samples exposed to drought water stress, Moddus-treatment or undergoing senescence, yielded six biomarker candidates uniquely important in YCS. From these candidates, a novel molecular biomarker test to identify plants affected by YCS was developed.

6.6.2.1. YCS Biomarker Candidate Discovery

RNAseq data from asymptomatic control, YCS, water-stressed, senescent, and Moddus-treated sugarcane leaf samples were each mapped to the YCS Reference transcriptome using CLC Genomics Workbench v12.0 software, with mapping parameters of 0.8 similarity and 0.8 length fraction match. A differential expression analysis of each treatment condition against the asymptomatic control was performed, controlling for tissue type, sampling batch, variety, and developmental stage. The results for each were then filtered for significance (Bonferroni < 0.0001) and fold change compared to the control (log_2 > absolute value of 1). The list of significant transcripts in each condition were compared in a Venn diagram using the webtool http://bioinformatics.psb.ugent.be/webtools/Venn/ (Figure 97).

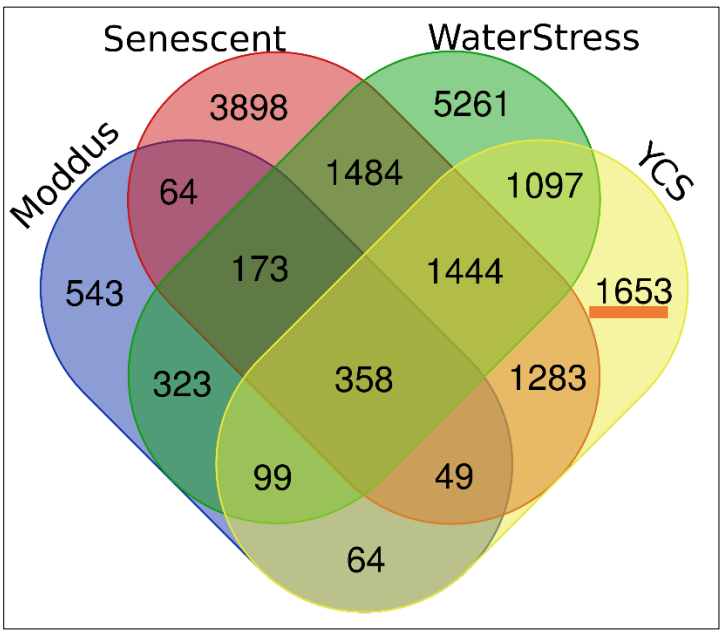

Figure 97 Venn diagram of the significantly differentially expressed transcripts in plants affected by these four conditions; YCS, Water-stress (drought), Senescence and Moddus-treated (GA inhibitor). The number of transcripts uniquely important in YCS is underlined

The list of 1653 transcripts that were uniquely important in YCS were then filtered using the criteria in Figure 98 to find transcript biomarker candidates that were significantly unique to YCS, upregulated in YCS, expressed in each of the YCS samples and not expressed in the control samples. This filtering process resulted in the discovery of five potential YCS biomarker candidates. An additional sixth potential candidate was identified in the same method as being important in both YCS and Moddus-treated plants. This sixth candidate was included in the biomarker testing process due to the similarity in symptoms between YCS and Moddus-treatment, and since Moddus is not used routinely in sugarcane fields. This makes the sixth candidate unlikely to be expressed due to

anything other than YCS under normal field conditions. This gives us a total of six potential YCS biomarker candidates to test.

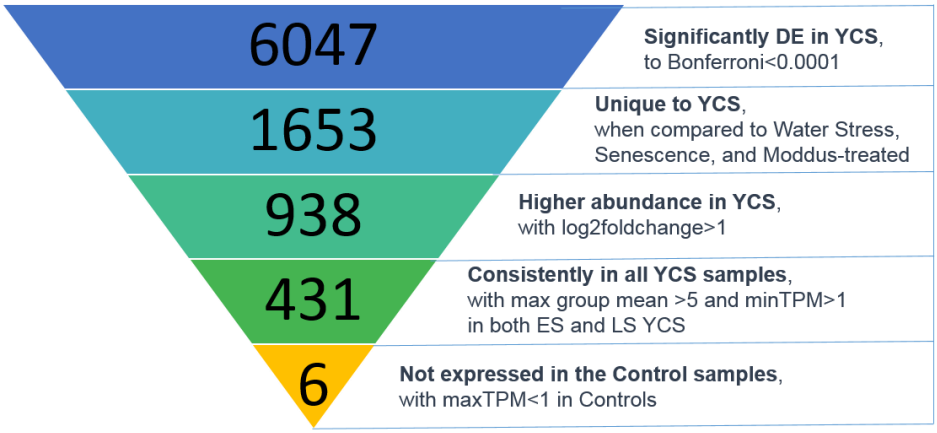

Figure 98 Bioinformatic filtering process to identify potential biomarker candidates unique to YCS

The six potential biomarker candidates were compared to the NCBI non-redundant proteins (nr) and nucleotide (nt) databases using BLAST to find their functions and annotations (Table 12).

Table 12 Annotations of biomarker transcript BLAST matches, and biomarker transcript lengths in bases

YCS Biomarker Candidate ID	Description from BLAST match	Size
YCS-1	Probable acyl-activating peroxisomal enzyme 1	771
YCS-2	Hypothetical protein SORBI_3009G207800 [Sorghum bicolor]	660
YCS-3	Unknown sequence [Saccharum hybrid cultivar]	570
YCS-4	Hypothetical protein SETIT 9G402200v2 [Setaria italica]	819
YCS-5	BTB POZ and TAZ domain-containing 2-like (BT2)	2181
YCS-6	Protein IN2-1 (safener-induced1)	1669

It is important to note here that each of the six YCS biomarker candidates were all plant sequences, and were transcripts expressed from plant genes. None of them were from non-sugarcane microorganisms. These biomarker candidates were all sugarcane genes expressed in YCS plants. Interestingly, the three annotated sequences are known to be expressed plant responses to oxidative stress. This suggests that the identified biomarker candidates may not be unique to YCS if this type of stress is also expressed sufficiently in other forms of sugarcane yellowing.

Oxidative stress can be caused by both biotic (pests and pathogens) and by abiotic (photosynthesis, metabolism, high light and temperature, water and nutrient limitations, high salt and heavy metal soils and elevated ozone) means (Apel and Hirt, 2004; Cakmak and Kirkby, 2008; Nishizawa et al., 2008; Keunen et al., 2013; Sham et al., 2014). To reiterate, our analyses have found no consistent evidence of any YCS-associated biotic factors such as bacterial, viral, or archaeal microorganisms in our sequencing data. It is far more likely that the oxidative stress response we see here in YCS-affected plants is due to abiotic factors.

To decide on a plant tissue type of choice for the biomarker sampling required analysis of the RNAseq data. This *in silico* differential expression analysis was performed comparing the expression

levels across all tissue types in the database (Table 13). The analysis identified the leaf lamina and midrib as the best tissue to test for the presence of the biomarker transcripts.

Table 13 YCS biomarker candidate expression in various tissue types

YCS Biomarker Candidate ID	Expression Fold Change in YCS					Mean TPM Abundance in YCS			
	ES YCS lamina	LS YCS lamina	YCS dewlap	YCS midrib	YCS internode	ES YCS lamina	LS YCS lamina	YCS dewlap	YCS midrib
YCS-1	7.8	19.8	79.3	141.4	-	4.4	14.4	0.6	26.3
YCS-2	203.3	383.7	57.4	818.1	1.1	11.2	17.7	9.4	57.2
YCS-3	57.5	61.8	13.4	45.4	1.8	8.0	11.4	2.6	12.0
YCS-4	16.5	24.4	1.7	21.4	1.4	6.9	13.5	3.7	12.5
YCS-5	11.2	45.3	17.0	50.9	-1.4	5.9	31.2	38.4	72.8
YCS-6	12.0	28.7	4.0	5.2	1.2	4.4	13.7	24.7	20.7

Of these candidates, YCS-2 had the highest TPM abundance and was unannotated. A series of primers were designed and optimised for this transcript (Table 14). PCR testing of early and late stage YCS and senescence, water stress, and asymptomatic controls yielded quite pleasing results (Figure 99). However, there was evidence of expression of this biomarker candidate in three of the late stage water-stress samples. It is possible that these water-stressed samples may have come from plants with an underlying YCS status.

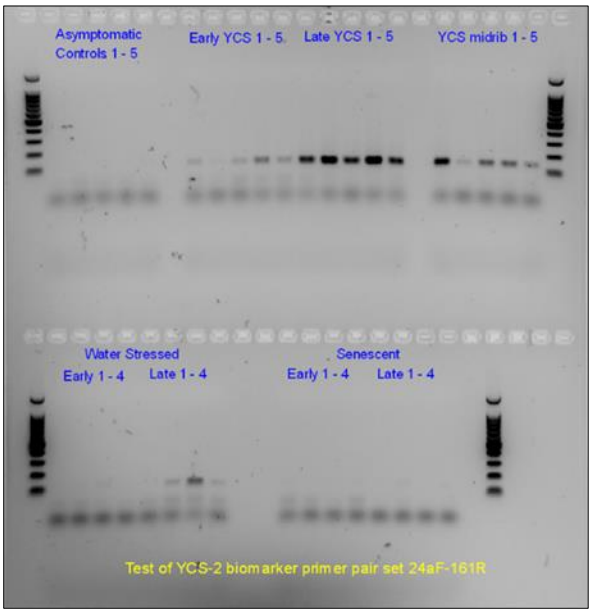

Figure 99 Gel image of YCS-2 biomarker candidate primer pair 24aF-161R (137bp region) (see Table 14) against asymptomatic controls, early and late-stage YCS leaf, YCS midrib, early and late-stage water stress and senescent samples

Table 14 YCS-2 biomarker candidate primers, forward (F) and (R) reverse sequences

Primer Name	YCS-2 Primer Sequence
Y2_24a_F	GCA ACA ACG AAG CAG AAG C
Y2_161_R	CCC ATT GGA TTG CTG GAC CT

To test this biomarker candidate further against as many forms of yellow leaf expression in sugarcane, samples were collected from positively identified (PCR molecular screening) diseased

plants from SRA Woodford station. During this field visit we used our optimised protocol for sample preservation in *RNAlater®* to ensure the technique could be rolled out to industry should our biomarker diagnostic be successful. Unfortunately, we saw a positive result in at least one replicate from each of the diseased plant samples (Figure 100). There was no improvement on this result when all potential biomarkers were assessed (data not shown). It is worth noting that at the time of sampling, the Woodford plants were extremely water stressed due a prolonged dry period. This result, while disappointing, confirmed that the biomarker candidates strongly expressed in YCS samples were not novel and potentially have a strong association with water deficit and oxidative stress.

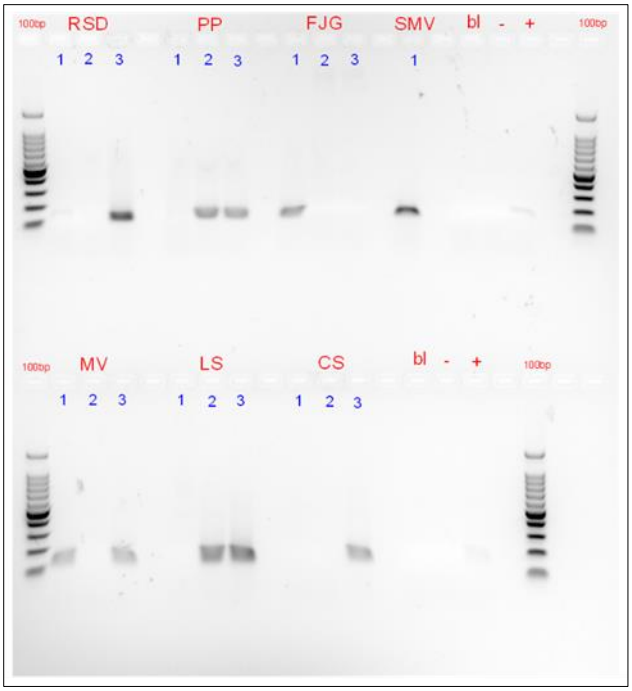

Figure 100 Gel photo of the YCS biomarker validation test of the Woodford diseased samples. Gel was run as a 1.5% agarose gel with 0.5x SYBRsafe at 90V for 60 minutes, using 100bp molecular weight ladder (Promega) as a marker. RSD: Ratoon Stunting Disease, PP: cane infected with rust, Pokkah Boeng and affected by cold chlorosis, FJG: Fiji Leaf Gall disease, SMV: Sugarcane Striate Mosaic disease; bl: no template blank control; - : negative Control from FV14 leaf4 sample barcode 5361; + : positive YCS control from FV14 leaf4 sample barcode 5363 (1:10 dilution); MV: Sugarcane Mosaic Virus; LS: Leaf Scald disease; CS: Chlorotic Streak Disease

In summary, the results concur with our research findings of a strong correlation between YCS yellowing and oxidative stress. As the cause of YCS is a source sink imbalance, there are many stressors that may be causal agents capable of inducing this physiological disorder. Therefore, it is highly unlikely, if not impossible, to discover a novel YCS biomarker of use to the industry.

6.7. Management

It is evident from the collective data presented within this report that the key driver of YCS is growth rate. A reduction in sink strength during the peak growing season increases the risk of photoassimilation exceeding the sink capacity. Therefore, any significant growth retardation preceding a period of increased carbon export from the source will increase the probability of YCS development and expression. An obvious remedy to this impending physiological disorder is to

mitigate or eliminate factors limiting culm growth or internode volume directly beneath the most photosynthetically active source leaves.

6.7.1. Growth rate and vigour

We investigated this further through a study of source leaf sucrose and starch content in fields of growers following best practice farming and consistently averaging >170t cane/ha. These growers anecdotally report that they see very little to no YCS symptoms across their farms. Fields that were mature and representing three widely grown genotypes (mostly 1st ratoon or plant crop cycle) were selected for sampling from five locations within three sites prior to harvest in September 2017. These fields were then monitored through the subsequent ratoon crop and further sampling conducted over the growing season to May 2018. Sucrose and total α-glucan content in the mid-upper canopy of three genotypes (KQ228$^{\Phi}$, Q208$^{\Phi}$, Q240$^{\Phi}$) in Burdekin irrigated fields was established for spring (September), summer (February) & autumn (May).

The top six source leaves of the canopy are leaves 1-6 (leaf 1 = FVD) of which mid canopy leaves 3-6 is where YCS symptom expression typically exhibits. Analysis of the sucrose and starch content within these canopy leaves, sampled between 8AM and 12:30PM, showed no excessive sucrose accumulation (i.e. above the tolerable threshold of 200 µmol/g DM) or any major redirection of carbon to α-glucan (Figure 101). Principle component analysis of leaf sucrose content for the three genotypes and sites over the growing period shows a tight cluster (Figure 102). This lack of separation between genotypes or sites shows these fields share a common parameter that maintains healthy levels of source leaf sucrose. As all fields chosen for this study were high yielding (>170 t cane/ha) it is highly likely that high sink strength is responsible for this maintenance.

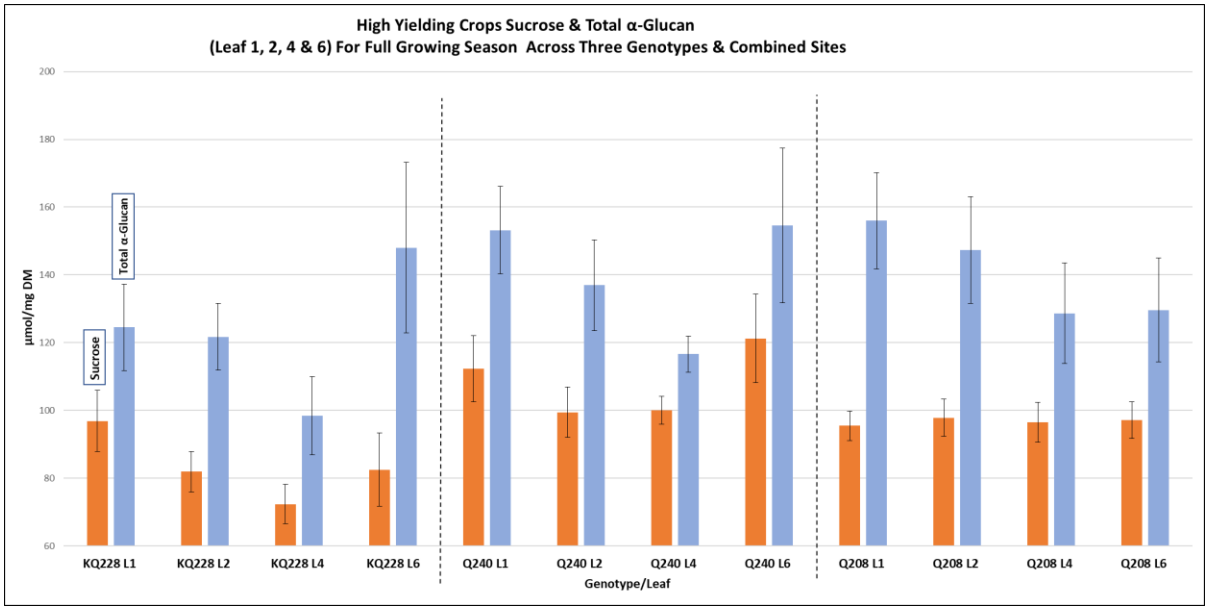

Figure 101 Leaf sucrose and total α-glucan levels in the mid-upper canopy (Leaf 1, 2, 4 & 6) of high yielding crops for varieties KQ228$^{\Phi}$, Q240$^{\Phi}$ & Q208$^{\Phi}$ across a full growing season

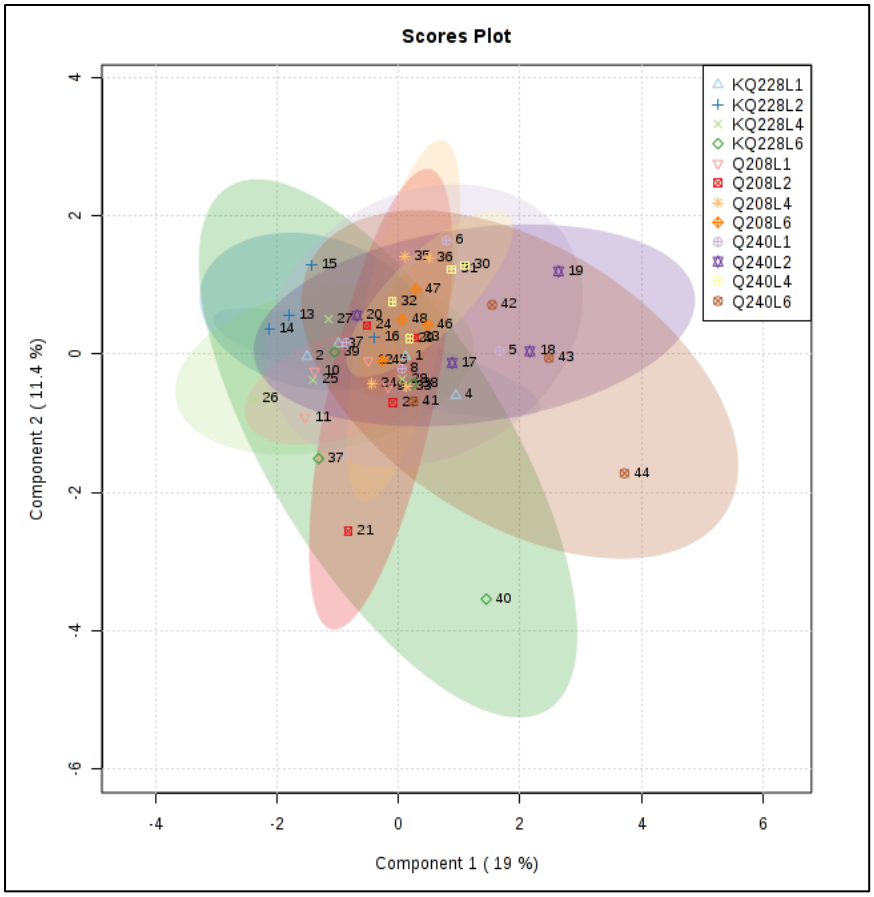

Figure 102 PCA analysis Q208$^{\Phi}$, Q240$^{\Phi}$, KQ228$^{\Phi}$ leaf sucrose, threes sites across a full growing season (Burdekin irrigated fields >170 t cane/ha)

The fact that levels of both metabolites are so low even though some sampling was as late as 12:30PM (when photosynthesis is approaching its peak), is indicative of a strong sugar gradient between the source and sink. This suggests that the entire source canopy of a high yielding crop maintains adequate sucrose export and carbon partitioning to α-glucan (soluble and starch) to ensure levels do not surpass a critical threshold that would trigger the onset of YCS. Therefore, maintenance of a healthy supply and demand balance is key to managing YCS. These results confirm that the current SRA recommendation to follow best farming practice, to ensure crop growth does not slow down during the peak growing season, remains one of the most important management strategies to mitigate the risk of YCS development.

6.7.2. Insecticide, YCS development, carbon partitioning and sink strength

Insecticide trials conducted as part of project 2014/049 show that the pyrethroid insecticide bifenthrin prevents the accumulation of sucrose and α-glucans (soluble and starch) in the source leaves and offers a potential YCS management option. Within the scope of our studies, here we present an evaluation of the collective data from the 2017/18 Burdekin trial.

The 2017/18 Burdekin insecticide trial investigated the effect of bifenthrin and the timing of application on internode (sink) size, sucrose and α-glucan accumulation in the source leaves and the development/expression of YCS. The trial consisted of untreated control (UTC) and weekly applications of bifenthrin (320 mL/ha) for the months of November through March, with some monthly treatments receiving five sprays while others received only three (Table 15). Included in this

trial was a magnesium sulphate ($MgSO_4$) treatment which was testing a YCS nutrient deficiency hypothesis and is included in this analysis in terms of sink strength.

6.7.2.1. Source leaf sucrose & α-glucan accumulation, YCS expression and sink strength

Appearance of first YCS symptoms coincided with the first rainfall event after a three-month dry period (Figure 103). Samples from leaves 2, 3 and 4 were collected each month for each treatment from the start of the trial (November 2017) and assayed for sucrose and α-glucan content (Bergmeyer and Bernt, 1974) . Levels of both metabolites did not exceed the upper tolerable threshold (approx. 200µmol/g DM) until February 2018. This correlates with the increase in YCS severity observed across the February, March, $MgSO_4$ & UTC treatments, but not with the Bifenthrin treatments. It is noteworthy that only leaf 4 showed elevated levels of sucrose and α-glucans above the threshold (Figure 104). This gives an insight into YCS symptom development, within and between the leaves of the mid-canopy. During this peak growth period one new leaf is produced approximately every 7 days depending on cumulative degree days (°Cd) (Table 15) (Inman-Bamber, 1994; Robertson, 1998). Therefore, leaf 4 will have been fixing carbon and exporting sucrose for one and two weeks more than leaf 3 and 2, respectively. If the disruption to carbon export is treated as a constant across the source leaves then accumulation of sucrose will have first occurred in Leaf 4 when it was chronologically a Leaf 1 or 2. Sucrose will then continue to build proportional to source leaf photosynthetic age as synthesis proceeds over the coming weeks. Leaf 4 will therefore be first to accumulate sucrose and α-glucans higher than the tolerable threshold (Figure 104) and exhibit signs of leaf yellowing. As time progresses yellowing will move from the YCS symptomatic leaf (in this case Leaf 4) to the asymptomatic leaf above and so forth up the canopy. Figure 103 shows a rapid increase in YCS severity through the canopy after February. It is important to note that only source leaves which have a supply demand imbalance will be affected, and it would be rare to see yellowing in Leaf 1 or 2 as there would be insufficient time for sucrose accumulation to reach levels high enough to induce symptoms. This is why YCS symptom development is a mid-canopy phenomenon that mostly affects leaves 3-6. Therefore, when YCS symptoms first appear there will usually be a band of green leaves below and green leaves above. Eventually the first YCS affected leaves will senesce and there will be no break in colour between these leaves and the developing YCS leaves above. This makes YCS difficult to diagnose if first observed at this point in time.

A disruption to carbon export will cause accumulation of sucrose and α-glucans in source leaves. Once the tolerable threshold is exceeded, the disruption to photosynthetic machinery and the production of reactive oxygen species will cause enough photooxidative damage to create visible yellowing. The magnitude and speed of disruption will be determined by the period where sucrose levels exceed the tolerable threshold. This magnitude can be determined by measuring sink strength or potential difference between the source and sink. However, it is worth noting that a strong sucrose gradient between the source and sink tissue is crucial if equilibrium is to be maintained between supply and demand during the peak photosynthetic months (Botha et al., 1996; Bihmidine et al., 2013).

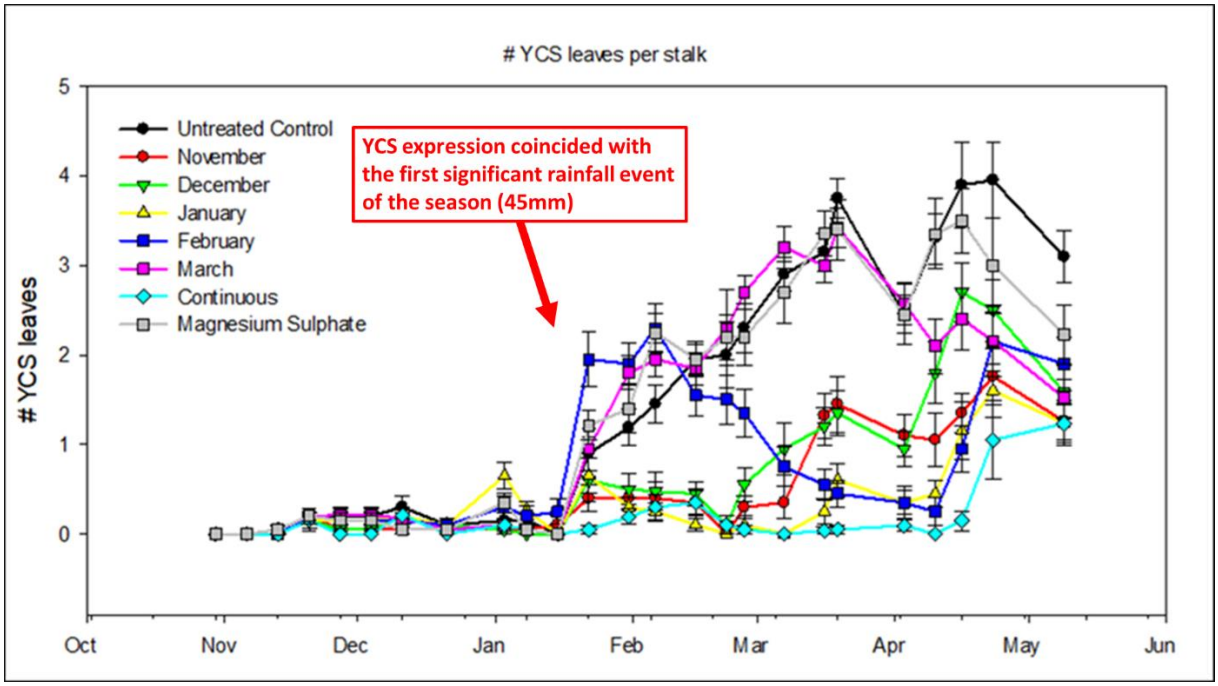

Figure 103 YCS expression appears after a rainfall event in late January

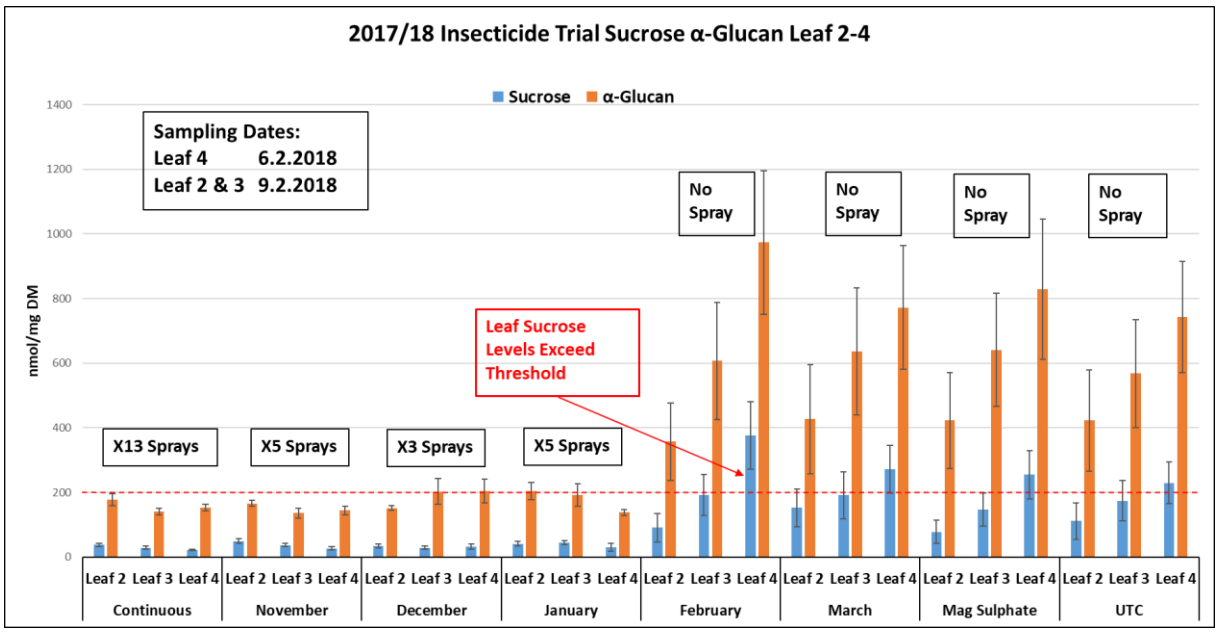

Figure 104 Source leaf sucrose and α-glucan accumulation exceeds toxic upper threshold in February (note: α-glucan units nmol glucose equivalent/mg DM)

Using a leaf base temperature (Tbase) of 18°C, sugarcane studies of Qld genotypes show that internodes elongate for approximately 380-degree days (°Cd), and given availability to water they will continue to expand for approximately a further 300 °Cd (Inman-Bamber, 1994; Robertson, 1998). Internode volumes measured in May 2018 were assigned calculated cumulative °Cd (Table 15) to enable an assessment of internode size at the time of bifenthrin treatment and any associated YCS symptom expression.

Table 15 Treatments and time of application, Cumulative °Cd and internode volume (Leaf Tbase = 8°C)

Date	Internode Cummulative °Cd		Internode #	Internode Volume cm^3 Continuous	Continuous		Internode Volume cm^3 UTC	UTC		Internode Volume cm^3 November	Nov		Internode Volume cm^3 December	Dec		Internode Volume cm^3 Januarys	Jan		Internode Volume cm^3 February	Feb		Internode Volume cm^3 March	March		Internode Volume cm^3 $MgSO_4$
6/05/2018	20.99		1	23.48			13.09			14.70			13.18			22.78			19.46			13.88			13.82
28/04/2018	58.09		2	27.23			16.16			18.61			17.69			23.49			25.08			17.34			16.83
19/04/2018	108.19		3	31.96			12.80			24.43			21.60			26.52			22.82			20.00			14.88
10/04/2018	169.27		4	37.18			14.67			27.64			21.63			26.57			26.11			20.10			15.41
2/04/2018	232.58	Final Bifenthrin Spray	5	37.51	Spray		14.08			21.86			22.72			31.94			27.07			21.75			16.91
25/03/2018	297.01		6	37.82	Spray		16.20			26.07			25.05			34.70			27.82			25.28	No Spray 100mL		19.88
17/03/2018	366.76	Internode Elongation Stops	7	40.04	Spray		16.86			26.26			26.96			37.14			28.68			25.04	Spray		19.85
9/03/2018	428.89		8	40.45	Spray		18.54			29.40			29.22			39.24			29.46			20.27	Spray		20.10
2/03/2018	490.92		9	38.91	Spray		18.57			33.08			31.35			39.11			28.26			19.96	Spray		22.07
22/02/2018	549.72		10	36.30	Spray		19.50			34.45			34.77			39.29			30.69	Spray		20.72			25.59
15/02/2018	624.31		11	38.17	Spray		20.41			33.87			36.49			42.29			31.54	Spray		20.60			24.53
8/02/2018	683.80	Internode Expansion Stops	12	37.16	Spray		21.98			35.28			36.32			40.69			30.67	Spray		22.26			23.93
1/02/2018	750.71		13	37.40	Spray		22.37			35.55			34.85			39.32			29.01	Spray		21.73			28.25
25/01/2018	816.52	YCS Appears	14	38.61	Spray		22.33			36.89			33.80			37.09	Spray		28.68			21.66			28.83
17/01/2018	883.49		15	38.57	Spray		21.83			34.71			33.12			35.51	Spray		25.46			22.88			26.40
10/01/2018	953.51		16	36.27	Spray		21.81			31.67			29.67			33.36	Spray		23.49			22.85			25.05
3/01/2018	1025.81		17	35.49	Spray		23.30			33.09			28.58			32.82	Spray		22.40			23.33			25.06
27/12/2017	1095.98		18	34.28	No Spray		24.24			32.09			27.66	No Spray		31.08			21.91			23.57			25.16
20/12/2017	1158.96		19	33.91	Spray		23.91			30.13			26.45	Spray		31.44			20.74			22.43			26.19
13/12/2017	1220.08		20	31.71	Spray		24.10			28.14			24.43	Spray		29.66			19.30			21.20			23.00
6/12/2017	1286.47		21	28.82	Spray		22.52			27.62			25.39	Spray		28.67			19.32			22.58			19.81
29/11/2017	1349.29		22	27.77	Spray		26.30			25.20	Spray		25.59			25.01			18.73			22.03			20.70
21/11/2017	1412.36		23	28.41	Spray		31.24			23.29	Spray		24.52			31.91			12.62			16.67			24.81
13/11/2017	1468.28		24	27.67	Spray		29.07			21.93	Spray								11.50						
5/11/2017	1528.23		25	26.07	Spray					23.14	Spray														
30/10/2017	1593.18	Bifentrin Treatment Starts	26	27.01	Spray					23.05	Spray														
20/10/2017	1644.27		27	27.08						19.62															

YCS symptoms first appeared in the untreated plots in late January (Figure 103) which aligns with Internode # 14 (Table 15). Figure 105 shows the proportional variation in internode volumes for each treatment in order of YCS severity.

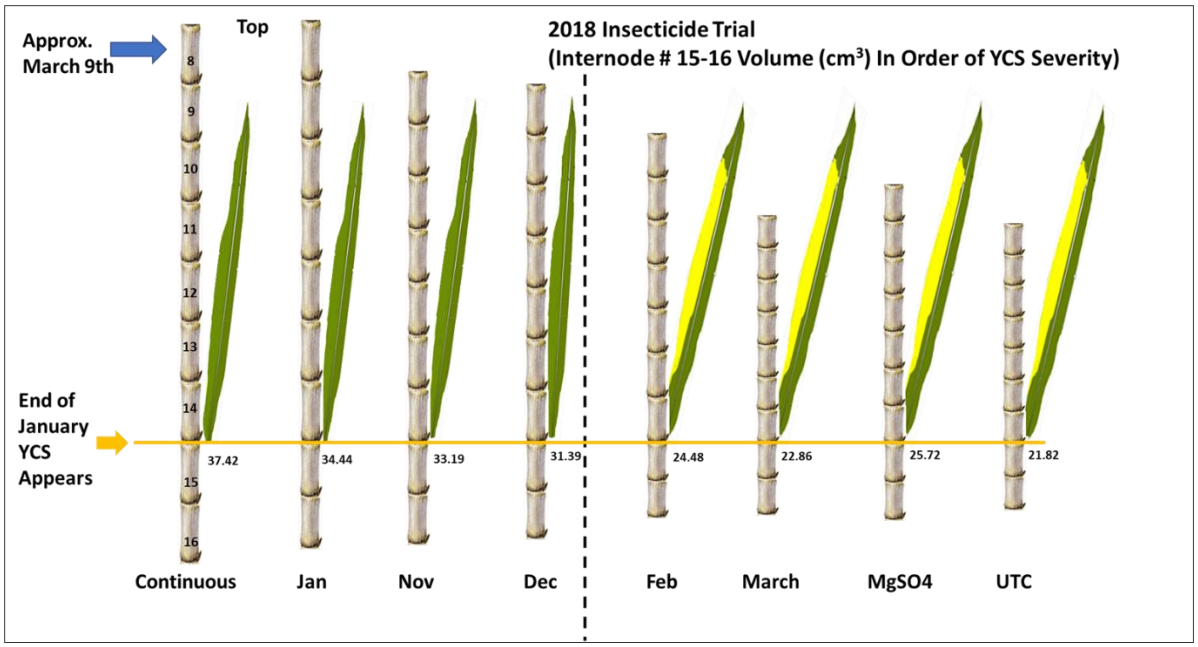

Figure 105 Bifenthrin treatment, YCS occurrence and internode size - internode numbering corresponds with true leaf number i.e. Internode #1 is the internode directly under the leaf sheath of true leaf # 1 = FVD).

The highest demand for sucrose from a source leaf is from the two internodes directly below it and the root system, with lower demand from the young upper sink culm and leaves (Botha and McDonald, 2010). Therefore, in terms of sink capacity or sink strength the size of internodes # 15 & 16 is of particular interest as they were sitting directly beneath the leaf first expressing YCS symptoms in late January in the insecticide field trial (Figure 105, Table 15). Interestingly, Figure 106A shows all plots sprayed with bifenthrin prior to February had significantly larger internodes # 15 & 16 volumes than those of the untreated plots and this correlates well with the level of YCS severity (Figure 106B). The period from when bifenthrin was first applied in the trial to the time of sampling and internode measurements equates to the top 23 internodes of the culm. Using the

average internode volume over this period as a proxy for plant vigour, plants treated with bifenthrin prior to February had higher vigour than the untreated controls (Figure 106C). Increased plant vigour correlates well with reduced YCS severity (Figure 106B & C). Independent of when bifenthrin was applied, the volume of actively growing internodes above the spray zone is larger than that of the untreated control (Table 15). Comparing the total volume of the top 23 internodes within each treatment indicates that the later the treatment was applied, the smaller the culm volume (Figure 107). Figure 108 shows there is a very strong correlation between culm volume and cane yield. This concurs with our study conducted in the Burdekin 2017/18 which found no YCS in several high yielding commercial crops with a large active sink (>170 t cane/ha).

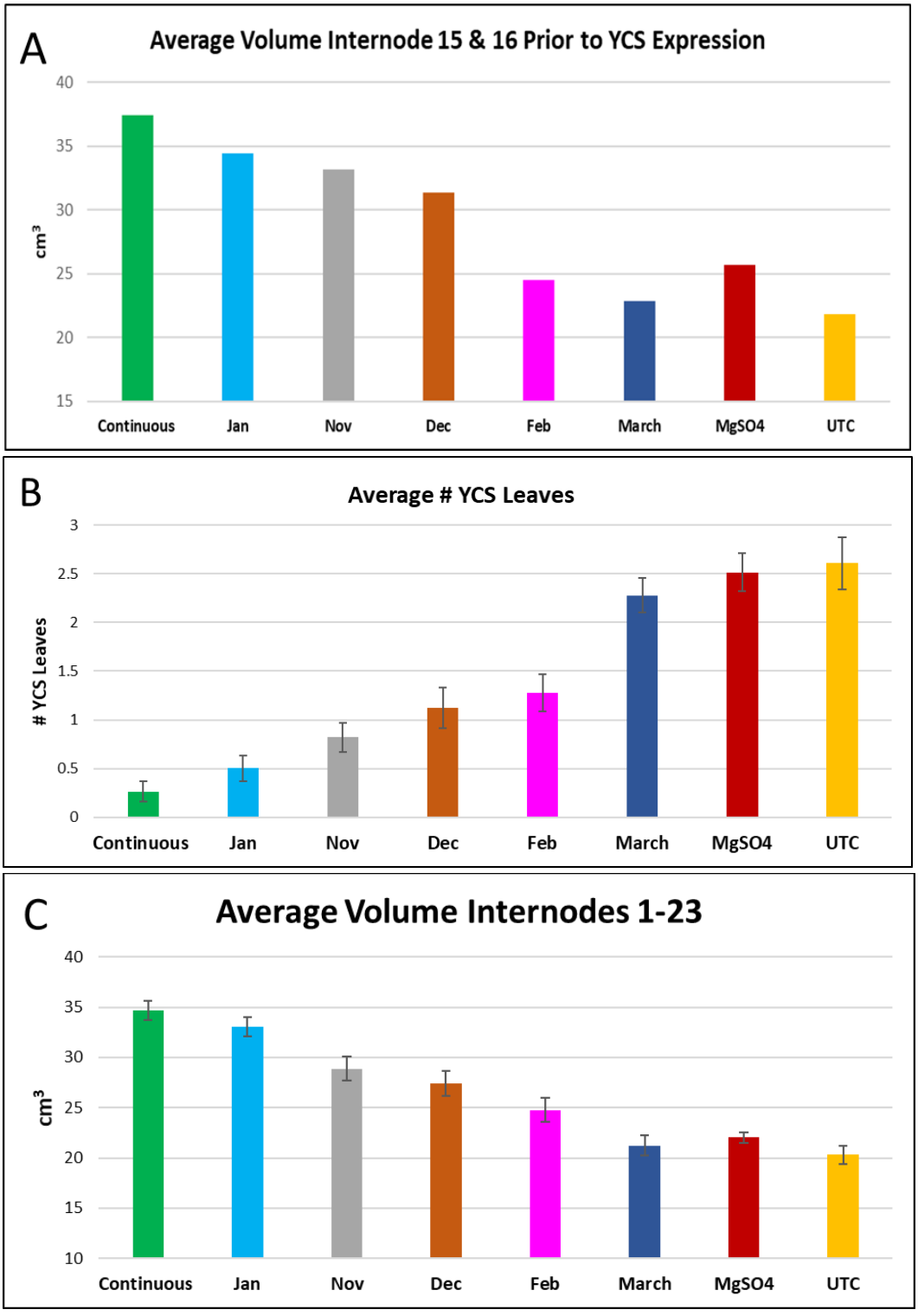

Figure 106 Untreated February, March, Mg SO_4 and UTC plants have reduced sink size A) higher YCS severity, compared to bifenthrin treated plants (Continuous, January, November and December) B) and reduced plant vigour C)

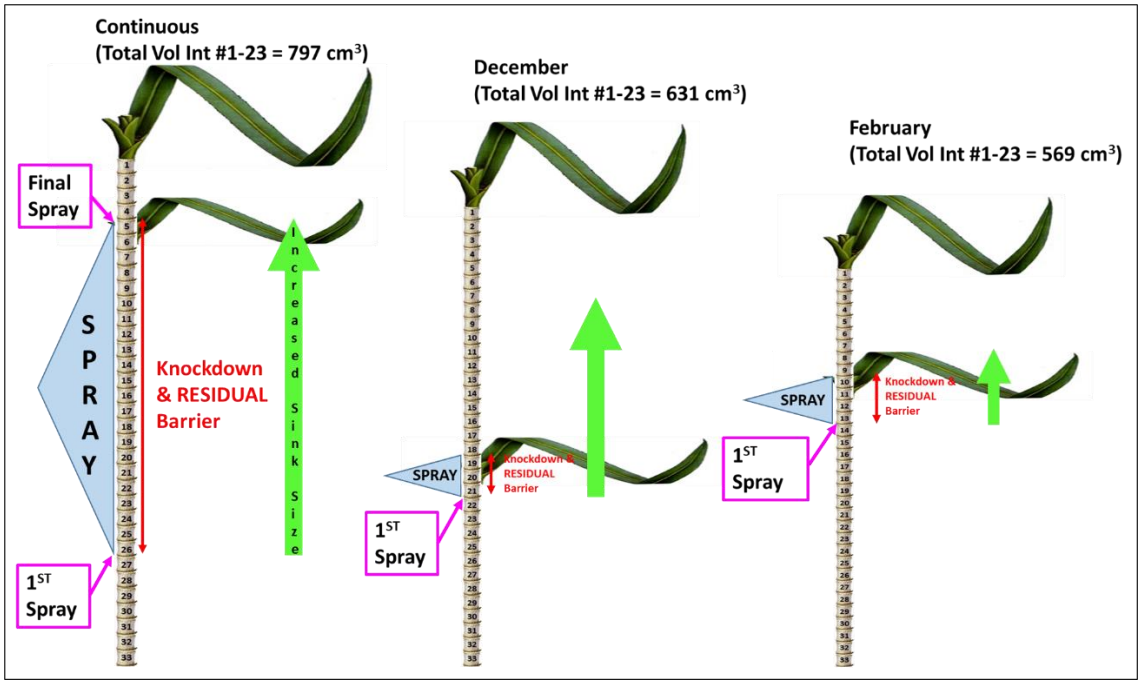

Figure 107 Sink size of top 23 internode volumes and bifenthrin treatment period

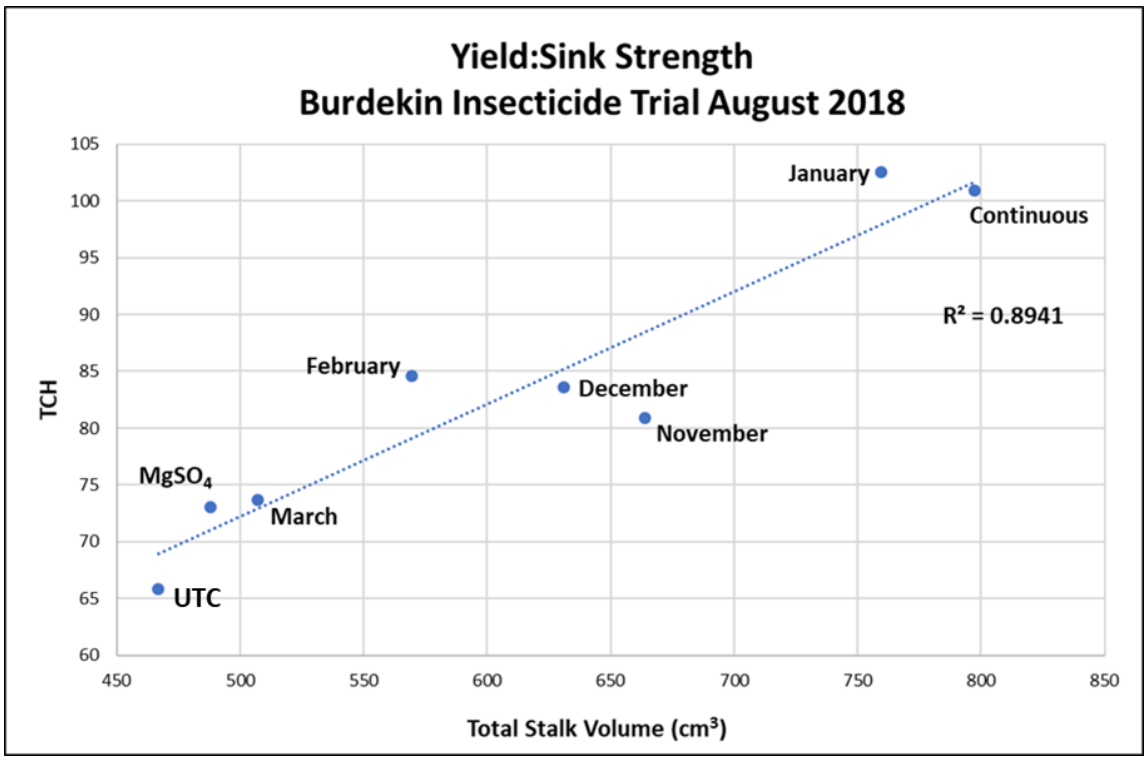

Figure 108 Burdekin insecticide trial 2017/18 yield (TCH) and sink strength (top 23 internode total volume representing the period from the first Bifenthrin spray which staggers monthly for each treatment except Continuous)

Bifenthrin is a broad-spectrum non-systemic insecticide that can kill or suppress both beneficial and non-beneficial insects. Complete removal or suppression of insects either i) prevents a plant defence response to wounding that would otherwise cause a physical blockage in the transport system (our data shows no callose accumulation in YCS symptomatic leaf tissue – see section 6.3.3.4 of this report) or ii) disrupts molecular signalling from the insects that is involved in the physiological

disruption of sink metabolism which reduces sink strength or competition with insect feeding or iii) prevents vectoring an agent that disrupts phloem transport (Note: phytoplasmas and other bacteria are at best intermittently detectable and only measurable at very low concentration in YCS leaf tissue), iv) prevents sink feeding that draws carbon away from sink growth or v) prevents a reduction in plant growth that may otherwise occur through upregulation of plant defence jasmonates (JAs) and reduced gibberellin (GA) synthesis in response to insect herbivory (Zhang et al., 2017; Yang et al., 2019). In any case, it suggests that bifenthrin maintains a healthy balance between supply and demand or growth and defence. This in turn prevents the accumulation of leaf sucrose to levels that initiate downregulation of photosystems I & II, leading to photooxidation and leaf yellowing.

The role of insects and the mechanism by which bifenthrin prevents accumulation of sucrose and α-glucans in the leaf is the subject of further investigation in the 2019/20 season. A possible insight to this from bifenthrin residue analysis conducted on the leaf and culm will be tested in the current season. Results showed that residue was found on the tops and culm at 2.4 and 4.6 months respectively after the last application (data not shown). Studies show that exposure to rainfall and sunlight increase the rate of degradation and reduce the efficacy of bifenthrin (Allan et al., 2009). The habit of sugarcane will therefore impact on bifenthrin efficacy as, after canopy closure at approximately 12 weeks, sunlight will be unable to penetrate and degrade insecticide applied under it and on the lower portion of the culm. Application of the insecticide in the Burdekin trial was by knapsack and to the point of saturation of the foliage and culm. When the plant is drenched like this the insecticide can penetrate behind leaf sheaths of older leaves which are not as tightly held to the culm. When this is considered it is not surprising that residue was detected on the culm 4.6 months after application. While rainfall will also reduce any residue, the fact that it is measurable in the tops 2.4 months after application suggests it is somewhat protected by the tight arrangement of leaves in this section of the plant. Therefore, bifenthrin residue may have a significant impact and needs to be considered when investigating the type of insect and its possible role in disrupting sink strength (internode volume) and phloem transport.

6.7.2.2. Plant response to insect attack

As illustrated in the previous section (6.7.2.1) and in previous publications (Olsen and Ward, 2019) it is highly likely that insect pressure could be one of the factors that can lead to YCS expression. Obviously, application of bifenthrin results in improved internode growth and at the same time results in lower leaf sucrose and glucan levels (see section 6.7.2. of this report Figure 106 & Figure 104). The observations that YCS expression and severity can be controlled to some extend by insecticide application does not come as a surprise. As highlighted throughout this report, YCS expression is the result of a suppression of growth.

The ‘growth–defence trade off’ phenomenon is well described in literature and was first observed in forestry studies of plant–insect interactions (for review Huot et al., 2014). Plant fitness is the balance between growth and defence. When plants need to activate a defence response it imposes a substantial demand for resources, which in turn reduces growth (Huot et al., 2014). However, recent work highlighted that defence-related growth repression is not merely competition for resources but involves complex hormone crosstalk and signalling pathways in balancing growth and defence in plants. Changes in both abiotic and biotic stresses will induce a reaction in signal molecules to facilitate appropriate plant responses (for review Ku et al., 2018). It would appear that salicylic acid (SA) is important in pathogen, jasmonate (JA) in insect activation (Huot et al., 2014; Patil et al., 2019)

and ABA in abiotic activation of plant defence responses. Balancing of growth versus defence involves the expression of these signalling pathways and the hormones auxin, brassinosteroids (BR), and gibberellins (GA)(Huot et al., 2014; Ku et al., 2018).

Enhanced deactivation of the JA pathway or defective JA receptors are associated with increased overall plant height and longer internodes (Yang et al., 2012; Kurotani et al., 2015; Patil et al., 2019). Elevated JA leads to increased lignification and reduced growth (Sehr et al., 2010; Agusti et al., 2011; Lin et al., 2016).

Not only changes in the JA-pathway but also the production of phenylpropanoids, flavonoids, secondary metabolites, stress-responsive transcription factors, disease resistance, lipid metabolism, cell wall metabolism, pathogen-related (PR) pathway and signal pathways, protein turnover and various transporters are associated with insect defence responses (Ma and Yamaji, 2006; Głowacki et al., 2011; Sham et al., 2014; Altmann et al., 2018; Miao et al., 2018; Chen et al., 2019; Du et al., 2019; Varsani et al., 2019; Xin et al., 2019). However, all of these responses are also induced in a multitude of other stress conditions, and their various signalling may overlap synergistically or interact antagonistically (Suzuki et al., 2014). Transcripts associated with these functions are in higher abundance in YCS.

Of all these responses, the JA pathway and DIMBOA benzoxazinoids have more often been associated with plant defence against insect attack and give the clearest indication of insect herbivory. We found 9 transcripts annotated as '60kDa jasmonate-induced –like' that were significantly differentially expressed in YCS (Bonferroni < 0.005). These transcripts ranged in size from 959 to 4086 bases. The expression fold changes ranged from -23 to 53, so they were not consistently upregulated, and all of them were weakly expressed.

For the DIMBOA expression in YCS, we found only two transcripts that were significantly differentially expressed in YCS (Bonferroni < 0.005). However, expression was weak and varied between samples, and these transcripts were not significantly differentially expressed in all datasets.

7. CONCLUSIONS

In this study we have established a link between sugar metabolism and YCS symptom development. YCS symptom development is induced premature senescence through which the crop rebalances its photosynthetic capacity with the demand for reduced carbon.

We have developed comprehensive metabolome, transcriptome and proteome databases and referenced to changes associated with YCS development and expression. This has not only revealed the level of disruption to source leaf metabolism in YCS plants but also established a metabolic reference base for sugarcane in Australia. This study showed how important it is to have a good solid understanding of the fundamentals of the physiology of the crop. As a result of the comprehensive understanding of sugarcane physiology attained through this study, the industry should now be in a better position to reach conclusions about any abnormal crop behaviour much faster than was the case with YCS.

Our data highlights the fundamental issue that underpins leaf metabolism and function in plants, and the differences between C_3 and C_4 crop species in dealing with it. Although the interception of

light is needed to drive photosynthesis and hence biomass production, it is also highly destructive if the absorbed energy is not used to drive carbon dioxide fixation. The consequence of not efficiently using the trapped light energy for photosynthesis is rapid destructive oxidation and yellowing of leaf tissue. The key to ensure continued CO_2 fixation is to maintain cellular sugars, especially sucrose levels, low. There are only two mechanisms that can be used for this purpose: firstly, the export of sugars to the non-photosynthetic actively growing tissues, or secondly, the conversion of sugars to water insoluble polymers such as starch. Many plants, and especially the C_3 species, have a huge capacity to convert sugars to starch and other polymers in the leaf and thereby ensuring that photooxidation and yellowing does not occur. When light interception exceeds the export and polymer production capacity, all plants will exhibit leaf yellowing which is merely reflecting the only option available to reduce light interception i.e. reduce the number of leaves that can capture light energy.

This study demonstrates that sugarcane (a C_4 species) has a very limited capacity to produce starch and other polymers. Evidently it has some ability to produce soluble glucans which can offer a limited 'overflow' for reduced carbon. The only real protective mechanism in sugarcane to prevent photooxidation and yellowing is to ensure that sucrose export from the leaf is closely matching the trapped light energy. Because of the limited buffering capacity in the leaf, sugarcane controls light interception primarily through a reduction in green leaf area and number of source leaves. In sharp contrast to the C_3 species, yellowing and premature leaf death is evident throughout the crop cycle. Previous studies have highlighted the rapid changes in green leaf numbers when sugarcane growth (demand for reduced carbon and sugar utilisation) is imposed on the crop due to abiotic stress conditions. This mechanism may be considered an evolutionary or adaptive response to minimise the collateral damage due to an inability to counter excess trapped energy caused by sink strength limitation. Sacrificing the light harvesting structures could well be a more energy efficient way to restore metabolic stasis and plant health.

The number of green leaves in the sugarcane canopy is a direct reflection of the demand for reduced carbon by the rest of the plant. Our data has clearly established that leaf sucrose is a very good indicator of the general health of the sugarcane plant. The leaves will remain green and functional when the leaf sucrose levels can be maintained at a level lower than 200 µmol/g DM. Starch in the midrib of the leaf is a good surrogate for leaf sucrose and something that can be easily measured as demonstrated by the simple starch stain we have developed.

Evidently, sucrose levels could exceed the acceptable threshold level as a result of (a) reduced growth of the non-photosynthetic (sink) tissues while photosynthesis remains at a high level, (b) accelerated photosynthesis while the demand from the sink tissues remain the same, or (c) a differential disruption in the leaf and sink metabolism through which photosynthate production exceeds the sucrose export rate. However, our data does not support either (a) or (b).

Based on our findings several scenarios can be predicted that will lead to mid canopy yellowing (YCS) in sugarcane. For example:

Scenario 1: Dry conditions at the time of peak irradiance (December to March). Internode elongation will slow up much faster than photosynthesis rates. Photosynthesis will be partially reduced due to stomatal resistance (water stress). If the crop receives water (rainfall or irrigation) after such a stress period photosynthesis will rapidly increase but sink demand will be slower to respond. The

consequence would be yellowing in the leaves that are primarily exporting carbon and have a high photosynthetic rate (typically leaf 4).

Scenario 2: A poorly developed root system caused by compaction, or a portion of the root system, especially new roots are taken out by predation, in the peak photosynthetic period. This will remove a substantial portion of the sink demand and lead to sucrose accumulation in the mid-canopy.

Scenario 3: The crop is exposed to insect pressure and this leads to an induction of the JA pathway and decrease in the GA, BR and auxin pathways which results in substantial reduction in internode length. The effect of the insect pressure is the same as what is achieved with water stress but in this scenario the cause is biotic– a reduction in sink demand and size and a source sink imbalance still ensues.

Over the duration of this project we have seen many examples such as poor soil and nutrient conditions, infrequent or no irrigation, shallow or severely compacted soil enhancing YCS (mid canopy yellowing) expression. In contrast we never saw major YCS expression in an actively growing crop and observed the crop growing out of YCS symptom expression under good growth conditions. In an extreme case we observed a complete prevention of YCS symptom development in a patch within a YCS symptomatic field where there was a continuous supply of grey water. This ensured even strong culm growth during the December to March period.

It is very important to note that mid-canopy yellowing as evident during YCS expression is due to reduced culm growth and not vice versa. The 'feast' status of internodes strongly correlates with internode sucrose levels and confirms there is no association between YCS and commercial cane sugar (CCS) penalty. The yellowing is the consequences of poor crop growth and merely a mechanism through which the plant rebalances the supply and demand for photosynthate.

We want to emphasise that there are two major findings in this project that could have significant implications for further crop improvement. Firstly, there is a significant induction of carbon partitioning to metabolic processes that produce antioxidants and hence provide temporary protection against photooxidation during YCS symptom development. Secondly, sugarcane produces significant quantities of soluble glucans and the leaf midrib and sheath become new secondary carbon sinks. This maintains carbon flow and energy utilisation in the leaf lamina during YCS development. Exploitation of these two traits could provide protection and minimise or prevent mid-canopy yellowing.

8. RECOMMENDATIONS FOR FURTHER RD&A

A rapidly changing environment over the past decade is likely to have contributed to increased crop stress and the physiological disorder known as YCS. Therefore, any continued investment should address i) how farm management practice will keep pace with climate change and ii) how genetic targets will improve crop resistance or tolerance to abiotic stress?

9. PUBLICATIONS

9.1 Journal publications

1) Marquardt A, Scalia G, Joyce P, Basnayake J, Botha FC. (2016). Changes in photosynthesis and carbohydrate metabolism in sugarcane during the development of Yellow Canopy Syndrome (YCS). *Functional Plant Biology* (submitted and accepted). (See Appendix 1)

2) Marquardt A, Scalia G, Wathen-Dunn K & Botha FC (2017) 'Yellow Canopy Syndrome (YCS) in Sugarcane is Associated with Altered Carbon Partitioning in the Leaf', *Sugar Tech*, vol. 19, no. 6, pp. 647-55. (See Appendix 1)

3) Marquardt A, Henry RJ & Botha FC (2019) 'Midrib Sucrose Accumulation and Sugar Transporter Gene Expression in YCS-Affected Sugarcane Leaves', *Tropical Plant Biology*, vol. 12, no. 3, pp. 186-205. (See Appendix 1)

9.2 Industry conference papers

4) Botha FC, Marquardt A, Scalia G, Wathen-Dunn1 K. (2016). Yellow Canopy Syndrome (YCS) is associated with disruption of sucrose metabolism in the leaf. *Proceedings of International Society of Sugarcane Technologists* (submitted). (See Appendix 1)
(presented by Frikkie Botha at ISSCT conference 2016).

5) Annelie Marquardt, Kate Wathen-Dunn, Robert J Henry and Frederik C Botha: “There’s yellow and then there’s yellow – which one is YCS?” In: Proceedings of the Australian Society of Sugar Cane Technologists, Volume 39, p89-98, 3-5 May, 2017.
(presented by Annelie Marquardt at ASSCT conference in 2017). (See Appendix 1)

10. ACKNOWLEDGEMENTS

We wish to thank our funding providers SRA and QDAF, the SRA RFU, other members of the YCS integrated project team who assisted directly with this research, Priya Joyce, Dave Olsen, Jaya Basnayake, Leana Hawkins and productivity and sugar services and the many growers who allowed access to their properties and assisted in sampling. We also thank the many technicians who assisted in sample collection and analyses. The feedback and insights provided by the Scientific Reference Panel for the SRA YCS Program and the other teams investigating YCS were also valuable in guiding the research

11. REFERENCES

Agusti J, Herold S, Schwarz M, Sanchez P, Ljung K, Dun EA, Brewer PB, Beveridge CA, Sieberer T, Sehr EM, Greb T (2011) Strigolactone signaling is required for auxin-dependent stimulation of secondary growth in plants. Proceedings of the National Academy of Sciences

Ahmad A (2014) Oxidative Damage to Plants: Antioxidant Networks and Signaling, Ed 1st. Academic Press

Allan SA, Kline DL, Walker D (2009) Environmental Factors Affecting Efficacy of Bifenthrin-treated Vegetation for Mosquito Control. Journal of the American Mosquito Control Association **25:** 338-346

Allison JCS, Weinmann H (1970) Effect of Absence of Developing Grain on Carbohydrate Content and Senescence of Maize Leaves. Plant Physiology **46:** 435

Altmann S, Muino JM, Lortzing V, Brandt R (2018) Transcriptomic basis for reinforcement of elm antiherbivore defence mediated by insect egg deposition. Molecular Ecology **27:** 4901-4915

Amano Y, Tsubouchi H, Shinohara H, Ogawa M, Matsubayashi Y (2007) Tyrosine-sulfated glycopeptide involved in cellular proliferation and expansion in Arabidopsis. Proc Natl Acad Sci U S A **104:** 18333-18338

Amm I, Sommer T, Wolf DH (2014) Protein quality control and elimination of protein waste: The role of the ubiquitin–proteasome system. Biochimica et Biophysica Acta (BBA) - Molecular Cell Research **1843:** 182-196

Andersen EJ, Ali S, Byamukama E, Yen Y, Nepal MP (2018) Disease Resistance Mechanisms in Plants. Genes **9:** 339

Apel K, Hirt H (2004) Reactive oxygen species: metabolism, oxidative stress, and signal transduction. Annual Review of Plant Biology **55:** 373-399

Arnér ESJ, Holmgren A (2000) Physiological functions of thioredoxin and thioredoxin reductase. European Journal of Biochemistry **267:** 6102-6109

Bai L, Zhang G, Zhou Y, Zhang Z, Wang W, Du Y, Wu Z, Song CP (2009) Plasma membrane-associated proline-rich extensin-like receptor kinase 4, a novel regulator of Ca signalling, is required for abscisic acid responses in Arabidopsis thaliana. Plant J **60:** 314-327

Baker NR (2008) Chlorophyll fluorescence: A probe of photosynthesis in vivo. *In* Annual Review of Plant Biology, Vol 59. Annual Reviews, Palo Alto, pp 89-113

Baker RF, Braun DM (2008) Tie-dyed2 functions with tie-dyed1 to promote carbohydrate export from maize leaves. Plant Physiology **146:** 1085-1097

Barratt DHP, Kölling K, Graf A, Pike M, Calder G (2011) Callose Synthase GSL7 Is Necessary for Normal Phloem Transport and Inflorescence Growth in Arabidopsis. Plant Physiology and Biochemistry **155:** 328-341

Bassi D, Menossi M, Mattiello L (2018) Nitrogen supply influences photosynthesis establishment along the sugarcane leaf. Scientific Reports **8:** 2327

Belesini AA, Carvalho FMS, Telles BR, de Castro GM, Giachetto PF, Vantini JS, Carlin SD, Cazetta JO, Pinheiro DG, Ferro MIT (2017) De novo transcriptome assembly of sugarcane leaves submitted to prolonged water-deficit stress. Genet Mol Res **16**

Bergmeyer H, Bernt E (1974) Sucrose. In: Bergmeyer HU (ed) Methods of enzymatic analysis, Vol 2. Verlag Chemie, , Weinheim, New York.

Beutler H (1984) Starch. In: Bergmeyer H (ed) Methods of enzymatic analysis., Vol 3, Verlag Chemie, Weinheim, New York

Bihmidine S, Hunter CT, Johns CE, Koch KE, Braun DM (2013) Regulation of assimilate import into sink organs: update on molecular drivers of sink strength. Front Plant Sci **4:** 177

Black CC, Lobodia T, Chen JQ, Sung S-JS (1995) Can sucrose cleavage enzymes serve as markers for sink strength and is sucrose a signal molecule during plant sink development? International Symposium on Sucrose Metabolism, Amer. Soc. of Plant Physiologists**:** 49-64

Bolger AM, Lohse M, Usadel B (2014) Trimmomatic: a flexible trimmer for Illumina sequence data. Bioinformatics **30:** 2114-2120

Bonnett GD (2014) Development stages (phenology) *In* PH Moore, FC Botha, eds, Sugarcane Physiology. Biochemistry & Functional Biology. John Wiley & sons, New Dehli, India, p 633

Botha FC, Marquardt A, Scalia G, Wathen-Dunn K (2016) Yellow Canopy Syndrome (YCS) is associated with disruption of sucrose metabolism in the leaf. Proceedings of the international Society of Sugar Cane Technologists **29:** 1348-1357

Botha FC, Marquardt A, Wathen-Dunn K, Scalia G, Joyce P (2015) Biological factors driving YCS (Final report Sugar Research Australia).

Botha FC, McDonald ZA (2010) Carbon partitioning in the sugarcane stalk. Proceedings Australian Society of Sugar Cane Technologists **32:** 486-496

Botha FC, Whittaker A, Vorster DJ, Black KG (1996) Sucrose accumulation rate, carbon partitioning and expression of key enzyme activities in sugarcane stem tissue. C S I R O, East Melbourne

Boughton BA, Damien L, Callahan CS, Jairus B, al. e (2011) Comprehensive profiling and quantitation of amine group containing metabolites. . Analytical Chemistry **83:** 7523-7530

Braun DM, Ma Y, Inada N, Muszynski MG, Baker RF (2006) Tie-dyed1 Regulates carbohydrate accumulation in maize leaves. Plant Physiolgy **142:** 1511-1522

Braun DM, Slewinski TL (2009) Genetic control of carbon partitioning in grasses: roles of sucrose transporters and tie-dyed loci in phloem loading. Plant Physiol **149:** 71-81

Cakmak I, Kirkby EA (2008) Role of magnesium in carbon partitioning and alleviating photooxidative damage. Physiologia Plantarum **133:** 692-704

Chaves MM, Flexas J, Pinheiro C (2008) Photosynthesis under drought and salt stress: regulation mechanisms from whole plant to cell. Annals of Botany **103:** 551-560

Chen L-Q, Hou B-H, Lalonde S, Takanaga H, Hartung ML, Qu X-Q, Guo W-J, Kim J-G, Underwood W, Chaudhuri B, Chermak D, Antony G, White FF, Somerville SC, Mudgett MB, Frommer WB (2010) Sugar transporters for intercellular exchange and nutrition of pathogens. Nature **468:** 527-U199

Chen S, Elzaki MEA, Ding C, Li Z, Wang J (2019) Plant allelochemicals affect tolerance of polyphagous lepidopteran pest Helicoverpa armigera (Hübner) against insecticides. Plant Signaling & Behavior **4:** 489-492

Chen XY, Kim JY (2009) Callose synthesis in higher plants. Plant Signaling & Behavior **4:** 489-492

Chepyshko H, Lai C-P, Huang L-M, Liu J-H, Shaw J-F (2012) Multifunctionality and diversity of GDSL esterase/lipase gene family in rice (Oryza sativa L. japonica) genome: new insights from bioinformatics analysis. BMC Genomics **13:** 309

Cui W, Lee JY (2016) Arabidopsis callose synthases CalS1/8 regulate plasmodesmal permeability during stress. Nature Plants **2:** 16034

Davies WJ, Kudoyarova G, Hartung W (2005) Long-distance ABA Signaling and Its Relation to Other Signaling Pathways in the Detection of Soil Drying and the Mediation of the Plant's Response to Drought. Journal of Plant Growth Regulation **24:** 285

Drake R, John I, Farrell A, Cooper W, Schuch W, Grierson D (1996) Isolation and analysis of cDNAs encoding tomato cysteine proteases expressed during leaf senescence. Plant molecular biology **30:** 755-767

Du H, Li X, Ning L, Qin R, Du Q, Wang Q (2019) RNA-Seq analysis reveals transcript diversity and active genes after common cutworm (Spodoptera litura Fabricius) attack in resistant and susceptible wild soybean lines. BMC Genomics **20:** 237

Du Y, Nose A, Kondo A, Wasano K (2000) Diurnal changes in photosynthesis in sugarcane leaves: II. Enzyme activities and metabolite levels relating to sucrose and starch metabolism. Plant Production Science **3:** 9-16

Dubin MJ, Mittelsten Scheid O, Becker C (2018) Transposons: a blessing curse. Current Opinion in Plant Biology **42:** 23-29

Dunaeva M, Goebel C, Wasternack C, Parthier B, Goerschen E (1999) The jasmonate-induced 60 kDa protein of barley exhibits N-glycosidase activity in vivo. FEBS Letters **452:** 263-266

Esau K (1957) Phloem Degeneration in Gramineae Affected by the Barley Yellow-Dwarf Virus. American Journal of Botany **44:** 245-251

Fan X, Naz M, Fan X, Xuan W, Miller AJ, Xu G (2017) Plant nitrate transporters: from gene function to application. J Exp Bot **68:** 2463-2475

Figueroa C, Lunn J (2016) A Tale of Two Sugars: Trehalose 6-Phosphate and Sucrose. Plant Physiology **172:** 7-27

Fontaniella B, Vicente C, Legaz ME, de Armas R, Rodríguez CW, Martínez M, Piñón D, Acevedo R, Solas MT (2003) Yellow leaf syndrome modifies the composition of sugarcane juices in polysaccharides, phenols and polyamines. Plant Physiology and Biochemistry **41:** 1027-1036

Foyer CH, Noctor G (2005) Oxidant and antioxidant signalling in plants: a re-evaluation of the concept of oxidative stress in a physiological context. Plant, Cell & Environment **28:** 1056-1071

Fujimoto S, Yonemura M, Matsunaga S, Nakagawa T, Uchiyama S, Fukui K (2005) Characterization and dynamic analysis of Arabidopsis condensin subunits, AtCAP-H and AtCAP-H2. Planta **222:** 293-300

Furbank RT (2011) Evolution of the C4 photosynthetic mechanism: are there really three C4 acid decarboxylation types? Journal of Experimental Botany **62:** 3103-3108

Geigenberger P (2011) Regulation of starch biosynthesis in response to a fluctuating environment. Plant physiology **155:** 1566-1577

Geiger DR, Koch KE, Shieh W (1996) Effect of environmental factors on whole plant assimilate partitioning and associated gene expression Journal of Experimental Botany **47:** 1229-1238

Ghannoum O (2009) C4 photosynthesis and water stress. Ann Bot **103:** 635-644

Gill SS, Tuteja N (2010) Reactive oxygen species and antioxidant machinery in abiotic stress tolerance in crop plants. Plant Physiology and Biochemistry **48:** 909-930

Gille S, de Souza A, Xiong G, Benz M, Cheng K, Schultink A, Reca I-B, Pauly M (2011) O-acetylation of Arabidopsis hemicellulose xyloglucan requires AXY4 or AXY4L, proteins with a TBL and DUF231 domain. The Plant cell **23:** 4041-4053

Glassop D, Stiller J, Bonnett GD, Grof CPL, Rae AL (2017) An analysis of the role of the ShSUT1 sucrose transporter in sugarcane using RNAi suppression. Functional Plant Biology **44:** 795-808

Głowacki S, Macioszek VK, Kononowicz AK (2011) R proteins as fundamentals of plant innate immunity. Cellular & Molecular Biology Letters **16:** 1-24

Goldschmidt EE, Huber SC (1992) REGULATION OF PHOTOSYNTHESIS BY END-PRODUCT ACCUMULATION IN LEAVES OF PLANTS STORING STARCH, SUCROSE, AND HEXOSE SUGARS. Plant Physiology **99:** 1443-1448

Gomes MP, Le Manac'h SG, Maccario S, Labrecque M, Lucotte M, Juneau P (2016) Differential effects of glyphosate and aminomethylphosphonic acid (AMPA) on photosynthesis and chlorophyll metabolism in willow plants. Pesticide Biochemistry and Physiology **130:** 65-70

Graham IA, Martin T (2000) Control of Photosynthesis, Allocation and Partitioning by Sugar Regulated Gene Expression. *In* RC Leegood, TD Sharkey, S von Caemmerer, eds, Photosynthesis: Physiology and Metabolism. Springer Netherlands, Dordrecht, pp 233-248

Grandbastien M-A (1998) Activation of plant retrotransposons under stress conditions. Trends in Plant Science **3:** 181-187

Gray J, Caparrós-Ruiz D, Grotewold E (2012) Grass phenylpropanoids: Regulate before using! Plant Science **184:** 112-120

Gupta AK, Kaur N (2005) Sugar signalling and gene expression in relation to carbohydrate metabolism under abiotic stresses in plants. Journal of Biosciences **30:** 761-776

Hamonts K, Trivedi P, Grinyer J, Holford P, Drigo B, Anderson IA, Singh BK (2018) Yellow Canopy Syndrome in sugarcane is associated with shifts in the rhizosphere soil metagenome but not with overall soil microbial function. Soil Biology and Biochemistry **125:** 275-285

Hatch MD, Glasziou KT (1964) Direct Evidence for Translocation of Sucrose in Sugarcane Leaves and Stems. Plant physiology **39:** 180-184

Herbers K, Tacke E, Hazirezaei M, Krause KP, Melzer M, Rohde W, Sonnewald U (1997) Expression of a luteoviral movement protein in transgenic plants leads to carbohydrate accumulation and reduced photosynthetic capacity in source leaves. Plant J **12:** 1045-1056

Hoang NV, Furtado A, Mason PJ, Marquardt A, Kasirajan L, Thirugnanasambandam PP, Botha FC, Henry RJ (2017) A survey of the complex transcriptome from the highly polyploid sugarcane genome using full-length isoform sequencing and de novo assembly from short read sequencing. BMC Genomics **18:** 395

Hoang NV, Furtado A, O'Keeffe AJ, Botha FC, Henry RJ (2017) Association of gene expression with biomass content and composition in sugarcane. PLoS One **12:** e0183417

Hoang NV, Furtado A, Thirugnanasambandam PP, Botha FC, Henry RJ (2018) De novo assembly and characterizing of the culm-derived meta-transcriptome from the polyploid sugarcane genome based on coding transcripts. *In* Heliyon, Vol 4, p e00583

Horváth BM, Magyar Z, Zhang Y, Hamburger AW, Bakó L, Visser RG, Bachem CW, Bögre L (2006) EBP1 regulates organ size through cell growth and proliferation in plants. The EMBO Journal **25:** 4909-4920

Huot B, Yao J, Montgomery BL, He SY (2014) Growth-defense tradeoffs in plants: a balancing act to optimize fitness. Mol Plant **7:** 1267-1287

Husted S, Schjoerring J (1995) Apoplastic pH and Ammonium Concentration in leaves of *Brassica napus* L. Plant Physiology **109:** 1453-1460

Idänheimo N (2015) The Role of Cysteine-rich Receptor-like Protein Kinases in ROS Signaling in Arabidopsis thaliana.

Inman-Bamber NG (1994) Temperature and seasonal effects on canopy development and light interception of sugarcane. Field Crops Research **36:** 41-51.

Inman-Bamber NG, Bonnett GD, Smith DM, Thorburn PJ (2005) Sugarcane physiology: Integrating from cell to crop to advance sugarcane production. Field Crops Research **92:** 115-117

Jeannette E, Reyss A, Gregory N, Gantet P, Prioul JL (2000) Carbohydrate metabolism in a heat-girdled maize source leaf. Plant Cell and Environment **23:** 61-69

Jensen SG (1996) Composition and metabolism of barley leaves infected with barley yellow dwarf virus. Phytopathology **59:** 1694-1698

Jiang CD, Shi L, Gao HY, Schansker G, Toth SZ, Strasser RJ (2006) Development of photosystems 2 and 1 during leaf growth in grapevine seedlings probed by chlorophyll a fluorescence transient and 820 nm transmission in vivo. Photosynthetica **44:** 454-463

Julius B, Slewinski TL, Baker RF, Tzin V, Braun DM (2018) Maize carbohydrate partitioning defective1 Impacts Carbohydrate Distribution, Callose Accumulation, and Phloem Function. Journal of Experimental Botany **69:** 3917-3931

Kelly G, Moshelion M, David-Schwartz R, Halperin O, Wallach R, Attia Z, Belausov E, Granot D (2013) Hexokinase mediates stomatal closure. The Plant Journal **75:** 977-988

Kenyon J, Turner JG (1990) Physiological changes in Nicotiana tabacum leaves during development of chlorosis caused by coronatine. Physiological and Molecular Plant Pathology **37:** 463-477

Keunen E, Remans T, Opdenakker K, Jozefczak M, Gielen H (2013) A mutant of the Arabidopsis thaliana LIPOXYGENASE1 gene shows altered signalling and oxidative stress related responses after cadmium exposure. Plant Physiol Biochem **63:** 272-280

Kim J, Yang J, Yang R, Sicher RC, Chang C, Tucker ML (2016) Transcriptome Analysis of Soybean Leaf Abscission Identifies Transcriptional Regulators of Organ Polarity and Cell Fate. Frontiers in Plant Science **7**

Kingston-Smith AH, Galtier N, Pollock CJ, Foyer CH (1998) Soluble acid invertase activity in leaves is independent of species differences in leaf carbohydrates, diurnal sugar profiles and paths of phloem loading. New Phytologist **139:** 283-292

Ko Y, Lin Y (2004) 1,3-beta-glucan quantification by a fluorescence microassay and analysis of its distribution in foods. Journal of Agriculture and Food Chemistry **52:** 3313-3318

Koch KE (1996) CARBOHYDRATE-MODULATED GENE EXPRESSION IN PLANTS. Annu. Rev. Plant Physiol. Plant Mol. Biol. **47:** 509-540

Koch KE (2004) Sucrose metabolism: regulatory mechanisms and pivotal roles in sugar sensing and plant development. Curr Opin Plant Biol **7:** 235-246

Kohle H, Jeblick W, Proten F, BLASCHEK W, KAUSS H (1984) Chitosan-Elicited Callose Synthesis in Soybean Cells as a Ca2+-Dependent Process. Plant Physiology and Biochemistry **77:** 544-551

Kowalski GM, De Souza DP, Burch ML, Hamley S, Kloehn J, Selathurai A, Tull D, O'Callaghan S, McConville MJ, Bruce CR (2015) Application of dynamic metabolomics to examine in vivo skeletal muscle glucose metabolism in the chronically high-fat fed mouse. Biochemical and Biophysical Research Communications **462:** 27-32

Krapp A, Stitt M (1995) AN EVALUATION OF DIRECT AND INDIRECT MECHANISMS FOR THE SINK-REGULATION OF PHOTOSYNTHESIS IN SPINACH - CHANGES IN GAS-EXCHANGE, CARBOHYDRATES, METABOLITES, ENZYME-ACTIVITIES AND STEADY-STATE TRANSCRIPT LEVELS AFTER COLD-GIRDLING SOURCE LEAVES. Planta **195:** 313-323

Kruger GHJ, Tsimilli-Michael M, Strasser RJ (1997) Light stress provokes plastic and elastic modifications in structure and function of photosystems II in camellia leaves. Physiologica Plantarum **101:** 265-277

Ku Y-S, Sintaha M, Cheung M-Y, Lam H-M (2018) Plant Hormone Signaling Crosstalks between Biotic and Abiotic Stress Responses. International Journal of Molecular Sciences **19:** 3206

Kumar A, Bennetzen JL (1999) Plant retrotransposons. Annu Rev Genet **33:** 479-532

Kurotani KI, Hattori T, Takeda S (2015) Overexpression of a CYP94 family gene CYP94C2b increases internode length and plant height in rice. Plant Signal Behav **10:** e1046667

Kwon SJ, Jin HC, Lee S, Nam MH, Chung JH, Kwon SI, Ryu C-M, Park OK (2009) GDSL lipase-like 1 regulates systemic resistance associated with ethylene signaling in Arabidopsis. The Plant Journal **58:** 235-245

Laskowski MJ, Dreher KA, Gehring MA, Abel S, Gensler AL, Sussex IM (2002) FQR1, a Novel Primary Auxin-Response Gene, Encodes a Flavin Mononucleotide-Binding Quinone Reductase. Plant Physiology **128:** 578

Lehrer AT, Komor E (2008) Symptom expression of yellow leaf disease in sugarcane cultivars with different degrees of infection by Sugarcane yellow leaf virus. Plant Pathology **57:** 178-189

Lemoine R, La Camera S, Atanassova R, Deedaldeechamp F, Allario T, Pourtau N, Bonnemain JL, Laloi M, Coutos-Theevenot P, Maurousset L, Faucher M, Girousse C, Lemonnier P, Parrilla J, Durand M (2013) Source-to-sink transport of sugar and regulation by environmental factors. Frontiers in Plant Science **4**

Li P, Zhou H, Shi X, Yu B, Zhou Y, Chen S, Wang Y, Peng Y, Meyer RC, Smeekens SC, Teng S (2014) The ABI4-induced Arabidopsis ANAC060 transcription factor attenuates ABA signaling and renders seedlings sugar insensitive when present in the nucleus. PLoS Genet **10:** e1004213

Lim CJ, Yang KA, Hong JK, Choi JS, Yun D-J, Hong JC, Chung WS, Lee SY, Cho MJ, Lim CO (2006) Gene expression profiles during heat acclimation in Arabidopsis thaliana suspension-culture cells. Journal of Plant Research **119:** 373-383

Lin YT, Chen LJ, Herrfurth C, Feussner I, Li HM (2016) Reduced Biosynthesis of Digalactosyldiacylglycerol, a Major Chloroplast Membrane Lipid, Leads to Oxylipin Overproduction and Phloem Cap Lignification in Arabidopsis. Plant Cell **28:** 219-232

Lipowsky G, Bischoff FR, Schwarzmaier P, Kraft R, Kostka S, Hartmann E, Kutay U, Görlich D (2000) Exportin 4: a mediator of a novel nuclear export pathway in higher eukaryotes. The EMBO journal **19:** 4362-4371

Long SP, Farage PK, Garcia RL (1996) Measurement of leaf and canopy photosynthetic CO2 exchange in the field. Journal of Experimental Botany **47:** 1629-1642

Loudet O, Michael TP, Burger BT, Le Metté C, Mockler TC, Weigel D, Chory J (2008) A zinc knuckle protein that negatively controls morning-specific growth in <em>Arabidopsis thaliana</em&gt. Proceedings of the National Academy of Sciences **105:** 17193

Love AJ, Yu C, Petukhova NV, Kalinina NO, Chen J, Taliansky ME (2017) Cajal bodies and their role in plant stress and disease responses. RNA biology **14:** 779-790

Lu Y, Sharkey TD (2006) The importance of maltose in transitory starch breakdown. Plant, Cell & Environment **29:** 353-366

Lunn J, Delorge I, Figueroa C, Van Dijck P, Stitt M (2014) Trehalose metabolism in plants. The Plant Journal **79:** 544-567

Lunn JE, Furbank RT (1997) Localisation of sucrose-phosphate synthase and starch in leaves of C4 plants. Planta **202:** 106-111

Ma JF, Yamaji N (2006) Silicon uptake and accumulation in higher plants. Trends in Plant Science **11:** 392-397

Marquardt A (2019) The molecular analysis of yellow canopy syndrome-induced yellowing in the sugarcane leaf. The University of Queeensland, The University of Queensland, Queensland Alliance for Agriculture and Food Innovation

Marquardt A, Henry RJ, Botha FC (2019) Midrib Sucrose Accumulation and Sugar Transporter Gene Expression in YCS-Affected Sugarcane Leaves. Tropical Plant Biology **12:** 186-205

Marquardt A, Scalia G, Joyce P, Basnayake J, Botha FC (2016) Changes in photosynthesis and carbohydrate metabolism in sugarcane during the development of Yellow Canopy Syndrome. Functional Plant Biology **43:** 523-533

Marquardt A, Scalia G, Wathen-Dunn K, Botha FC (2017) Yellow Canopy Syndrome (YCS) in Sugarcane is Associated with Altered Carbon Partitioning in the Leaf. Sugar Tech **19:** 647-655

Mattiello L, Riaño-Pachón DM, Martins MCM, da Cruz LP, Bassi D, Marchiori PER, Ribeiro RV, Labate MTV, Labate CA, Menossi M (2015) Physiological and transcriptional analyses of developmental stages along sugarcane leaf. BMC plant biology **15:** 300-300

McCormick AJ, Cramer MD, Watt DA (2008) Regulation of photosynthesis by sugars in sugarcane leaves. Journal of Plant Physiology **165:** 1817-1829

Miao Y, Jia H, Li Z, Liu Y, Hou M (2018) Transcriptomic and Expression Analysis of the Salivary Glands in Brown Planthoppers, Nilaparvata lugens (Hemiptera: Delphacidae). Journal of Economic Entomology **111:** 2884-2893

Moore PH, Botha FC (2013) Sugarcane Physiology, Biochemistry & Functional Biology. Hoboken : Wiley, Hoboken

Morey SR, Hirose T, Hashida Y, Miyao A, Hirochika H, Ohsugi R, Yamagishi J, Aoki N (2018) Genetic Evidence for the Role of a Rice Vacuolar Invertase as a Molecular Sink Strength Determinant. Rice (N Y) **11:** 6

Morey SR, Hirose T, Hashida Y, Miyao A, Hirochika H, Ohsugi R, Yamagishi J, Aoki N (2019) Characterisation of a rice vacuolar invertase isoform, OsINV2, for growth and yield-related traits. Functional Plant Biology **46:** 777-785

Morgan T, Jackson P, McDonald L, Holtum J (2007) Chemical ripeners increase early season sugar content in a range of sugarcane varieties. Australian Journal of Agricultural Research **58:** 233-241

Mueller MJ, Berger S (2009) Reactive electrophilic oxylipins: Pattern recognition and signalling. Phytochemistry **70:** 1511-1521

Myers AM, Morell MK, James MG, NBall SG (2000) Recent Progress toward Understanding Biosynthesis of the Amylopectin Crystal. Plant Physiology **122:** 989-997

Nanchen A, Fuhrer T, Sauer U (2007) Determination of metabolic flux ratios from 13C-experiments and gas chromatography-mass spectrometry data: protocol and principles. Methods Mol Biol **358:** 177-197

Negi P, Rai AN, Suprasanna P (2016) Moving through the Stressed Genome: Emerging Regulatory Roles for Transposons in Plant Stress Response. Frontiers in plant science **7:** 1448-1448

Nishizawa A, Yabuta Y, Shigeoka S (2008) Galactinol and raffinose constitute a novel function to protect plants from oxidative damage. Plant Physiology **147:** 1251-1263

Nounjan N, Chansongkrow P, Charoensawan V, Siangliw JL, Toojinda T, Chadchawan S, Theerakulpisut P (2018) High Performance of Photosynthesis and Osmotic Adjustment Are Associated With Salt Tolerance Ability in Rice Carrying Drought Tolerance QTL: Physiological and Co-expression Network Analysis. Frontiers in plant science **9:** 1135-1135

Nuccio ML, Wu J, Mowers R, Zhou H-P, Meghji M, Primavesi LF, Paul MJ, Chen X, Gao Y, Haque E, Basu SS, Lagrimini LM (2015) Expression of trehalose-6-phosphate phosphatase in maize ears improves yield in well-watered and drought conditions. Nature Biotechnology **33:** 862-869

Olsen DJ, Ward AL (2019) Effect of neonicotinoid, pyrethroid and spirotetramat insecticides and a miticide on incidence and severity of Yellow canopy syndrome. Proceedings Australian Society of Sugar Cane Technologists **41:** 359-366

Olsen JV, Blagoev B, Gnad F, Macek B, Kumar C, Mortensen P, Mann M (2006) Global, In Vivo, and Site-Specific Phosphorylation Dynamics in Signaling Networks. Cell **127:** 635-648

Osmond CB, Foyer CH, Bock G, Grace SC, Logan BA (2000) Energy dissipation and radical scavenging by the plant phenylpropanoid pathway. Philosophical Transactions of the Royal Society of London. Series B: Biological Sciences **355:** 1499-1510

Patil V, McDermott HI, McAllister T, Cummins M, Silva JC, Mollison E, Meikle R, Morris J, Hedley PE, Waugh R, Dockter C, Hansson M, McKim SM (2019) APETALA2 control of barley internode elongation. Development **146:** dev170373

Peng H, Zhang J (2009) Plant genomic DNA methylation in response to stresses: Potential applications and challenges in plant breeding. Progress in Natural Science **19:** 1037-1045

Peumans WJ, Damme EJMV (2001) Ribosome-inactivating proteins from plants: more than RNA N-glycosidases? The FASEB Journal **15:** 1493-1506

Pokorska B, Zienkiewicz M, Powikrowska M, Drozak A, Romanowska E (2009) Differential turnover of the photosystem II reaction centre D1 protein in mesophyll and bundle sheath chloroplasts of maize. Biochimica Et Biophysica Acta-Bioenergetics **1787:** 1161-1169

Qin YM, Hu CY, Pang Y, Kastaniotis AJ, Hiltunen JK, Zhu YX (2007) Saturated very-long-chain fatty acids promote cotton fiber and Arabidopsis cell elongation by activating ethylene biosynthesis. Plant Cell **19:** 3692-3704

Rae AL, Martinelli P, Dornelas MC (2014) Anatomy and Morphology. *In* PH Moore, FC Botha, eds, Sugarcane: Physiology, Biochemistry, and Functional Biology. John Wiley & Sons, Inc, UK

Rae AL, Pierre J (2018) Sugarcane root systems for increased productivity; development and application of a root health assay: Final report submitted Sugar Research Australia.

Rajcan I, Tollenaar M (1999) Source:sink ratio and leaf senescence in maize:: II. Nitrogen metabolism during grain filling. Field Crops Research **60:** 255-265

Robertson MJ, Bonnett G. D., Hughes R. M., Muchow R. C. and Campbell J. A. (1998) (1998) Temperature and leaf area expansion of sugarcane: integration of controlled-environment, field and model studies. Australian Journal of Plant Physiology **25:** 819-828

Rodziewicz P, Swarcewicz B, Chmielewska K, Wojakowska A, Stobiecki M (2014) Influence of abiotic stresses on plant proteome and metabolome changes. Acta Physiologiae Plantarum **36:** 1-19

Russin WA, Evert RF, Vanderveer PJ, Sharkey TD, Briggs SP (1996) Modification of a Specific Class of Plasmodesmata and Loss of Sucrose Export Ability in the sucrose export defective1 Maize Mutant. The Plant Cell **8:** 645

Sasaki H, Hara T, Ito S, Uehara N, Kim HY, Lieffering M, Okada M, Kobayashi K (2007) Effect of free-air CO_2 enrichment on the storage of carbohydrate fixed at different stages in rice (Oryza sativa L.). Field crops research **100:** 24-31

Saunders EC, de Souza DP, Chambers JM, Ng M, Pyke J, McConville MJ (2015) Use of (13)C stable isotope labelling for pathway and metabolic flux analysis in Leishmania parasites. Methods Mol Biol **1201:** 281-296

Schansker G, Tóth SZ, Strasser RJ (2005) Methylviologen and dibromothymoquinone treatments of pea leaves reveal the role of photosystem I in the Chl a fluorescence rise OJIP. Biochimica et Biophysica Acta (BBA) - Bioenergetics **1706:** 250-261

Schöttler MA, Tóth SZ (2014) Photosynthetic complex stoichiometry dynamics in higher plants: environmental acclimation and photosynthetic flux control. Frontiers in Plant Science **5**

Schreiber U, Neubauer C (1987) The Polyphasic Rise of Chlorophyll Fluorescence upon Onset of Strong Continuous Illumination: II. Partial Control by the Photosystem II Donor Side and Possible Ways of Interpretation. **42:** 1255

Schultink A, Naylor D, Dama M, Pauly M (2015) The Role of the Plant-Specific ALTERED XYLOGLUCAN9 Protein in Arabidopsis Cell Wall Polysaccharide O-Acetylation. Plant Physiology **167:** 1271-1283

Schulz S, Chachami G, Kozaczkiewicz L, Winter U, Stankovic-Valentin N, Haas P, Hofmann K, Urlaub H, Ovaa H, Wittbrodt J, Meulmeester E, Melchior F (2012) Ubiquitin-specific protease-like 1 (USPL1) is a SUMO isopeptidase with essential, non-catalytic functions. EMBO reports **13:** 930-938

Schürmann P, Jacquot J-P (2000) PLANT THIOREDOXIN SYSTEMS REVISITED. Annual Review of Plant Physiology and Plant Molecular Biology **51:** 371-400

Schwacke R, Ponce-Soto GY, Krause K, Bolger AM, Arsova B, Hallab A, Gruden K, Stitt M, Bolger ME, Usadel B (2019) MapMan4: A Refined Protein Classification and Annotation Framework Applicable to Multi-Omics Data Analysis. Molecular Plant **12:** 879-892

Sehr EM, Agusti J, Lehner R, Farmer EE, Schwarz M, Greb T (2010) Analysis of secondary growth in the Arabidopsis shoot reveals a positive role of jasmonate signalling in cambium formation. Plant J **63:** 811-822

Sham A, Al-Azzawi A, Al-Ameri S, Al-Mahmoud B, Awwad F (2014) Transcriptome Analysis Reveals Genes Commonly Induced by Botrytis cinerea Infection, Cold, Drought and Oxidative Stresses in Arabidopsis. PLoS ONE **9**

Sharp RE, Wu Y, Voetberg GS, Saab IN, LeNoble ME (1994) Confirmation that abscisic acid accumulation is required for maize primary root elongation at low water potentials. Journal of Experimental Botany **45:** 1743-1751

Shedletzky E, Unger C, Delmer DP (1997) A microtiter-based fluorescence assay for (1,3)-beta-glucan synthases. Analytical Biochemistry **249:** 88-93

Sheen J (1990) Metabolic repression of transcription in higher plants. The Plant Cell **2:** 1027

Sheen J (1994) Feedback control of gene expression. Photosynthesis Research **39:** 427-438

Shiriga K, Sharma R, Kumar K, Yadav SK, Hossain F, Thirunavukkarasu N (2014) Genome-wide identification and expression pattern of drought-responsive members of the NAC family in maize. Meta Gene **2:** 407-417

Simão FA, Waterhouse RM, Ioannidis P, Kriventseva EV, Zdobnov EM (2015) BUSCO: assessing genome assembly and annotation completeness with single-copy orthologs. Bioinformatics **31:** 3210-3212

Slewinski TL, Braun DM (2010) The psychedelic genes of maize redundantly promote carbohydrate export from leaves. Genetics **185:** 221-232

Slewinski TL, Meeley R, Braun DM (2009) Sucrose transporter1 functions in phloem loading in maize leaves. J Exp Bot **60:** 881-892

Smith GJ (2007) Starch and Cellulose *In* Organic Chemistry, Second Edition The McGraw-Hill Companies, Inc.

Srivastava A, Guissé B, Greppin H, Strasser RJ (1997) Regulation of antenna structure and electron transport in Photosystem II of Pisum sativum under elevated temperature probed by the fast polyphasic chlorophyll a fluorescence transient: OKJIP. Biochimica et Biophysica Acta (BBA) - Bioenergetics **1320:** 95-106

Stitt M, Quick WP (1989) Photosynthetic carbon partitioning: its regulation and possibilities for manipulation. Physiologia Plantarum **77:** 633-641

Strand DD, Livingston AK, Satoh-Cruz M, Froehlich JE, Maurino VG, Kramer DM (2015) Activation of cyclic electron flow by hydrogen peroxide in vivo. Proceedings of the National Academy of Sciences of the United States of America **112:** 5539-5544

Strasser RJ, Srivastava A, Tsimili-Michael M (2000) The fluorescence transient as a tool to characterize and screen photosynthetic samples. *In* M Yunus, U Pathre, P Mohanty, eds,

Probing Photosynthesis: Mechanism, Regulation and Adaptation. Taylor and Francis, London, UK, pp 443-480

Sung SJS, Xu DP, Galloway CM, Black CC (1988) A REASSESSMENT OF GLYCOLYSIS AND GLUCONEOGENESIS IN HIGHER-PLANTS. Physiologia Plantarum **72:** 650-654

Suzuki N, Rivero RM, Shulaev V, Blumwald E (2014) Abiotic and biotic stress combinations. New Phytologist **203:** 32-43

Takahashi H, Imamura T, Konno N, Takeda T, Fujita K, Konishi T, Nishihara M, Uchimiya H (2014) The Gentio-Oligosaccharide Gentiobiose Functions in the Modulation of Bud Dormancy in the Herbaceous Perennial Gentiana. The Plant Cell **26:** 3949-3963

Takemiya A, Sugiyama N, Fujimoto H, Tsutsumi T, Yamauchi S, Hiyama A, Tada Y, Christie J, Shimazaki K-i (2013) Phosphorylation of BLUS1 kinase by phototropins is a primary step in stomatal opening. Nature communications **4:** 2094

Thangasamy S, Chen P-W, Lai M-H, Chen J, Jauh G-Y (2012) Rice LGD1 containing RNA binding activity affects growth and development through alternative promoters. The Plant Journal **71:** 288-302

Tollenaar M, Daynard T (1982) Effect of source-sink ratio on dry matter accumulation and leaf senescence of maize. Canadian Journal of Plant Science - CAN J PLANT SCI **62:** 855-860

Tsimilli-Michael M, Strasser RJ (2008) Experimental Resolution and Theoretical Complexity Determine the Amount of Information Extractable from the Chlorophyll Fluorescence Transient OJIP. In JF Allen, E Gantt, JH Golbeck, B Osmond, eds, Photosynthesis. Energy from the Sun. . Springer Netherlands Dordrecht

Tsimilli-Michael M, Strasser RJ (2013) The energy flux theory 35 years later: formulations and applications. Photosynth Res **117:** 289-320

Uehara N, Sasaki H, Aoki N, Ohsugi R (2009) Effects of the Temperature Lowered in the Daytime and Night-time on Sugar Accumulation in Sugarcane. Plant Production Science **12:** 420-427

Ueki S, Citovsky V (2014) Plasmodesmata-associated proteins: can we see the whole elephant? Plant Signaling & Behavior **9:** e27899

van Heerden PDR, Swanepoel JW, Krüger GHJ (2007) Modulation of photosynthesis by drought in two desert scrub species exhibiting C3-mode CO2 assimilation. Environmental and Experimental Botany **61:** 124-136

Varsani S, Grover S, Zhou S, Koch KG, Huang P (2019) 12-Oxo-Phytodienoic Acid Acts as a Regulator of Maize Defense against Corn Leaf Aphid. Plant Physiology and Biochemistry **179:** 1402-1415

Wahid A, Close TJ (2007) Expression of dehydrins under heat stress and their relationship with water relations of sugarcane leaves. Biologia Plantarum **51:** 104-109

Wang C, Yan X, Chen Q, Jiang N, Fu W, Ma B, Liu J, Li C, Bednarek SY, Pan J (2013) Clathrin Light Chains Regulate Clathrin-Mediated Trafficking, Auxin Signaling, and Development in <em>Arabidopsis</em&gt. The Plant Cell **25:** 499

Wang J, Wang Y, O'Halloran TJ (2006) Clathrin Light Chain: Importance of the Conserved Carboxy Terminal Domain to Function in Living Cells. Traffic **7:** 824-832

Watt DA, McCormick AJ, Govender C, Carson DL, Cramer MD, Huckett BI, Botha FC (2005) Increasing the utility of genomics in unravelling sucrose accumulation. Field Crops Research **92:** 149-158

Weise SE, van Wijk KJ, Sharkey TD (2011) The role of transitory starch in C3, CAM, and C4 metabolism and opportunities for engineering leaf starch accumulation. Journal of Experimental Botany **62:** 3109-3118

Widodo, Patterson JH, Newbigin E, Tester M, Bacic A, Roessner U (2009) Metabolic responses to salt stress of barley (Hordeum vulgare L.) cultivars, Sahara and Clipper, which differ in salinity tolerance. Journal of experimental botany **60:** 4089-4103

Will T, van Bel AJ (2006) Physical and chemical interactions between aphids and plants. Journal of Experimental Botany **57:** 729-737

Witt S, Galicia L, Lisec J, Cairns J, Tiessen A, Araus J, Palacios Rojas N, Fernie A (2011) Metabolic and Phenotypic Responses of Greenhouse-Grown Maize Hybrids to Experimentally Controlled Drought Stress. Molecular plant **5:** 401-417

Wood DE, Salzberg SL (2014) Kraken: ultrafast metagenomic sequence classification using exact alignments. Genome Biology **15:** R46

Xia J, Sinelnikov IV, Han B, Wishart DS (2015) MetaboAnalyst 3.0--making metabolomics more meaningful. Nucleic Acids Res **43:** W251-257

Xin Z, Chen S, Ge L, Li X, Sun X (2019) The involvement of a herbivore-induced acyl-CoA oxidase gene, CsACX1, in the synthesis of jasmonic acid and its expression in flower opening in tea plant (Camellia sinensis). Plant Physiology and Biochemistry **135:** 132-140

Yan N, Doelling JH, Falbel TG, Durski AM, Vierstra RD (2000) The Ubiquitin-Specific Protease Family from Arabidopsis.AtUBP1 and 2 Are Required for the Resistance to the Amino Acid Analog Canavanine. Plant Physiology **124:** 1828-1843

Yan SL, Lehrer AT, Hajirezaei MR, Springer A, Komor E (2008) Modulation of carbohydrate metabolism and chloroplast structure in sugarcane leaves which were infected by Sugarcane Yellow Leaf Virus (SCYLV). Physiological and Molecular Plant Pathology **73:** 78-87

Yang DL, Yao J, Mei CS, Tong XH, Zeng LJ, Li Q, Xiao LT, Sun TP, Li J, Deng XW, Lee CM, Thomashow MF, Yang Y, He Z, He SY (2012) Plant hormone jasmonate prioritizes defense over growth by interfering with gibberellin signaling cascade. Proc Natl Acad Sci U S A **109:** E1192-1200

Yang J, Duan G, Li C, Liu L, Han G, Zhang Y, Wang C (2019) The Crosstalks Between Jasmonic Acid and Other Plant Hormone Signaling Highlight the Involvement of Jasmonic Acid as a Core Component in Plant Response to Biotic and Abiotic Stresses. Frontiers in Plant Science **10**

Yoo SY, Kim Y, Kim SY, Lee JS, Ahn JH (2007) Control of flowering time and cold response by a NAC-domain protein in Arabidopsis. PLoS One **2:** e642

Yoshida-Moriguchi T, Willer T, Anderson ME, Venzke D, Whyte T, Muntoni F, Lee H, Nelson SF, Yu L, Campbell KP (2013) SGK196 is a glycosylation-specific O-mannose kinase required for dystroglycan function. Science (New York, N.Y.) **341:** 896-899

Zhang L, Zhang F, Melotto M, Yao J, He SY (2017) Jasmonate signaling and manipulation by pathogens and insects. Journal of experimental botany **68:** 1371-1385

Zhang Q, Hu WC, Zhu F, Wang LM, Yu QY, Ming R, Zhang JS (2016) Structure, phylogeny, allelic haplotypes and expression of sucrose transporter gene families in Saccharum. Bmc Genomics **17**

12. APPENDIX

12.1. Appendix 1 Publications

https://doi.org/10.1071/FP15335

https://doi.org/10.1007/s12355-017-0555-1

https://doi.org/10.1007/s12042-019-09221-7


Botha FC 2016 Yellow Canopy Synd


Marquardt_ASSCT.pdf

12.2. Appendix 2 Academic publications


Marquardt A s4140264_phd_thesi


KateWD_UQ_June2017.pdf

12.3. Appendix 3 Presentations


GPMB congress_Botha.pdf


P2015016 Appendix C AMarquardt_Trop

Industry webinar https://www.youtube.com/watch?v=SDe4L00cBLI&t=7s

12.4. Appendix 4 Posters


P2015016 Appendix C Kate-TropAg-Poste


P2015016 Appendix C Trop Ag 13C Poste


TropAg_BiomarkerTest_YCS_Poster_2019 F


TropAg_YCS_Identification_Poster_2019 F_n


Botha F 2017 Poster PAG.pdf


Annelie Poster PAG.pdf

12.5. Appendix 5 Data


2015016 Appendix A Phytoplasmas and

12.6. Appendix 6 METADATA DISCLOSURE

Table 16: Metadata disclosure 1

Data	Raw and trimmed RNA sequencing data files, and de novo assembled sugarcane YCS transcriptomes (leaf/internode/combined)
Stored Location	1) Sugar Research Australia: portable hard drives, cloud storage account and Linux computer used by Kate Wathen-Dunn 2) NCBI Sequence Reads Archive, under BioProjects PRJNA480179 and PRJNA474042
Access	1) Sugar Research Australia staff only, or by request 2) Anyone with an internet connection
Contact	Gerard Scalia (gscalia@sugarresearch.com.au) or Steve Comerford (scomerford@sugarresearch.com.au) for access

Table 17: Metadata disclosure 2

Data	All data, scripts, images, analyses, files, reports and presentations associated with the project
Stored Location	Sugar Research Australia "J:\2014090YCS\"
Access	Access is restricted
Contact	Gerard Scalia (gscalia@sugarresearch.com.au) or SRA's IT Department/Steve Comerford (scomerford@sugarresearch.com.au) for access